MECHANISTIC INSIGHTS INTO THE ORIGIN OF ENANTIOSELECTIVITY OF THE ORGANOCATALYTIC ASYMMETRIC CHLOROLACTONIZATION

By

S. Roozbeh Yousefi

A DISSERTATION

Submitted to
Michigan State University
in partial fulfillment of the requirements
for the degree of

DOCTOR OF PHILOSOPHY

Chemistry

2012

ABSTRACT

MECHANISTIC INSIGHTS INTO THE ORIGIN OF ENANTIOSELECTIVITY OF THE ORGANOCATALYTIC ASYMMETRIC CHLOROLACTONIZATION

By

S. Roozbeh Yousefi

Mechanistic studies of the $(DHQD)_2PHAL$ catalyzed asymmetric chlorolactonization reaction of alkenoic acids have led to some surprising conclusions. Deuterium labeling studies of the catalyzed reaction have revealed that the face selectivity of the delivery of the chlorenium ion to olefins is neither a necessary nor a sufficient condition to deliver the product lactones with high enantioselectivities. The reaction likely proceeds via a carbocation intermediate with the enantioselectivity originating as a result of "templation" of the cyclization of the acid nucleophile by the chiral catalyst. Reaction progress kinetic analysis (RPKA) competition studies revealed that the rate-determining step is the formation of the chloronium ion. Taken together, these results suggest that the rate determining step and the enantioselectivity determining step are segregated. Moreover, NMR studies lead us to a plausible resting state of the asymmetric chlorolactonization.

Dedicated to my beloved parents

ACKNOWLEDGEMENTS

There are a number of people who have helped me throughout my journey in graduate school. This thesis would be incomplete without conveying my heartfelt thanks for the help and support I have received.

First and foremost, I would like to thank my advisor, Babak Borhan. During my time in your lab I have learned a great deal from you, and much of who I am as a scientist is directly due to your influence. Thank you for helping me to learn how to think critically and to have the confidence to put my ideas into practice. I am particularly grateful for the freedom you granted me in allowing me to pursue my desires in physical organic chemistry. Thanks for everything you have done for me and sorry if I bother you sometimes. Our personalities are completely different but we still enjoy being friends so I guess I can call this a true friendship.

I would also like to thank the members of my committee: Professor James (Ned) Jackson, Professor William Wulff, and Professor Dan Jones. Thank you for your guidance and support during my time here at MSU. I would like to specially thank Professor Ned Jackson, not just because you were my second reader. I want to thank you, because I learned a lot from you from the first day of your 851 lecture to the end of my PhD program when we had hours-long meetings. Thank you for being both tough and nice to me.

It has been my great pleasure to work with such a dedicated group of scientists. I have learned a great deal from each of you. Additionally, I have thoroughly enjoyed getting to

Table of Contetnts

List of Tables

List of Figures

Key to Symbols and Abbreviation

Å	Angstrom
AcOH	Acetic acid
Boc	*tert*-Butyl carbamate
CCl_4	Carbon tetra chloride
CH_2Br_2	Dibromomethane
CH_2Cl_2	Dichloromethane
$CHCl_3$	Chloroform
CsOH	Cesium Hydroxide
d	Day
D_2O	Deuterium oxide
DABCO	1,4-Diazabicyclo[2.2.2]octane
DBDMH	1,3-Dibromo-5,5-dimethylhydantoin
DCC	*N,N'*-Dicyclohexylcarbodiimide
DCDMH	1,3-Dichloro-5,5-dimethylhydantoin
DCDPH	1,3-Dichloro-5,5-diphenylhydantoin
$(DHQ)_2AQN$	Hydroquinidine (anthraquinone-1,4-diyl) diether
$(DHQD)_2PHAL$	Hydroquinidine 1,4-phthalazinediyl diether
$(DHQD)_2PYR$	Hydroquinidine-2,5-diphenyl-4,6-pyrimidinediyl diether
DMAP	4-Dimethylaminopyridine
DMF	Dimethylformamide

dr	Diastereomeric ratio
E	Enzyme
ee	Enantiomeric ratio
Et_2O	Diethyl ether
EtOH	Ethanol
h	Hour
H_2O_2	Hydrogen peroxide
HCl	Hydrogen chloride
Hex	Hexane
HMPA	Hexamethylphosphoramide
HPLC	High-performance liquid chromatography
I_2	Iodine
iPr_2NEt	N,N-Diisopropylethylamine
K_2CO_3	Potassium carbonate
KOCl	Potassium hypochlorite
KOH	Potassium hydroxide
MeCN	Acetonitrile
Min	Minute
Mol	Molar
MS	Molecular sieves
NaH	Sodium Hydroxide
$NaHCO_3$	Sodium bicarbonate

NaOAc	Sodium acetate
NaOCl	Sodium hypochlorite
NaOH	Sodium hydroxide
NBS	*N*-Bromosuccinimide
nBuLi	*n*-Butyllithium
NMR	Nuclear Magnetic Resonance
NQR	Nuclear quadrupole resonance
Nu	Nucleophile
Pd	Palladium
PDC	Pyridinium dichromate
PhCl	Chlorobenzene
PPM	Parts per million
PTC	Phase transfer catalyst
PTSA	p-Toluenesulfonic acid
Py	Pyridine
ROESY	Rotating Frame Overhause Effect SpectroscopY
RT	Room temperature
Sat	Saturated
Sec	Second
SmI_2	Samarium iodide
TCCA	Trichloroisocyanuric acid
TFA	Trifluoroacetic acid

THF   Tetrahydrofurane

TMS   Trimethylsilyl

List of Schemes

Chapter 1: Cinchona Alkaloid Derivatives in Organocatalysis

1.1: Introduction

Cinchona alkaloids are isolated from the bark of different cinchona trees[1] (Figure 1.1)[2]. The Cinchona alkaloids history started in the beginning of the seventeenth century when their barks were used in European markets as an antimalarial herbal medicine. In 1820, the Cinchona active compound, quinine, was isolated by Pierre-Joseph Pelletier and Joseph Bienaime Caventou and since then Cinchona alkaloids, especially quinine, have been used and played an important role in human society as medicines.[3] Nowadays, around 700 metric tons of Cinchona alkaloids are extracted per year and almost half of that is used in the food and beverage industry as a bitter
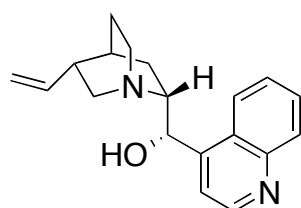
I-1
Cinchonine
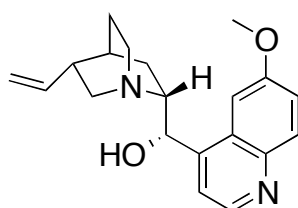
I-2
Quinidine
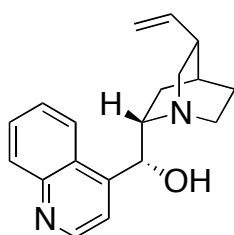
I-3
Cinchonidine
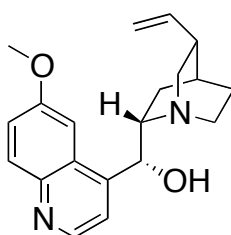
I-4
Quinine

Scheme I-1. Cinchona alkaloids extracted from the bark of the cinchona trees. (For interpretation of the references to color in this and all other figures, the reader is referred to the electronic version of this dissertation)
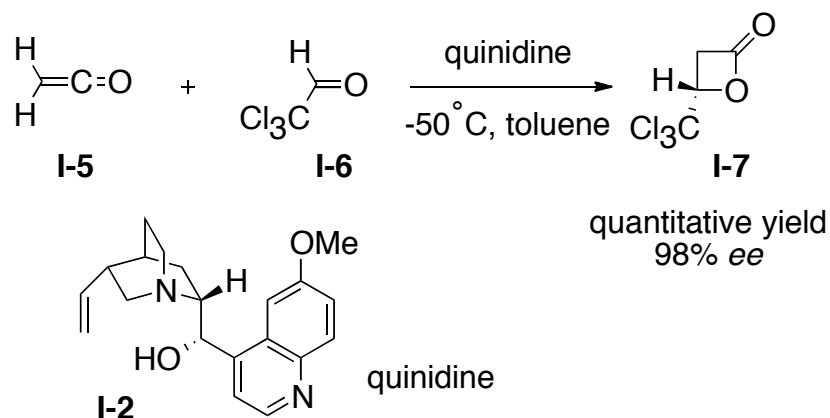
Scheme I-2. Cinchona alkaloids used in asymmetric β-lactones synthesis.

additive. The remaining quinine and quinidine is used as antimalaria drug, muscle relaxant compound, and as antiarrhythmic (cardiac depressant).

The cinchona alkaloids era in organic chemistry started in 1853 when Pasteur used them as resolving agents.[4,5] Since then many have used cinchona alkaloids as powerful resolving agents.[6] Beside the classical resolution process, in the past two decades tremendous development has also been achieved in the fields of cinchona-based enantioseparations and enantioselective analytical tools. However, the most important application of the cinchona alkaloids in chemistry in recent decades has been their use in enantioselective reactions as homogenous and heterogeneous catalysts. The first asymmetric reaction that used a cinchona base was reported by two German chemists, Bredig and Fisk in 1912. They discovered that quinine and quinidine, the pseudoenantiomeric alkaloids, can catalyze the addition of HCN to benzaldehyde in enantioselective fashion with almost 10% *ee*.[7,8] Almost 40 years later, Pracejus and coworkers applied the cinchona alkaloid derivative, *O*-acetylquinine, as a catalyst (1
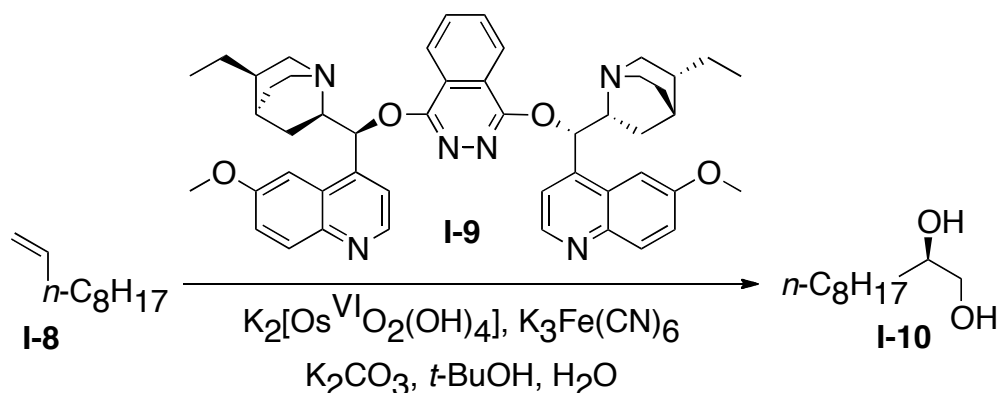
Scheme I-3. Sharpless asymmetric dihydroxylation

mol%) in an asymmetric reaction. They controlled the enantioselectivity of addition of methanol to phenylmethylketene in the presence of *O*-acetylquinine to synthesize (-)-α-phenyl methylpropionate in 74 % *ee*.[9,10] In the late 1970s and early 1980s, Wynberg and coworkers took the usage of the cinchona alkaloid to a new level.[11] Their extensive studies on the use of cinchona alkaloids as chiral Lewis base/nucleophilic catalysts demonstrated that cinchona alkaloid derivatives can be used in a wide range of enantioselective reactions. For example this class of alkaloids was used in addition of ketenes to carbonyl compounds to yield β-lactones (Scheme I-2).[12]

Since Wynberg's pioneering studies, the usage of cinchona alkaloids in asymmetric catalysis has become very popular, with a number of successful examples, reported in the late 1980s and early 1990s. For example the Sharpless asymmetric dihydroxylation of olefins (Scheme I-3) that utilizes the dimeric form of the alkaloids **I-9** as a chiral catalyst inducer has had a great impact on synthetic chemistry and for that he won the Nobel Prize in chemistry in 2001.[13-15] Since 2000 the use of chiral organocatalysts

has expanded dramatically. In this period of time cinchona alkaloids and derivatives have seen a resurgence in use as organocatalysts.[3]

1.2. Active Sites in Cinchona Alkaloids and Their Derivatives

The most common cinchona alkaloids are quinine, quinidine, cinchonidine and cinchonine and also two common dimer derivatives, $(DHQD)_2PHAL$ and $(DHQ)_2PHAL$ with a phthalazine linker. Their success in asymmetric catalysis is directly related to key features in their structures such as their diverse chiral skeleton and also their easily tunable sites. The presence of the 1,2-amino alcohol moiety containing the highly basic and bulky quinuclidine is mainly responsible for their catalytic activity.

The quinuclidine moiety makes them effective ligands for a variety of metal-catalyzed reactions such as the Sharpless asymmetric dihydroxylation where osmium binds to the quinuclidine (Scheme I-3). In addition to its utility for metal binding, the quinuclidine moiety can act as a chiral base or nucleophile in different organocatalytic
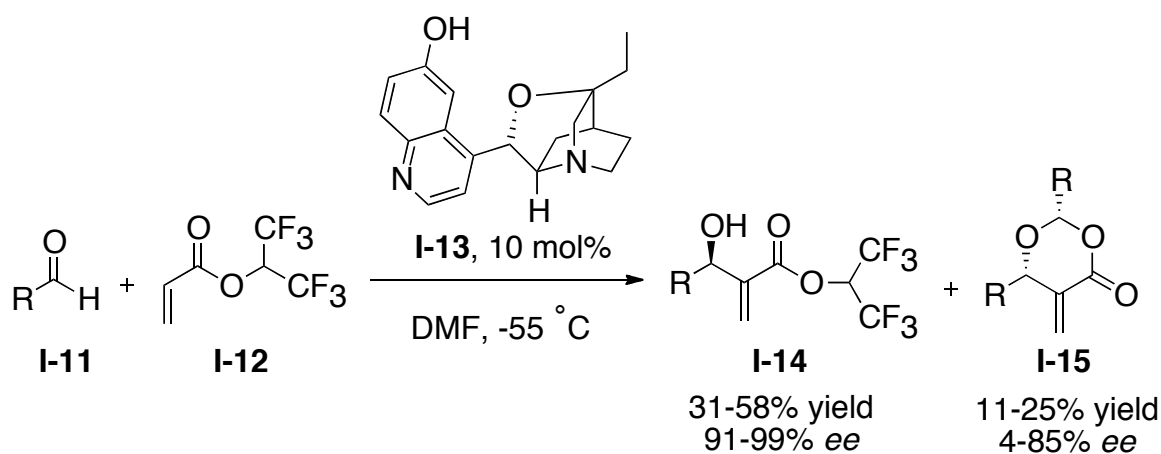
Scheme I-4. Asymmetric Morita-Baylis-Hillman reaction

4

reactions. For example Hatakeyama and coworkers used β–isocupreidine **I-13**, derived from quinidine, as a catalyst (10 mol%) in the catalytic asymmetric Morita-Baylis-Hillman reaction (Scheme I-4).[16] Enantioselectivity as high as 99% was achieved in the reaction of a variety of aldehydes **II-11** with the electrophilic hexafluoroisopropyl acrylate **II-12**.[16]

The corresponding quaternized ammonium salts of cinchona alkaloids have been used as chiral phase transfer catalysts, where asymmetric induction occurs through a chiral ion pairing mechanism between the cationic ammonium species and an anionic nucleophile. For example, Conn and coworkers conducted the Michael addition of 2-propyl-1-indanone **I-16** with methyl vinyl ketone **I-17** under biphasic conditions (aq 50% NaOH/toluene) using the cinchona/cinchonidine-derived phase-transfer catalyst **I-18** to get the desired product **I-19** in 80% *ee.[17]*

Besides the quinuclidine moiety, the secondary 9-hydroxy group can serve as an acid site or hydrogen bond donor.[18] By derivatization of the OH group into ureas,
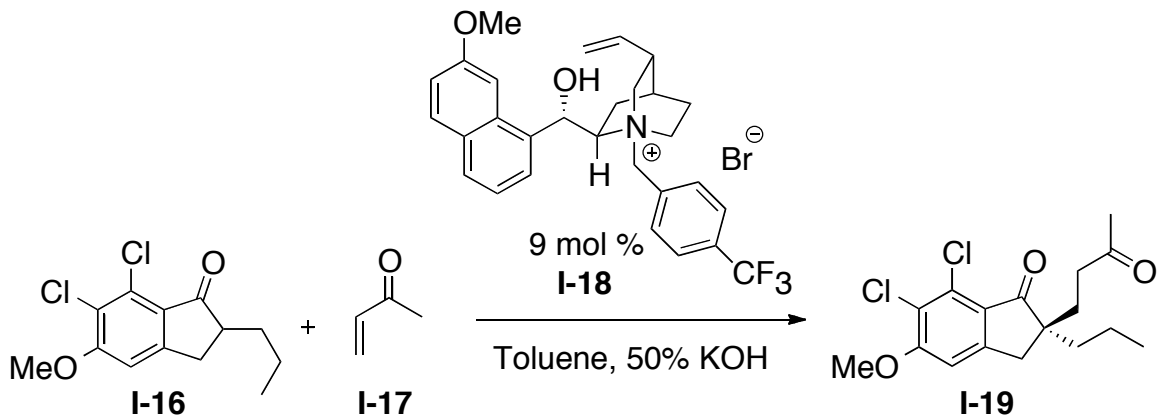
Scheme I-5. PTC-catalyzed enantioselective Michael addition reactions

amides and so on, with either retention or inversion of the hydroxyl carbon, can provide more acidic or hydrogen donor sites. Moreover, the substitution of 9-OH into a free amino group can make this class of alkaloids into effective chiral aminocatalysts. These catalysts can be used in enamine[19] and iminium catalysis.[20]

The other active site of this class of alkaloids is the 6'-methoxy group of the quinoline, which can be easily converted to a free hydroxyl group or a thiourea, moieties, which are also effective hydrogen-bond donors. Furthermore, in many cases,

A. Nitrogen of quinuclidine
1) Metal binding ability: chiral ligand or chiral modifiers
2) General base: deprotonation
3) Nucleophilic catalyst
4) N-alkylation: chiral phase transfer catalyst

B. R = OH or thioureas
1) H-bond donor or acid

B. R = OH or thioureas
1) H-bond donor or acid

C. X = OH
1) H-bond donor or acid
2) Metal coordination

D. X = NH$_2$ or further derivatization
1) Amino catalysis (enamine and iminium catalysis)
2) H-Bond donors (e.g. ureas, amides, thioureas...)

X = OH

R = H
R$'$ = CH=CH$_2$; Cinchonidine
R$'$ = CH$_2$CH$_3$; Dihydrocinchonidine
R = OMe
R$'$ = CH=CH$_2$; quinine
R$'$ = CH$_2$CH$_3$; Dihydroquinine

X = OH

R = H
R$'$ = CH=CH$_2$; Cinchonine
R$'$ = CH$_2$CH$_3$; Dihydrocinchonine
R = OMe
R$'$ = CH=CH$_2$; quinidine
R$'$ = CH$_2$CH$_3$; Dihydroquinidine

Scheme I-6. Active sites in cinchona alkaloids and their derivatives

6

I-9

I-23

I-20

I-24

I-21

I-25

I-26

I-22

I-27
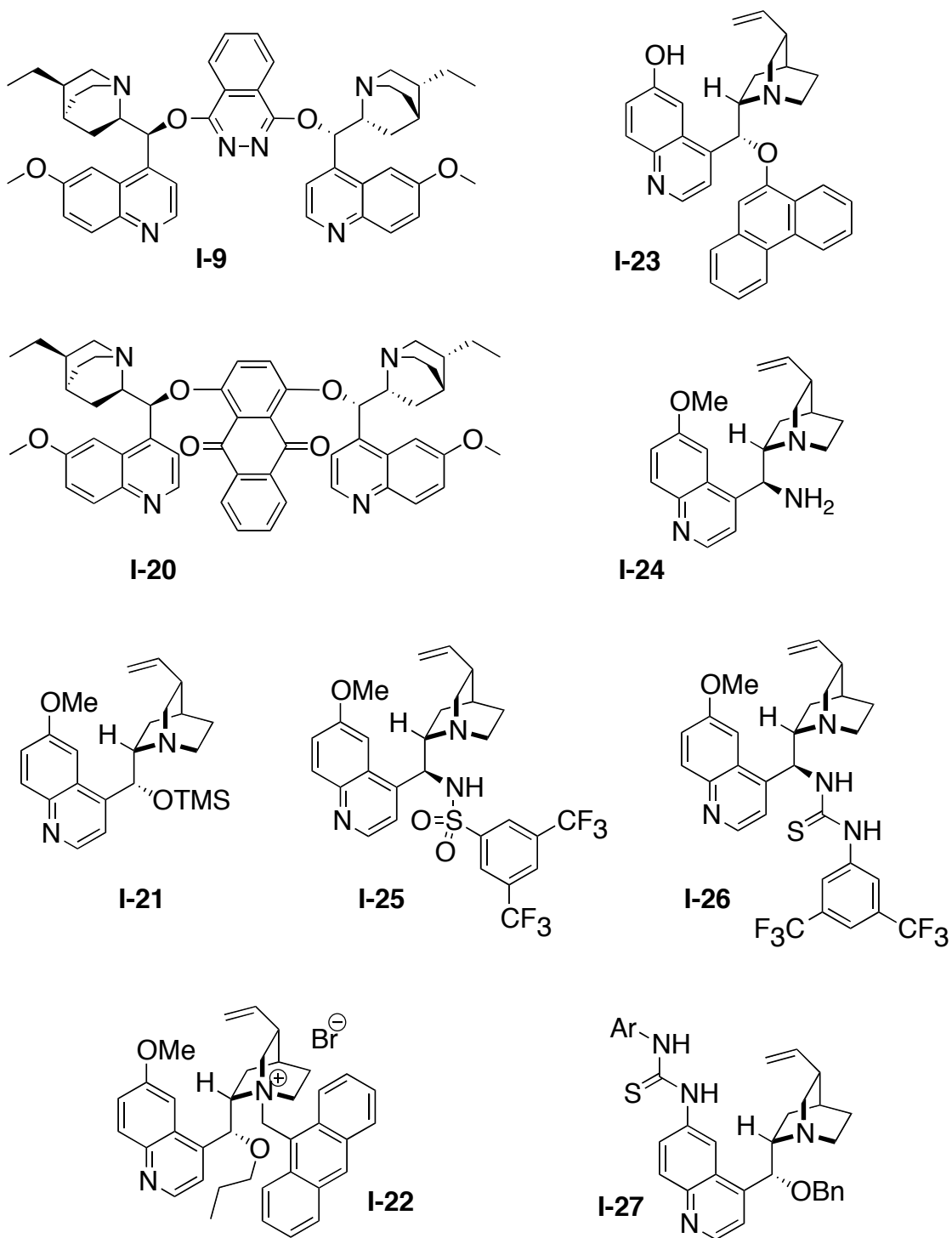
Scheme I-7. Representative examples of cinchona alkaloid derivatives in organocatalysis

the catalysis is also supported by a π–π interaction with quinoline and also the aromatic linker in the case of the dimer derivatives such as $(DHQD)_2PHAL$.

The active sites in cinchona alkaloids and their derivatives are summarized in Scheme **I-6**. In general these active sites in this class of alkaloids act in catalysis not independently but cooperatively. Scheme **I-7** illustrates some representative cinchona alkaloid derivatives.

This chapter illustrates the importance of cinchona alkaloids and their derivatives as organocatalysts by highlighting some examples of their application in oxidation, reduction, nucleophilic α–substitution of carbonyl derivatives, enantioselective protonation, cycloaddition, nucleophilic conjugate addition to electron deficient C=C double bonds, nucleophilic 1,2 addition to C=O and C=N bonds, desymmetrization and kinetic resolution.

R=H ; 80% yield, 55% *ee*
R=OMe ; 92% yield, 54% *ee*
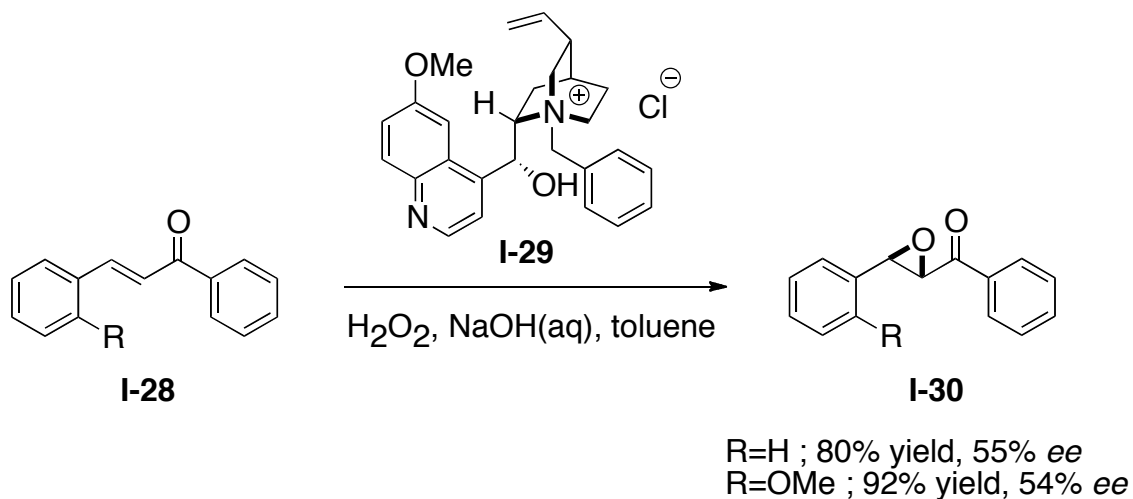
Scheme I-8. Epoxidation of *trans*-chalcone using cinchona-based chiral PTC

1.3: Cinchona-Based Organocatalyst for Asymmetric Oxidations and Reductions

1.3.1: Introduction

Facial selectivity of sp^2 carbons through asymmetric oxidation and reduction is a very common and important strategy to control the absolute configuration of sp^3 centers. The use of transition-metal based catalysts has been well established in oxidation and reduction of sp^2 carbons but practical issues such as high sensitivity to moisture and oxygen and toxic metal contamination in the product restrict their application, especially in large scale.

1.3.2: Epoxidation of Enones and $\alpha,\beta-$unsaturated Sulfones Using Cinchona-Based Chiral Phase-transfer Catalyst

Phase-transfer catalysts (PTC) have been used in the asymmetric epoxidation of electron-deficient olefins such as enones and $\alpha,\beta-$unsaturated sulfones. The use of
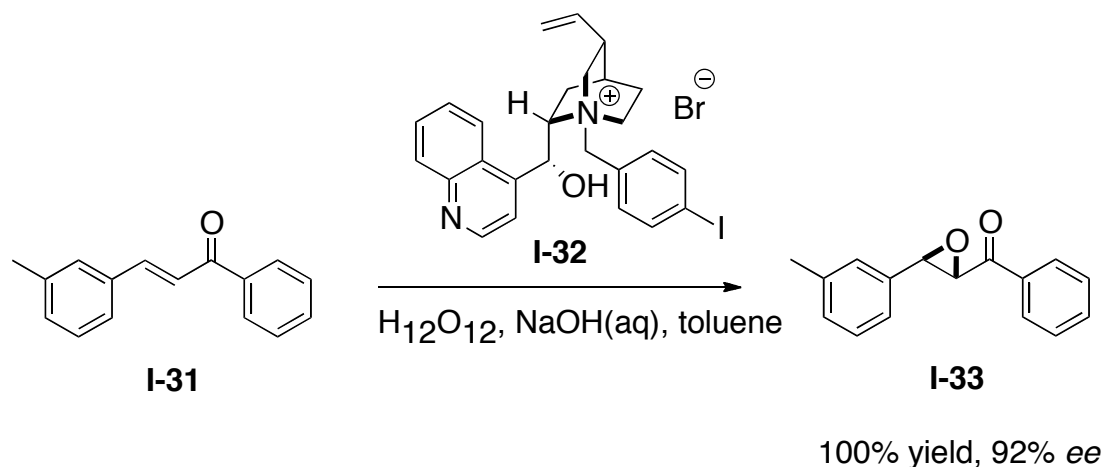
Scheme I-9. Arai modification on Wynberg's PTC epoxidation

cinchona-based chiral PTC was initiated by Wynberg in the 1970s. In Wynberg's pioneering studies only low to moderate *ee* (up to 55%) values were achieved in the epoxidation of *trans*-chalcones with basic hydrogen peroxide in the presence of the *N*-benzylquininium chloride as a PTC (Scheme I-8).[21,22]

Much higher enantioselectivity (up to 92% *ee*) was achieved simply by introducing the iodo group at the para position on the phenyl ring of the PTC **I-29** (Wynberg catalyst) by Arai and co workers (Scheme I-9).[23,24] These results indicate that the substituent on the benzyl moiety is important for achieving higher *ee* (authors didn't rationalize the observed higher ee).
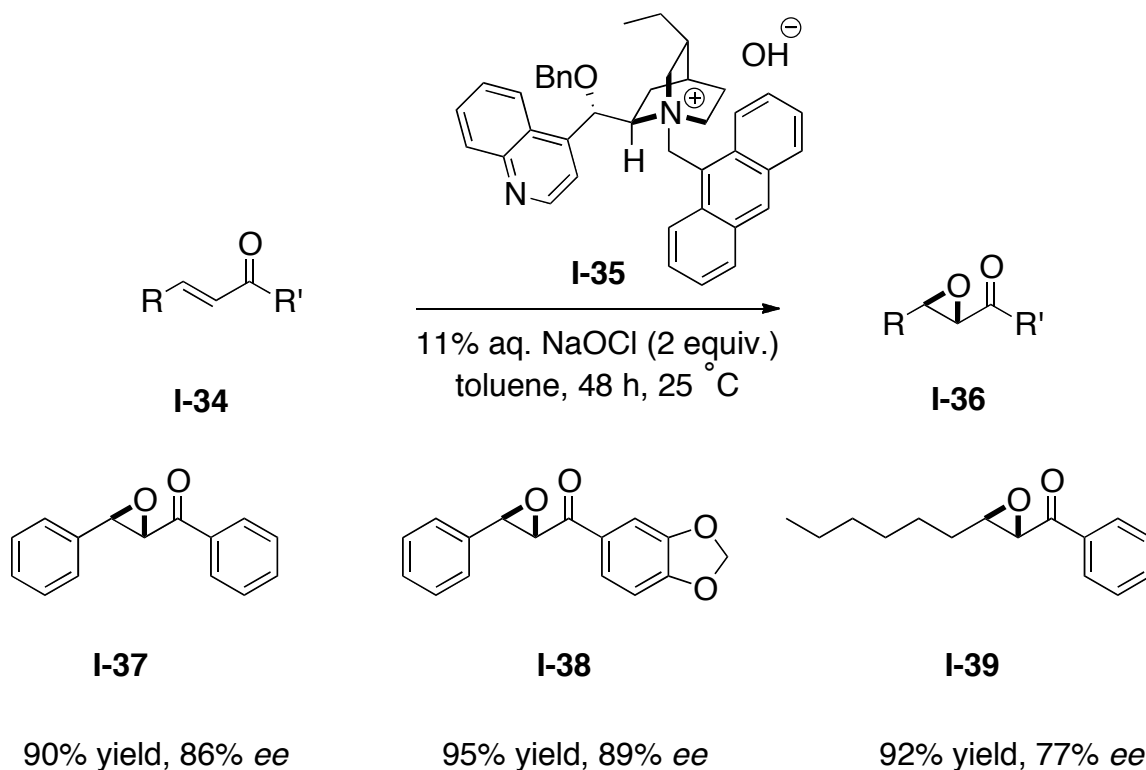
Scheme I-10. Lygo *O*-benzylated *N*-anthracenylmethyl dihydro cinchonodinium hydroxide PTC
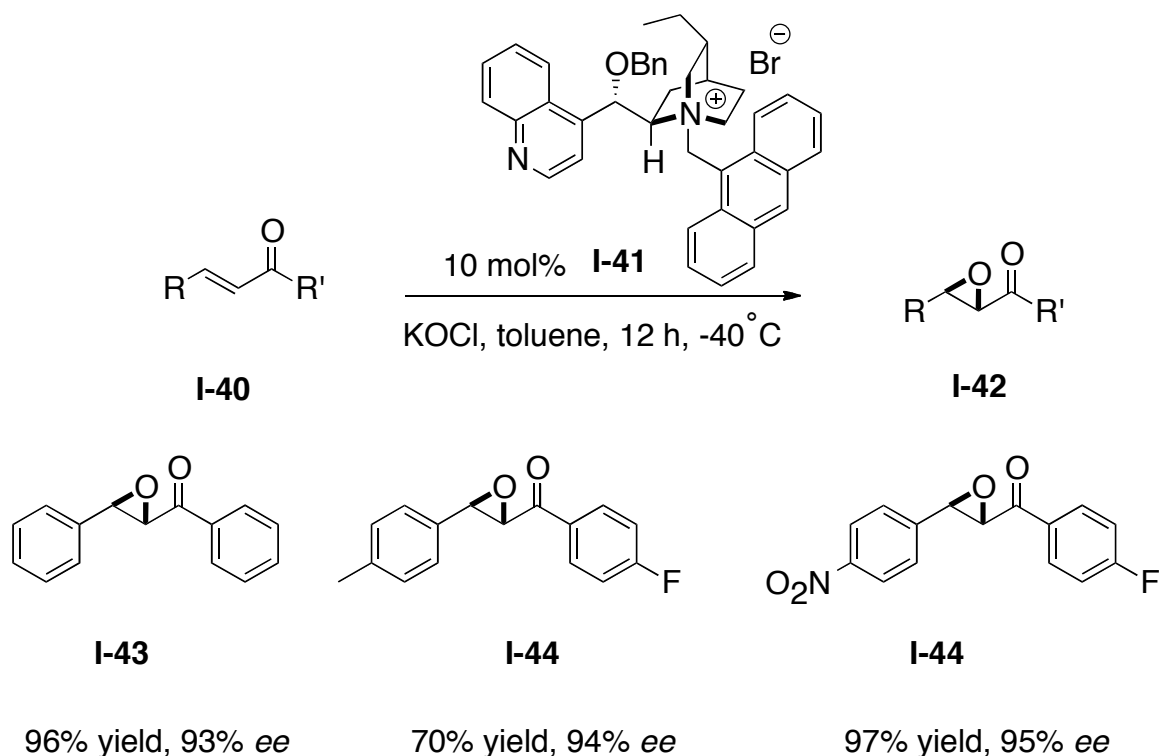
Scheme I-11. Corey *O*-benzylated *N*-anthracenylmethyl dihydro cinchonodinium bromide PTC

Later, Lygo and Corey achieved high enantioselectivity by using a new class of PTC, *O*-benzylated *N*-anthracenylmethyl dihydro cinchonodinium hydroxide and bromide respectively.[25,26] Lygo and coworkers obtained high enantioselectivity (76%-89%) by using 10 mol% of PTC **I-35** (hydroxide as a counter ion) in the presence of aqueous sodium hypochlorite as an oxidant (Scheme I-10).[25,26] A further improvement was achieved by Corey and coworkers by replacing the hydroxide with bromide. These authors found high enantioselectivity in reactions of various α,β-enones with aqueous KOCl and 10 mol% of the catalyst **I-41**, in toluene at -40˚C (Scheme I-11).[27]
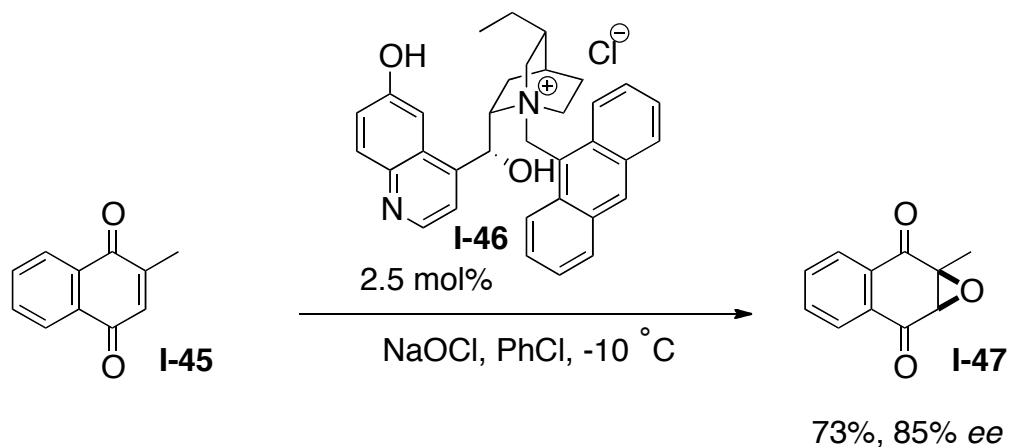
Scheme I-12. Asymmetric epoxidation of α,β-enones

The asymmetric epoxidation of the α,β–cyclic enones using cinchona-based chiral PTCs gave generally poor or moderate enantioselectivities. In 2007 Berkessel and coworkers achieved the highest enantioselectivity for the oxidation of cyclic enones with PTC. They could reach 85% *ee* with 73% yield for the epoxidation of the 2-methylnaphthoquinone (precursor of vitamin K_3) with an aqueous solution of NaOCl at -10 $^{\circ}$C , using PTC **I-46.**[28]

It is believed that the salt of the oxidant in aqueous solution or solid phase is transferred to the organic phase as a counter ion of the chiral PTC. Once in the organic
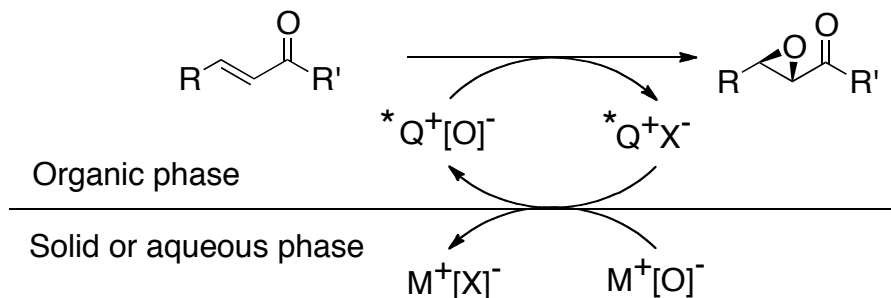
Scheme I-13. General mechanism of epoxidation of enones with PTCs

12
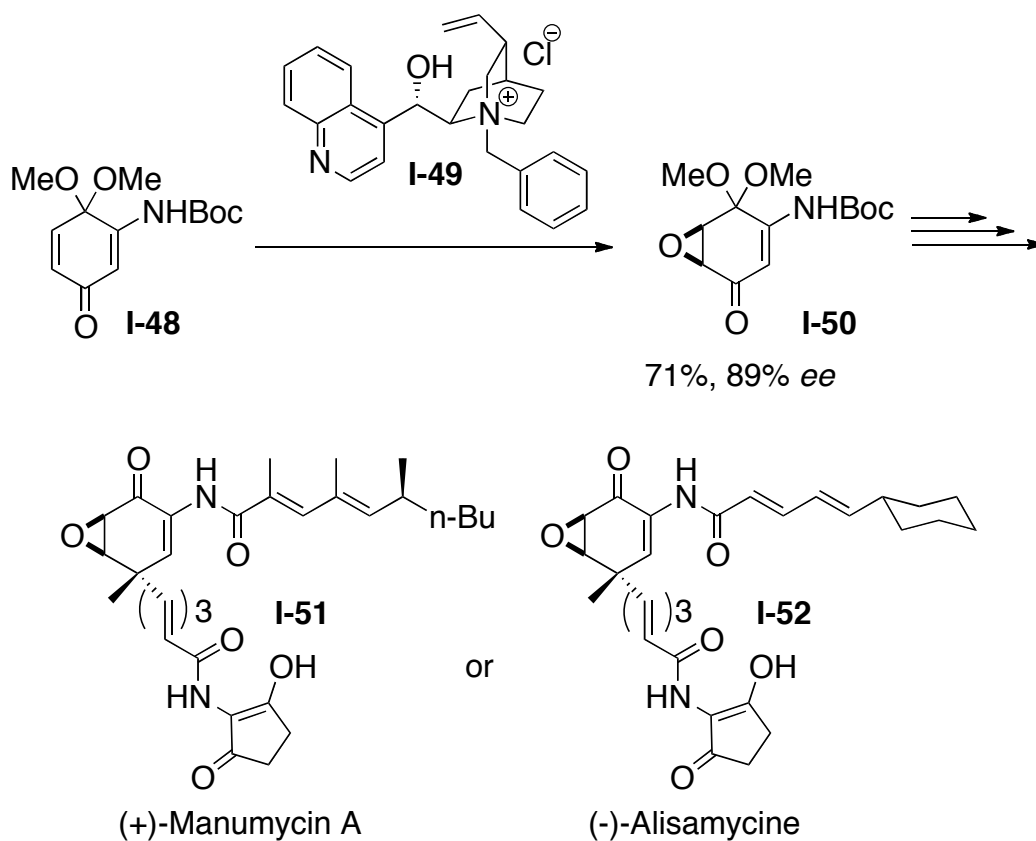
Scheme I-14. Synthetic application of the asymmetric epoxidation of enones using chiral PTCs

phase, it can oxidize enones in asymmetric fashion due to the presence of the oxidant in chiral environment (Scheme I-13).

Application of Wynberg's epoxidation in total synthesis of the (+)-manumycin A, (-)-alisamycin and (+)-MT 35214 highlights the importance of this class of transformation. For these total syntheses Taylor and coworkers used Wynberg's PTC **I-49** to synthesize epoxide **I-50** in 89%*ee* and 71% yield, which was converted in multiple steps to (+)-manumycin A **I-51**, (-)-alisamycin **I-52** and (+)-MT 35214 **I-53**.[29,30]

1.3.3: Epoxidation of $\alpha,\beta-$Unsaturated Sulfones Using Cinchona-Based Chiral Phase-transfer Catalysts

Asymmetric epoxidation of $\alpha,\beta-$unsaturated sulfones **I-54** has been achieved in 2006 by Dorow and coworkers. In this asymmetric epoxidation, *N*-anthracenylmethyl cinchona alkaloid derivative **I-55**, was used in the presence KOCl as an oxidant at low temperature. Dorrow and coworkers found that the size and the electronic characteristic of the ether substituent at C9 (O) has a great effect on both the reaction conversion and the enantioselectivity.[31]

1.3.4: Epoxidation of Enones via Iminium Catalysis by Using Cinchona-Based Chiral Primary Amine

As mentioned before, poor to moderate enantioselectivity was observed in the epoxidation of $\alpha,\beta-$enones using chinchona based chiral PTCs. A breakthrough in epoxidation of cyclic enones was made by the List group in 2008, using the bis TFA
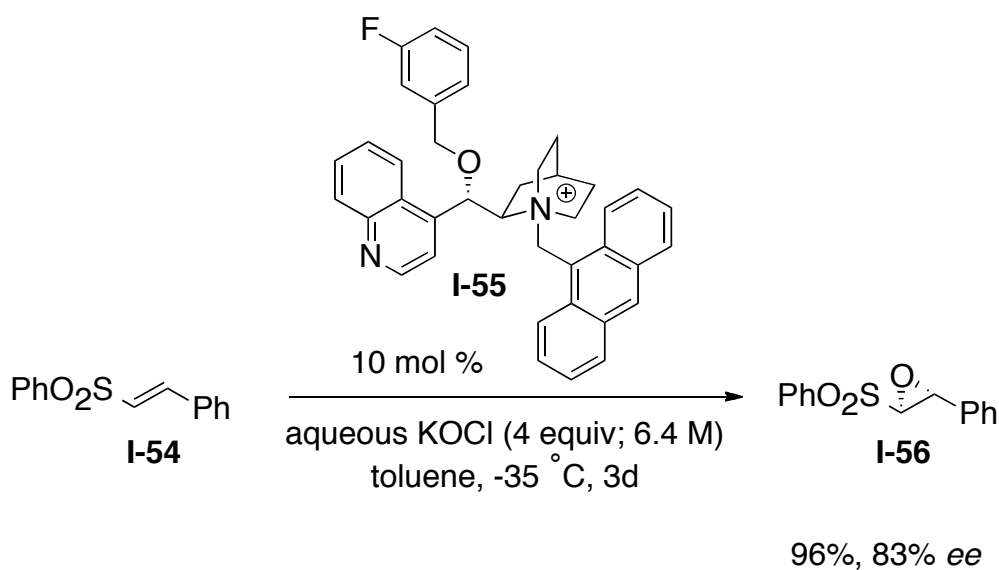
Scheme I-15. Asymmetric epoxidation of $\alpha,\beta-$unsaturated Sulfones

(trifluoroacetic acid) salt of 9-amino-9-(deoxy)-epi-quinine. List and coworkers reached up to 99% *ee* in epoxidation of β-substituted cyclopentenone, cyclohexenone, and cycloheptenone (Scheme I-16).[32] Based on the unreactivity of the α-substituted enones under the same reaction condition and the lower activity of the quinine, quinidine and also the nonprotonated version of catalyst **I-58**, the authors suggest that the reaction goes through an iminium pretransition state (Scheme I-16). Soon afterward Deng and coworkers applied the same methodology for the epoxidation of acyclic enones (96-97% *ee*).[33]
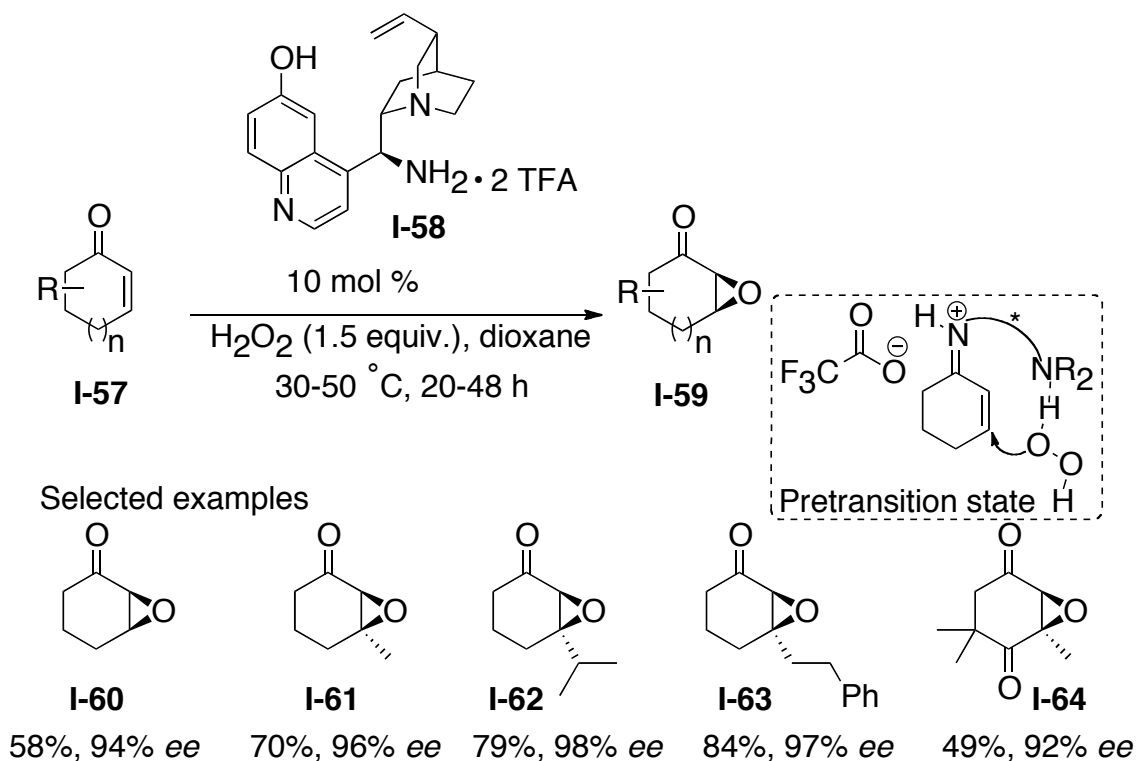
Scheme I-16. Asymmetric epoxidation of enones via iminium catalysis
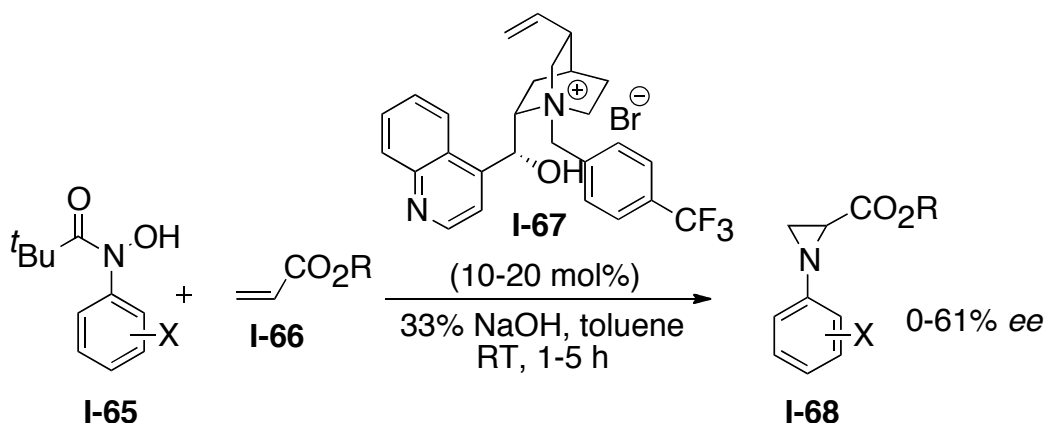
Scheme I-17. Asymmetric aziridation of enones using PTCs

1.3.5: Aziridination of Enones Using Cinchona-Based Chiral Phase-Transfer Catalyst.

Aziridines are useful precursors for the synthesis of biologically active species such as amino acids, β-lactams and alkaloids.[34,35] Most of the highly enantioselective aziridinations have been achieved by transition-metal based chiral catalysts. As mentioned before, a nontoxic organocatalyst would be desirable for industrial large scale production from an environmental point of view. Prabhakar and coworkers (Scheme I-17) have used PTCs for the first time for the aziridination of acrylates. PTC **I-67** in the presence of hydroxamic acid **I-65** was used to obtain low to moderate *ee* values (0-61% *ee*).[36,37] In 2005, Siva and coworkers achieved to up to 95% *ee* with PTCs **I-71** and **I-72** (Scheme I-18) in the reaction of electron-deficient olefins with *N*-acyl-*N*-arylhydroxylamines as nitrogen transfer reagent under biphasic condition (toluene/aqueous NaOH).[38]
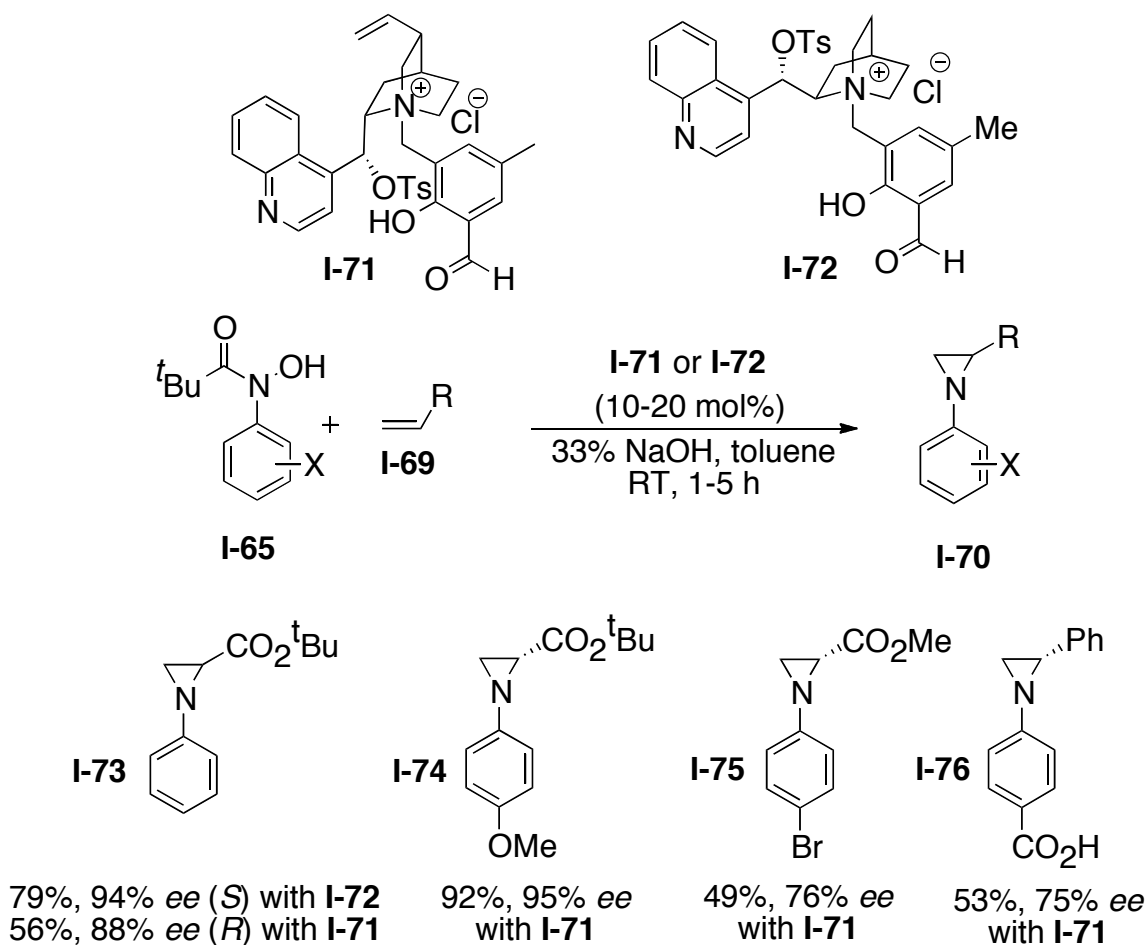
Scheme I-18. Asymmetric aziridination of enones using PTCs **I-71** & **I-72**

1.3.6: Cinchona-Based Organocatalysts in Asymmetric Reductions

Despite the importance of asymmetric reductions, use of cinchona alkaloids in asymmetric reductions has been limited to the reduction of aromatic ketones. Colonna and coworkers in 1978 introduced the first example of asymmetric reduction of alkyl aryl ketones in the presence of the cinchona-based PTCs. Alkyl aryl ketones can be reduced with inexpensive sodium borohydride under aqueous-organic biphasic condition. Colonna and coworkers could only obtain 5-32% *ee* in the presence of the 5 mol%

benzylquininium chloride.[39,40] Later on, Lawrence reached to up to 71% *ee* in the presence of the PTC **I-78** with tris(trimethylsiloxy)silane as the hydride donor (Scheme I-19). The authors believed that the hydride source is activated by attack of the nucleophile, presumably fluoride. The enantioselectivity can be controlled by the presence of the resulting activated hydride source in a chiral environment as a counter ion to stay close to benzylquinium.[41]

1.4 Cinchona-Based Catalysis in Nucleophilic α-Substitution of Carbonyl Derivatives

1.4.1 Introduction

Nucleophilic α-substitution of carbonyls can be achieved through two different approaches. One involves the *in situ* formation of a chiral enamine through a covalent
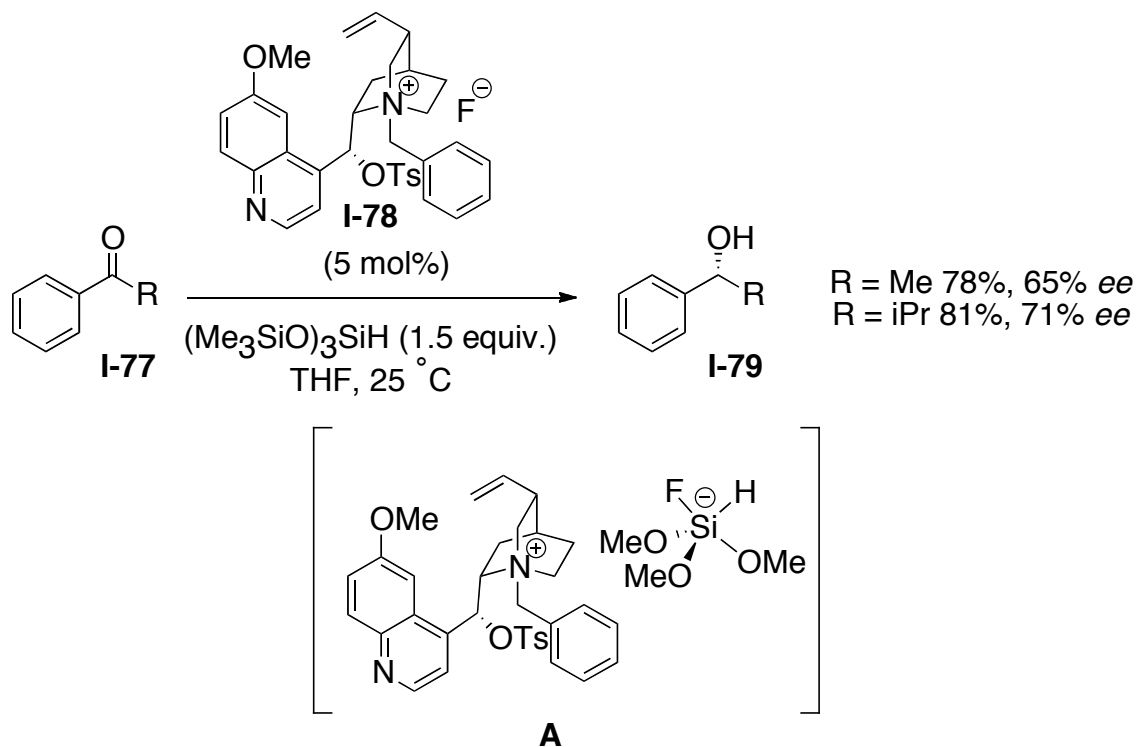
Scheme I-19. Reduction of aromatic ketones with cinchona-based PTCs

18

bond between a chiral secondary amine such as proline and the substrate, such as an aldehyde, followed by asymmetric bond formation between the α carbon and electrophile.[19,42] The other relies on noncovalent interactions, such as hydrogen bonding[18,43] or ion-pair formation,[44,45] between the substrate and organocatalyst. Cinchona alkaloids usually take part as catalysts in this transformation through the second approach, mostly as PTCs. A mechanistic illustration for the nucleophilic α-substitution of carbonyls under phase-transfer condition is depicted in Scheme I-19 This process generally proceeds via the following three steps: In the first step the α proton to the carbonyl is removed by the base, typically a metal hydroxide, at the interface between the organic and aqueous (or solid) phases to yield the corresponding metal enolate (**B**). This metal enolate **B** stays near the interface until cation exchange occurs between the metal cation and the lipophilic phase-transfer catalyst. The resulting chiral ion-pair **C** is able to move into the organic phase to react with the electrophile, in the third step. The chirality in this process is controlled by the presence of the chiral
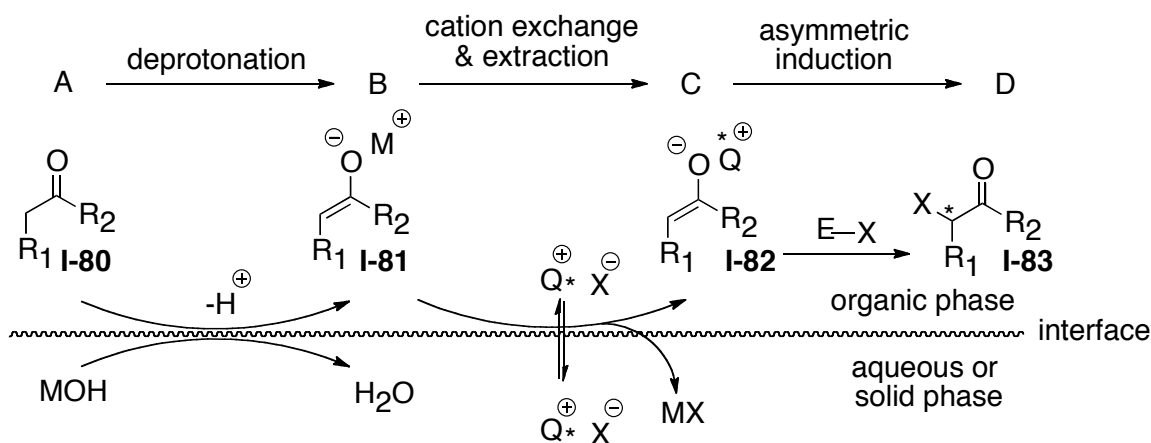
Scheme I-20. Mechanistic scheme for the α-monosubstitution of carbonyl compounds under phase-transfer conditions
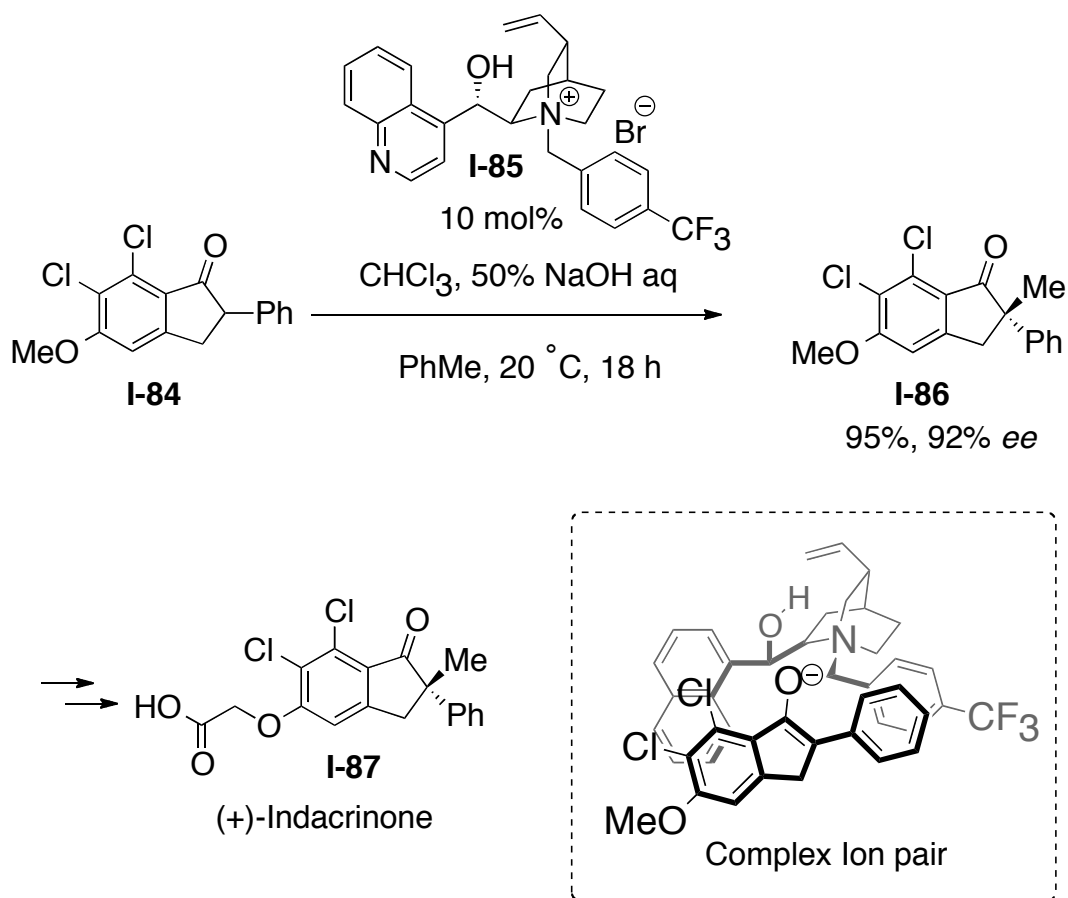
Scheme I-21. First asymmetric α-methylation of carbonyl compounds under phase-transfer conditions

lipophilic-onium (Q*) as ion pair close to the enolate.[46-48] As mentioned above cinchona alkaloids can be easily derivatized to a variety of PTCs by alkylation of the quinuclidine moiety. Due to this ability they have been used in numerous examples in highly enantioselective nucleophilic α-substitutions of carbonyl compounds. This section tries to illustrate some examples of cinchona-based PTCs in asymmetric nucleophilic α-substitution of carbonyl (Scheme I-20).

1.4.2 Nucleophilic α-Substitution of Carbonyl Derivatives via Cinchona Based Phase-transfer Catalysts

1.4.2.1 Pioneering advancements in Use of Phase Transfer Catalysts in Nucleophilic α-Substitution of Carbonyl Derivatives

In 1984, Dolling and coworkers reported the first successful use of cinchona PTC in asymmetric α-substitution of carbonyls. PTC **I-85** was used in methylation of 6,7-dichloro-5-methoxy-2-phenyl-1-indanone to obtain the methylated product in 95% yield and 92% ee. Later on, the methylated product was transformed to (+)-indacrinone in three steps (Scheme I-21).[49] They proposed that as the enolate anion of **I-84** has an almost planar structure, both substrate and catalyst can interact and fit on top of each other. Hydrogen-bonding and π-π stacking can further stabilize this interaction. Because the PTC **I-85** blocks the rear side of the enolate, the alkylation preferentially occurs from the front side of the enolate.
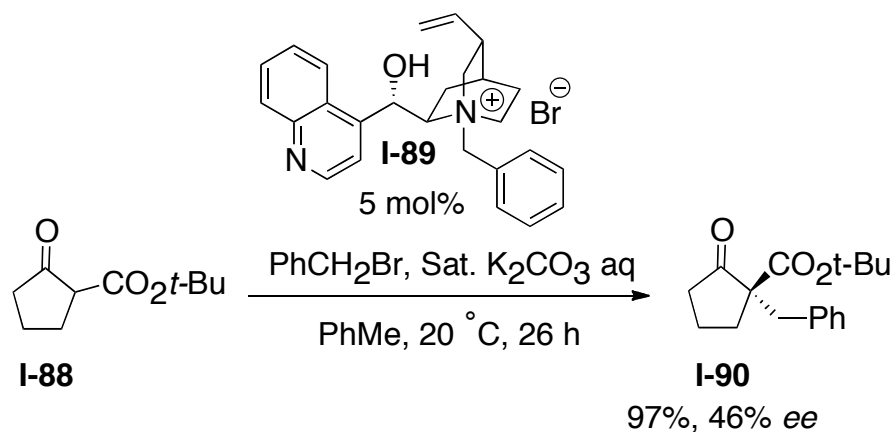
Scheme I-22. Asymmetric α-benzylation of cyclic β-ketoester
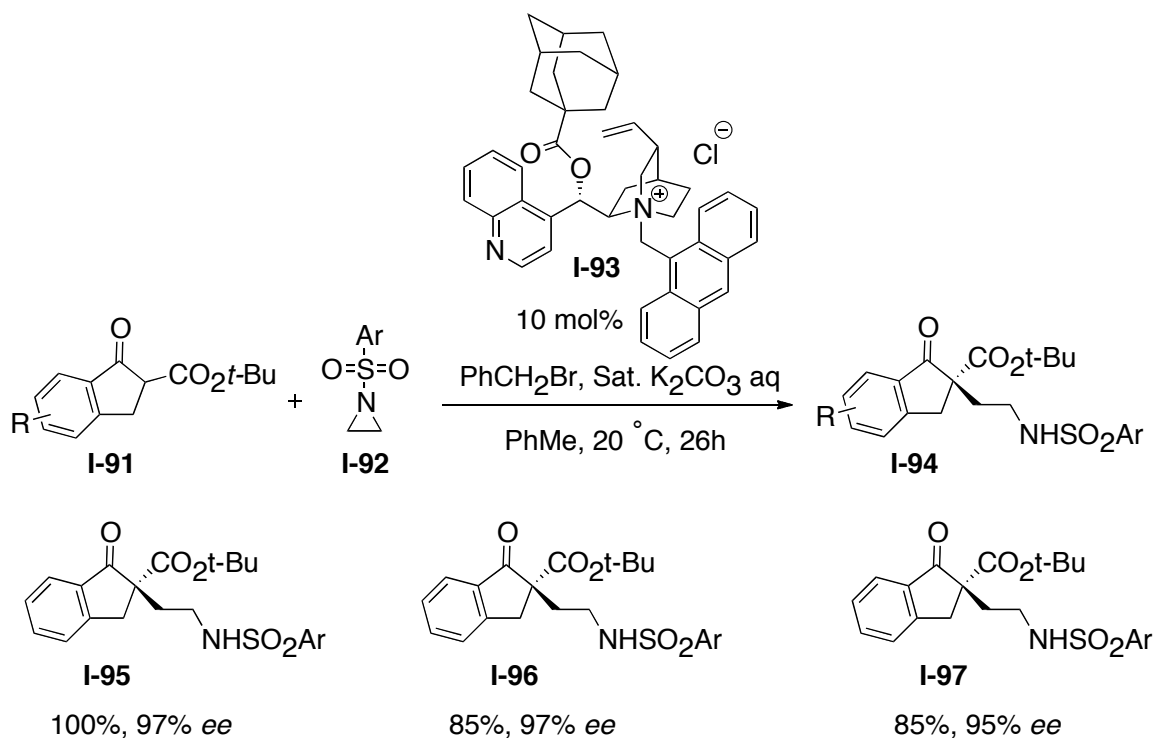
Scheme I-23. Asymmetric α-alkylation of cyclic β-ketoester with aziridines

1.4.2.2 α-Substitution of β-Keto Carbonyl Compounds

Asymmetric alkylation of β-Keto carbonyl derivatives under phase-transfer conditions is an efficient and useful approach to synthesize a chiral quaternary carbon center. Dehmlow and coworkers were able to benzylate cyclic β-ketoester, 2-(tert-butoxycarbonyl)cyclopentanone **I-88** in the presence of the cinchoninium PTC **I-89** in high yield and with 46% *ee* (Scheme I-22). [50]

Very recently, Dixon and coworkers achieved high chemical and optical yield for the α-alkylation of β-keto carbonyl derivatives with aziridines in the presence of the cinchona based PTC **I-93** (Scheme I-23).**[51]**
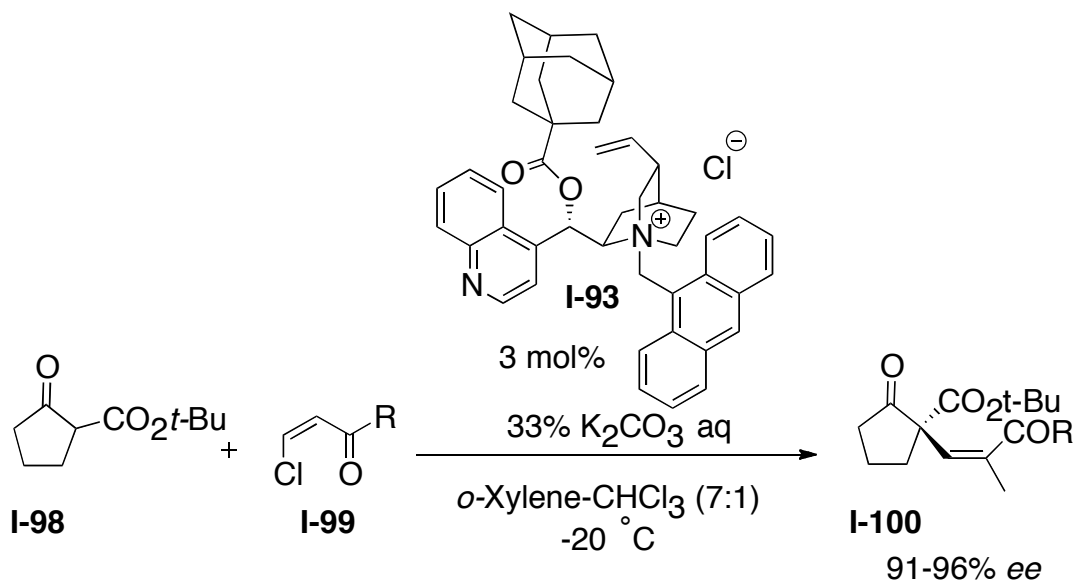
Scheme I-24. A catalytic enantioselective vinylic substitution of β-ketoester

Jorgensen and coworkers reported the first example of catalytic asymmetric vinylic substitution in 2006. They used hydrocinchoninium PTC **I-93** incorporating a highly bulky substituent on the C-9, 1-adamantoyl moiety, to catalyze this highly enantioselective reaction (Scheme I-24). By applying PTC **I-93** they could introduce α,β-
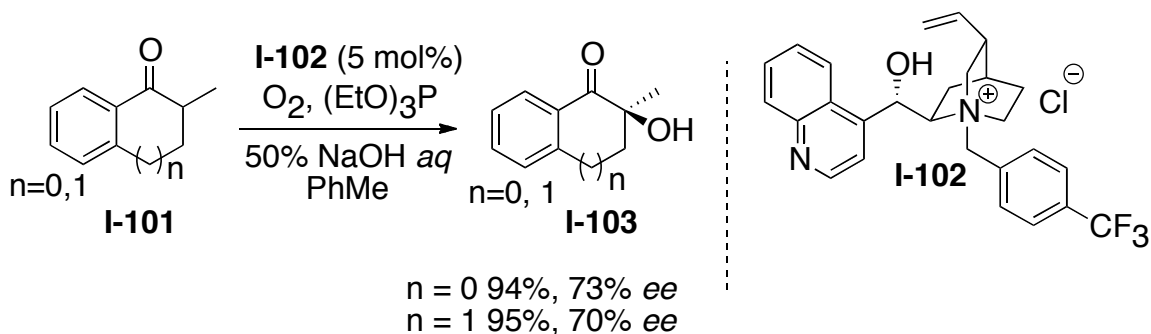
Scheme I-25. Asymmetric α-hydroxylation ketones with PTCs

unsaturated carbonyl groups to the α-position of the cyclic β–ketoester **I-98** in high enantioselectivity (91%-96%).[52] In 2007, the same group could also achieved the highly enantioselective (90-96% *ee*) α-alkynylation of cyclic β-ketoester in the presence of the PTC **I-93**.[53]

1.4.2.3 α-Hydroxylation of Carbonyl Derivatives

α-Hydroxylation of carbonyl derivatives was explored earlier than other heteroatoms in the literature. The first synthesis of optically active α-hydroxy ketones was reported in 1988 by Shioiri and coworkers. In this asymmetric catalysis molecular oxygen was used as an electrophile, along with triethylphosphite in the presence of the PTC **I-102** to synthesize α-hydroxyindanone and α-hydroxytetralone from the corresponding cyclic

Ar = Ph 81%, 83% *ee*
Ar = Tol 80%, 87% *ee*
Ar = 2-Naph 87%, 76% *ee*

R = Me (n=1) 93%, 54% *ee*
R = Me (n=2) 94%, 42% *ee*
R = Bn (n=1) 99%, 89% *ee*
R = Bn (n=1) 95%, 71% *ee*
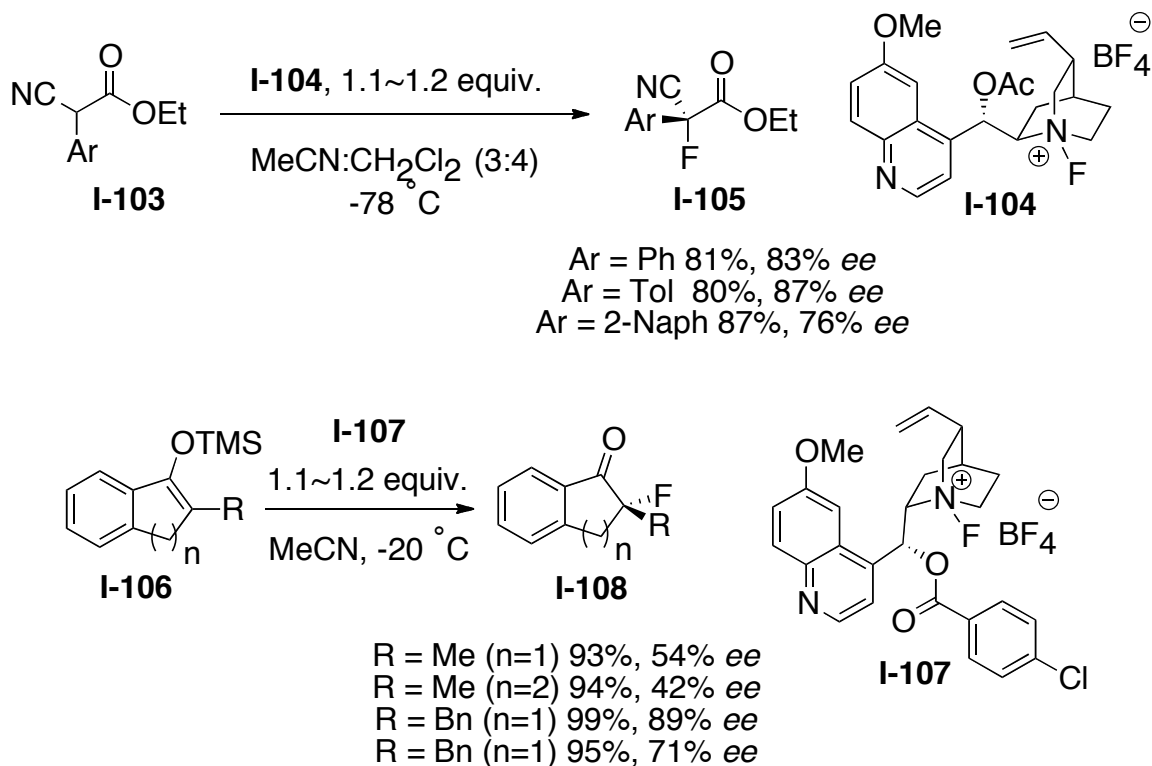
Scheme I-26. Asymmetric α-fluorination of carbonyl derivatives

24

ketone (Scheme I-25).[54]

1.4.2.4 α-Fluorination of Carbonyl Derivatives

Chiral organofluorine compounds are a useful class of compounds in analytical, biological, medicinal and polymer chemistry. Moreover, they have b*ee*n used frequently in enzyme mechanistic studies. Thus, the development of efficient asymmetric α– fluorination has been explored greatly. For example, Shibata and coworkers reported in 2000 the direct fluorination of α-cyano ester **I-103** and trimethylsilylenol ethers **I-106** using *in-situ N*-fluoro-*O*(9)-acyl hydroquininium and quinidinium salts, **I-104**, **I-107** respectively. By using these two chiral fluorine salts, they could achieve from 42 to 89% *ee* (Scheme I-26).[55,56]
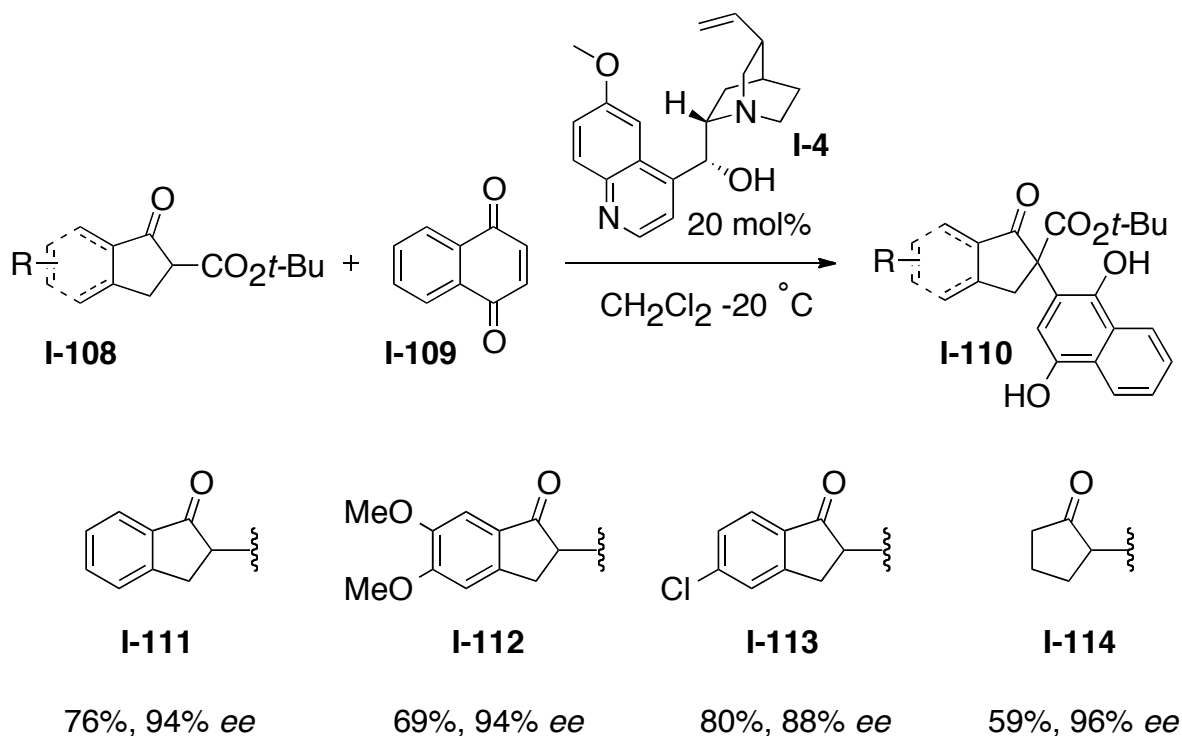
Scheme I-27. Asymmetric α-arylation of carbonyl derivatives

1.4.3 Nucleophilic α-Substitution of Carbonyl Derivatives via Non-PTC

Asymmetric nucleophilic α-substitution of carbonyl derivatives by using cinchona based organocatalysts in non-biphasic homogeneous conditions have been extensively explored in recent years. In this section some examples of this class of catalysis will be reviewed.

1.4.3.1 α-Arylation of Carbonyl Derivatives

(−)-Quinine was used as an organocatalyst in the asymmetric α-arylation of β-ketoester **I-108** by Jorgenson and coworkers.[57] They obtained the corresponding α-arylated product **I-110** in high enantioselectivity under homogeneous condition (Scheme I-27). In this reaction quinine acts as a chiral base in deprotonation of the β-ketoester to form the enolate. The corresponding enolate as counter ion of the protonated quinine attacks 1,4-naphthoquinone in an enantioselective fashion to form the desired product.

R = Me	R = Et	R = Bn
95%, 68% *ee*	83%, 72% *ee*	98%, 73% *ee*
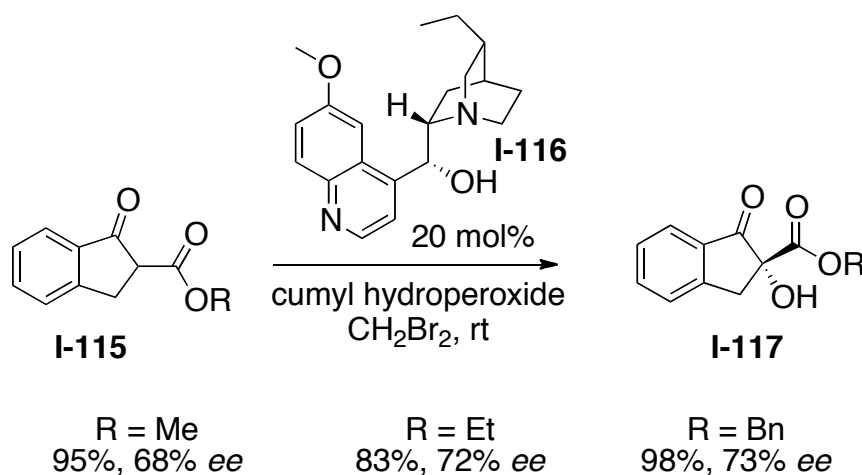
Scheme I-28. Asymmetric α-hydroxylation of β-keto esters
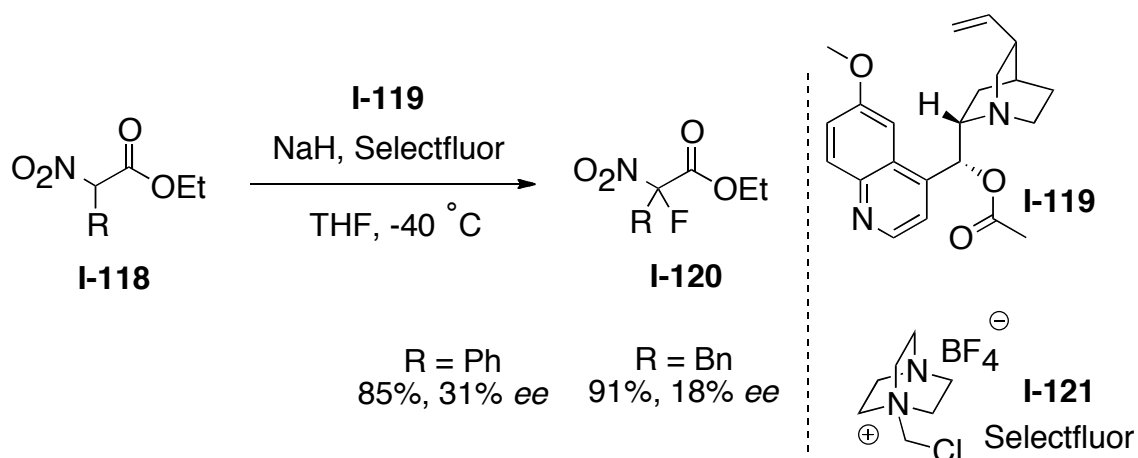
Scheme I-29. Asymmetric α-fluorination of α-nitro esters

1.4.3.2 α-Hydroxylation of Carbonyl Derivatives

Jorgensen and coworkers were also able to disclose α-hydroxylation of 1,3-dicarbonyl compounds under nonbiphasic condition. In this methodology, they used hydroquinine as the organocatalyst and cumyl hydroperoxide as the oxidant. They obtained the corresponding α-hydroxylated β-keto esters with enantioselectivity up to 80% *ee* (Scheme 1-28). During the optimization of this reaction they realized that the *O*(9)-OH group of the hydroquinine is important in controlling the enantioselectivity of this reaction.[58]

1.4.3.3 α-Halogenation of Carbonyl Derivatives

Togni and coworkers used a cinchona alkaloid catalyst **I-119** to perform stereoselective α-fluorination of α-nitro esters with Selectfluor **I-121** (Scheme I-29). Under basic conditions they were able to obtain the desired fluorinated products in high yield but low enantioselectivities (up to 31%).[59]
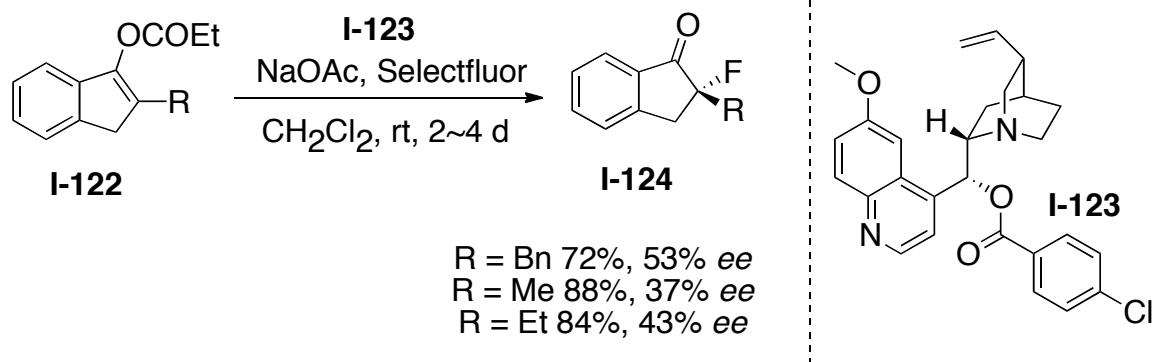
Scheme I-30. Asymmetric α-fluorination of acyl enol esters

Shibata and coworkers were able to extend this methodology to fluorination of the acyl enol esters in the presence of the cinchona alkaloid catalyst **I-123** to obtain α-fluoroketone with up to 53% *ee* (Scheme I-30).[60]

Cahard and coworkers reached higher enantioselectvity in fluorination of silyl enol ethers **I-125** with polystyrene-bound cinchona alkaloids (PS-CA, **I-126**). Selectfluor along with this soluble-phase PS-CA gave both good chemical and optical yields (Scheme I-31). They were also able to recover their catalyst and reuse it a couple of
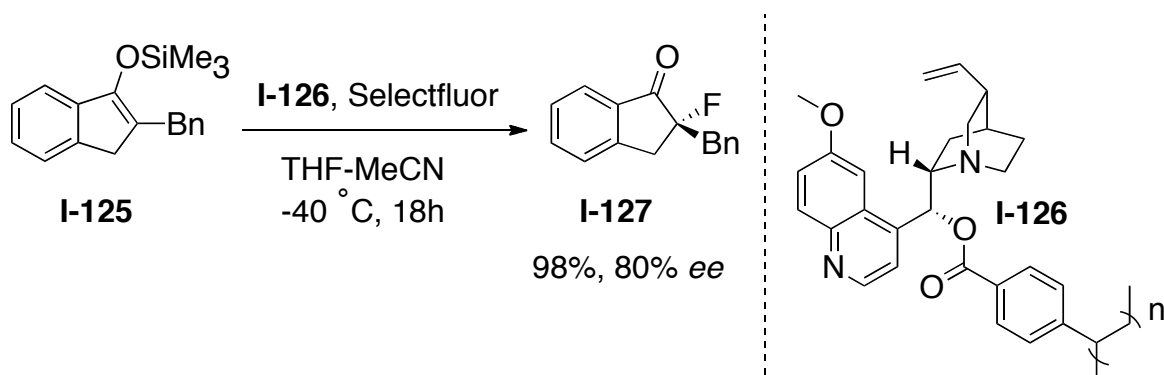
Scheme I-31. Asymmetric α-fluorination of silyl enol esters
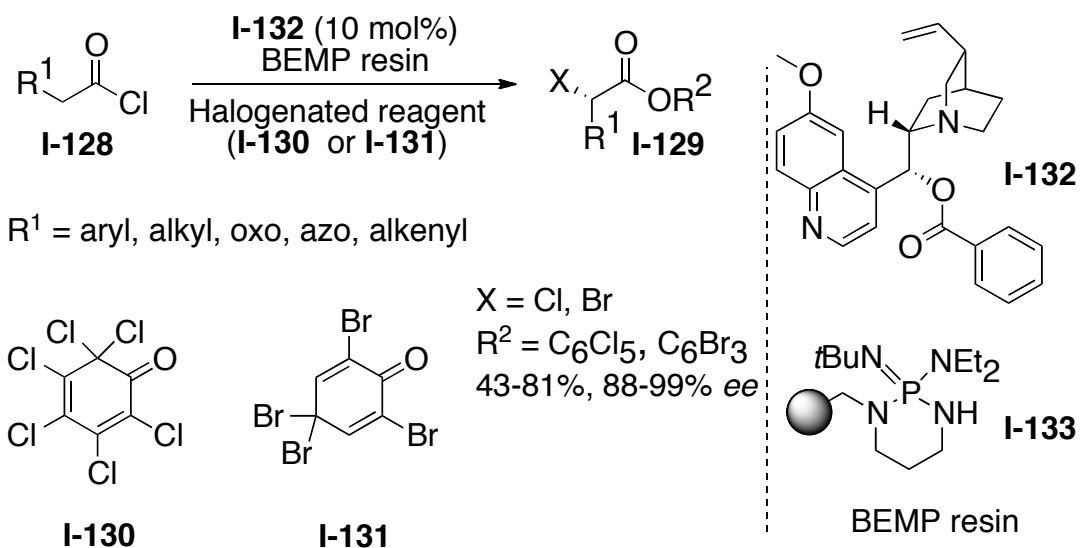
Scheme I-32. Asymmetric α-bromination and α-chlorination

times without any loss of enantioselectivity.[61]

In 2001, Lectka and coworkers developed α-chlorination and α-bromination with cinchona-based organocatalysts. They generated a ketene intermediate from the acid chloride with either BEMP resin or proton sponge. By addition of *O*-benzoylquinine to the ketene, a zwitterionic enolate was formed, which was halogenated with perhydroquinones **I-130** and **I-131**. Finally a haloaromatic phenolate replaced the *O*-benzoylquinine moiety to form the desired chiral α-halocarbonyl products with up to 99% *ee* (Scheme I-32).[62]

Later on in 2006, Lectka and coworkers upgraded the enantioselective α-bromination with (*R*)- proline incorporated cinchona catalyst **I-136** and with their new bromination agent **I-135** (Scheme I-33). During the optimization they found out that by

replacing the (*R*)- proline with its enantiomer the enantioselectivity dropped from 95% *ee* to 88% *ee*.[63]

1.4.3.4 α-Amination of Carbonyl Derivatives

Catalytic asymmetric construction of nitrogen substituted quaternary centers is an important and challenging task in asymmetric synthesis. In 2004, Pihko and coworkers reported the first α-amination using cinchona alkaloids. They obtained the desired α-aminated cyclic and acyclic β-ketoesters **I-140** in high yield and low to moderate enantioselectivity (27 to 88% *ee*) in the presence of cinchonine or cinchonidine (I-**1, I-3**) as the chiral catalyst base and dibenzyl azo dicarboxylate **I-139** as the nitrogen source.[64] Enantioselectivity in this reaction was again controlled by the presence of the protonated chiral catalyst as a counterion to the corresponding enolate.

Later on, Jorgensen and coworkers accomplished highly enantioselective α-amination of α-aryl-α-cyanoacetates. They obtained up to 98% *ee* by using di-tert-butyl

R = Ph, PhOMe, PhCH$_2$CH$_2$, *n*-pentyl

41~68% yield
96 ~99% *ee*
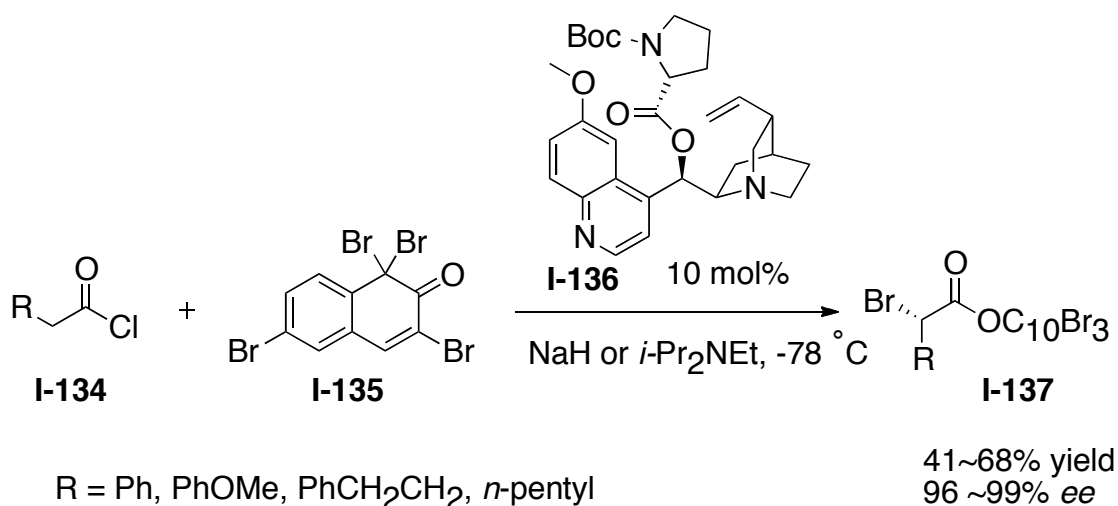
Scheme I-33. Asymmetric α-bromination with proline-corporated cinchona based catalyst
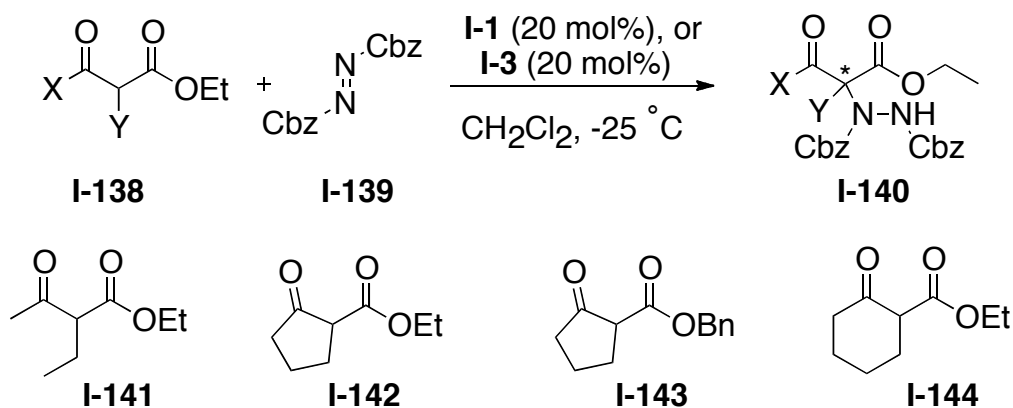
Scheme I-34. Asymmetric α-amination of β-ketoesters

azodicarboxylate in the presence of the catalytic amount of the α-isocupreidine.[65]

Chen and coworkers reported the first α-amination of aromatic ketones in 2007. They obtained the desired product in low to moderate yield but with high optical purity (88~99%ee) in the presence of the 1-amino-9-deoxyepicincona alkaloid **I-147** as the catalyst and azodicarboxylate as the nitrogen source (Scheme I-35). Since the reaction proceeds through an enamine intermediate, they found that addition of the 4 Å molecular sieve was necessary for the removal of the water during enamine formation.[66]
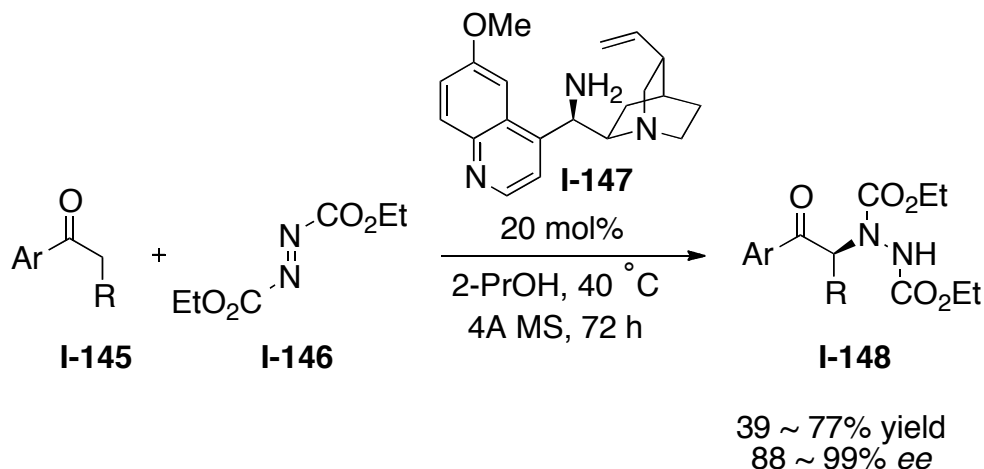
Scheme I-35. Asymmetric α-amination of aromatic ketones

1.4.3.5 α- Sulfenylation of Carbonyl Derivatives

In 2005, cinchona alkaloid dimeric derivatives were used for the asymmetric α-sulfenylation of activated C−H bonds in lactones, lactams and β-dicarbonyl compounds. Jorgensen and coworkers achieved high chemical and optical yield of α-sulfenylation in the presence of (DHQD)$_2$PYR and the electrophilic sulfur reagent **I-150** (Scheme I-36).[67]

1.4.3.6 Conclusions

The asymmetric α-substitution of carbonyl derivatives in the presence of cinchona-based chiral catalysts, especially as a phase- transfer catalyst, is a powerful and efficient method for the synthesis of a variety of synthetically and/or biologically active compounds in an asymmetric fashion. As reviewed here in this section different derivatives of cinchona alkaloids and cinchona alkaloids ammonium salts have been
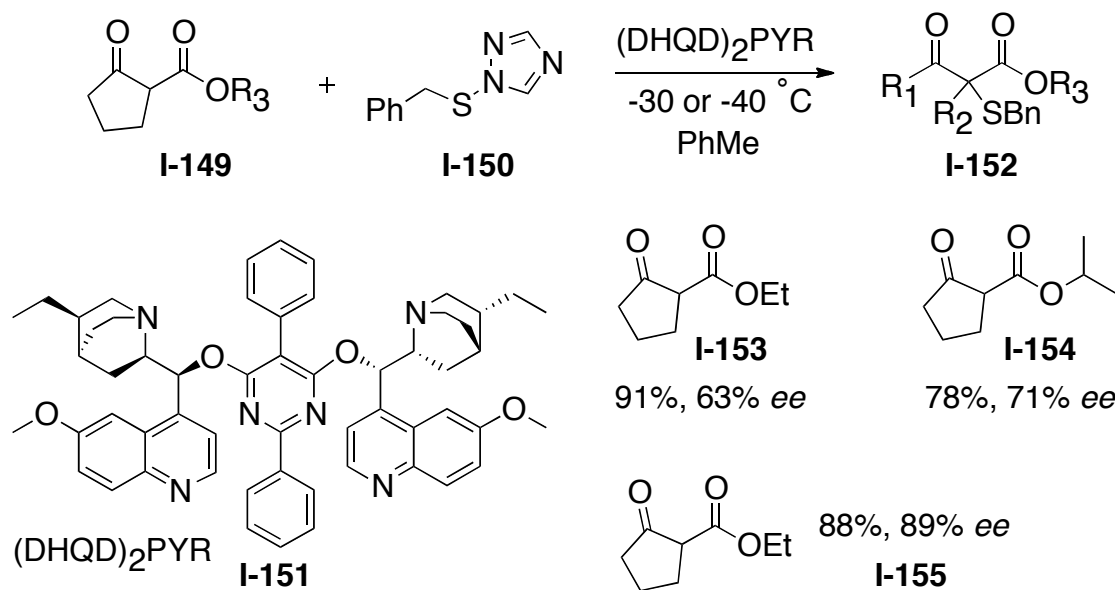
Scheme I-36. Asymmetric α-sulfenylation of carbonyl derivatives

developed to control the enantioselectivity in a variety of α-substitutions of different carbonyl compounds.

1.4.4 Cinchona-Based Enantioselective Protonation

1.4.4.1 Introduction

One of the oldest methods to control the configuration of an asymmetric carbon is taking the advantage of asymmetric protonation of a prochiral carbon center such as an enolate or an enol. In general there are some difficulties for this class of asymmetric reactions, despite its simplicity. Some of the problems in controlling the enantioselectivity of protonation of the prochiral carbon centers are: 1) difficulties in controlling the approach of the smallest electrophile, proton, toward a prostereogenic nucleophilic carbon due to its size and fast diffusion, 2) the problem of O-protonation of

the carbonyl functional group, which leads reversibly to the enol that can racemize the

chiral center α to the carbonyl, and 3) the presence of the two possible

diastereoisomers Z and E of the enolate that can lead to opposite enantiofacial

selectivities. Beside all of these issues, other complexities merit mention such as metal

aggregation, solvation and complexation.[68-70]

The cinchona alkaloids in this class of asymmetric reactions can act as a direct

protonating reagent of the enolate or as an acid-base bifunctional catalyst. In the

second case, cinchona alkaloids act as a base to deprotonate the substrate to generate

the enolate and then as an acid by reprotonating the prochiral carbon of the enolate.

Enantioselectivity can be categorized into four groups based on the type of reaction
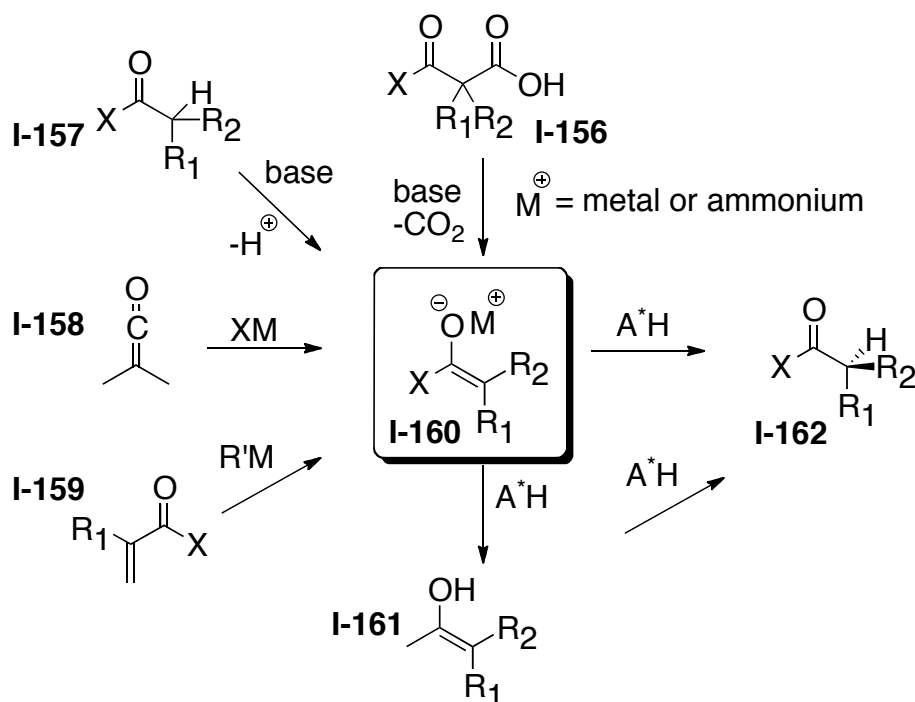
Scheme I-37. Four categories in enantioselective protonation

34

and substrate. In all of these four categories the key prochiral enolate or enol will form as depicted in Scheme I-37. These four categories are: decarboxylation, deprotonation, ketene addition, and Michael addition. In this section these four classes of Cinchona-mediated enantioselective protonation are discussed with some examples.

1.4.4.2 Preformed Enolates and Equivalents

The first direct asymmetric protonation of an enolate (via enamine analogues) was reported in 1976 by Duhumel and coworkers.[71] In 1992 Takeuchi and coworkers used cinchona alkaloids in asymmetric protonation of the enolate.[72] In their methodology samarium diodide was used to reduce the benzil to the corresponding enediolate **I-164**, which was then protonated in an asymmetric fashion by HCl in the presence of the quinidine as a chiral catalyst to the desired (*R*)-benzoin **I-165** in 91% *ee*. Although Takeuchi obtained the desired product in high enantioselectivity, their approach suffered from limited substrate scope (one substrate was described) and the use of a super-stoichiometric amount (3 equiv.) of the quinidine.[72]`
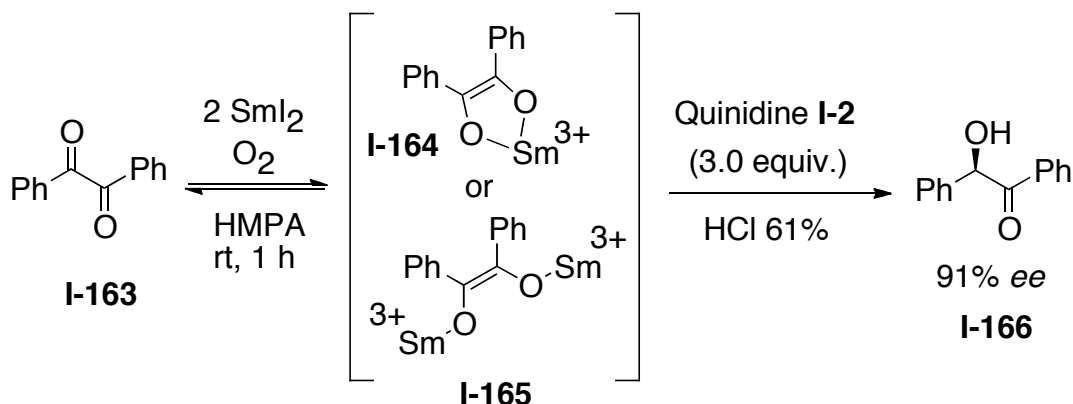
Scheme I-38. Takeuchi's benzil-to-benzoin reductive asymmetric protonation

In 2007 Levacher and coworkers introduced the first organocatalytic enantioselective protonation of silyl enol ethers **I-167** in the presence of the (DHQ)$_2$AQN. In this methodology desired ketones were obtained in as high as 92% *ee* in the presence of the mixture of benzoyl fluoride and ethanol as a latent source of HF (Scheme I-39). [73]

1.4.4.3 Nucleophilic addition on ketenes

The nucleophilic addition of substituted ketenes is a well-known method to generate a prochiral enolate that can be further protonated in an asymmetric fashion. The addition of chiral tertiary amines as catalyst to the ketene generates the chiral zwitterionic intermediate **I-171**. After rapid diastereoselective protonation of the
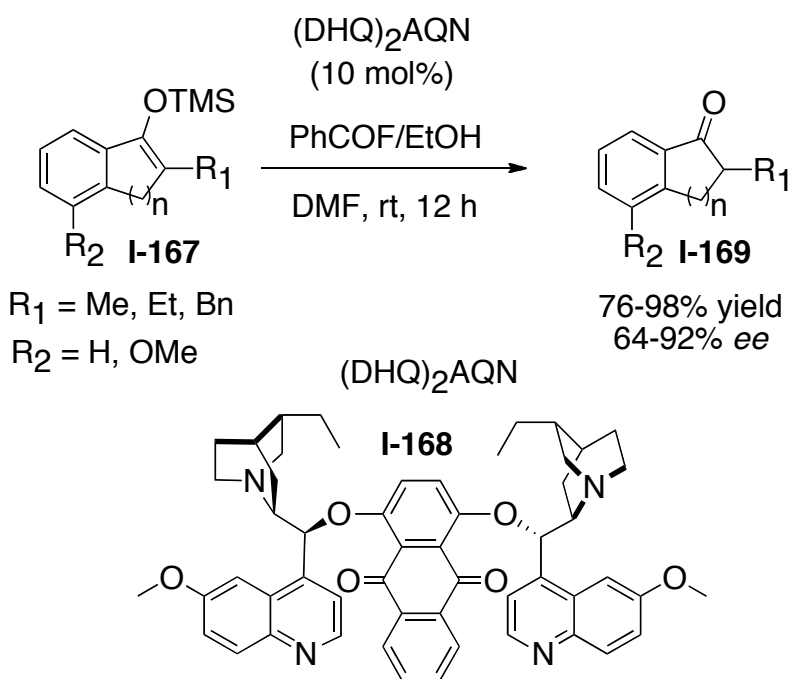
Scheme I-39. Levacher's organocatalytic asymmetric protonation of silyl enol ethers
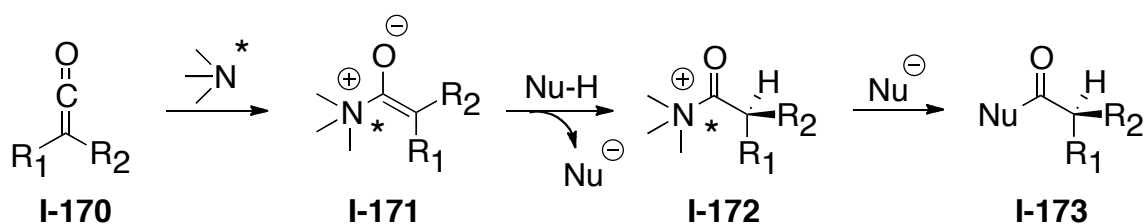
Scheme I-40. Chiral tertiary amine catalyzed addition of heteroatomic nucleophiles on ketenes

intermediate **I-171** the chiral acylammonium **I-172** is formed. This acylammonium intermediate further reacts with nucleophile to form the final product **I-173** and release the chiral tertiary amine catalyst to continue the reaction cycle (Scheme I-40).

The pioneering studies in this field were done by Precejus and coworkers in the 1960s.[9,74-76] The best asymmetric protonation, 74% *ee*, was observed for the addition of methanol to phenylmethylketene **I-174** in the presence of the 9-*O*-acetylquinine **I-175** as a catalyst at -110 $^\circ$C (Scheme I-41a). The reaction selectivity was sensitive to the temperature; the *ee* of the same reaction at -70 $^\circ$C dropped dramatically to less than 5%.[9]

Later on, Simpkins and coworkers introduced a similar approach for the addition of thiophenol to prochiral silylketenes.[77] The nucleophilic addition of thiophenol to trialkylsilylketenes occurred in the presence of 10 mol% of 9-*O*-benzoylquinine **I-179** at -78 $^\circ$C. They were able to obtain the desired α-silylthioesters **I-180** with enantiomeric excesses ranging from 84 to 93% *ee* (Scheme I-141b). The conversion of the thioester group into a ketone, an aldehyde, or a primary alcohol and silyl moiety into a protected alcohol illustrates the importance of this asymmetric protonation.

Despite the importance of cinchona alkaloids as bifunctional chiral catalysts for the nucleophilic addition/enantioselective protonation of prochiral ketenes, no further contribution has been made in this field.

1.4.4.4 Michael Additions

Michael addition is a widely used reaction for the formation of C-C or C-heteroatom bonds. In the first step the nucleophile attacks to the β-carbon, forming an enolate
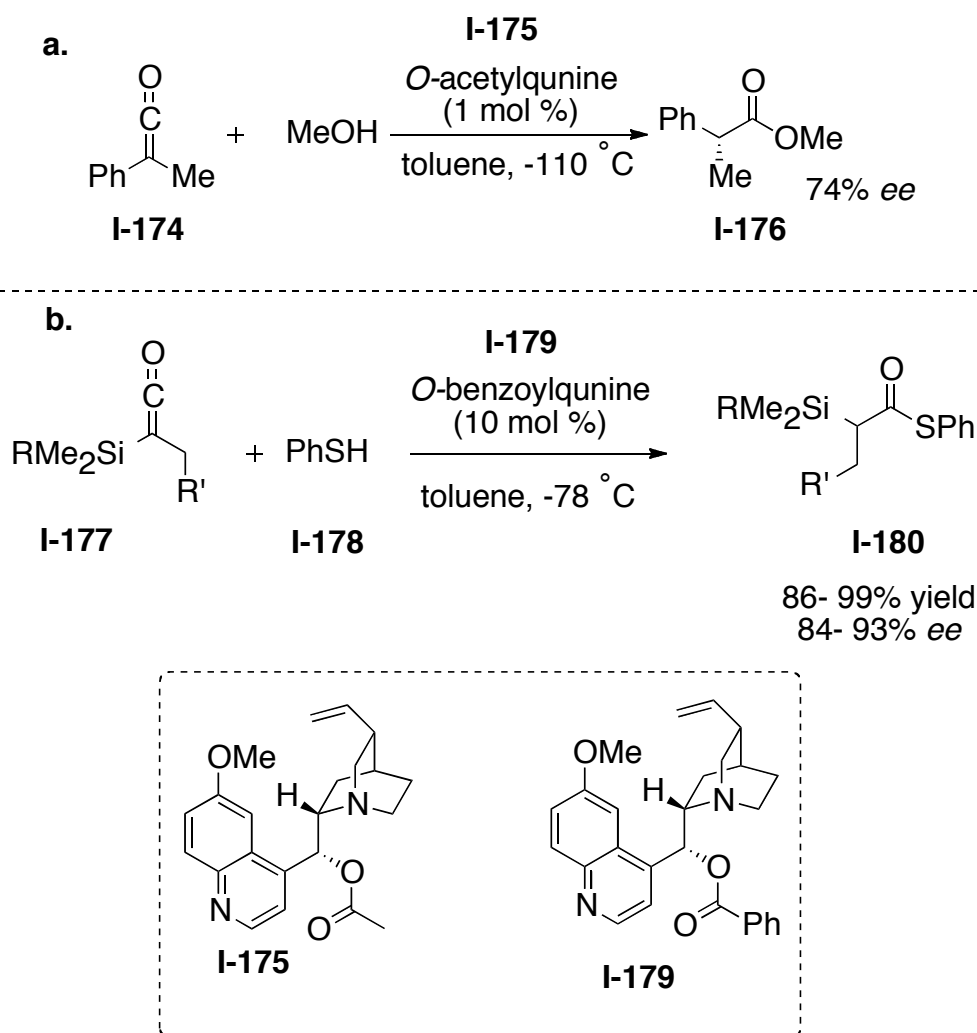
Scheme I-41. a) Tandem methanol addition/asymmetric protonation on phenylmethylketene. b) Simpkins's thiophenol addition on silylketenes
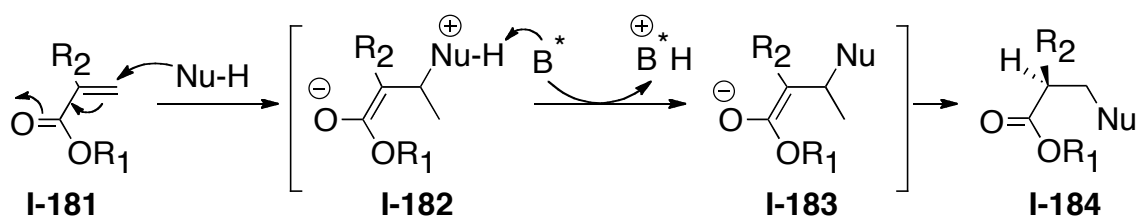
Scheme I-42. Asymmetric protonation induced by Michael additions

intermediate (Scheme I-42). When the Michael acceptor has a substituent on the α-position, the resulting enolate bears a prochiral carbon. Despite the importance of the Michael reaction in organic synthesis, the tandem conjugate addition asymmetric protonation has not been studied extensively. There are only a few publications that demonstrate the use of cinchona alkaloids as bifunctional organocatalysts to catalyze the Michael reaction and control the configuration of the chiral carbon created during protonation of the enolate intermediate.

Pracejus and coworkers published the first tandem Michael addition/enantioselective protonation mediated by cinchona alkaloids in 1977. They
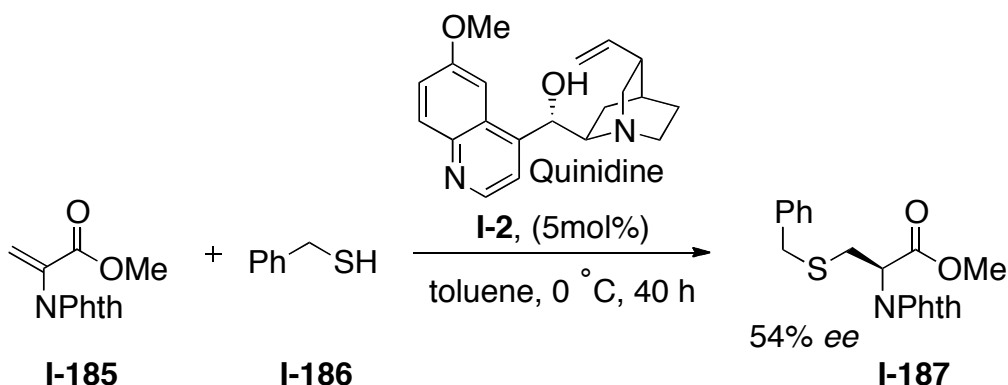
Scheme I-43. Pracejus's benzyl thiol addition on α-substituted Michael acceptor
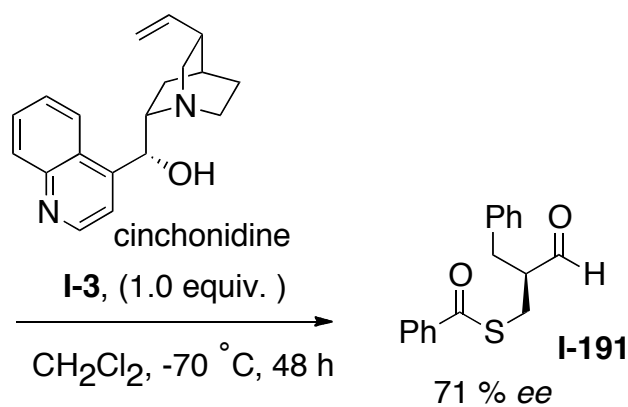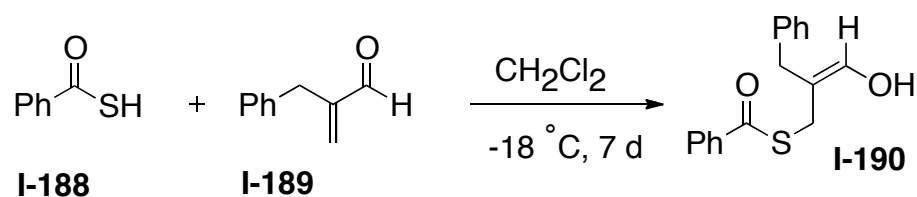
Scheme I-44. Asymmetric tautomerization of enols

used 5 mol% quinidine **I-2** to achieve moderate enantioselectivity (54% ee) in the addition of benzyl thiol **I-186** with 2-phthalimidoacrylate **I-185** (Scheme I-143).[78]

Duhamel and co workers were able to synthesize the stable enol **I-190** by the conjugate addition of thiobenzoic acid **I-188** on 2-benzylacrolein **I-189** at -18 (*Z*: *E* ratio >95:5). Following asymmetric tautomerization of this configurationally pure enol, the desired aldehyde **I-191** was obtained in the presence of a stoichiometric amount of cinchonidine at -70 °C with 71% *ee*.[79]

In 2006 Deng and coworkers developed an unprecedented transformation where two nonadjacent stereocenters were created with up to 98% *ee*. In this reaction β-keto esters or β-keto nitriles add to 2-chloroacrylonitrile (Scheme I-45.[80] The

enantioselectivity in this reaction is controlled by a 6' -OH cinchona alkaloid such as **I-194**. The authors proposed that the enantioselectivity in this tandem reaction resulted from a network of hydrogen-bonding interactions between the catalyst and substrates and also between the catalyst and the enol intermediate in the protonation step. In the first step the β-keto ester or β-keto nitrile gets deprotonated by the catalyst. The protonated catalyst can control the enantioselectivity of the Michael reaction presumably by hydrogen bonding. The protonated catalyst then acts as a chiral acid and participates in enantioselective protonation of the enolate intermediate.[80]

1.4.4.5 Enantioselective Decarboxylative Protection

The first example of an asymmetric reaction in chemical history surprisingly is the
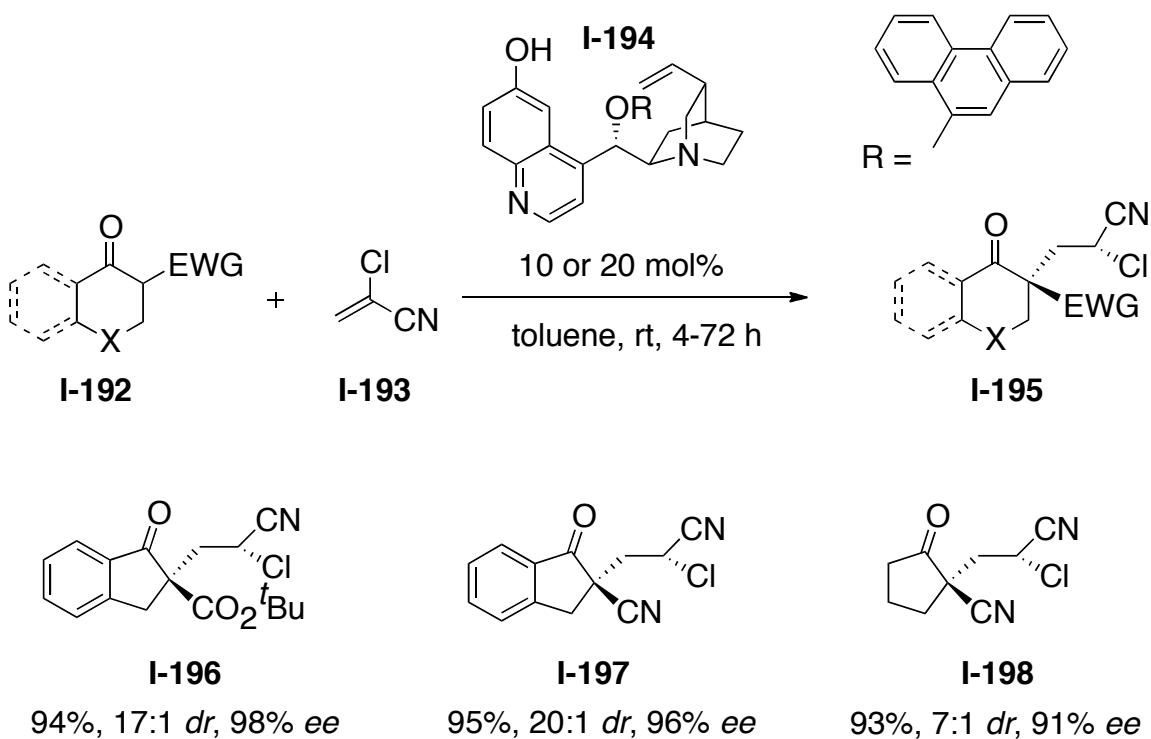
Scheme I-45. Deng's tandem Michael addition/enantioselective protonation

enantioselective decarboxylative protonation. In this first example Marckwal and coworkers used brucine, a readily available optically pure compound, as a chiral inductor.[81,82] Acidic and basic conditions lead to different reaction pathways. In acidic condition an enol intermediate is formed by the unimolecular decomposition of the starting material upon loss of CO_2 that occurs through proton transfer in a cyclic transition state. In basic condition an enolate intermediate is formed after deprotonation of the acid followed by rapid loss of CO_2. In both acidic and basic conditions a prochiral intermediate forms. The chirality in the final product is controlled at last step of the mechanism and is induced by an optically active source, which intimately and noncovalently is involved in the enantioselective protonation of the prochiral carbon (Scheme I-46).

The first efficient organocatalyzed enantioselective decarboxylative protonation, EDP, was reported by Brunner and Schmidt for the synthesis of a precursor of (*S*)-
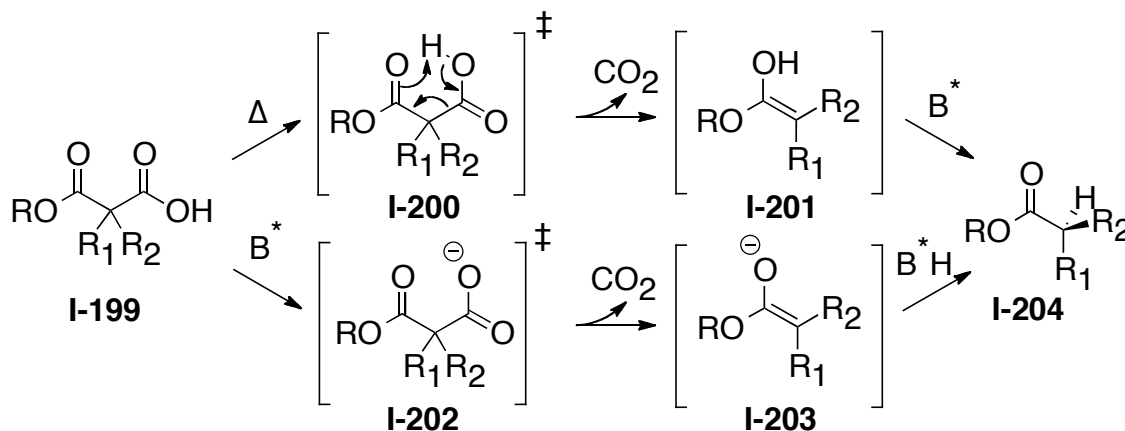
Scheme I-46. Proposed mechanisms of enantioselective decarboxylation/protonation
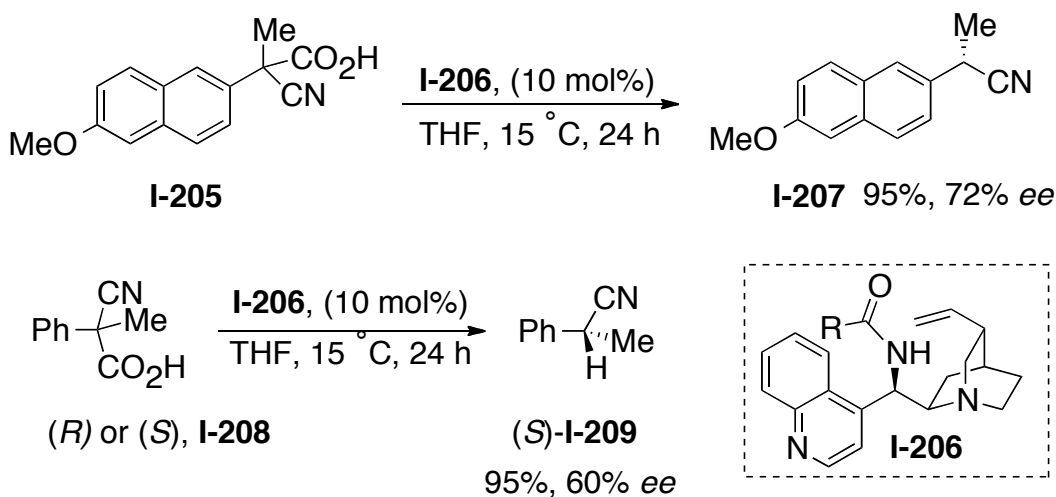
Scheme I-47 Brunner's enantioselective decarboxylation/protonation
of 2-cyanopropionic acid derivatives

naproxen.[83] They screened many bases and found that cinchona alkaloids are the

most efficient catalyst. A selectivity up to 72% (Scheme I-47) was achieved by using 10

mol% of 9-*epi*-cinchonine benzamide derivative **I-206** in the EDP of aryl substituted 2-

cyano propionic acid **I-205**. The EDP of 2-cyano-2-phenyl propionitrile **I-208** carried out

under same condition gave 60% *ee*. Mechanistic studies showed that when both

enantiomers of 2-cyanopropanoic derivative **I-208** or the racemic substrate were

subjected to the reaction condition, the same enantioselectivity was observed for the

product (Scheme I-47). This result suggests a two-step decarboxylation/protonation

mechanism via planar intermediates followed by asymmetric protonation.

Amere and coworkers in 2007 achieved the most enantioselective decarboxylative

protonation for the synthesis of a variety of cyclic and acyclic α-amino acids with 83-

93% *ee*. Optimization of the reaction condition showed that the highest selectivities

were achieved in polar solvent at 0 $^{\circ}C$ in the presence of the thiourea derivatives of cinchona alkaloids (Scheme I-48).[84]

1.4.5 Cinchona-Catalyzed Nucleophilic 1,2 Addition to C=O and C=N Bonds

1.4.5.1 Introduction

The enantioselective nucleophilic addition to prochiral C=O and C=N moieties yielding the corresponding chiral products is one of the most important areas of research in asymmetric catalysis. Over the past few decades, remarkable scientific achievements have been made in these research areas by using a variety of transition metal chiral catalysts and also by using chiral organocatalysts. As mentioned earlier the naturally occurring cinchona alkaloids have proven to be powerful organocatalysts in
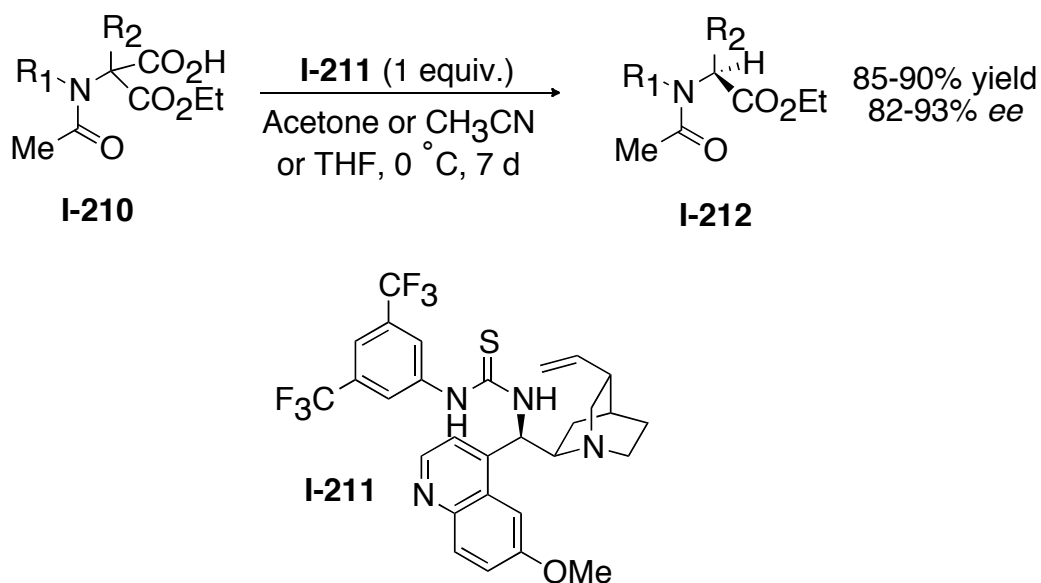
Scheme I-48 Asymmetric synthesis of α-amino esters in the presence of cinchona thiourea

44

different chemical reactions. These cinchona alkaloid based organocatalysts have also been used extensively in the nucleophilic 1,2 addition to C=O and C=N bonds such as aldol, Henry, Mannich, Darzene, Morita-Baylis-Hillman, aza-Morita-Baylis-Hillman and cyanation (cyanohydrin synthesis) reactions. In the following section some examples of aldol and aza-Morita-Baylis-Hillman reactions will be reviewed.

1.4.5.2 Aldol reaction.

The asymmetric aldol reaction is a common method in synthesizing chiral β-hydroxy ketones. In 1993, Shioiri and coworkers introduced the first cinchona- catalyzed enantioselective Mukaiyama-type aldol reaction of benzaldehyde with the silyl enol ether **I-212** in the presence of the *N*-benzylcinchoninium fluoride **I-214** (Scheme I-49)**.**
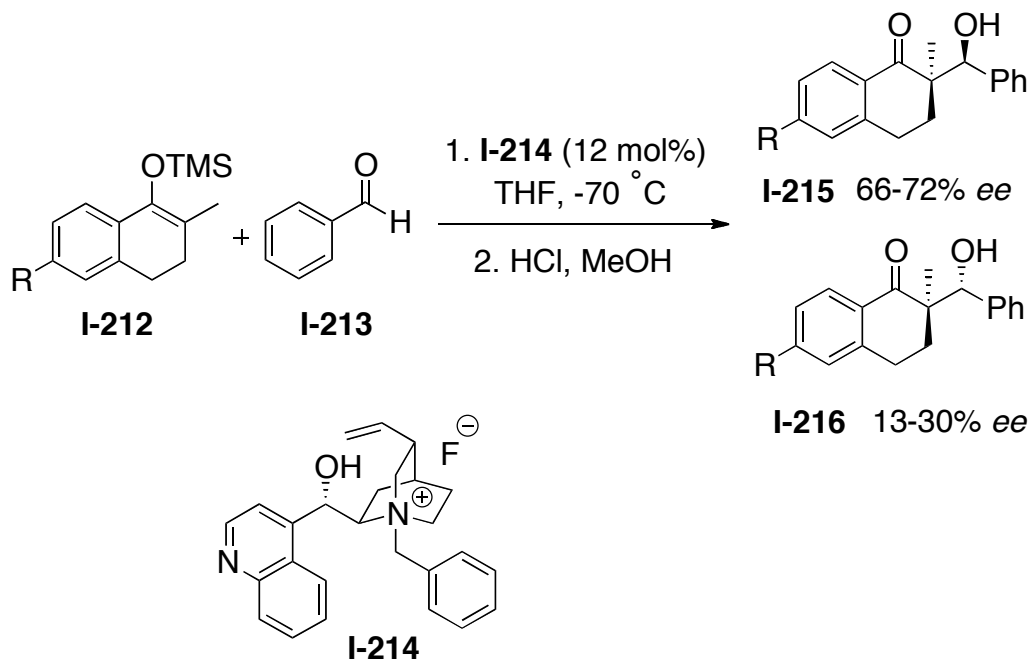
Scheme I-49 The first cinchona- catalyzed enantioselective
Mukaiyama-type aldol reaction
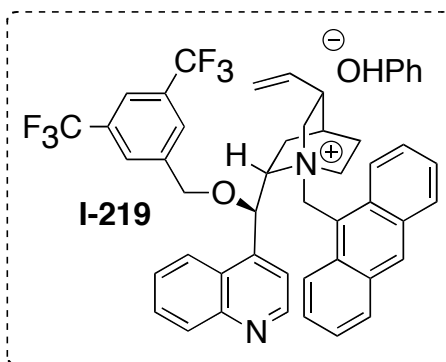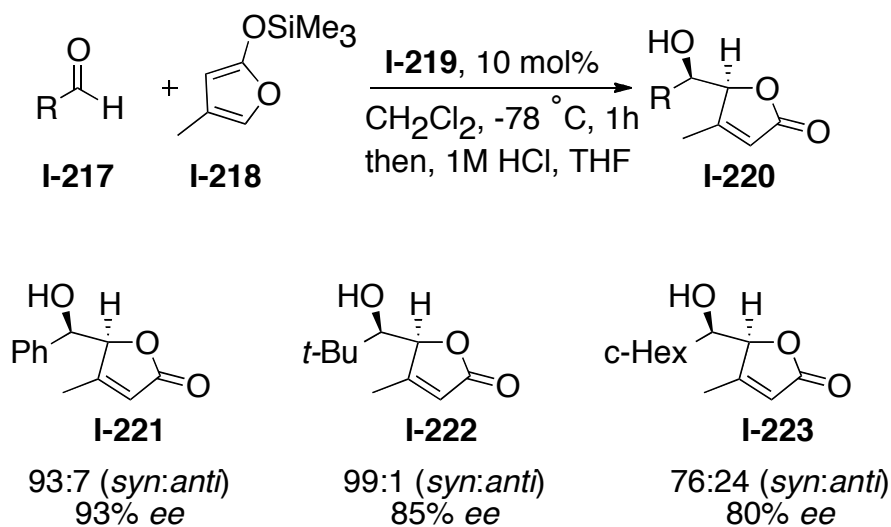
Scheme I-50 Enantioselective Mukaiyama-type aldol reaction
with phenoxide as an activator

However, they obtained the desired β-hydroxy ketones with low to moderate enantio-
and diastereoselectivity. The observed asymmetric induction can be explained by a dual
activation mode of the catalyst. In this reaction fluoride acts as a nucleophile activator
by deprotection of the silyl enol ethers and the chiral ammonium cation activates the
carbonyl group.[85]

Recently the Mukaiyama group developed a methodology in which the phenoxide
anion was used as an activator of silyl enol ethers, instead of fluoride.[86] In this
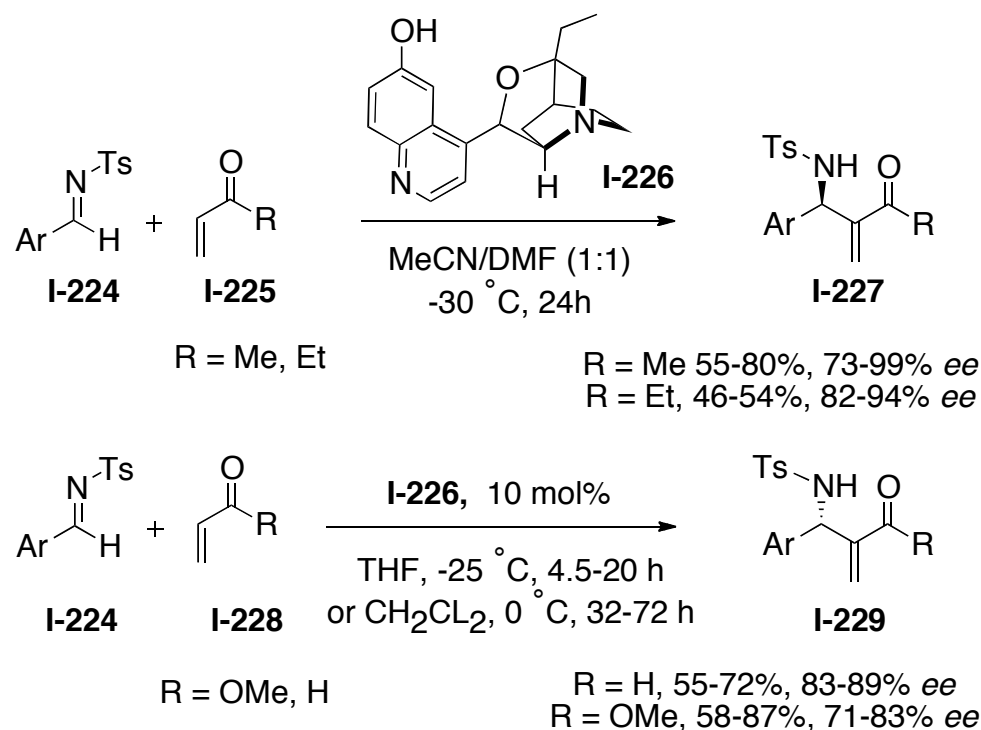
Scheme I-51 Aymmetric aza-Morita-Baylis-Hillman reaction

methodology a range of aliphatic and aromatic aldehydes underwent the vinylogous

Mukaiyama-type aldol reaction with silyl enol ether **I-218** in the presence of the

cinchona-based catalyst **I-219** bearing a phenoxide anion (Scheme I-50).

1.4.5.3 Aza-Morita-Baylis-Hillman reaction

The Aza-Morita-Baylis-Hillman reaction provides easy access to highly

functionalized allylic amines. In general, this reaction can be catalyzed by simple

amines or phosphines, which can attack as a Michael donor to electron deficient

Michael acceptor alkenes. The resulting enolate intermediate undergoes the Mannich

reaction with C=N to form the desired allylic alcohol.

Hatakeyama[87] and Shi[88,89] and Adolfsson[90] have extensively studied the aza-MBH reactions. They report that β-ICD **I-226** is an efficient and also general catalyst for the asymmetric aza-MBH of activated aryl imines with various activated olefin. For example Shi[88,89] has shown that by using ethyl and methyl vinyl ketone (EVK, MVK) as a Michael acceptors, product with up to 99% *ee* are obtained (Scheme 1-51). However, interestingly, the adduct **I-227** derived from MVK and EVK show the opposite configuration to those obtained with acrolein and methylacrylate. This interesting outcome was explained on the basis of the mechanism depicted in Scheme I-52. This outcome, controlled by the rate of the elimination step of the two betain intermediates **I-230** and **I-231**, is stabilized by intramolecular hydrogen bonding betw*ee*n the amidate and phenolic OH.
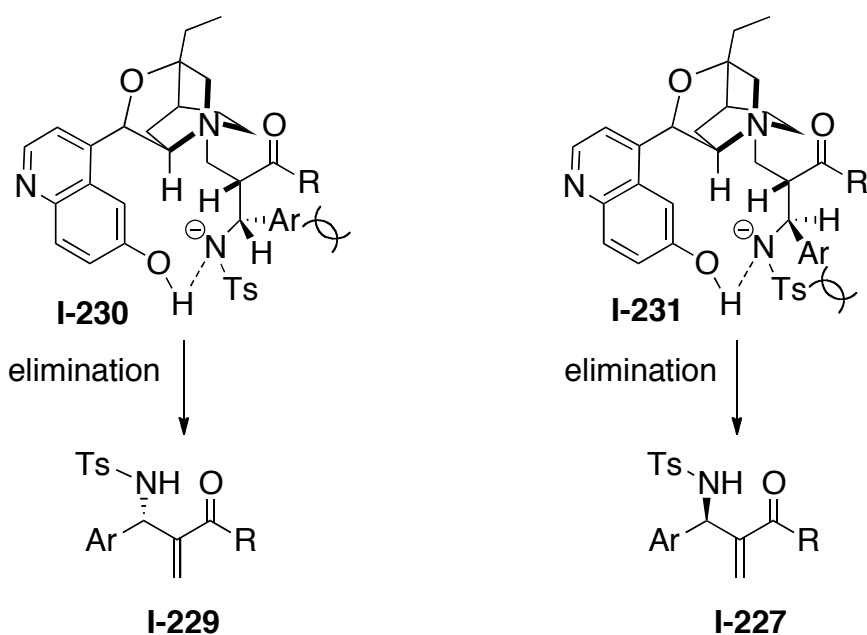
Scheme I-52 Elimination step of the two possible betaine intermediates

1.4.6 Cinchona-Catalyzed Nucleophilic Addition of Electron-Deficient C=C Double bonds

1.4.6.1 Introduction

Asymmetric conjugate addition reactions are common and important to synthesize highly functionalized products that are readily transformed into a variety useful chiral intermediates. In the late 1970s and early 1980s Wynberg[91-93] and coworkers showed that cinchona alkaloids can be useful for asymmetric conjugate addition reactions. Since then, numerous examples of these reactions have been reported. The importance of this class of alkaloids in asymmetric conjugate addition reactions will be presented in the form of a couple of examples.

1.4.6.2 PTC-Catalyzed Enantioselective Michael Addition Reaction.

Asymmetric Michael additions have been studied extensively under phase-transfer conditions with achiral bases in the presence of the cinchona alkaloid-derived chiral phase transfer catalysts. In 1986, Conn and coworkers for the first time used cinchonine/cinchonidine-derived chiral phase-transfer catalysts. However, low to moderate *ee*'s were obtained.[17] In 1997 Corey and coworkers improved the *ee* to 99% by using *O*(9)-allyl-*N*-(9-anthracenylmethyl) cinchonidinium bromide as PTC **I-237**.[94,95] This methodology was useful in synthesizing various functionalized α-alkyl-amino acids (Scheme I-53). Later on, Corey and coworkers expanded the substrate scope to include nitromethane and silyl enolethers by small modification of PTC **I-237**.[96]

In 2007, Jorgensen and coworkers reported the first example of an asymmetric 1,6-addition of β-ketoesters to electron-poor δ–unsubstituted dienes using PTC **I-241**.

I-233
85%, 91% *ee*

I-236
88%, 99% *ee*

I-232

I-237 (10mol %)
CH$_2$Cl$_2$/50% KOH aq
-55 °C

I-237 (10mol %)
CsOH-H$_2$O/CH$_2$Cl$_2$
-78 °C

I-237 (10mol %)
CsOH-H$_2$O/CH$_2$Cl$_2$
-78 °C

I-237 (10mol %)
CsOH-H$_2$O/CH$_2$Cl$_2$
-78 °C

I-235
85%, 91% *ee*

I-234
85%, 95% *ee*

I-237
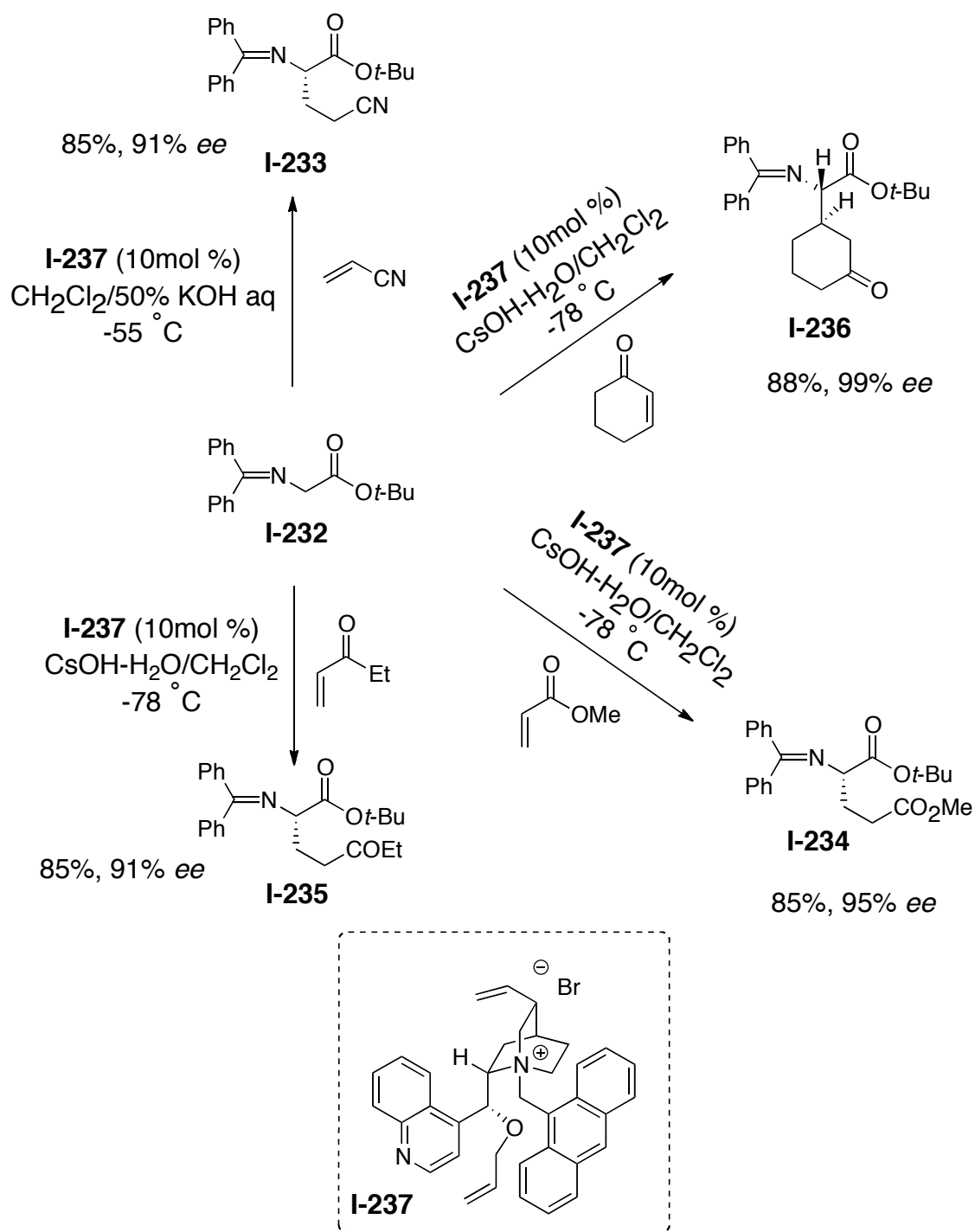
Scheme I-53 PTC-catalyzed enantioselective Michael addition reactions

50
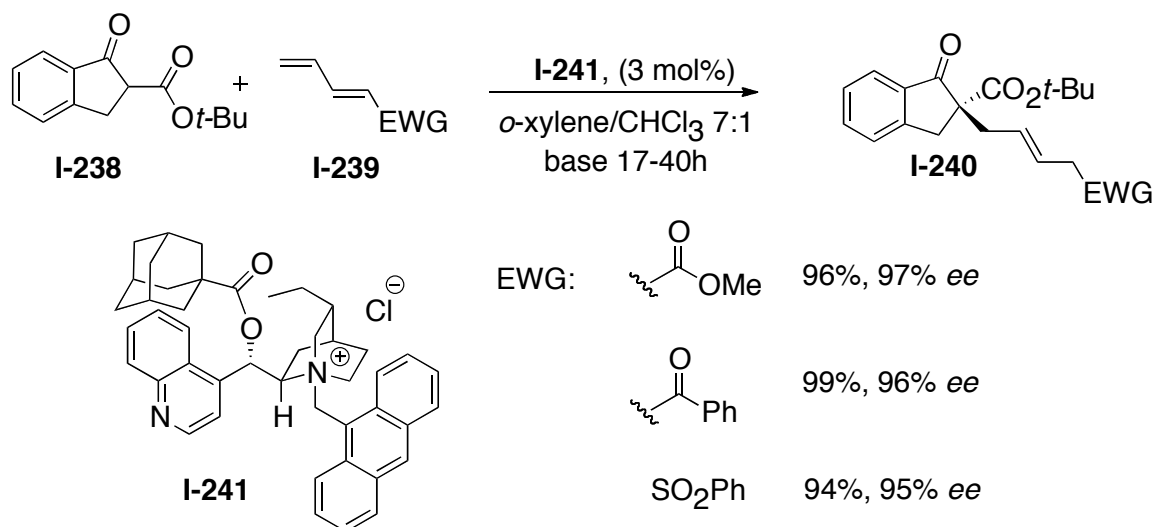
Scheme I-54 PTC-catalyzed asymmetric 1,6-addition of β-ketoesters to electron-poor δ−unsubstituted dienes

Various electron-poor δ-unsubstituted dienes bearing ketones, esters and sulfones have been used in this reaction with β-keto esters **I-238** to obtain the desired product in high yield and *ee*.[97]

1.4.6.3 Non-PTC-Catalyzed Enantioselective Michael Addition Reaction.

In 2004, Jorgensen and coworkers obtained high chemical and optical yields for the conjugate addition of 1,3-diketones to alkynones in the presence of Sharpless' bis-cinchona alkaloid (DHQ)$_2$PHAL. They obtained the desired addition products in high enatioselectivity (up to 95% *ee*) for both aromatic and aliphatic alkynones. In both cases mixture of *E/ Z*-isomers were formed, which were selectively isomerized to the more

stable *E*- isomer (>50:1) by treating the mixture with catalytic amounts of Bu$_3$P or I$_2$ (Scheme I-155).[98]

In 2007 Wang and coworkers found that the quinine-derived thiourea catalyst is an efficient catalyst for the tandem thio-Michael-aldol reaction of various 2-mercaptobenzaldehydes with α-β-unsaturated oxazolidinones (Scheme I-56). They obtained the desired benzothiopyranes with thr*ee* stereogenic centers in high chemical and optical yield. The authors believe that the high stereoselectivity is controlled by multiple hydrogen bonding between the catalyst and the substrate **I-251**.[99]

1.4.6.4 Epoxidation and Aziridination

Peroxides or hypochlorites as Michael donors can attack electron-deficient olefins to give epoxides via a conjugate addition-intramolecular cyclization sequence. For example primary amine cinchona based bifunctional catalysts were used by Wang and
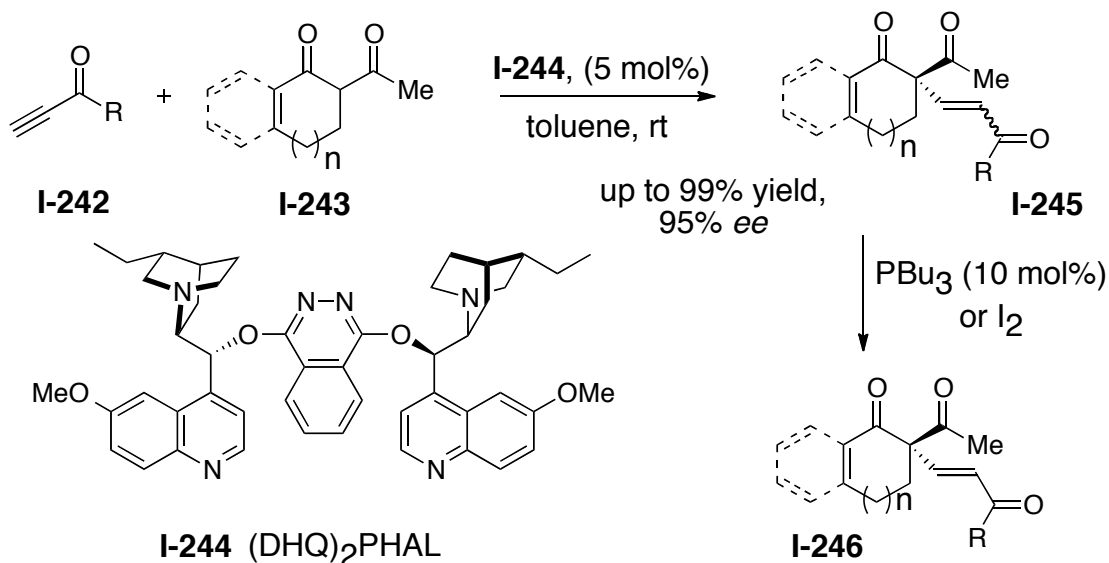
Scheme I-55 (DHQ)$_2$PHAL catalyzed asymmetric conjugate addition of 1,3-diketones to alkynones

coworkers for the epoxidation of different cyclic enones via imminium catalysis (Scheme I-57).[32] In another example cinchona-based PTCs were used by Corey and coworkers in the asymmetric epoxidation of acyclic enones via a chiral ion pairing mechanism.[27]

In a similar fashion , Pesciaioli and coworkers controlled the enantioselectivity of acyclic enone aziridinations by using **I-257** PTC. *N*-Hydroxamates were used as the nitrogen source to obtain the desired *N*-arylaziridines via conjugate addition in high chemical and optical yield (Scheme I-58).

1.4.7 Cinchona-Catalyzed Cycloaddition Reactions

1.4.7.1 Introduction

Asymmetric pericyclic reactions are among the most common methods to synthesize enantioenriched cyclic compounds. High enantioselectivity is obtained by
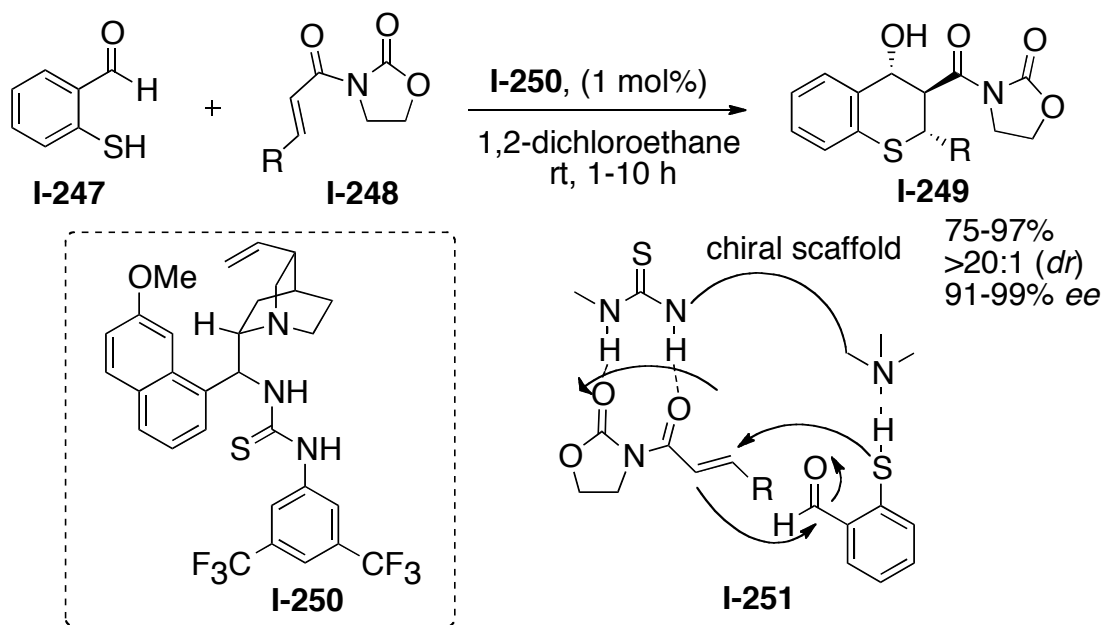
Scheme I-56 Quinine-derived thiourea catalyzed tandem thio-Michael-aldol reaction
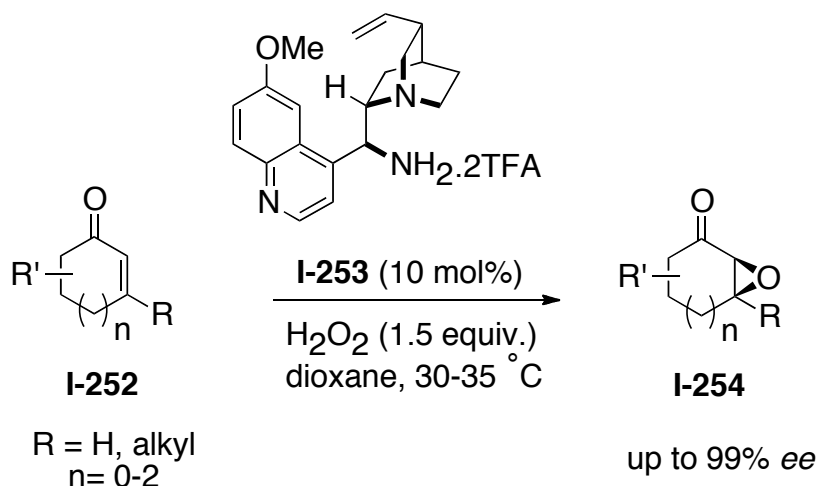
Scheme I-57 Asymmetric epoxidation of cyclic enones via iminium catalysis

using chiral metal complexes and also small organocatalysts.[100-102]

Cinchona alkaloid based catalysts have also contributed to this area, since they are multifunctional and also can be easily tuned. In this section, the application of cinchona alkaloids and their derivatives in asymmetric cycloaddition will be illustrated with a couple of examples.
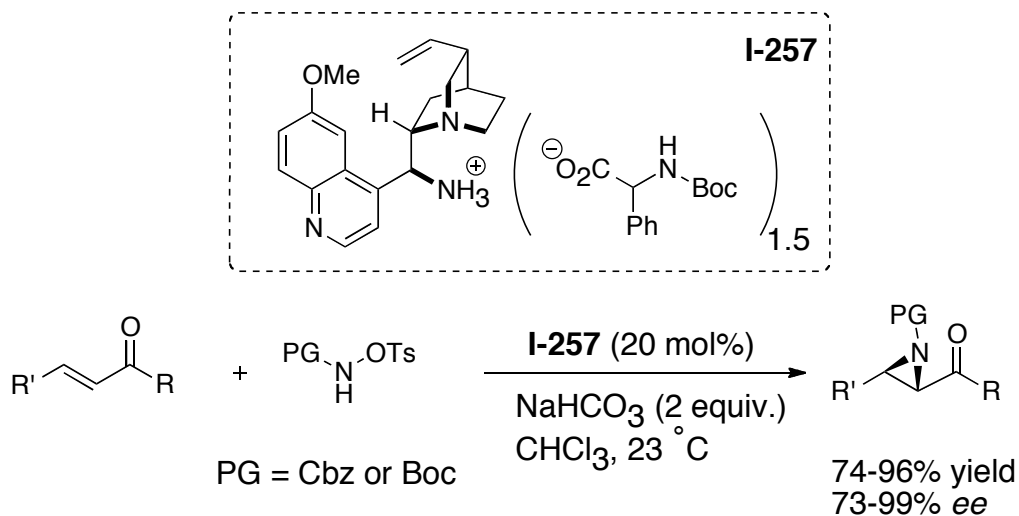
Scheme I-58 Asymmetric aziridination of acyclic enones with PTC
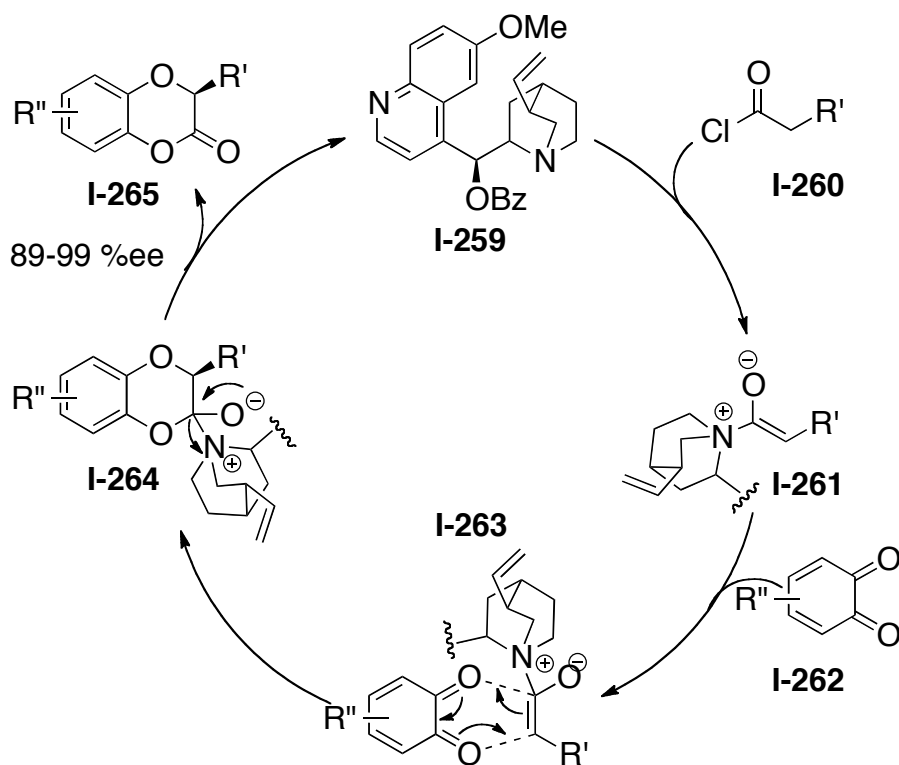
Scheme I-59 Catalytic cycle for the [4 + 2] cycloaddition of ketene enolate and *o*-quinone

1.4.7.2 Quinoclidine tertiary amines catalyzed asymmetric cycloadditions

Cinchona alkaloids possess a nucleophilic quinoclidine moiety that reacts with acyl chloride as a Lewis base to generate a ketene enolate *in situ*. Lectka *et al.* in 2006 used this ketene enolate intermediate in an inverse electron demand [4 + 2] cyclo addition with electron deficient o-quinones. In this reaction the desired lactone adduct was obtained in high yield and enantioselectivity by applying 10 mol% of benzoylquinidine (Scheme I-59).[103]

Apart from acting as an effective Lewis base catalyst, the protonated quinuclidine can act as a Bronsted acid to participate in other cycloaddition reactions. For example, Calter and coworkers proposed that the protonated cinchona alkaloid would catalyze the asymmetric 'interrupted' Feist-Benary reaction between ethylbromopyruvates and cyclohexane-1,3-dione, as a Bronsted acid. In this reaction, hydrogen-bonding interaction between catalyst and α-ketoester moiety, renders it more electrophilic towards attack by either enol or enolate of cyclohexane-1,3-dione. The resulting product undergoes intermolecular alkylation to afford the desired [3 + 2] cycloadduct in high yield and enantioselectivity (Scheme I-60).[104]
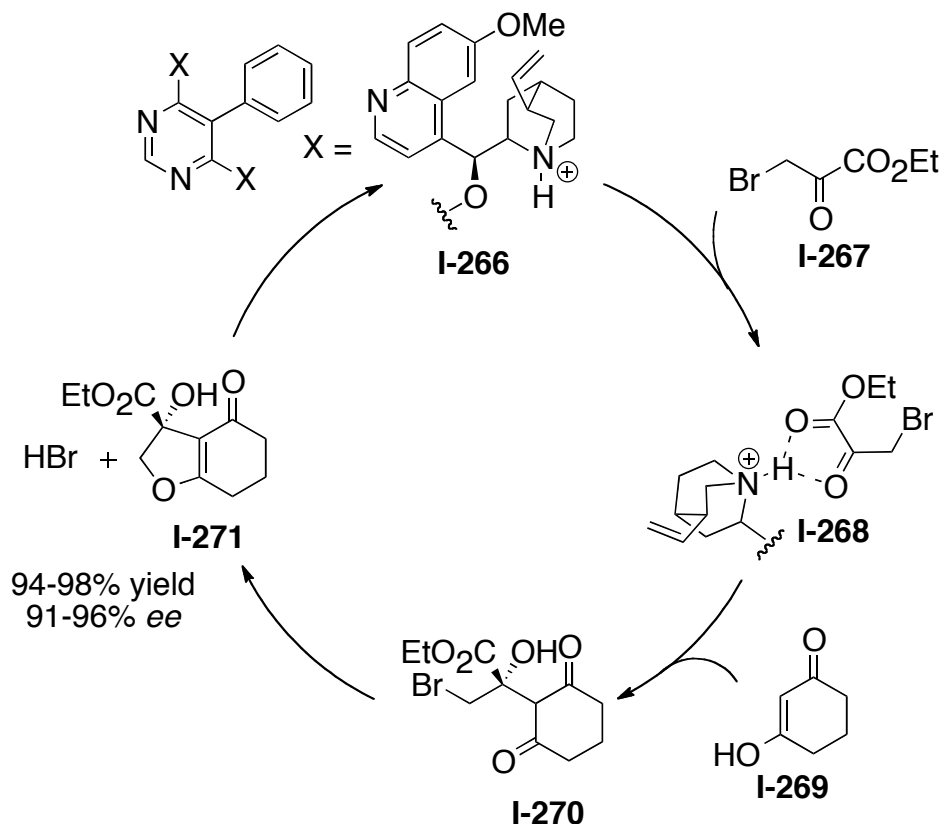
Scheme I-60 Catalytic mechanism for the asymmetric interrupted
Feist-Benary reaction

1.4.7.3 Asymmetric Cycloaddition Catalyzed by Bifunctional Cinchona Alkaloids

Natural cinchona alkaloids by themselves are bifunctional amino alcohols. This bifunctional characteristic can be beneficial in asymmetric reaction through concerted activation modes. Nakatani et al. explored the usage of natural cinchona alkaloids for the first time in controlling the enantioselectivity of the Diels-Alder reaction. In the Diels-Alder reaction of 3-hydroxy-2-pyrone with *N*-methylmaleimide, modest enantioselectivity was obtained by using stoichiometric amounts of cinchonidine. The formation of the rigid complex between 3-hydroxy-2-pyrone and cinchonidine was essential to control the enantioselectivity of the reaction as depicted in Scheme I-61. [105]

In 2000, MacMillan and coworkers reported the first amine catalyzed 1,3-dipolar

endo:exo = 11:1, 77% *ee*
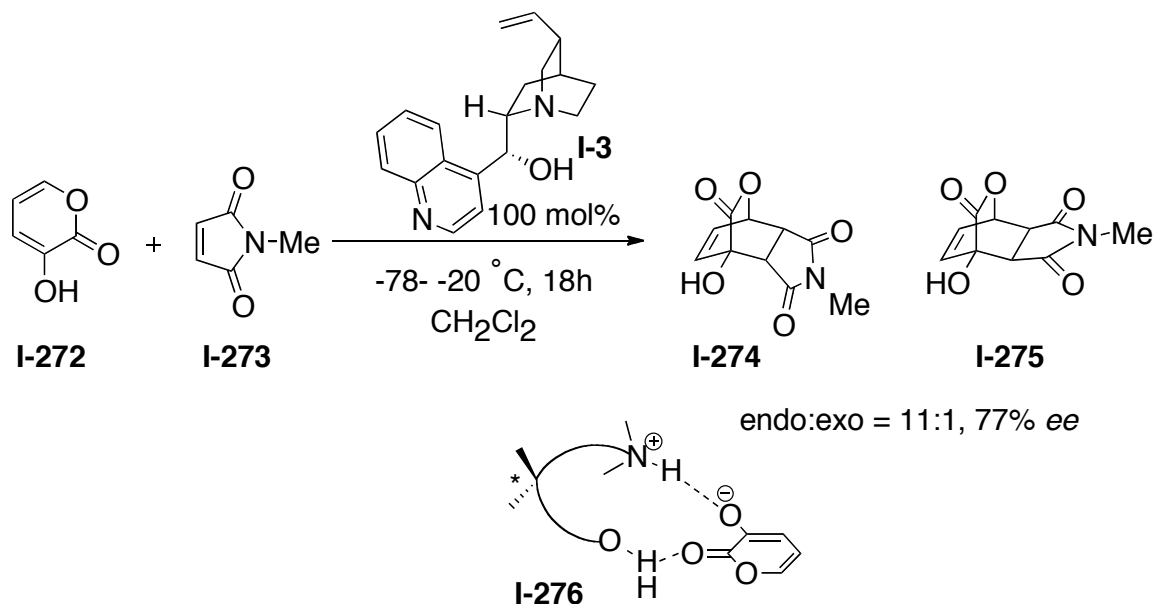
Scheme I-61 Diels-Alder reaction of 3-hydroxy-2-pyrone
with *N*-methylmaleimide

cycloaddition of α,β-unsaturated aldehydes and nitrones by LUMO- activation.[106]

Later on in 2007, Chen *et al.* found that 9-amino-9-deoxyepiquinine **I-281** can catalyze the 1,3-dipolar cycloaddition of azomethine imine and 2-cyclohexen-1-one in the presence of a catalytic amount of acid. The desired tricyclic product was obtained in moderate *ee* and high diastereoselectivity. They were able to improve the *ee* up to 89% by a newly designed multifunctional primary amine, 6'-hydroxy-9-amino-9-deoxyepiquinine **I-278**. The authors proposed that the free hydroxyl group plays an important rule in this reaction as both reactivity and enantioselectivity were increased
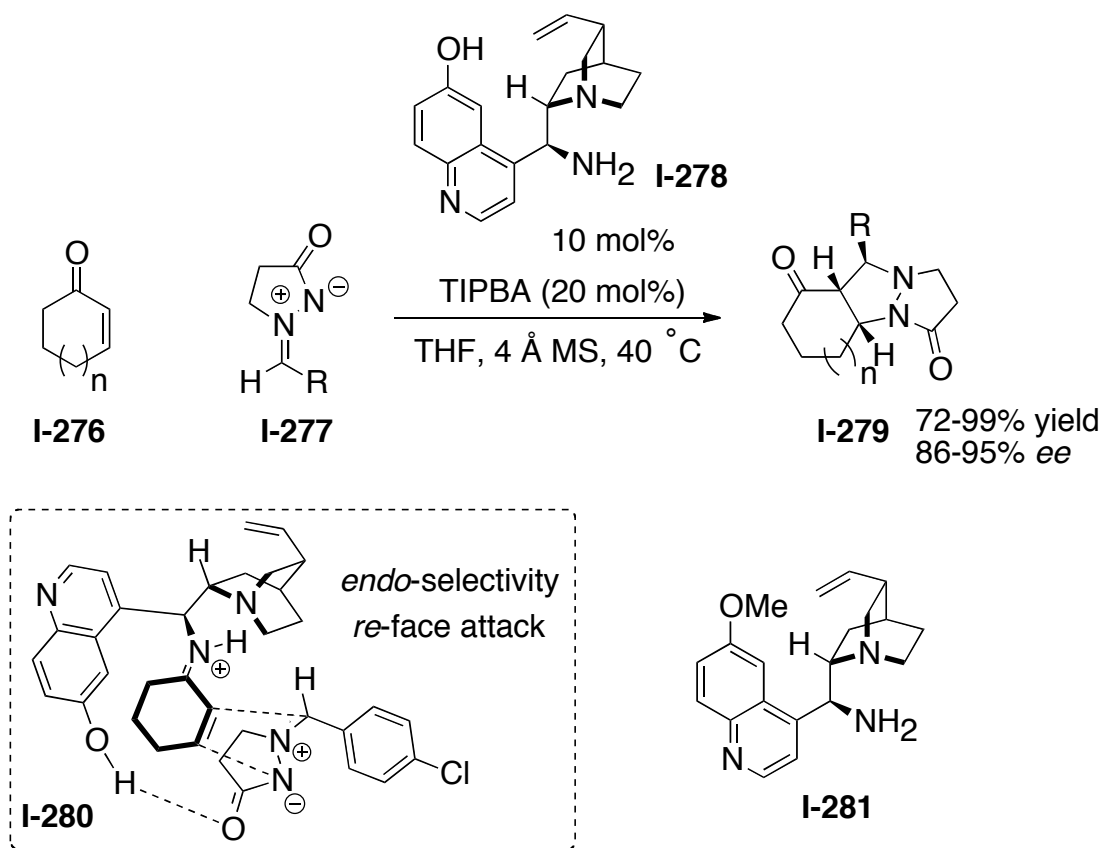
Scheme I-62 Asymmetric 1,3-dipolar cycloaddition of cyclic enones and azomethine imines
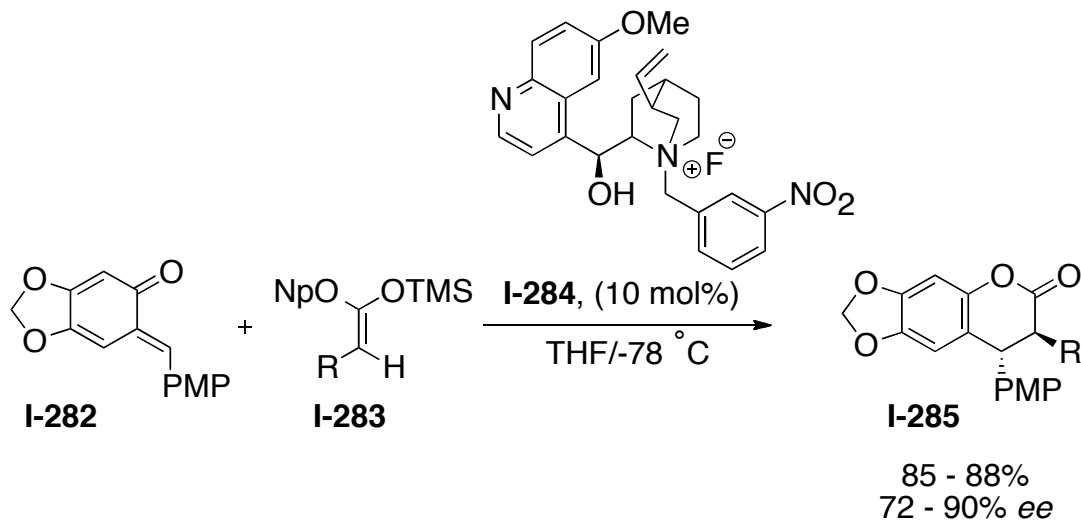
Scheme I-63 Asymmetric cycloaddition of *o*-quinone
methide with silyl ketene acetal

dramatically. They believed that these observed effects could be due to *ee* the formation

of hydrogen-bonds between the 6'-OH group and the dipoles carbonyl group as

depicted in Scheme I-62. Moreover, addition of the four angstrom molecular sieves

helped to improve the by removing the trace amount of water that is generated during

the formation of the active iminium intermediate. This *ee* improvement supports the

proposal of a hydrogen bonding complex since the presence of water could interrupt the

formation of hydrogen bonds between the substrate and catalyst.[107]

1.4.7.4 Asymmetric Cycloaddition Catalyzed by Cinchona-Based Phase-Transfer Catalyst

After developing a successful catalytic [4 + 2] cycloaddition,[8] the Lectka group

developed another highly enantioselective cycloaddition by using cinchona-based PTC.

They used *N*-(3-nitrobenzyl)quinidinium fluoride as PTC **I-284** to catalyze asymmetric

cycloaddition of *o*-quinone methide (*o*-QM) **I-282** with silyl ketene acetals **I-283**. The desired cycloadducts **I-285** were obtained in excellent chemical yield and good *ee*. In this reaction fluoride possibly deprotects the silyl ketene acetal and the resulting enolate intermediate reacts with *o*-QM in an asymmetric fashion in the presence of the chiral PTC as a counter ion. They have also found that the free hydroxyl group of PTC was essential to get high enantioselectivity in this reaction.[35]

1.4.8 Cinchona-Based Organocatalysts for Desymmetrization of meso-Compounds and (Dynamic) Kinetic Resolution of Racemic Compounds.

1.4.8.1 Introduction

The desymmetrization of *meso*-compounds is a practical and common method in preparation of enantioenriched molecules from achiral compounds in a single step. Dynamic Kinetic Resolution (DKR) a variant of desymmetrization, enables the conversion of racemic reactants with 100% theoretical yield to highly pure optically active molecules. In DKR, as both reacting enantiomers engage in chemical equilibrium, the faster reacting enantiomer is replenished in the course of the reaction at the expense of the slower reacting one.

Since the usage of the cinchona alkaloids as resolving agents by Pasteur[4,5] in 1953, remarkable achievements have been reported in this area by taking advantage of this class of alkaloids. The presence of the Lewis basic quinoclidine nitrogen and Lewis acidic substituents at the C9 position, such as hydroxyl thiourea and sulfonamide groups, are again the key structural features for their successful utility. In this section,

60

examples will highlight the importance of cinchona alkaloids and their derivatives in these two areas.

1.4.8.2 Desymmetrization of *meso-Diols*

The enantioselective discrimination of the hydroxyl groups of *meso*-diols can lead to chiral mono protected diols, which can be used as important intermediates for asymmetric organic synthesis. Besides the common enzymatic methods, a number of chemical approaches have been reported that utilize different chiral catalysts such as

98%, 91% *ee*
I-290

99%, 86% *ee*
I-291

80%, 93% *ee*
I-292

85%, 94% *ee*
I-293

Desymmetrization of
meso-1,3 and 1,4 diol
70-99% *ee*
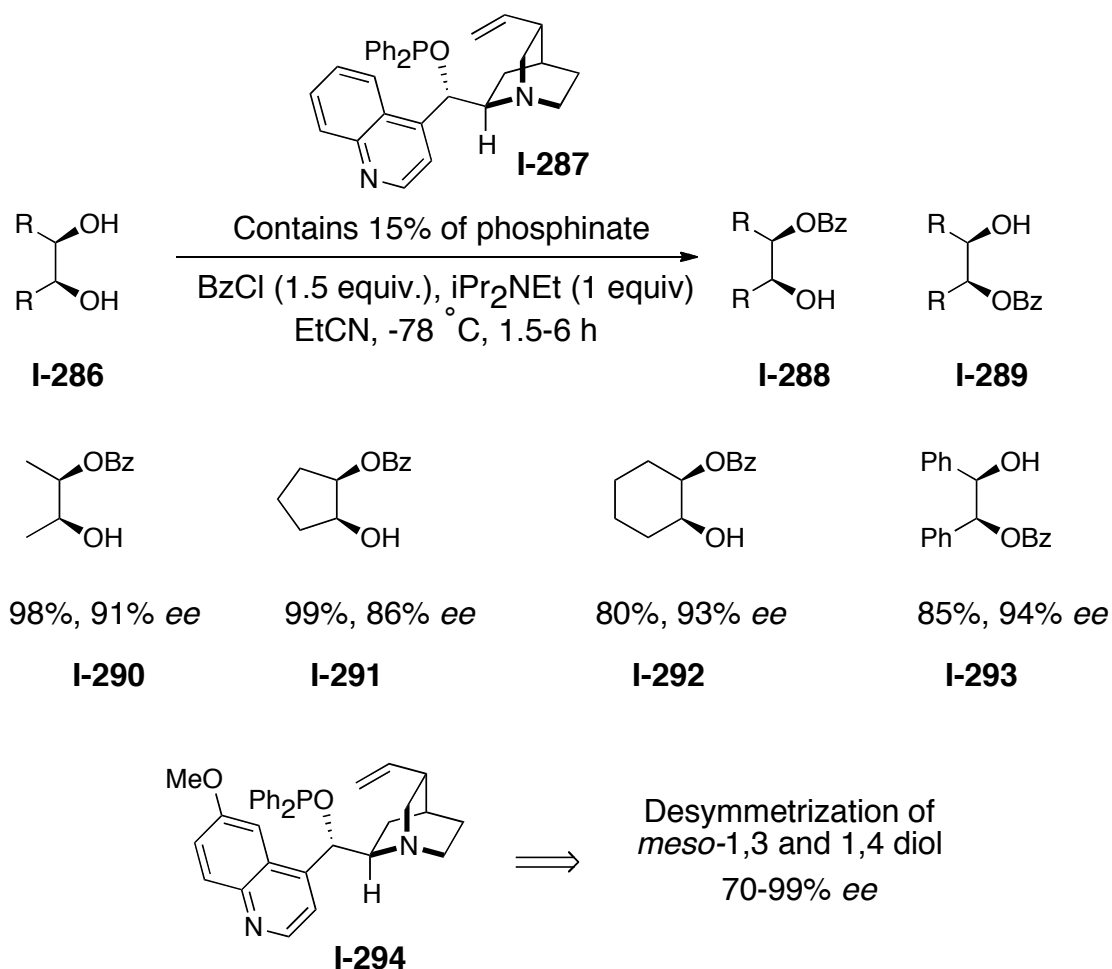
Scheme I-64 Desymmerization of *meso*-diols with
phosphinite cinchona alkaloid derivative

61

1,2-diamine catalysts, chiral phospholane-based catalysts and planar chiral DMAP derivatives.[108,109] Duhmel and coworkers for the first time used cinchona alkaloids in the desymmetrization of *meso* diols, achieving up to 47%*ee* by using *O*-benzoylquinidine.[110] In 2003, Yamamoto and coworkers improved the enantioselectivity of their diol desymmetrization by using a phosphinite derivative of cinchonine **I-287** as the catalyst. In this desymmetrization a range of 1,2-*meso*-diols were mono protected with benzoyl chloride in the presence of the 15 mol% of phosphinite catalyst in high chemical and optical yield (Scheme I-65). The authors propose that the reaction is initiated through the activation of the acylating reagent (benzoyl chloride) by the trivalent Lewis basic phosphinite group.[111] They were also able to use the same methodology for the desymmetrization of the *meso*-1,3 and 1,4-diols by using the phosphinite catalyst **I-294**.[112]

1.4.8.3 Desymmetrization of *meso*-Cyclic Anhydride

The resulting hemiesters obtained from the stereoselective alcoholysis of anhydrides are versatile intermediates in the synthesis of many bioactive compounds.[113-115] As a result a large amount of effort has been devoted to this class of desymmetrization through enzymatic and nonenzymatic catalytic systems.[108] To date cinchona alkaloid- based catalysts have proved to be the most efficient chiral organocatalysts in desymmetrization of *meso*-cyclic anhydrides. In 1985 Oda *et al.* found that natural cinchona alkaloids, cinchonine, quinidine, cinchonidine and quinine, can catalyze the methanolytic desymmetrization of *cis*-2,4-dimethyl glutaric anhydride **I-295**. In the case of using cinchonine as a catalyst they obtained the desired hemiester
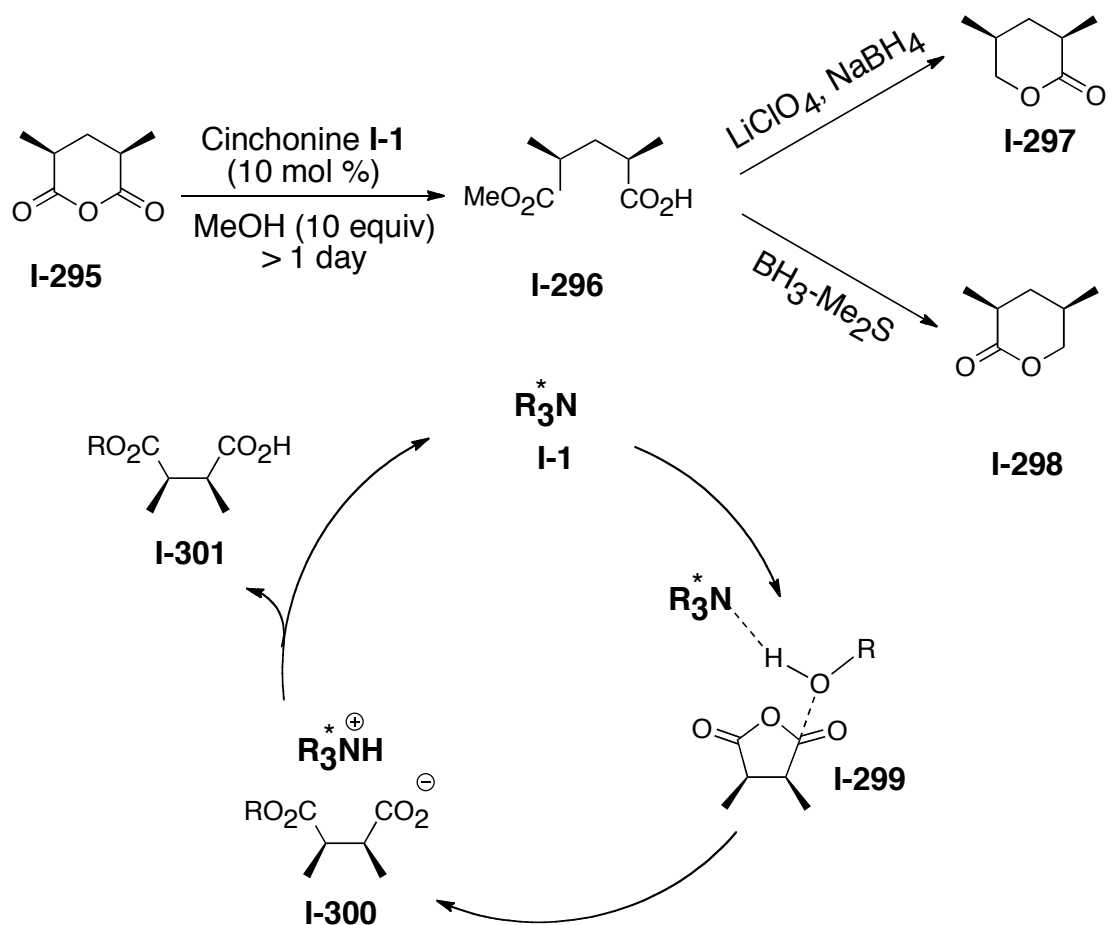
Scheme I-65 Desymmetrization of *meso*-cyclic anhydride with cinchonine and the proposed mechanism by Oda

I-296 in high yield but moderate *ee* (70%).[116] Further more the hemiester **I-296** was easily converted to the lactone **I-297** and its enantiomer **I-298** by selective reduction of either the carbonyl group of the ester or acid.[117]

In 1999 Bolm and coworkers reported the more efficient but not very practical protocol for the enantioselective desymmetrization of *meso*-cyclic anhydrides. After optimization of the reaction they found that in the presence of 110 mol% quinidine a

range of different *meso*-cyclic anhydrides underwent alcoholysis to give methyl hemiesters in 61-99% yield and 85-99% *ee*.[118] Due to the impractical 110 mol% catalyst loading, they tried to reduce the amount of the quinidine to 10-mol%. In the presence of the 10-mol% catalyst they realized a dramatic drop in *ee* and conversion. They found that by adding a base additive, the protonated quinidine gets activated again and comes back to the cycle. After exhaustively screening different tertiary amines, pempiridine was found to be the ideal base additive. Thus in the presence of the 10 mol% quinidine and 1 equiv. pempiridine at -55 °C, they could desymmetrize different *meso*-cyclic anhydrides in high enantioselectivity and conversion in six days (Scheme I-66).[118-120]
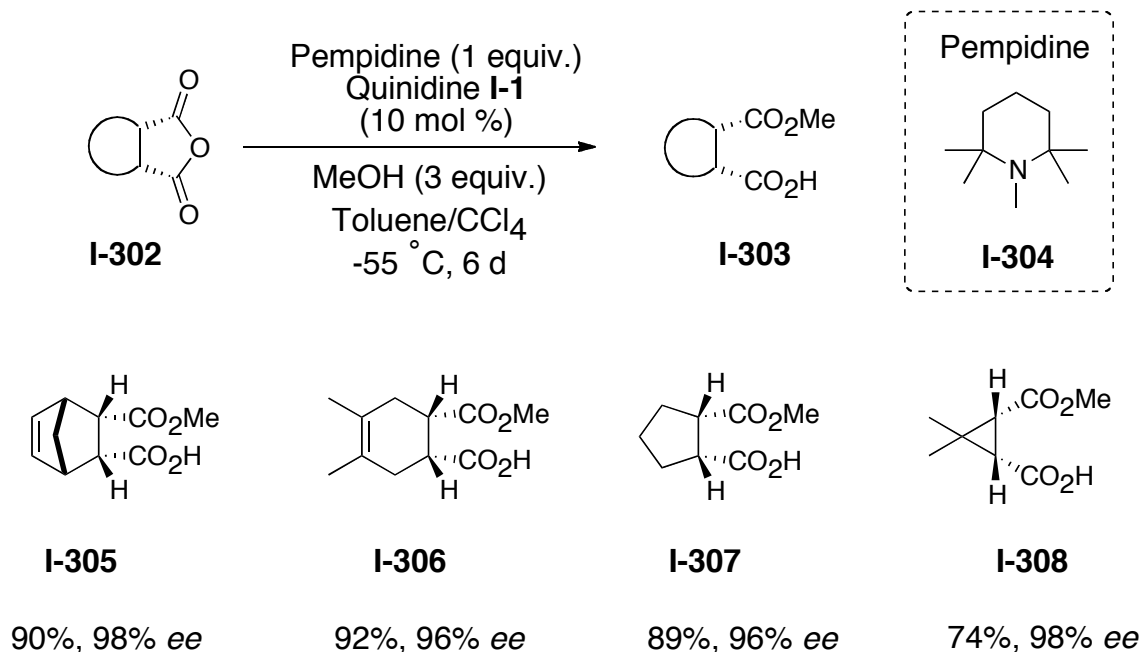
Scheme I-66 Desymmetrization of *meso*-cyclic anhydride with quinidine and pempidine as an additive

64

Although Bolm and coworkers improved their methodology, they could not increase the rate of the reaction to overcome the long reaction times. In 2008, The song and Connon groups, independently, overcame this drawback by using bifunctional cinchona-based thiourea catalyst **I-309**. It was proposed by the authors that this class of bifunctional catalyst could activate the nucleophile by its basic quinoclidine moiety and also at the same time activate the anhydride (electrophile) by double hydrogen bonding with its thiourea moiety (Scheme I-67). After optimizing the condition they desymmetrized a range of anhydrides smoothly at room temperature in high chemical and optical yield in the presence of 1-to 10-mol% catalyst.[121-123]

1.4.8.4. Dynamic Kinetic Resolution of Racemic *N*-Cyclic Anhydride

Deng and coworkers reported the kinetic resolution of the *N*-urethane protected *N*-carboxyanhydrides by methanolysis in the presence of (DHQD)$_2$AQN **I-168** in order to
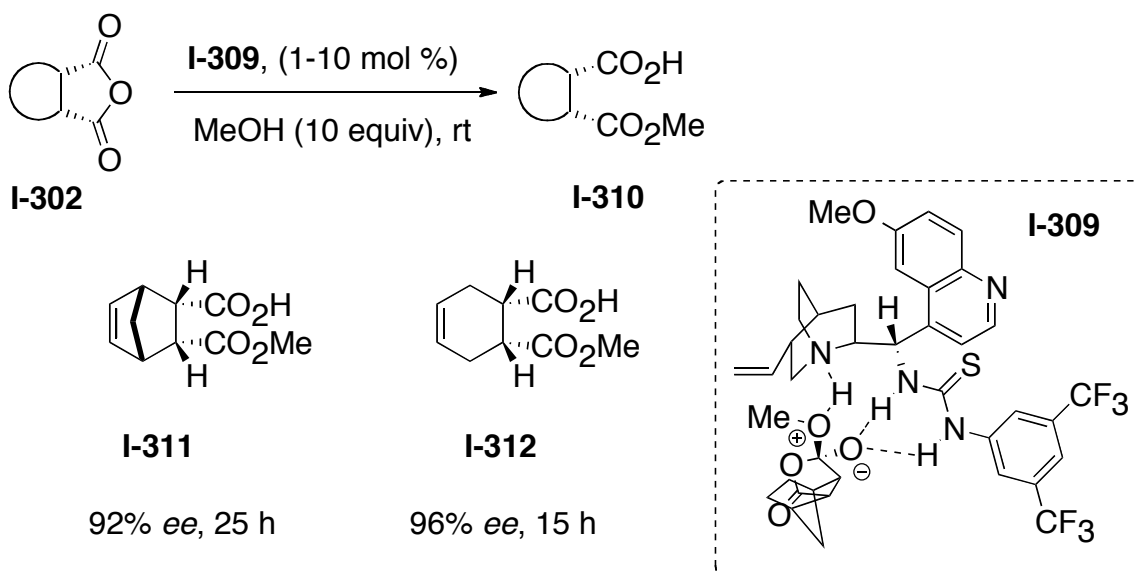
Scheme I-67 Desymmetrization of *meso*-cyclic anhydride with cinchona-based thiourea catlalyst
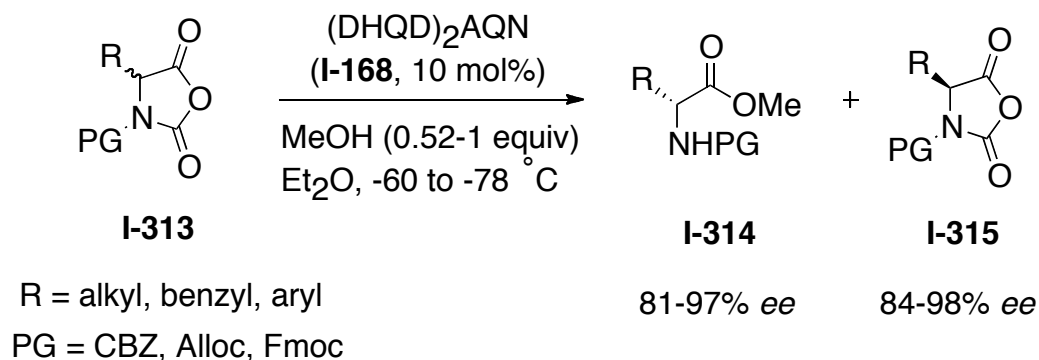
Scheme I-68 Kinetic resolution of racemic *N*-cyclic anhydride

synthesize enantiomerically pure α-amino acids (Scheme I-68). They resolved a range

of racemic substrates **I-313** to the *N*-protected α-amino esters **I-314** (up to 97% *ee*),

leaving the unreacted (*S*) **I-315** starting material that was enriched to 98% *ee*.[124]

Later on they found that by increasing the temperature, the racemization of the 5-

aryl *N*-carboxy anhydrides proceeds fast enough to enable dynamic kinetic resolution.

By using (DHQD)$_2$AQN, they achieved highly efficient dynamic kinetic resolution with

high enantioselectivity and almost quantitative conversion to the desired

enantioenriched amino esters **I-317** (Scheme I-69).[125]

The authors propose the dual role for (DHQD)$_2$AQN as depicted in Scheme I-69. In

this proposed mechanism the catalyst acts as a general base to racemize the *N*-

carboxy anhydrides and also activate the nucleophile (R"OH).

1.5. Summary

This chapter described the current stage in the application of cinchona alkaloid in

organocatalysis and also highlighted their key features responsible for their success.

Cinchona alkaloids in general, are readily available, relatively inexpensive and can be

modified easily to access catalyst with desired functionality. These valuable key features were highlighted by some examples of their application in oxidation, reduction, nucleophilic α–substitution of carbonyl derivatives, enantioselective protonation, cycloaddition, nucleophilic conjugate addition to electron deficient C=C double bonds, nucleophilic 1,2 addition to C=O and C=N bonds, desymmetrization and kinetic resolution. Despite the scientific achievements that have been made in this field, only a
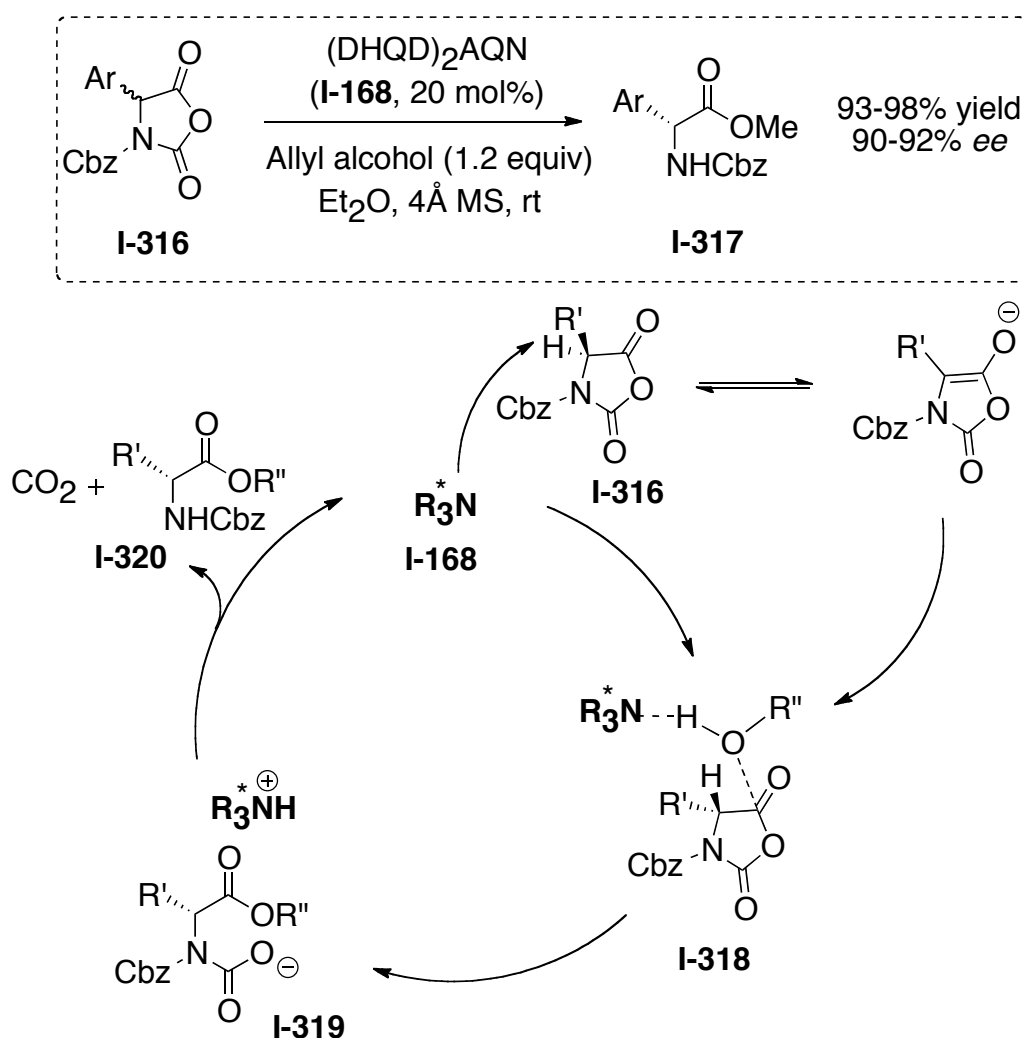
Scheme I-69 Dynamic kinetic resolution of racemic *N*-cyclic anhydride and dual catalytic role of (DHQD)$_2$AQN

few such reactions have reached the level of synthetic practicability. Thus, more systematic mechanistic studies are vital to lead us to more efficient and practical systems. It has been shown recently by Borhan group, followed by some other groups, that cinchona alkaloids can also be used in halocyclization reactions. In next three chapters, extensive mechanistic studies on our chlorolactonization have been presented in order to design more efficient and practical systems in near future.

REFERENCES

REFERENCES:

1.   Garfield, S. *Mauve*; Faber &Faber: London, 2000.

2.   Garnier, J. M.; Robin, S.; Rousseau, G. *European Journal of Organic Chemistry* **2007**, 3281.

3.   Song, C. E. *Cinchona Alkaloids in synthesis and catalysis*; WILEY-VCH: Weinheim, 2009.

4.   Pasteur, L. *Academy of Science* **1853**, *37*, 162.

5.   Pasteur, L. *Liebigs Annalen der Chemie* **1853**, *88*, 209.

6.   Jacques, J., Collet, A., and Wilen, S. H *Enantiomers, Racemates and Resolutions*; John Wiley & Sons, Inc., 1981.

7.   Bredig, G.; Fiske, P. S. *Biochemische Zeitschrift* **1912**, *46*, 7.

8.   Bredig, G.; Minaeff, M. *Biochemische Zeitschrift* **1932**, *249*, 241.

9.   Pracejus, H. *Annalen Der Chemie-Justus Liebig* **1960**, *634*, 9.

10.   Pracejus, H.; Matje, H. *Journal Fur Praktische Chemie* **1964**, *24*, 195.

11.   Wynberg, H. *Topics in Stereochemistry* **1986**, *16*, 87.

12.   Wynberg, H.; Staring, E. G. J. *Journal of the American Chemical Society* **1982**, *104*, 166.

13.   Johnson, R. A. a. S., K. B. *in Catalytic Asymmetric Synthesis*; 2nd ed.; Wiley & Sons, Inc.: New York, 2000.

14.   Kolb, H. C. *In Transition Metals for Organic Synthesis*; Wiley-VCH Verlag Gmbh: Weinheim, 1998; Vol. 2.

15.   Kolb, H. C.; Vannieuwenhze, M. S.; Sharpless, K. B. *Chemical Reviews* **1994**, *94*, 2483.

16.   Iwabuchi, Y.; Nakatani, M.; Yokoyama, N.; Hatakeyama, S. *Journal of the American Chemical Society* **1999**, *121*, 10219.

17. Conn, R. S. E.; Lovell, A. V.; Karady, S.; Weinstock, L. M. *Journal of Organic Chemistry* **1986**, *51*, 4710.

18. Doyle, A. G.; Jacobsen, E. N. *Chemical Reviews* **2007**, *107*, 5713.

19. Mukherjee, S.; Yang, J. W.; Hoffmann, S.; List, B. *Chemical Reviews* **2007**, *107*, 5471.

20. Erkkila, A.; Majander, I.; Pihko, P. M. *Chemical Reviews* **2007**, *107*, 5416.

21. Helder, R.; Hummelen, J. C.; Laane, R.; Wiering, J. S.; Wynberg, H. *Tetrahedron Letters* **1976**, 1831.

22. Wynberg, H.; Greijdanus, B. *Journal of the Chemical Society-Chemical Communications* **1978**, 427.

23. Arai, S.; Tsuge, H.; Oku, M.; Miura, M.; Shioiri, T. *Tetrahedron* **2002**, *58*, 1623.

24. Arai, S.; Tsuge, H.; Shioiri, T. *Tetrahedron Letters* **1998**, *39*, 7563.

25. Lygo, B.; Wainwright, P. G. *Tetrahedron Letters* **1998**, *39*, 1599.

26. Lygo, B.; Wainwright, P. G. *Tetrahedron* **1999**, *55*, 6289.

27. Corey, E. J.; Zhang, F. Y. *Organic Letters* **1999**, *1*, 1287.

28. Berkessel, A.; Guixa, M.; Schmidt, F.; Neudoerfl, J. M.; Lex, J. *Chemistry-A European Journal* **2007**, *13*, 4483.

29. Alcaraz, L.; Macdonald, G.; Ragot, J. P.; Lewis, N.; Taylor, R. J. K. *Journal of Organic Chemistry* **1998**, *63*, 3526.

30. Macdonald, G.; Alcaraz, L.; Lewis, N. J.; Taylor, R. J. K. *Tetrahedron Letters* **1998**, *39*, 5433.

31. Dorow, R. L.; Tymonko, S. A. *Tetrahedron Letters* **2006**, *47*, 2493.

32. Wang, X.; Reisinger, C. M.; List, B. *Journal of the American Chemical Society* **2008**, *130*, 6070.

33. Lu, X.; Liu, Y.; Sun, B.; Cindric, B.; Deng, L. *Journal of the American Chemical Society* **2008**, *130*, 8134.

34.   Sweeney, J. B. *Chemical Society Reviews* **2002**, *31*, 247.

35.   Tanner, D. *Angewandte Chemie-International Edition in English* **1994**, *33*, 599.

36.   Aires-de-Sousa, J.; Prabhakar, S.; Lobo, A. M.; Rosa, A. M.; Gomes, M. J. S.; Corvo, M. C.; Williams, D. J.; White, A. J. P. *Tetrahedron-Asymmetry* **2002**, *12*, 3349.

37.   AiresdeSousa, J.; Lobo, A. M.; Prabhakar, S. *Tetrahedron Letters* **1996**, *37*, 3183.

38.   Murugan, E.; Siva, A. *Synthesis-Stuttgart* **2005**, 2022.

39.   Balcells, J.; Colonna, S.; Fornasier, R. *Synthesis-Stuttgart* **1976**, 266.

40.   Colonna, S.; Fornasier, R. *Journal of the Chemical Society-Perkin Transactions 1* **1978**, 371.

41.   Drew, M. D.; Lawrence, N. J.; Watson, W.; Bowles, S. A. *Tetrahedron Letters* **1997**, *38*, 5857.

42.   List, B. *Accounts of Chemical Research* **2004**, *37*, 548.

43.   Taylor, M. S.; Jacobsen, E. N. *Angewandte Chemie-International Edition* **2006**, *45*, 1520.

44.   Dehmlow, E. V. a. D. S. S. *Phase Transfer Catalysis*; 3rd ed.; Wiley-VCH Verlag GmbH: Weinheim, 1993.

45.   Sasson, Y. a. N., R. *Handbook of Phase-Transfer Catalysis*; Blackie Academic & Professional: London, 1997.

46.   O' Donnell, M. J., Esikova, I.A., Mi, A., Shullenberger, D. F., and Wu, S. *In Phase-Transfer Catalysis: Mechanism and Synthesis*; American Chemical Society: Washington, DC, 1997.

47.   O'Donnell, M. J. *In Catalytic Asymmetric Synthesis*; 2nd ed.; Wiley-VCH Verlag GmbH, : New York, 2000.

48.   Rabinovitz, M.; Cohen, Y.; Halpern, M. *Angewandte Chemie-International Edition in English* **1986**, *25*, 960.

49.   Dolling, U. H.; Davis, P.; Grabowski, E. J. J. *Journal of the American Chemical Society* **1984**, *106*, 446.

50. Dehmlow, E. V.; Duttmann, S.; Neumann, B.; Stammler, H. G. *European Journal of Organic Chemistry* **2002**, 2087.

51. Moss, T. A.; Fenwick, D. R.; Dixon, D. J. *Journal of the American Chemical Society* **2008**, *130*, 10076.

52. Poulsen, T. B.; Bernardi, L.; Bell, M.; Jorgensen, K. A. *Angewandte Chemie-International Edition* **2006**, *45*, 6551.

53. Poulsen, T. B.; Bernardi, L.; Aleman, J.; Overgaard, J.; Jorgensen, K. A. *Journal of the American Chemical Society* **2007**, *129*, 441.

54. Masui, M.; Ando, A.; Shioiri, T. *Tetrahedron Letters* **1988**, *29*, 2835.

55. Shibata, N.; Suzuki, E.; Asahi, T.; Shiro, M. *Journal of the American Chemical Society* **2001**, *123*, 7001.

56. Shibata, N.; Suzuki, E.; Takeuchi, Y. *Journal of the American Chemical Society* **2000**, *122*, 10728.

57. Aleman, J.; Richter, B.; Jorgensen, K. A. *Angewandte Chemie-International Edition* **2007**, *46*, 5515.

58. Acocella, M. R.; Mancheno, O. G.; Bella, M.; Jorgensen, K. A. *Journal of Organic Chemistry* **2004**, *69*, 8165.

59. Ramirez, J.; Huber, D. P.; Togni, A. *Synlett* **2007**, 1143.

60. Fukuzumi, T.; Shibata, N.; Sugiura, M.; Nakamura, S.; Toru, T. *Journal of Fluorine Chemistry* **2006**, *127*, 548.

61. Thierry, B.; Audouard, C.; Plaquevent, J. C.; Cahard, D. *Synlett* **2004**, 856.

62. Wack, H.; Taggi, A. E.; Hafez, A. M.; Drury, W. J.; Lectka, T. *Journal of the American Chemical Society* **2001**, *123*, 1531.

63. Dogo-Isonagie, C.; Bekele, T.; France, S.; Wolfer, J.; Weatherwax, A.; Taggi, A. E.; Lectka, T. *Journal of Organic Chemistry* **2006**, *71*, 8946.

64. Pihko, P. M.; Pohjakallio, A. *Synlett* **2004**, 2115.

65. Saaby, S.; Bella, M.; Jorgensen, K. A. *Journal of the American Chemical Society* **2004**, *126*, 8120.

66.   Liu, T.-Y.; Cui, H.-L.; Zhang, Y.; Jiang, K.; Du, W.; He, Z.-Q.; Chen, Y.-C. *Organic Letters* **2007**, *9*, 3671.

67.   Sobhani, S.; Fielenbach, D.; Marigo, M.; Wabnitz, T. C.; Jorgensen, K. A. *Chemistry-a European Journal* **2005**, *11*, 5689.

68.   Duhamel, L.; Duhamel, P.; Plaquevent, J. C. *Tetrahedron-Asymmetry* **2004**, *15*, 3653.

69.   Eames, J.; Weerasooriya, N. *Tetrahedron-Asymmetry* **2001**, *12*, 1.

70.   Fehr, C. *Angewandte Chemie-International Edition in English* **1996**, *35*, 2567.

71.   Duhamel, L. *Comptes Rendus Hebdomadaires Des Seances De L Academie Des Sciences Serie C* **1976**, *282*, 125.

72.   Takeuchi, S.; Miyoshi, N.; Hirata, K.; Hayashida, H.; Ohgo, Y. *Bulletin of the Chemical Society of Japan* **1992**, *65*, 2001.

73.   Poisson, T.; Dalla, V.; Marsais, F.; Dupas, G.; Oudeyer, S.; Levacher, V. *Angewandte Chemie-International Edition* **2007**, *46*, 7090.

74.   Tille, A.; Pracejus, H. *Chemische Berichte-Recueil* **1967**, *100*, 196.

75.   Pracejus, H.; Tille, A. *Chemische Berichte-Recueil* **1963**, *96*, 854.

76.   Pracejus, H.; Kohl, G. *Annalen Der Chemie-Justus Liebig* **1969**, *722*, 1.

77.   Blake, A. J.; Friend, C. L.; Outram, R. J.; Simpkins, N. S.; Whitehead, A. J. *Tetrahedron Letters* **2001**, *42*, 2877.

78.   Pracejus, H.; Wilcke, F. W.; Hanemann, K. *Journal Fur Praktische Chemie* **1977**, *319*, 219.

79.   Henze, R.; Duhamel, L.; Lasne, M. C. *Tetrahedron-Asymmetry* **1997**, *8*, 3363.

80.   Wang, Y.-Q.; Song, J.; Hong, R.; Li, H.; Deng, L. *Journal of the American Chemical Society* **2006**, *128*, 8156.

81.   Marckwald, W. *Berichte Der Deutschen Chemischen Gesellschaft* **1904**, *37*, 349.

82.   Marckwald, W. *Berichte Der Deutschen Chemischen Gesellschaft* **1904**, *37*, 1368.

83.   Brunner, H.; Schmidt, P. *European Journal of Organic Chemistry* **2000**, 2119.

84.   Amere, M.; Lasne, M.-C.; Rouden, J. *Organic Letters* **2007**, *9*, 2621.

85.   Ando, A.; Miura, T.; Tatematsu, T.; Shiori, T. *Tetrahedron Letters* **1993**, *34*, 1507.

86.   Nagao, H.; Yamane, Y.; Mukaiyama, T. *Chemistry Letters* **2007**, *36*, 8.

87.   Kawahara, S.; Nakano, A.; Esumi, T.; Iwabuchi, Y.; Hatakeyama, S. *Organic Letters* **2003**, *5*, 3103.

88.   Shi, M.; Xu, Y. M. *Angewandte Chemie-International Edition* **2002**, *41*, 4507.

89.   Shi, M.; Xu, Y. M.; Shi, Y. L. *Chemistry-a European Journal* **2005**, *11*, 1794.

90.   Balan, D.; Adolfsson, H. *Tetrahedron Letters* **2003**, *44*, 2521.

91.   Hermann, K.; Wynberg, H. *Journal of Organic Chemistry* **1979**, *44*, 2238.

92.   Hiemstra, H.; Wynberg, H. *Journal of the American Chemical Society* **1981**, *103*, 417.

93.   Wynberg, H.; Helder, R. *Tetrahedron Letters* **1975**, 4057.

94.   Corey, E. J.; Noe, M. C.; Xu, F. *Tetrahedron Letters* **1998**, *39*, 5347.

95.   Zhang, F. Y.; Corey, E. J. *Organic Letters* **2000**, *2*, 1097.

96.   Corey, E. J.; Zhang, F. Y. *Organic Letters* **2000**, *2*, 4257.

97.   Bernardi, L.; Lopez-Cantarero, J.; Niess, B.; Jlrgensen, K. A. *Journal of the American Chemical Society* **2007**, *129*, 5772.

98.   Bella, M.; Jorgensen, K. A. *Journal of the American Chemical Society* **2004**, *126*, 5672.

99.   Zu, L.; Wang, J.; Li, H.; Xie, H.; Jiang, W.; Wang, W. *Journal of the American Chemical Society* **2007**, *129*, 1036.

100.   Dalko, P. I.; Moisan, L. *Angewandte Chemie-International Edition* **2004**, *43*, 5138.

101.   K., M. *In Catalytic Asymmetric Synthesis*; Wiley-VCH Verlag GmbH: New York, 2000.

102.   Shen, J.; Tan, C.-H. *Organic & Biomolecular Chemistry* **2008**, *6*, 3229.

103.   Bekele, T.; Shah, M. H.; Wolfer, J.; Abraham, C. J.; Weatherwax, A.; Lectka, T. *Journal of the American Chemical Society* **2006**, *128*, 1810.

104.   Calter, M. A.; Phillips, R. M.; Flaschenriem, C. *Journal of the American Chemical Society* **2005**, *127*, 14566.

105.   Okamura, H.; Nakamura, Y.; Iwagawa, T.; Nakatani, M. *Chemistry Letters* **1996**, 193.

106.   Jen, W. S.; Wiener, J. J. M.; MacMillan, D. W. C. *Journal of the American Chemical Society* **2000**, *122*, 9874.

107.   Chen, W.; Du, W.; Duan, Y.-Z.; Wu, Y.; Yang, S.-Y.; Chen, Y.-C. *Angewandte Chemie-International Edition* **2007**, *46*, 7667.

108.   Garcia-Urdiales, E.; Alfonso, I.; Gotor, V. *Chemical Reviews* **2005**, *105*, 313.

109.   Rendler, S.; Oestreich, M. *Angewandte Chemie-International Edition* **2008**, *47*, 248.

110.   Duhamel, L.; Herman, T. *Tetrahedron Letters* **1985**, *26*, 3099.

111.   Mizuta, S.; Sadamori, M.; Fujimoto, T.; Yamamoto, I. *Angewandte Chemie-International Edition* **2003**, *42*, 3383.

112.   Mizuta, S.; Tsuzuki, T.; Fujimoto, T.; Yamamoto, I. *Organic Letters* **2005**, *7*, 3633.

113.   Atodiresei, L.; Schiffers, I.; Bolm, C. *Chemical Reviews* **2007**, *107*, 5683.

114.   Spivey, A. C.; Andrews, B. I. *Angewandte Chemie-International Edition* **2001**, *40*, 3131.

115.   Tian, S. K.; Chen, Y. G.; Hang, J. F.; Tang, L.; McDaid, P.; Deng, L. *Accounts of Chemical Research* **2004**, *37*, 621.

116.   Hiratake, J.; Yamamoto, Y.; Oda, J. *Journal of the Chemical Society-Chemical Communications* **1985**, 1717.

117. Hiratake, J.; Inagaki, M.; Yamamoto, Y.; Oda, J. *Journal of the Chemical Society-Perkin Transactions 1* **1987**, 1053.

118. Bolm, C.; Schiffers, I.; Dinter, C. L.; Gerlach, A. *Journal of Organic Chemistry* **2000**, *65*, 6984.

119. Bolm, C.; Schiffers, I.; Atodiresei, I.; Hackenberger, C. P. R. *Tetrahedron-Asymmetry* **2003**, *14*, 3455.

120. Bolm, C.; Schiffers, I.; Dinter, C. L.; Defrere, L.; Gerlach, A.; Raabe, G. *Synthesis-Stuttgart* **2001**, 1719.

121. Connon, S. J. *Chemical Communications* **2008**, 2499.

122. Peschiulli, A.; Gun'ko, Y.; Connon, S. J. *Journal of Organic Chemistry* **2008**, *73*, 2454.

123. Rho, H. S.; Oh, S. H.; Lee, J. W.; Lee, J. Y.; Chin, J.; Song, C. E. *Chemical Communications* **2008**, 1208.

124. Hang, J. F.; Tian, S. K.; Tang, L.; Deng, L. *Journal of the American Chemical Society* **2001**, *123*, 12696.

125. Hang, J. F.; Li, H. M.; Deng, L. *Organic Letters* **2002**, *4*, 3321.

Chapter 2: Mechanistic Studies of Asymmetric Chlorolactonization.

2.1: Introduction

In contrast to the large number of known examples of substrate controlled stereoselective halolactonizations,[1,2] *reagent-controlled* processes are rare, and have only begun to attract attention within the last 15 to 20 years. The importance of a successful approach to a reagent-controlled halolactonization are obvious, as such methodology would provide easy access to highly functionalized halolactones in one step from achiral substrates. The first enantioselective halolactonization was reported in 1992 by Taguchi and coworkers when a single alkenoic acid substrate (**II-1**) was cyclized by treatment with iodine and a stoichiometric amount of a chiral titanium complex, generated from titanium (IV) *iso*-propoxide and ligand **II-2**, returning iodolactones **II-3** in 67% yield with 65% *ee* (Scheme II-1, eq. 1).[3] This report was subsequently followed by a number of reports employing stoichiometric or super-stoichiometric amounts of a chiral amine promoter to effect iodolactonization. Nearly all of these methodologies rely upon the formation of a dimeric iodonium salt (*i.e.* [(L*)$_2$I$^+$]Y$^-$, where L* is a chiral amine promoter, and Y is a non-nucleophilic counter ion, see **II-9**).[3-7] Two of the most highly selective variants of this strategy were presented by Wirth[5,6] (eq. 2) and Rousseau[7] (eq. 3). Aside from the obvious disadvantage of committing up to ~5 equivalents of chiral promoter in some cases, these approaches lead to the desired product in poor enantioselectivities (15 to 45% *ee*) and limited substrate scope. It is also important to highlight that all of these methodologies proceed

via an iodocyclization; reports on analogous chloro and bromolactonizations are absent, except for a singular example reported by Cui and Brown where a bromolactone was produced in only 5% *ee* by action of an analogous chiral bromonium/pyridine dimer.[8]

Gao and coworkers reported the first published catalytic protocol whereby *trans*-5-

Taguchi:

$$\text{II-1} \xrightarrow[\substack{\text{Py, iodine} \\ \text{2. PTSA, PhH}}]{\substack{\text{1. Ti(O}i\text{-Pr)}_4 \\ \text{II-2 (1 equiv.)}}} \text{II-3} \qquad (1)$$

67% , *dr* = 58:1, 65% *ee*

Wirth:

$$\text{II-4} \xrightarrow[\text{DCM, -78 }^{\circ}\text{C}]{\text{II-5 (2 equiv.), ICl}} \text{II-6} \qquad (2)$$

82%, 45% *ee*

Rousseau:

$$\text{II-7} \xrightarrow[\text{AgSbF}_6,\ \text{I}_2,\ \text{DCM, -78 }^{\circ}\text{C}]{\substack{\text{N-methylephedrine} \\ \text{(4.8 equiv.)}}} \text{II-8} \qquad (3)$$

92% yield (from I$_2$), 45% *ee*

II-2   II-5   II-9
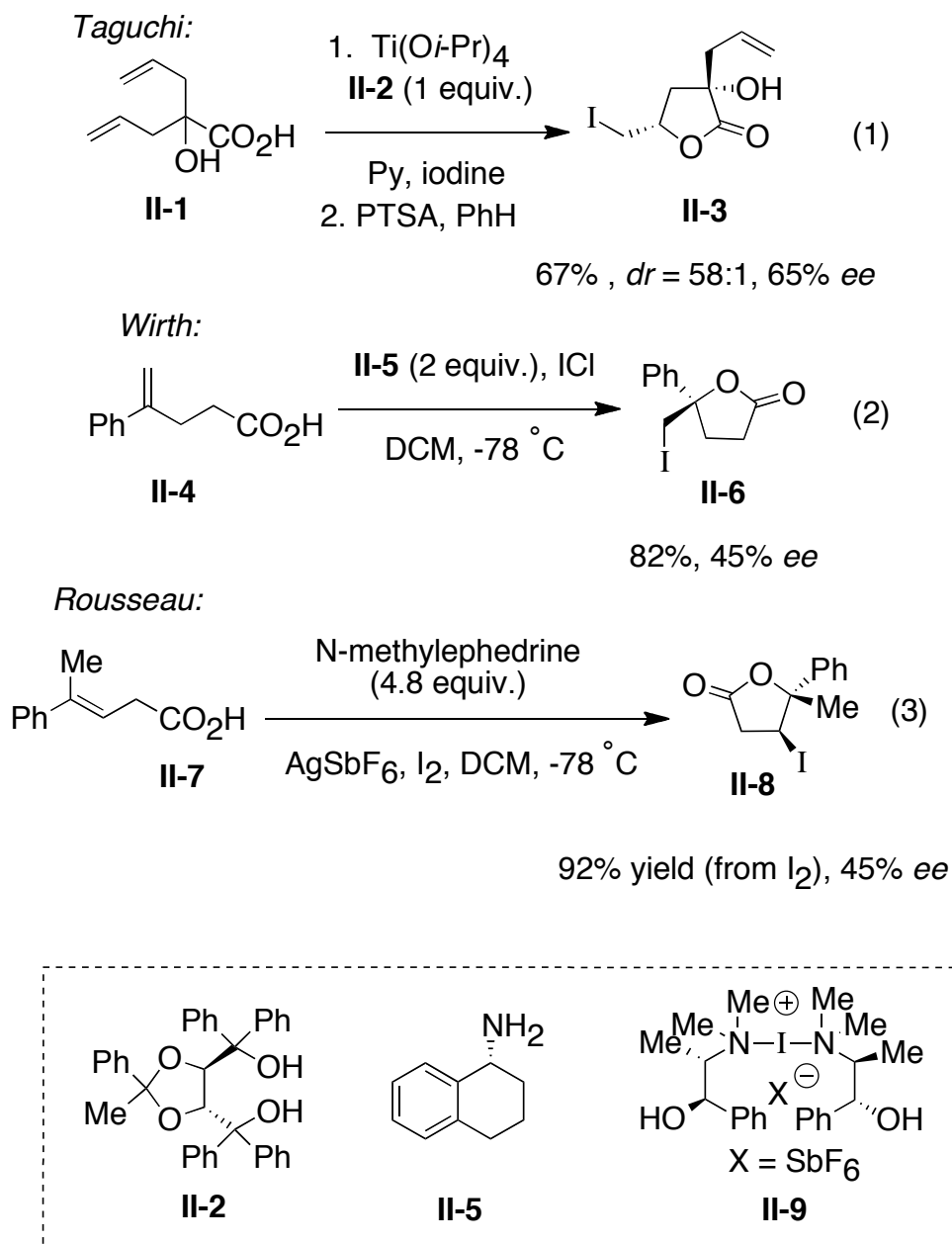
Scheme II-1. Asymmetric halolactonization protocols.

aryl-4-pentenoic acids such as **II-10** were cyclized in the presence of iodine and 30 mol% of a quaternary ammonium salt derived from cinchonidine **II-11** (Scheme II-2).[9,10] The desired iodolactones were returned in nearly a 1:1 ratio of *exo* **II-12** and *endo* **II-13** isomers with marginal enantioselectivities (*exo* = 16% *ee*, *endo* = 31% *ee*). Finally, Braddock and coworkers have attempted to catalyze the formation of chiral bromolactones by action of a chiral amidine organocatalyst, but racemic products were isolated.[11]

To better understand the potential difficulties in controlling the enantioselectivity of the halolactonization and in general all types of halocyclization reactions, we need first to look at their mechanism. The general mechanism of all halocyclizations including halolactonization (Scheme II-3a) involves the formation of a halonium intermediate **II-15**, which then undergoes attack by an intramolecular nucleophile to create a ring **II-16**.[12] The two main challenges (Scheme II-3b) in this class of asymmetric transformations
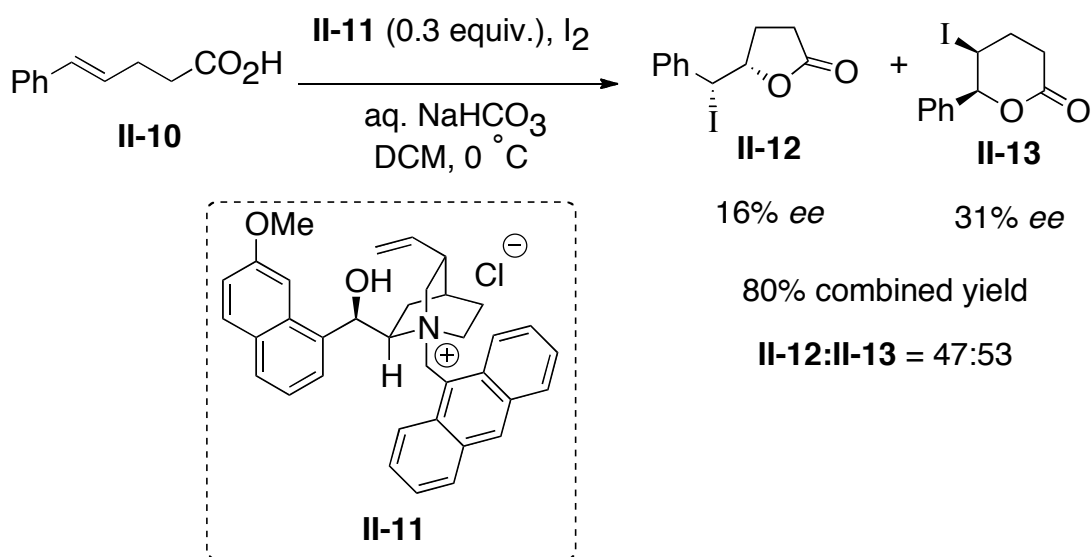
Scheme II-2. Gao's organocatalytic iodolactonization.
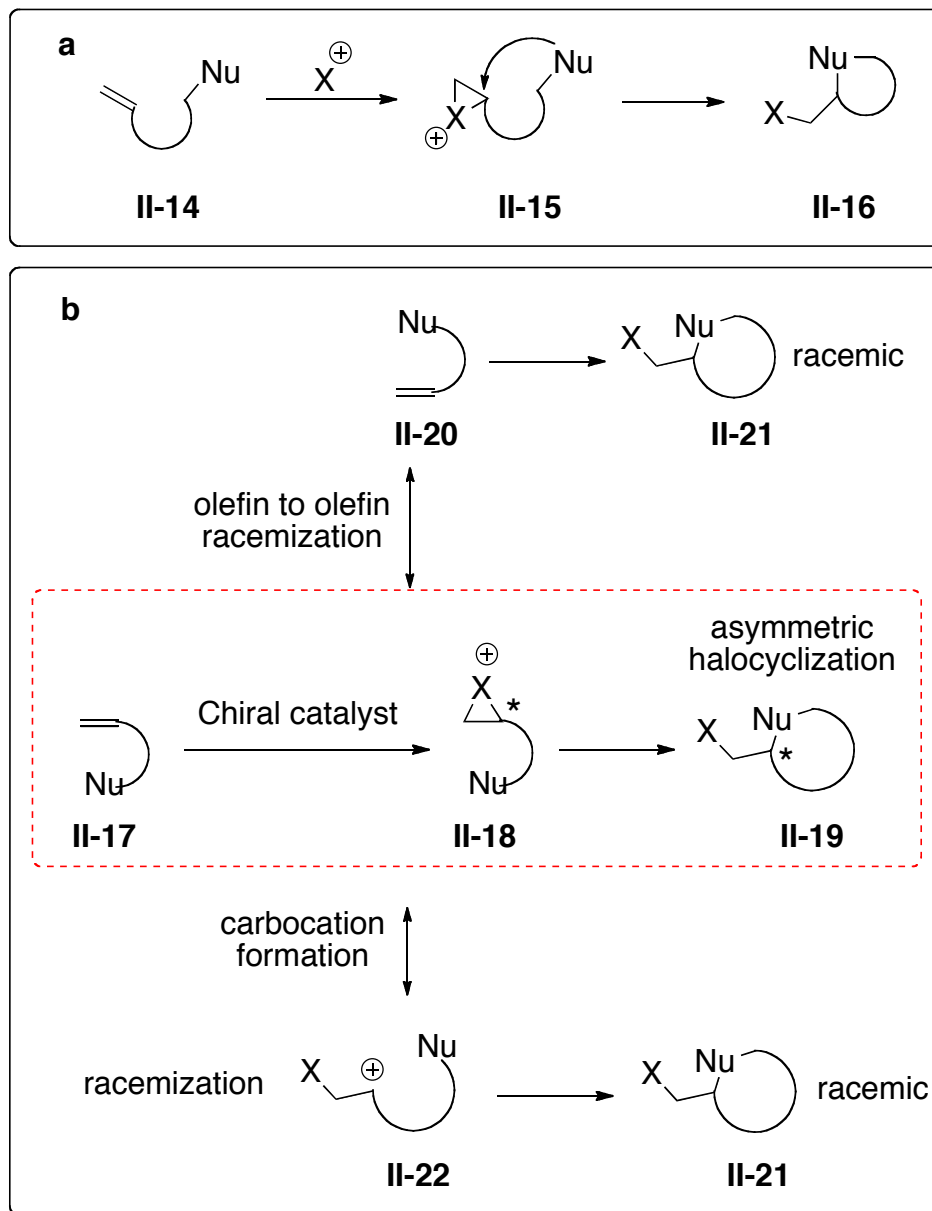
Scheme II-3. (a) General halocyclization mechanism. (b) Main challenges in asymmetric halocyclization.

are: 1) developing an efficient catalyst system, which delivers the halonium to the olefin in an enantioselective fashion (Scheme II-3), and 2) preventing racemization of the resulting chiral halonium, which can be eroded by a process known as olefin- to-olefin
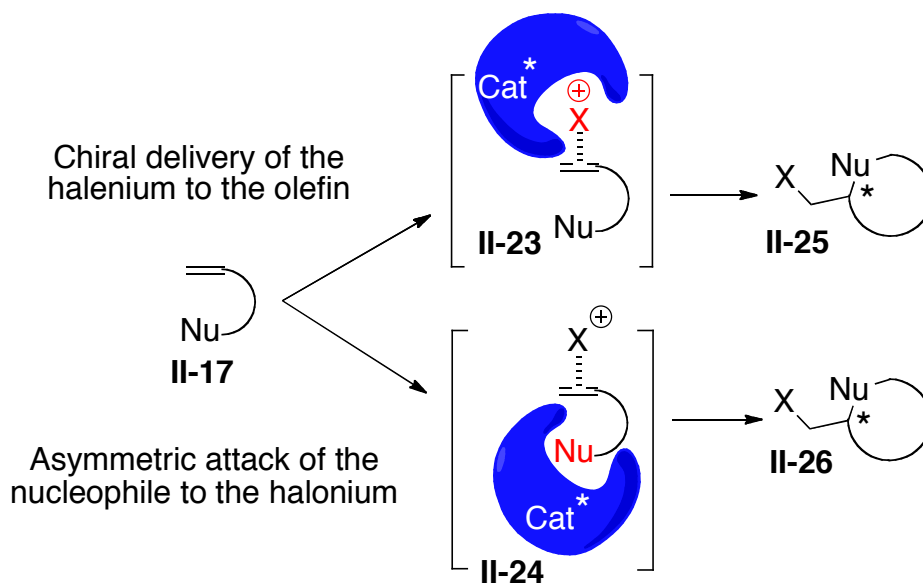
Scheme II-4. Two strategies in getting high enantioselectivity in halocyclization reactions, chiral delivery of the halenium to the olefin and asymmetric attack of the nucleophile to the halonium.

transfer, which was recently demonstrated in elegant work by Denmark and co-workers.[13] Racemization can also occur due to the opening of the chiral halonium intermediate to halocarbenium, especially when fluorine or chlorine is used as a halogen source.

To overcome the first challenge in halocyclization reactions, the halenium source has to be engulfed in a chiral environment to deliver the halenium in an asymmetric fashion to the olefin. This can be achieved by either covalent or noncovalent binding of the halenium source to a chiral catalyst (Scheme II-4). After controlling the enantioselectivity of the halonium formation, racemization needs to be blocked. Covering the halonium intermediate by a bulky group can stop olefin-to-olefin racemization. Chiral catalyst as a bulky moiety **II-23** can do this by staying close to the

halonium intermediate as a counter ion to stop the olefin-to-olefin racemization (Scheme II-4). As mentioned previously, halocarbenium ion formation can also lead to the racemization of the halonium intermediate. Inhibiting this is not easy but the problem (racemic product) can be minimized if a chiral environment around the carbocation intermediate is able to direct the nucleophile in an asymmetric fashion. The presence of the catalyst here again as a counter ion to the carbocation intermediate can lead to discrimination of one side of the carbocation sp^2 carbon by the nucleophile over the other side. In both cases the overall enantioselectivity of the halocyclization reaction is set and controlled in the first step of the reaction, the halenium delivery to the olefin.

In another approach, enantioselectivity of the halocyclization can be controlled in the second step, the ring-closing step. Basically in this approach there is no need to deliver the halenium in an enantioselective manner. By providing a chiral environment around the nucleophile **II-24**, one side of the halonium or halocarbonium intermediate can be discriminated by the chiral nucleophile. To apply this approach the presence of the chiral catalyst close to the nucleophile is needed as depicted in Scheme II-4. The difference between these two approaches is, whether the first step is the enantio-determining step or the second step.

A recent breakthrough in the Borhan laboratory has led to the development of a catalytic, enantioselective chlorolactonization of alkenoic acids **II-27** (Scheme II-5a).[14] We assumed that high enantioselectivity in our chlorolactonization is the consequence of the binding of the chlorine source, hydantoin, to the catalyst, $(DHQD)_2PHAL$. This association between $(DHQD)_2PHAL$ and hydantoin can lead to the delivery of the
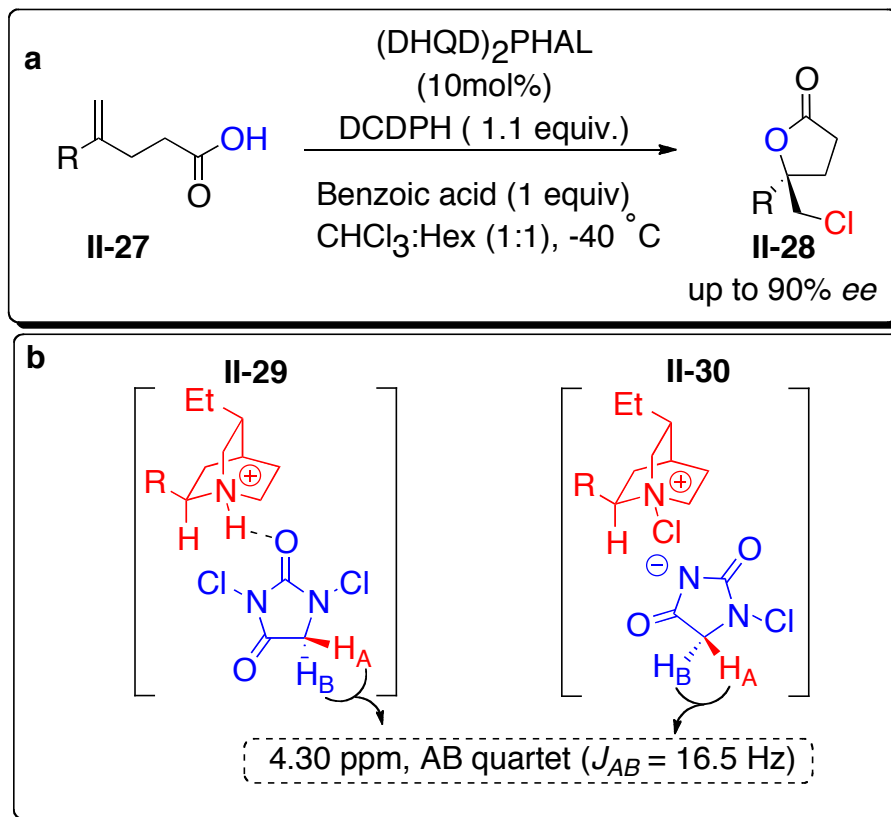
Scheme II-5 (a) Our asymmetric chlorolactonization. (b) Associative complex between hydantoin and (DHQD)$_2$PHAL.

chlorine to the olefin in an asymmetric fashion. The observation of an AB quartet in ^{1}H NMR studies of complexes **II-29** and **II-30** (Scheme II-5b) discussed in detail in Chapter three, supports this hypothesis. This observation leads us to the proposition that asymmetric delivery of the halonium to the olefin in the first step, controls the enantioselectivity of the reaction (Scheme II-4).

Later on in another example, Veitch and Jacobsen reported the highly enantioselective iodolactonization of hexenoic acid derivatives, catalyzed with chiral tertiary aminourea catalysts.[15] The desired iodolactones were obtained (up to 96% *ee*)

in the presence of the chiral tertiary aminourea, *N*-iodoimide **II-32**, and a catalytic amount of I$_2$ (Scheme II-6). Low temperature NMR studies on the mixture of catalyst and *N*-iodoimide **II-32** suggest the formation of complex **II-36** (Scheme II-7)**.** Quench of complex **II-36** with aqueous sodium thiosulfate regenerates catalyst **II-33** as well as the corresponding secondary amine. The secondary amine is presumably formed from complex **II-36** by elimination of HI and subsequent iminium hydrolysis. A proposed mechanism of iodolactonization is depicted in Scheme II-7. Iodination of hexenoic acid **II-31** with the active complex **II-36** leads to the formation of the iodonium intermediate. Subsequent cyclization is proposed to occur as the rate- and enantio-determining step, based on the observation of differing reactivities, under otherwise identical conditions, of pentenoic, hexenoic, and heptenoic acid substrates to generate the corresponding 5-, 6-, and 7- membered lactone products (5 > 6 >> 7). In this proposed mechanism urea-bound phthalimide in complex **II-37** serves as the base in the enantio-determining cyclization step. Moreover, in another mechanistically designed experiment they found
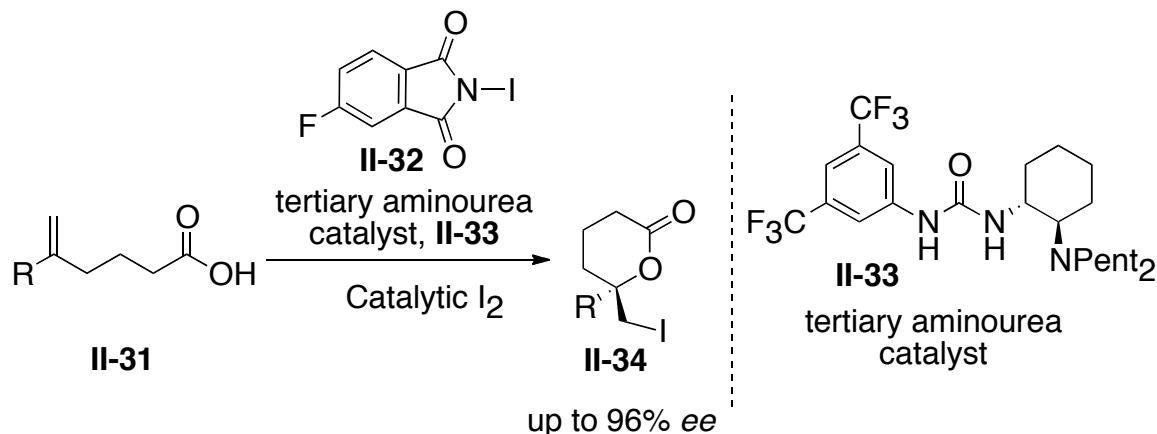
Scheme II-6. Tertiary aminourea catalyzed enantioselective iodolactonization
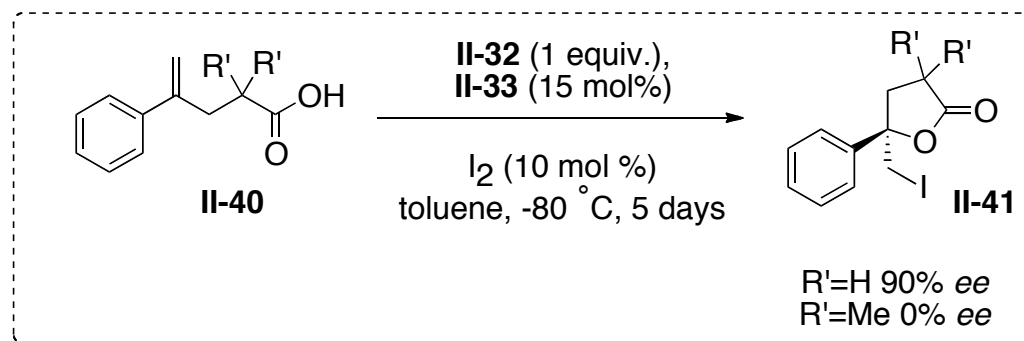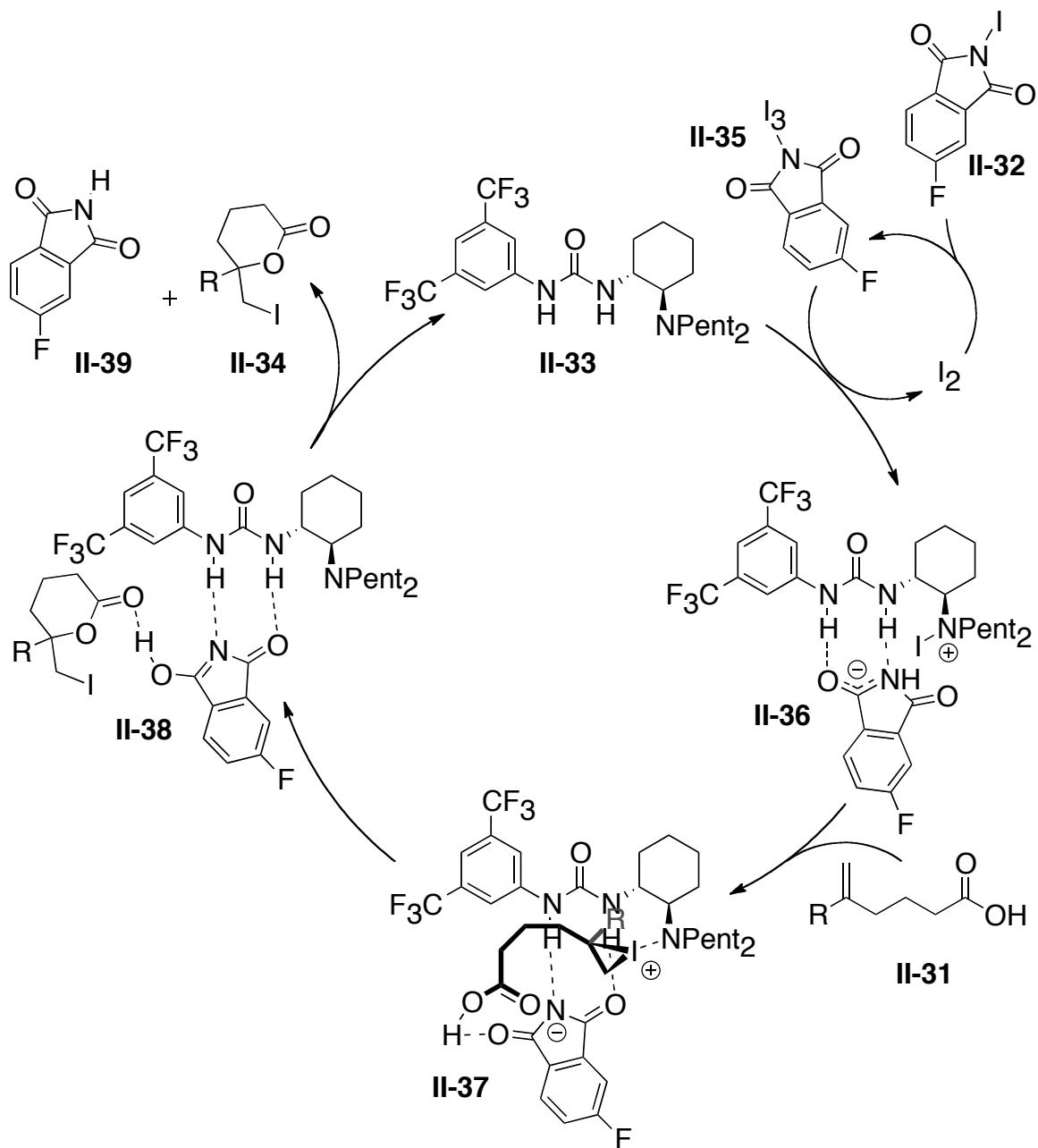
Scheme II-7. Proposed catalytic cycle for iodolactonization

86

that that gem-dimethyl-substituted pentenoic substrate was found to undergo cyclization to give racemic product under the optimized conditions. In general, they proposed that any factor that accelerates the cyclization of the iodonium ion intermediate (**II-37**, Scheme II-7) leads to diminished enantioselectivities. It is believed that increasing the rate of the cyclization step changes the identity of the rate- and enantio-determining step, presumably to the formation of the iodonium ion. The decreased enantioselectivity would then be the result of poor facial selectivity in the iodination of the alkene.

In the same year, 2010, Murai and coworkers reported a highly enantioselective bromolactonization catalyzed by a C_3-symmetric chiral trisimidazoline **II-43**.[16] The desired bromolactones were obtained from a variety of 5-substituted 5-hexenoic acids **II-42** in high optical (72-91%*ee*) and chemical yields (Scheme II-8a). Murai and coworkers propose that asymmetric attack of the nucleophile onto the achiral halonium intermediate, plays a crucial role in their highly enantioselective bromolactonization. By NMR studies they found that three molecules of acid substrate, 5-phenylhex-5-enoic acid, bind to their C3-symmetric chiral trisimidazoline, which provides a chiral environment around the nucleophile (Scheme II-8b). They ruled out the hypothesis of asymmetric bromine delivery to olefin as an enantio-determining step by performing the bromoetherification under the same condition. If the trisimidazoline **II-43** also interacted with NBS or DBDMH, and a complex formed by such an interaction mainly engaged in the reaction, bromocyclization of the alcohol **II-45** should also lead to high enantioselectivity. However, after submitting the alcohol **II-45** to the reaction tetrahydropyran **II-46** was produced in almost racemic form (4% *ee*). It was also
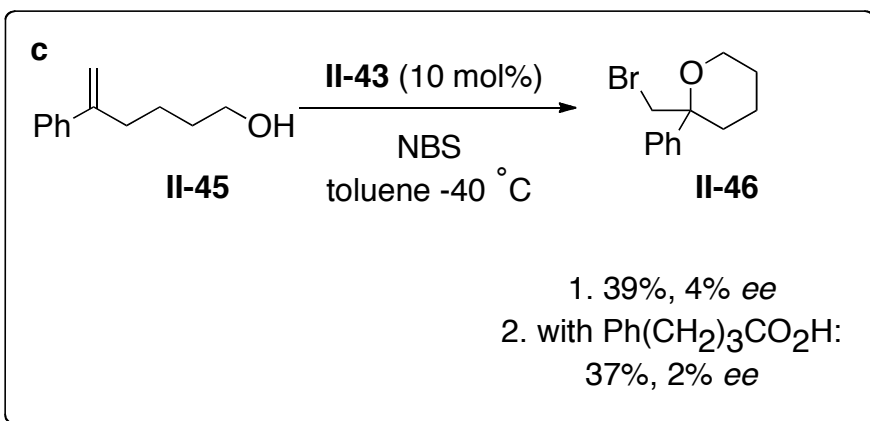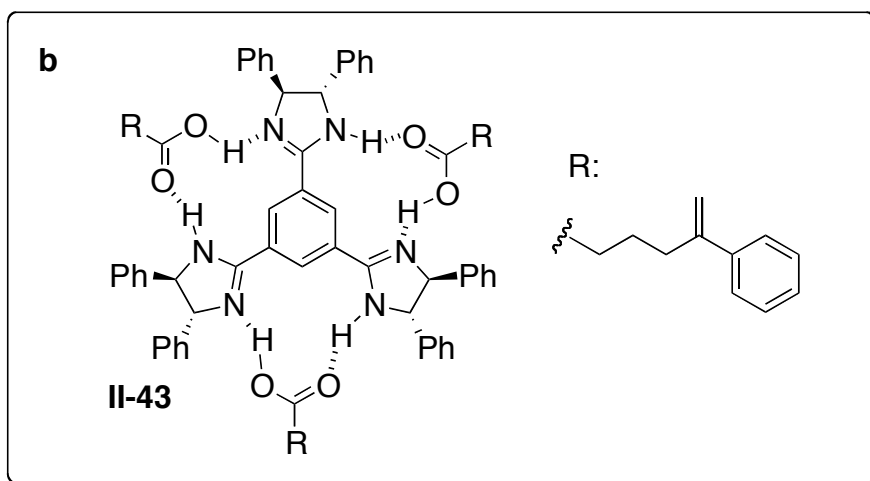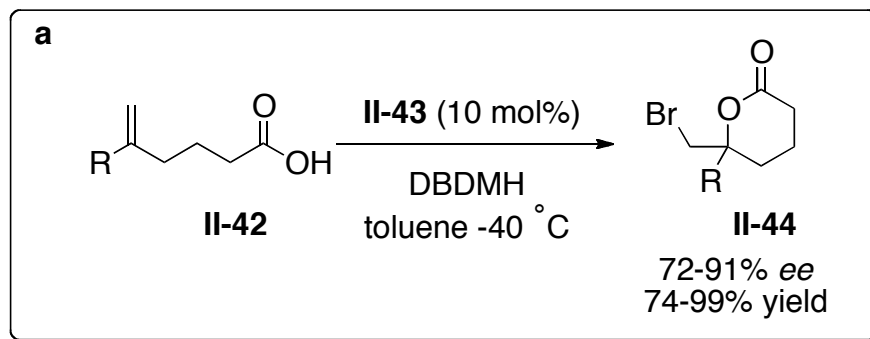
Scheme II-8. a. Asymmetric bromolactonization catalyzed by a C3-symmetric chiral trisimidazoline b. Plausible 1:3 mixture of **II-43** and **II-42** c. Control experiment with alcohol **II-45**

possible that the imidazolium salt generated from **II-43** and a carboxylic acid might function as a proton donor to activate NBS or DBDMH and thus create a chiral environment. In a control experiment (Scheme II-8c) they observed that the bromocyclization of **II-45** in the presence of 4-phenylbutyric acid also gave **II-46** in almost racemic form. Based on these mechanistic studies they proposed that like Jacobsen's iodolactonization, the second step is enantio-determining step in their bromolactonization.

Zhang and coworkers also achieved highly enantioselective bromolactonization of conjugated (*Z*)-enynes (80-99% *ee*) in the presence of bifunctional urea modified cinchona alkaloids catalysts and NBS as the bromine source (Scheme II-9).[17] They proposed that in their methodology NBS is activated by hydrogen bonding with urea moiety and/or protonated quinuclidine. The binding of the bromine source will likely transfer the bromine to the olefin in an asymmetric fashion.

With the growing interest in halocyclizations the importance of detailed mechanistic studies is apparent. In the first part of this chapter we design a labeled substrate to

dr= 10:1 to 20:1
ee = 80% 99%
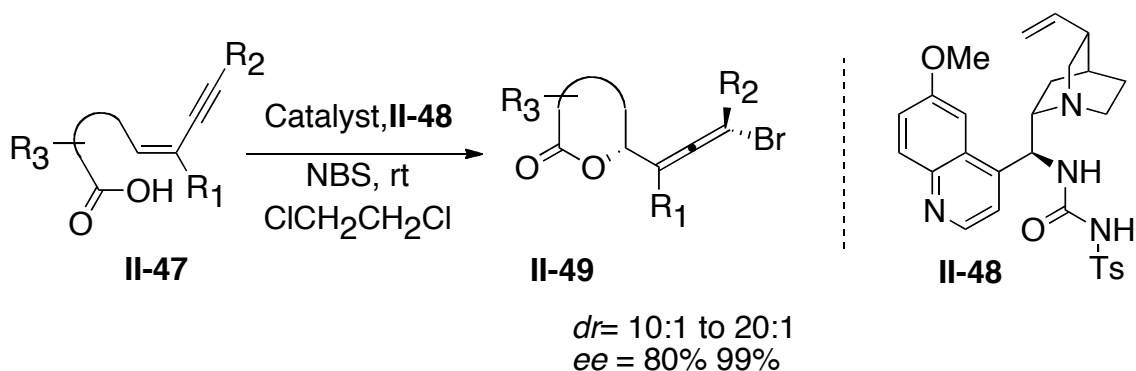
Scheme II-9. Enantioselective bromolactonization of conjugated (Z)-enynes
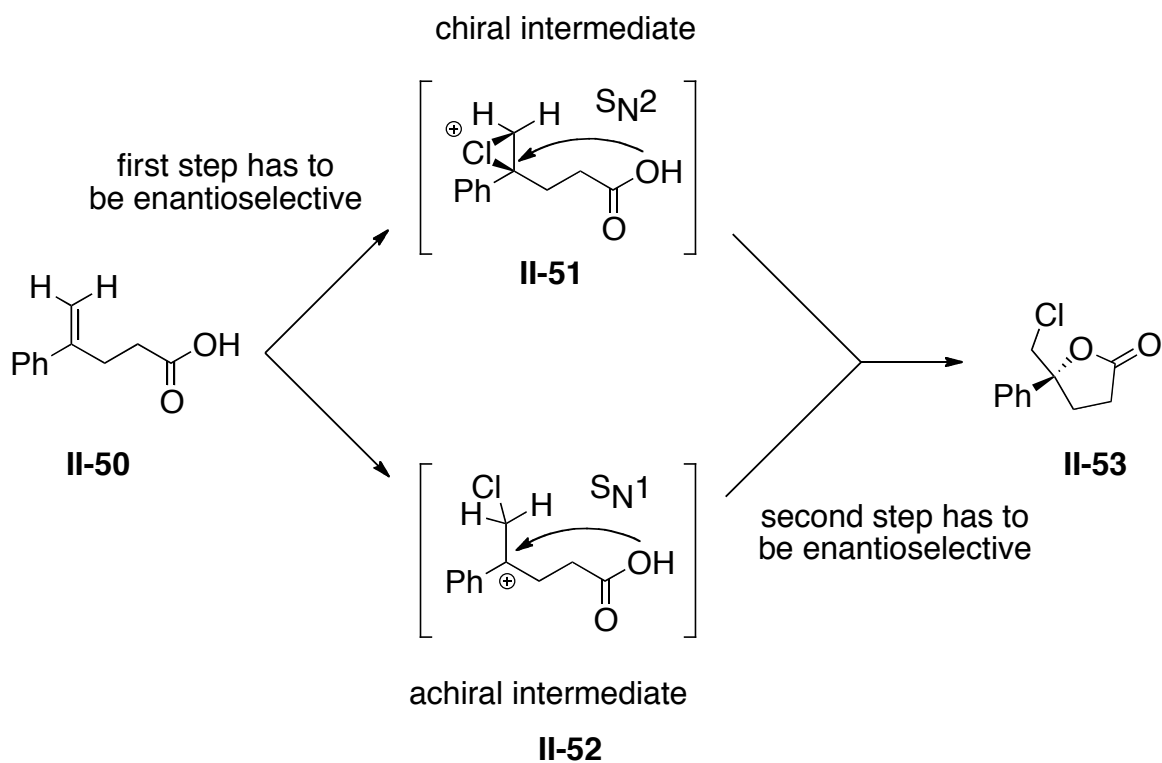
Scheme II-10. The difference between carbocation and chloronium intermediates in the *enantio*-determining step.

distinguish the enantio-determining step of the chlorolactonization reaction. This labeled

substrate is utilized to reveal the nature of the intermediate, halonium vs halocarbonium.

In the second part, extensive kinetics studies will be presented to understand the

mechanism of the reaction and reveal the rate-determining step (RDS) for the

asymmetric chlorolactonization methodology.

2.2: Labeling Studies.

The first step towards understanding the mechanism of the asymmetric

chlorolactonization is to find out whether the chlorolactonization proceeds through the

halocarbonium (Markovnikov-type open form) or the halonium (bridged form) as

singlet, 3.41 ppm   quartet, 6.35 ppm

$$\overset{\oplus}{\underset{Me \quad Me}{Me \ Cl \ H}}$$

II-54

major

doublet, 2.49 ppm

$$Me \overset{\oplus}{Cl} H \quad \rightleftharpoons \quad \underset{Me \quad Me}{\overset{Me}{\oplus}}C \overset{H}{=} C \leftarrow Cl \quad \rightleftharpoons \quad Me \overset{\oplus}{Cl} Me$$

II-55   **II-56**   **II-57**

septet, 6.24 ppm   triplet, 4.23 ppm

$$Cl \rightarrow \underset{H}{\overset{H}{\triangleleft}} \underset{Me}{\overset{Me}{\oplus}}$$

major

II-58
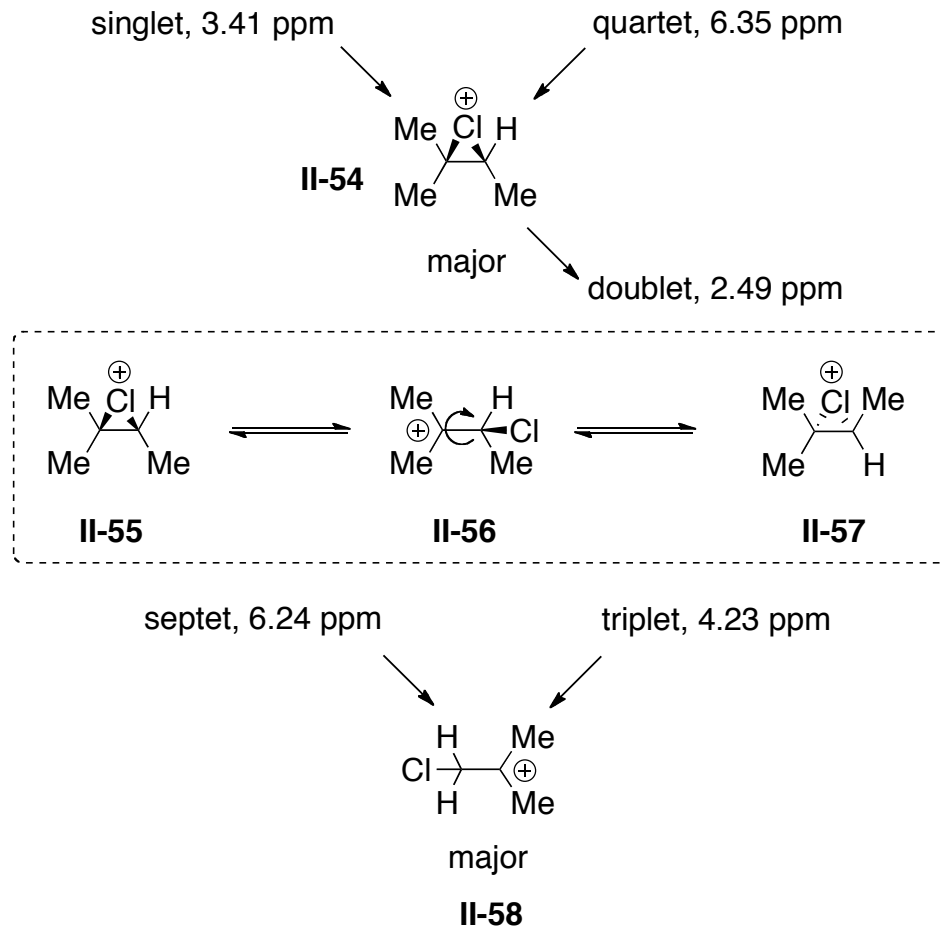
Scheme II-11. Olah's NMR studies on halonium ion formation

depicted in Scheme II-10. Halocyclization of **II-50** leads to a single chiral center since the starting material is a 1,1-disubstituted olefin. It is important to note that chlorine ends up on a non-chiral carbon. If the reaction proceeds through the halocarbonium intermediate, then the enantioselectivity of this reaction is solely controlled by the ring closing, as the absolute stereochemistry (in case of asymmetric delivery of the chlorine to the olefin) is lost by formation of the planar carbocation intermediate. However, if the reaction goes through the chloronium bridge form then the enantioselectivity is

91

controlled by the asymmetric delivery of the chlorine as the oxygen opens the chloronium intermediate through an S_N2 displacement (Scheme II-10).

Olah et al demonstrated through NMR studies that 2,3-dimethyl-2-butene and 2-methyl-2-butene form the chloronium bridge, whereas 2-methylpropene exists in the open halocarbonium form (Scheme II-11).[18,19] For these studies, Olah and co-workers used antimony pentafluoride in sulfur dioxide solution to ionize 2-fluoro-3-chloro-2-methylbutane and 1-chloro-2-fluoro-2-methylpropane at -78 °C. For the case of 2-fluoro-3-choloro-2-methylbutane, observation of a singlet peak around 3.4 ppm could be the result of rapid equilibration of the bridge form to the open form, following by rotation around the C-C bond (Scheme II-11 box). Moreover, the lack of a measurable long-range coupling shows that the concentration of open ion is relatively small. Overall, these results show that with 2-fluoro-3-choloro-2-methylbutane the bridged chloronium **II-54** dominates. When 1-chloro-2-fluoro-2-methylpropane was ionized, long-range coupling between methyl and methylene protons through the planar sp^2-hybridized carbonium ion carbon atom was observed **II-58**, suggesting the predominance of carbocation. By analogy, we could infer that the 4-substituted 4-pentanoic acid substrates also go through the open form. This will be examined experimentally as described below.

To support this hypothesis we envisioned that by replacing one of the vinylic protons with deuterium the product could have two chiral carbons, the quaternary carbon and the carbon attached to the chlorine. Having two chiral centers on the final product will provide the opportunity to investigate whether the reaction goes through the

carbocation intermediate or the bridged halonium. If the reaction goes through the carbocation intermediate in the ring-closing step (S_N1 reaction) the carboxylic acid can attack from either the *Si*-face of the carbocation or the *Re*-face of the carbocation. The result of the S_N1 reaction will be the formation of the two diastereomers. If the reaction goes through the chloronium intermediate, the ring-closing step will be a S_N2 type reaction. In that case the carboxylic acid will always attack the opposite face of the chloronium, which leads to the formation of just one diastereomer.
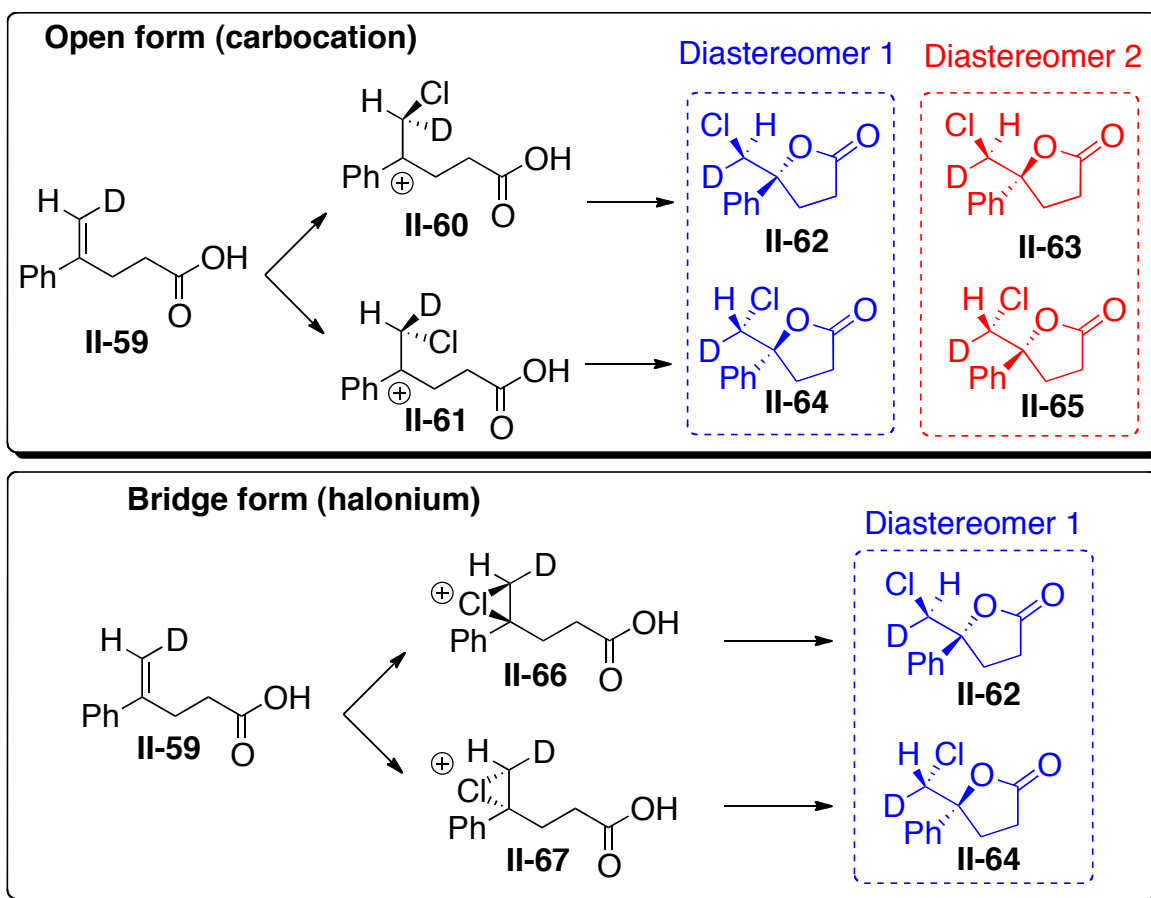
Scheme II-12. Two plausible intermediates: Open form (formation of the two diastereomers, and bridged form (formation of the one diastereomer)

According to the latter analysis, we can judge the nature of the intermediate, carbocation vs halonium, based on the number of diastereomers isolated from the deuterium-labeled substrate. (Scheme II-12). To execute this idea the deuterated acid substrate **II-59** was synthesized from a deuterated alkyne and phenyl boronic acid. Alkyne **II-68** was deprotonated in the presence of NaH and then quenched with D_2O providing the desired alkyne **II-69** in 80% yield. In the next step the phenyl boronic acid was cross-coupled with deuterated alkyne **II-69** in the presence of the catalytic amount of the Pd(0).[20] The resultant alcohol **II-70** was then oxidized with PCC to yield the labeled 4-phenylpentenoic acid **II-59** (Scheme II-13).
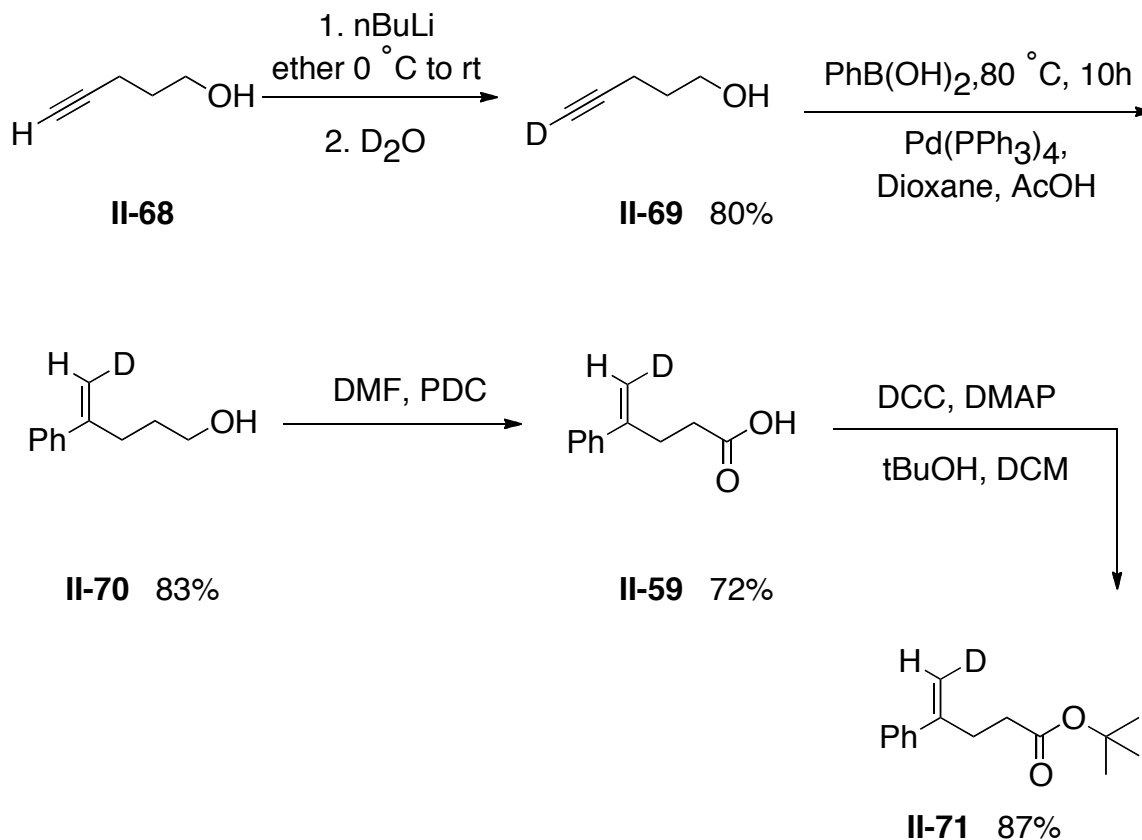
Scheme II-13. Synthesis of deuterated substrate acid **II-58** and deuterated ester **II-70**
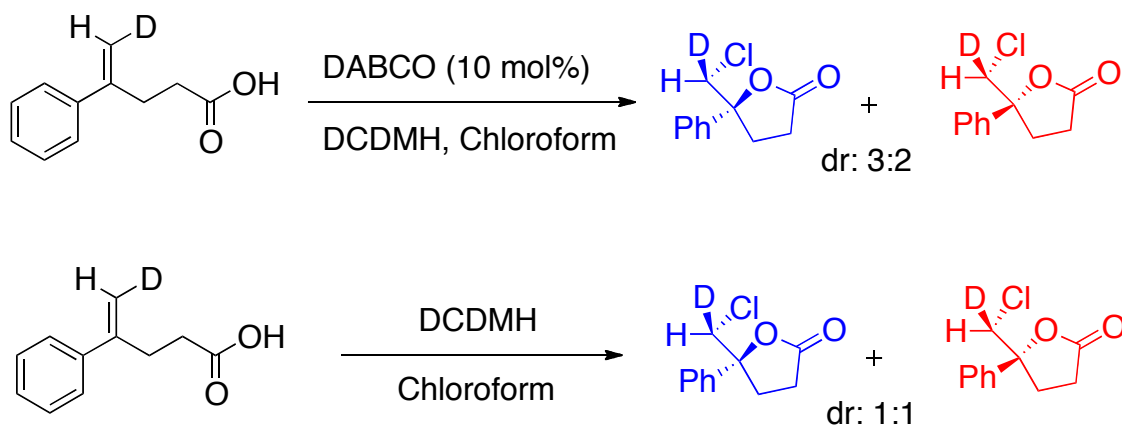
Figure II-1. Formation of the two diastereomers: an evidence
for carbocation intermediate.

Cyclization of the labeled acid **II-59** in the presence of DCDMH and 10-mol%
DABCO as an achiral catalyst, led to the production of two diastereomers in a 3:2 *dr*
based on NMR analysis (Figure II-1). In the absence of the DABCO, a 1:1 *dr* was
observed   (Figure II-1). This result suggests that the reaction goes through the
carbocation intermediate as two diastereomers were observed.

Based on discussion summarized in Scheme II-10 and the latter results the high
enantioselectivity of the final lactone must be the result of high facial selectivity of the
ring-closing step. Although likely that the second step is the enantio-determining step,
the nature of the chlorine delivery was not clear. Understanding the enantioselectivity of
the first is important to fully comprehend the role of the chiral catalyst, and further
designs for cis or trans 1,2-disubstituted, tri and tetra substituted olefins in future.
Although we have clear evidence for an intimate pairing of the dichlorohydantoin and
cinchona alkaloid catalyst (Scheme II-5b), the question of chiral chlorine delivery
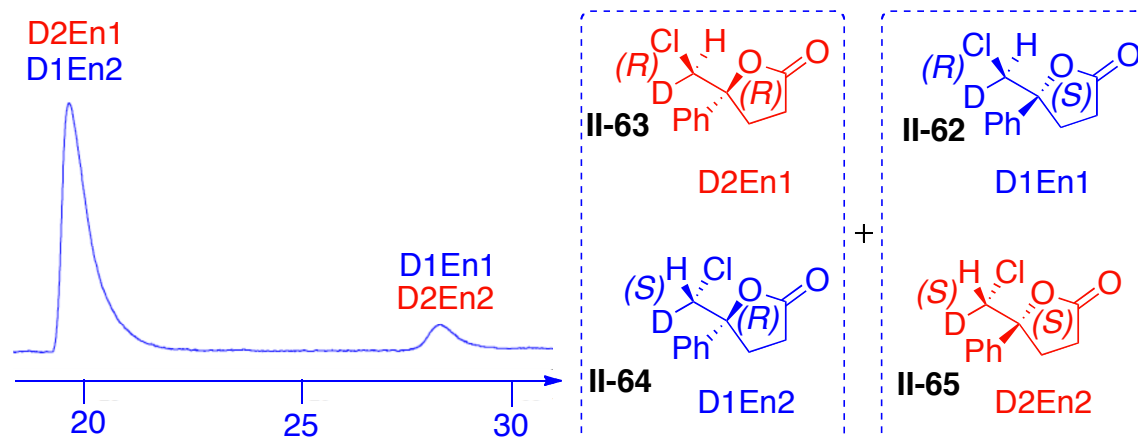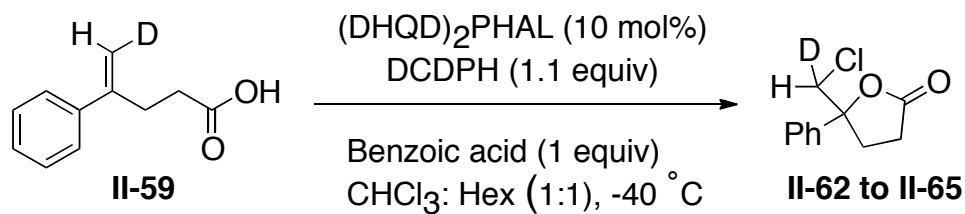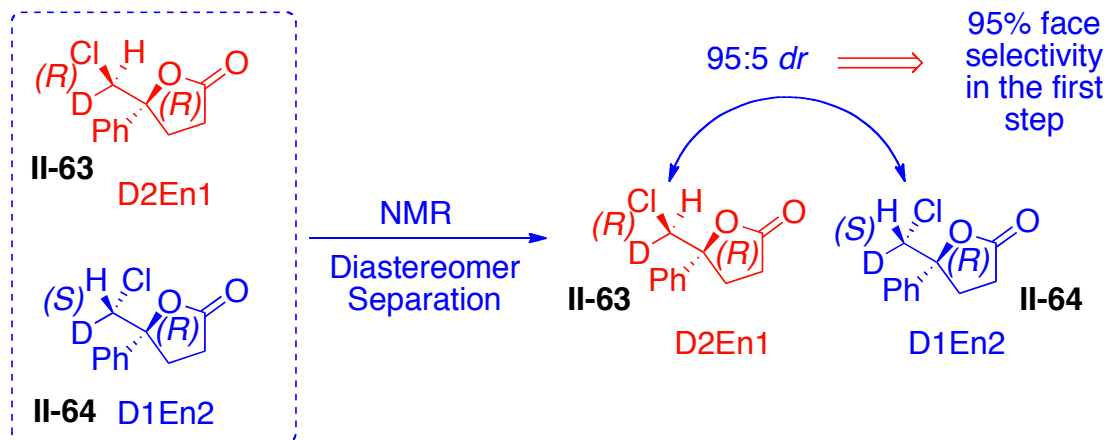
Figure II-2. Face selectivity in chlorine delivery were measured by using chiral HPLC and NMR.

remains unanswered because the chlorine ends up on a non-chiral carbon (Scheme II-5a).

To measure the face selectivity of the first step, the deuterated substrate was utilized. Reaction of the labeled substrate under optimized asymmetric catalytic condition results in products that enable analysis of olefin face selectivity for chlorine delivery in first step by using chiral HPLC and NMR spectroscopy (Figure II-2).

The four possible products of the reaction, D1EN1, D1EN2, D2EN1 and D2EN2 (**II-62** to **II-65)** are depicted in Figure II-2. The product mixture of the reaction was submitted to chiral HPLC separation. The chiral HPLC column cannot distinguish between deuterated and protiated compounds. D2EN1 and D1EN2 (**II-63** and **II-64)**, having *R* chirality on the quaternary carbon, elute together as the major product, while D1EN1 and D2EN2 (**II-62** and **II-65)** with *S* chirality on the quaternary carbon were isolated as one peak. The HPLC ratio provides the enantioselectivity of the reaction at the quaternary carbon. The major products (D2EN1 and D1EN2) was submitted to NMR analysis, providing *dr* of the reaction since the proton vs. deuterium signals could be distinguished. As these two diastereomers have same chirality, (*R*) on the quaternary
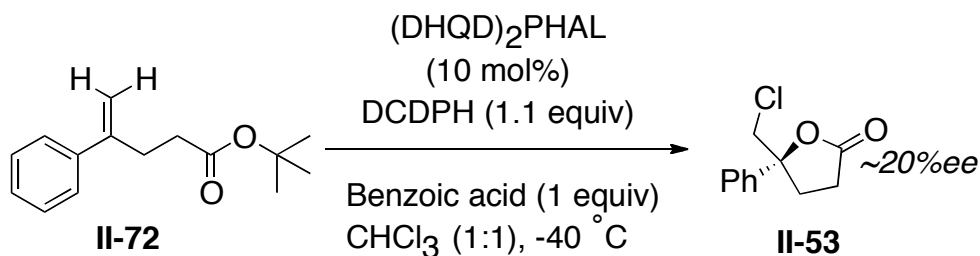
Scheme II-14. Low enantioselectivity in chlorolactonization of **II-72**
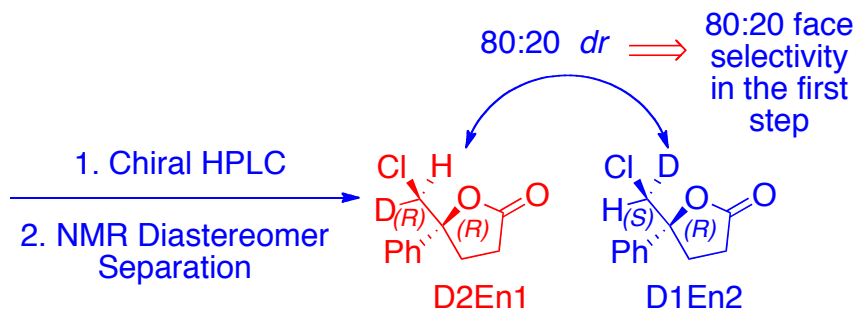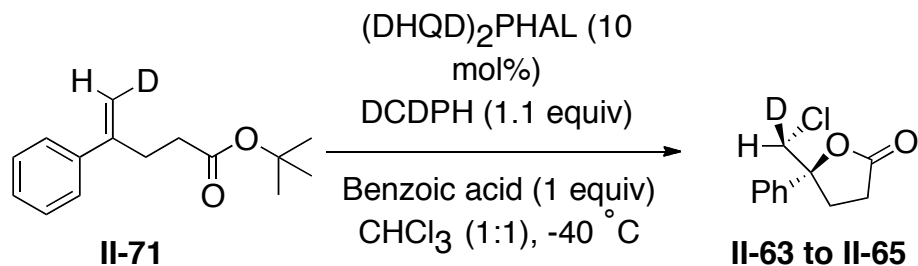
Figure II-3. Deuterated ester substrate was used to show that face selectivity in each step is independently controlled.

carbon, the *dr* value comes from the ratio of different chirality on the labeled carbon. The measured *dr* value of 95% equals the face selectivity in the first step (Figure II-2). Clearly the chlorine delivery to the olefin is highly enantioselective (see experimental section for determination of absolute chirality of the labeled carbon).

The origin of high face selectivity in both steps can be due to the binding of the substrate to the protonated catalyst or could be controlled independent from each other. To elucidate and separate the origin of the enantioselectivity for each step the cyclization of the *t*-butyl ester **II-72** was pursued. Chlorolactonization of **II-72** under standard catalytic asymmetric conditions led to the desired product with much reduced - 20% enantioselectivity (Scheme II-14). This experiment shows that having the

carboxylic acid moiety is essential for getting high enantioselectivity of the quaternary carbon. This can be due to binding of the substrate through hydrogen binding or ionic interactions with the protonated catalyst. To check whether or not replacing the carboxylic acid with an ester has any effect on the face selectivity of the chlorine delivery to the labeled version of the *t*-butyl ester **II-72** was synthesized (Scheme II-13) and submitted to identical reaction conditions. Surprisingly, chiral HPLC separation and NMR analysis indicates high selectivity in the first step (80:20) (Figure II-3). which suggests the carboxylic acid does not have any effect on the olefin face selectivity of chlorine delivery.

The low selectivity (-20 *ee* %) on the quaternary carbon and the relatively high face selectivity (80:20 *dr*) on labeled carbon suggest that both steps, chlorine delivery to the olefin and also the ring closing step, are highly face selective, and furthermore the
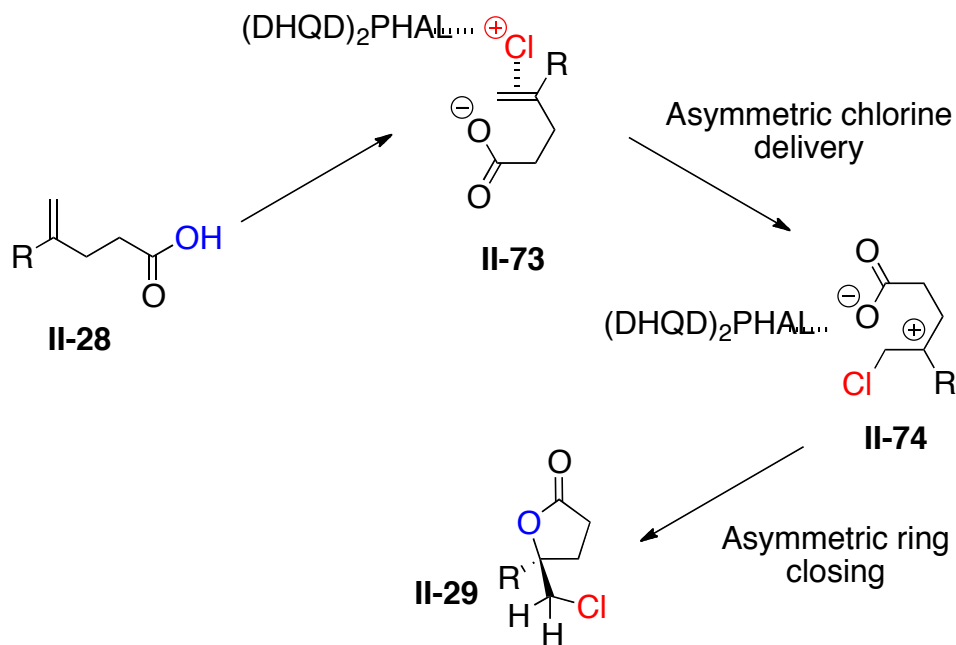
Scheme II-15. High face selectivity in chlorine delivery to olefin and ring closing steps
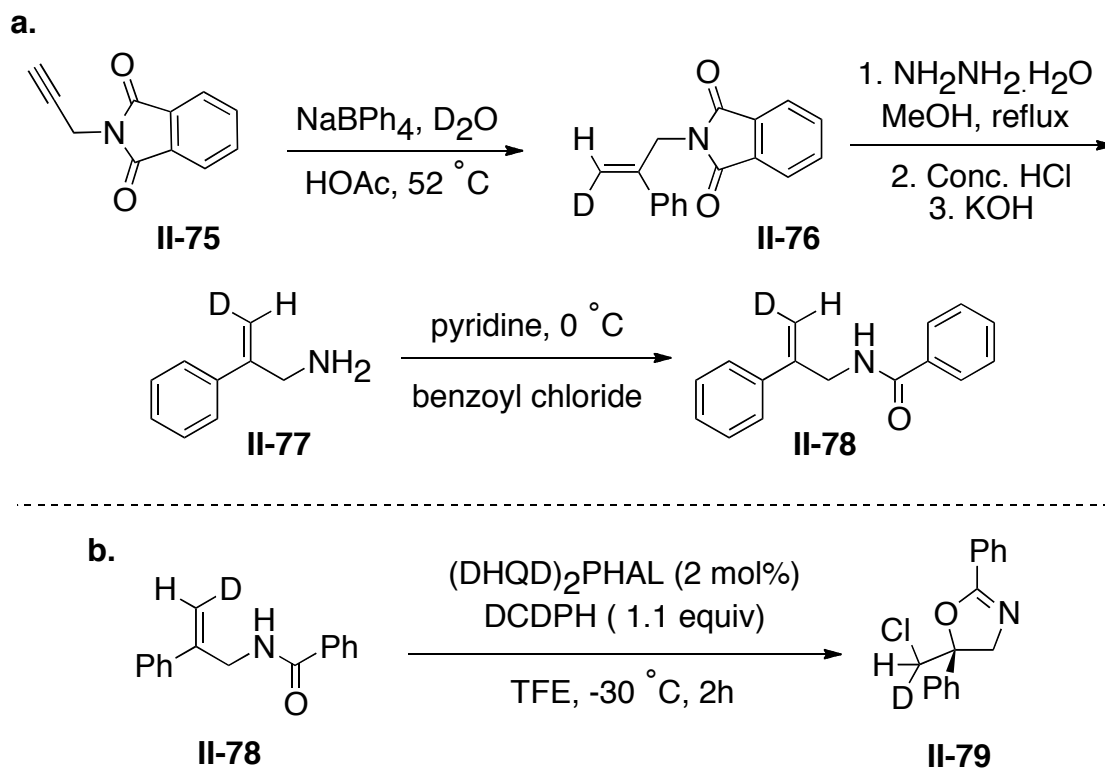
Scheme II-16. a. Synthesis of deuterated amide **II-78**   b. Deuterated amide leads to diastereomic differentiation to probe olefin face selectivity

factors that control face selectivity for each step are independent (Scheme II-15). The high selectivity in the first step can be due to the binding of the chlorinated hydantoin to the catalyst and delivery of the chlorine in the chiral environment. The selectivity for the second step might be controlled by templation and binding of the substrate to the catalyst, which controls the face selectivity of the ring closing step.

To show that this method can be generalized to other halocyclization reactions, the same idea was also applied to 1,1-disubstituted unsaturated amide chlorocyclization[21]

by synthesizing the corresponding deuterated substrate (Scheme II-16a). After HPLC separation and *dr* measurement by NMR, it became clear that chlorine delivery occurs with high face selectivity (99%, Scheme II-16b).

2.3: Kinetic Analysis:

2.3.1: Introduction

Kinetics investigation of multistep organic reactions can provide a better understanding of reaction mechanism by revealing the order of each reaction components and rate-determining step (RDS). Moreover, with kinetics studies, the rate, and possibly equilibrium constants of each step can be measured. Kinetic Information can help to optimize the synthetic route by providing mechanistic understanding of the reaction. All these points highlight the importance of kinetic measurements.
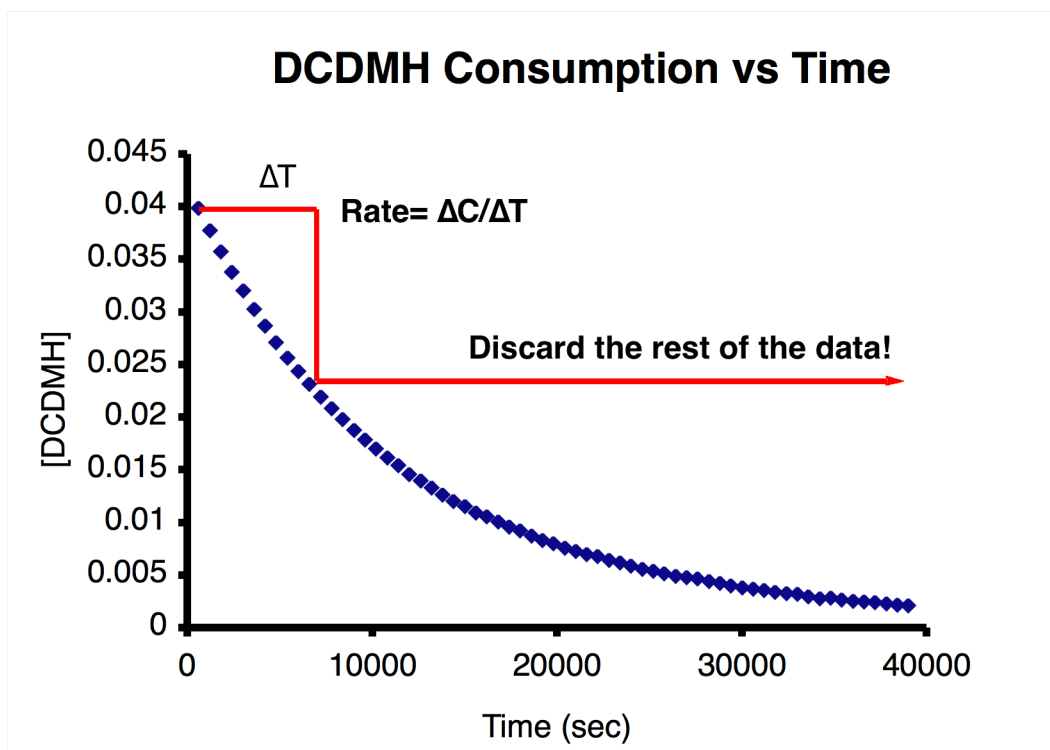
Figure II-4. Classical kinetic methodology
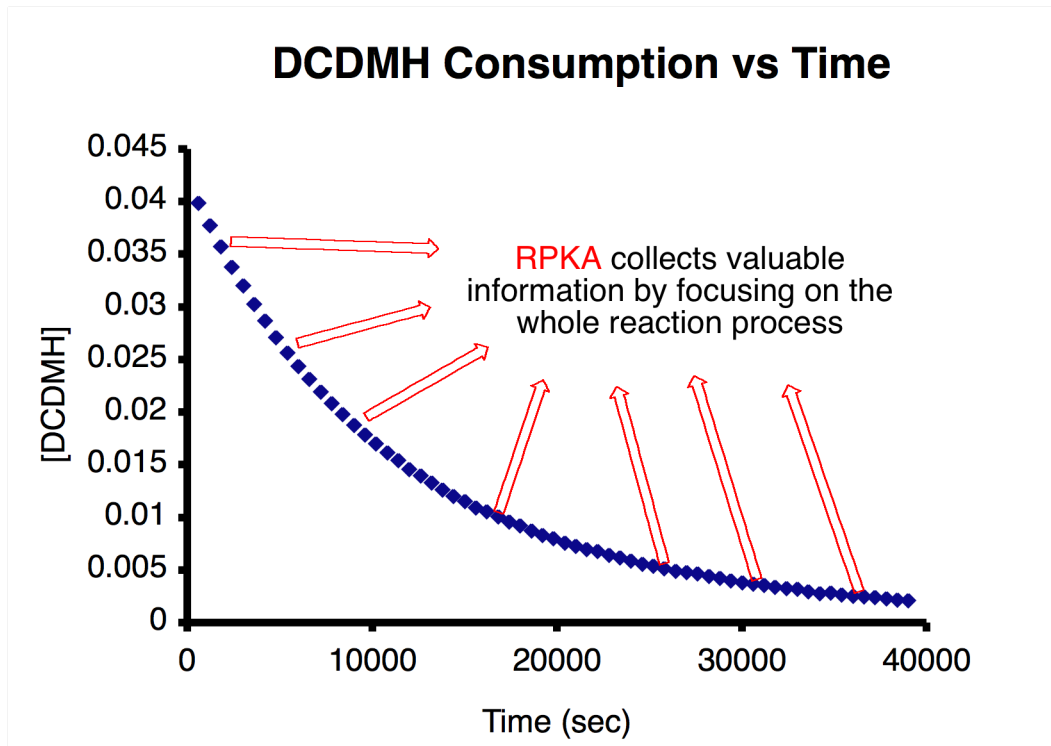
Figure II-5. Reaction progress kinetic analysis

Conventional method, classical kinetics analysis, relies on initial rate data, which can be obtained by establishing pseudo first order conditions in multi component reactions. In pseudo first order condition one of the reactants is present in large excess, such that its change in concentration is negligible. Initial rate data may be blind to complications including side reactions. Moreover, Initial rate data do not reveal how the reaction proceeds in high conversion. In addition, pseudo first order conditions are far removed relative to optimized conditions, and do not mimic real-reaction conditions.[22]

These difficulties and problematic issues in classical kinetics analysis have led to an easier and more reliable method to study the kinetics of different reactions. In 2005 Blackmond and coworkers designed a powerful methodology, reaction progress kinetic

II-80   II-81   II-82
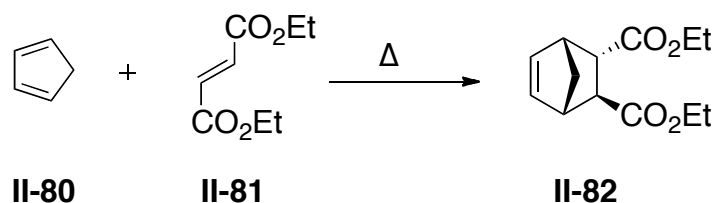
$$\text{Rate} = k\,[\textbf{II-80}]\,[\textbf{II-81}]$$

Scheme II-17. . Diels-Alder, a model Reaction

analysis (RPKA), to study the mechanism of complex catalytic reactions. RPKA is designed to get the necessary information out of fewer experiments. By following the reaction from beginning to end, RPKA can provide better understanding of the reaction mechanism, especially since it follows reactions performed with their idealized conditions. Moreover, RPKA helps analyze process robustness by addressing the role of side reactions and catalyst deactivation and activation.[22-24]

Classical kinetics methodology measures a small change in concentration, ΔC, over a short time at the beginning of the reaction, Δt, at C_0 to calculate the rate and reveal the order of the each individual reactant. In order to develop the rate law, the reaction needs to be repeated for many values of the initial concentration. In classical methodology the rest of the data, typically 90% of the reaction progress is not used and usually is discarded (Figure II-4). A large portion of valuable kinetic information is discarded and in fact, often the very same information is measured latter as reactions in different with initial concentrations are evaluated. RPKA extracts valuable information from the data that is collected during the whole course of reaction (Figure II-5).

a

[cyclopentadiene]= constant at 4M

Rate = k [II-80] [II-81]

Rate (M/min)

0.07
0.06
0.05
0.04
0.03
0.02
0.01
0

0.25 0.27 0.29 0.31 0.33 0.35 0.37 0.39

[diethyl fumarate] (M)

b

[diethyl fumarate]= constant at 2M

Rate = k [II-80] [II-81]

Rate (M/min)

0.04
0.035
0.03
0.025
0.02
0.015
0.01
0.005
0

0   0.05   0.1   0.15   0.2

[cyclopentadiene] (M)
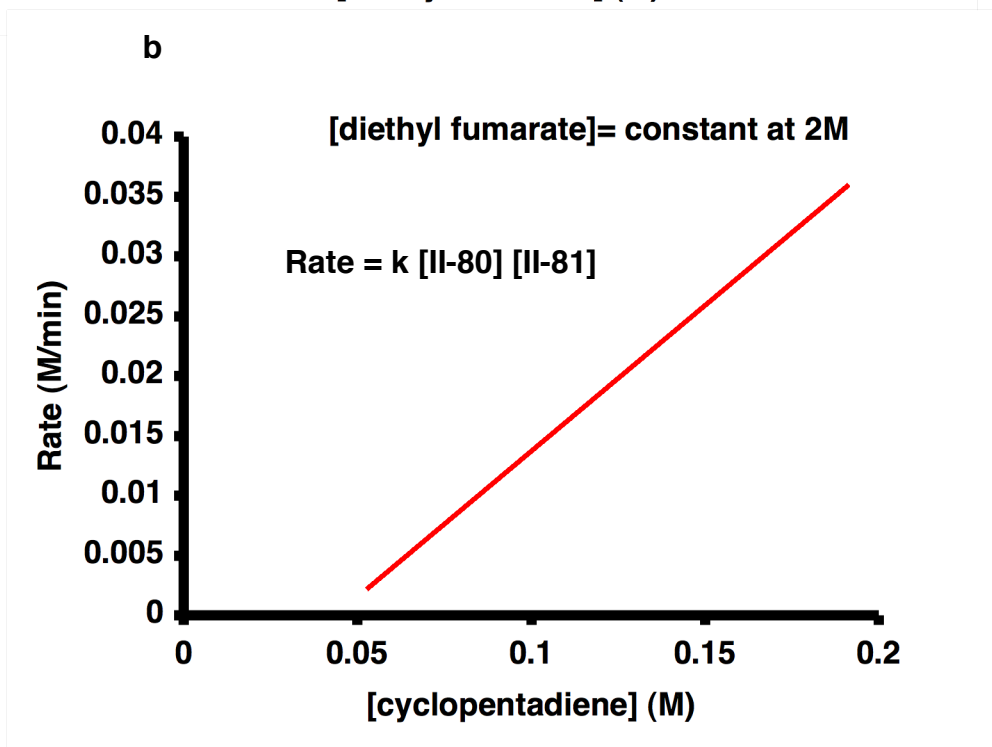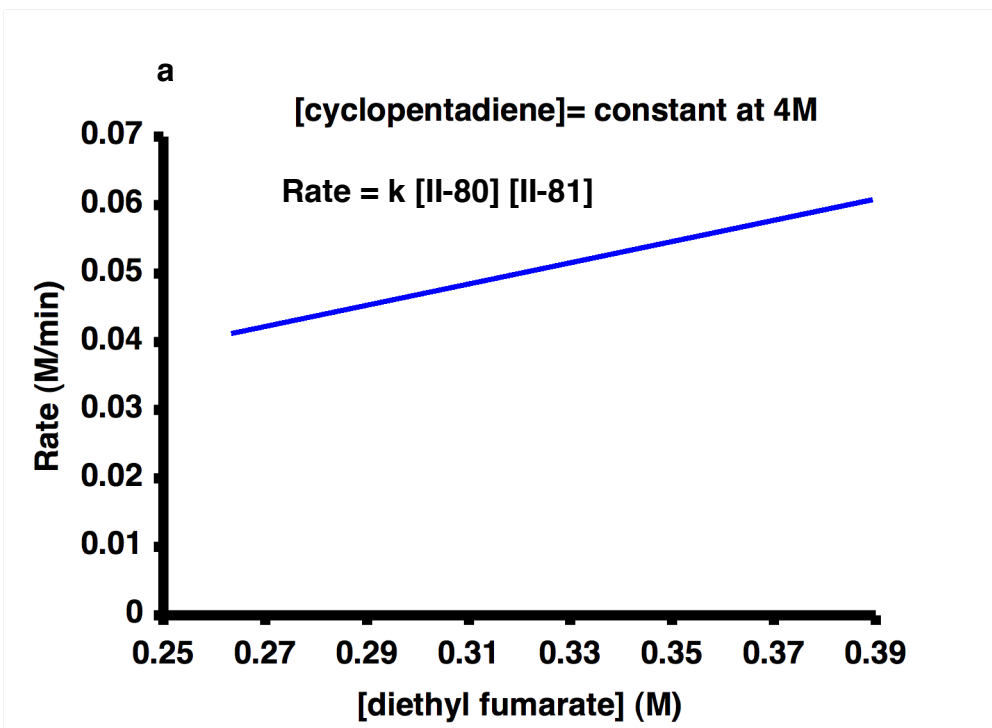
Figure II-6. Classical kinetic studies of Diels-Alder reaction
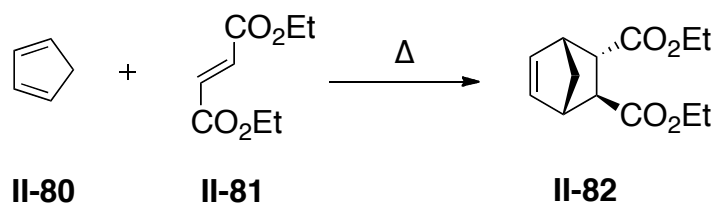
	$[\text{II-80}]_0$	$[\text{II-81}]_0$	excess
EXP A	0.2 M	0.6 M	0.4 M
EXP B	0.2 M	0.4 M	0.2 M

Table II-1. Different excess protocol

RPKA is supported by rigorous mathematical treatment of the minimum number of separate experiments required to extract kinetic information. RPKA can provide concentration dependences or in another word reaction order, rate constants and also catalyst stability analysis (catalyst deactivation). [22-24]

To effectively use RPKA, an accurate means of monitoring reaction progress over time is needed. This can be done by measuring the concentration or rate as a function of time, using some form of in-situ spectroscopy or reaction calorimetry. The key point is the need for fairly high data density in order to carry out the necessary data manipulation. To better understand the differences and advantages of RPKA, a classical kinetics approach will be compared with RPKA for a model reaction.[22-24]

A Diels-Alder reaction, a bimolecular one step transformation is chosen as a model reaction. The reaction rate in this bimolecular reaction depends on the concentration of both substrates; rate = k [**II-80**] [**II-81**] (Scheme II-17).[23]
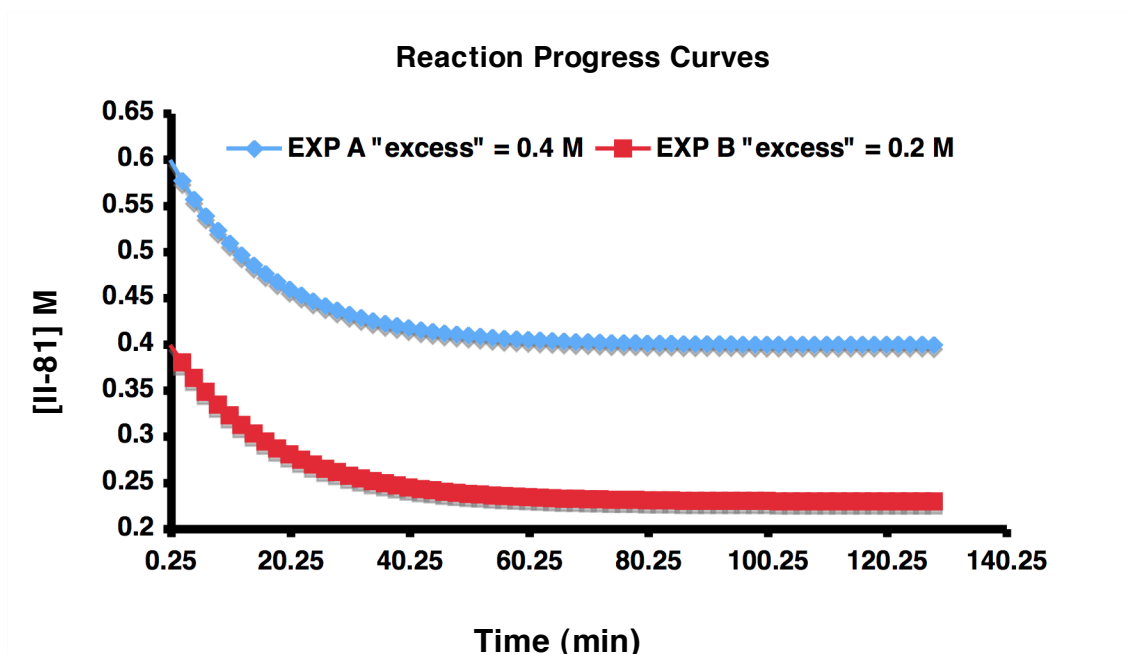
Figure II-7. Reaction progress curves

In the classical kinetic methodology two sets of reactions are carried out. First substrate **II-80** is held constant, while substrate **II-81**'s initial concentration is varied and the initial rate in separate experiments is measured as depicted in Figure II-6. Next the converse is done by holding **II-81** constant and varying **II-80**. Two plots (Figure II-6) from two separate sets of initial rate experiments are produced. The straight lines confirm the first order behavior for each substrate and from the slope the rate constant is calculated. Although the classical method looks plausible and perfect it has some serious drawbacks. First, it requires a large number of separate experiments, as an example nine experiments for each substrate, overall eighteen separate experiments. More importantly, the concentration is distorted from synthetically relevant conditions. Typically, ten fold excess of one substrate concentration over the other one is used.

106

Classicalkinetics method conditions are far away form the real and optimized conditions, which can lead to erroneous results in some cases.

Instead of carrying out multiple experiments to build two plots, the RPKA method requires only two separate experiments. The reaction conditions are carefully designed to ensure the same information from two-reaction progress experiments are obtained instead of carrying out a large number of experiments. More importantly, both substrates are allowed to react in similar ratio to those used in optimized conditions instead of keeping either substrate concentration constant. Basically in RPKA both substrate concentrations change during the course of the reaction. The stoichiometry of the reaction must be considered carefully. For example in the latter example, one diene **II-80** reacts with one molecule of dienophile **II-81**. In RPKA, a parameter called *"excess"* has been defined to relate one substrate concentration to the other. In this model, with a one to one stoichiometry the "*excess*" is defined as the difference between two concentrations (*"**excess**"* = [**II-80**]$_0$ - [**II-81**]$_0$ = [**II-80**] - [**II-81**]). If the initial concentration is measured, the *"excess"* for the reaction stays constant through out the reaction. The *"excess"* is not going to change during the course of the reaction, as one diene is reacting with one dienophile. Thus, we can solve for one substrate concentration in terms of the other ([**II-80**] = [*"**excess**"*] - [**II-81**]). As such if the concentration of one reactant is known, the concentration of the other can be easily calculated. *"Excess"* has units of concentration like molarity and it can be positive negative or zero. *"Excess"* is not the same as the number of equivalents or the % excess concentration, both of which

Reaction Rate vs [II-80]
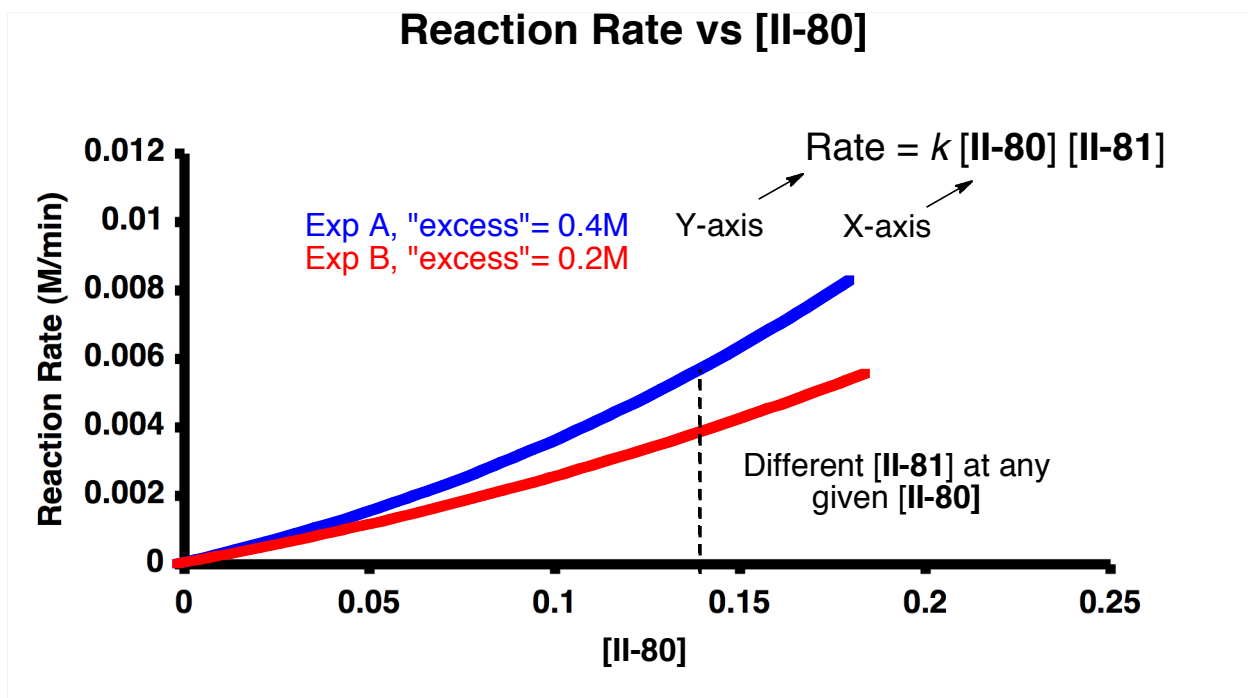
Figure II-8. Reaction rate vs [II-80].

do change during the course of reaction. Moreover, *"excess"* can be large or small. If it is a large number classical kinetics is mimicked. [22-24]

RPKA can be separated into two protocols; different *"excess"* sets of experiment and same *"excess"* sets of experiment. These are explained in the following two sections.

2.3.2: Different "*Excess*" Protocol

In order to define the order of two substrate concentrations, two experiments at different *"excess"* are carried out. As depicted in Table II-1 for the model reaction two experiments with different *"excess"* values, one with 0.4 M and the other one with 0.2 M are performed. The initial concentrations are not critical here and could vary (in this
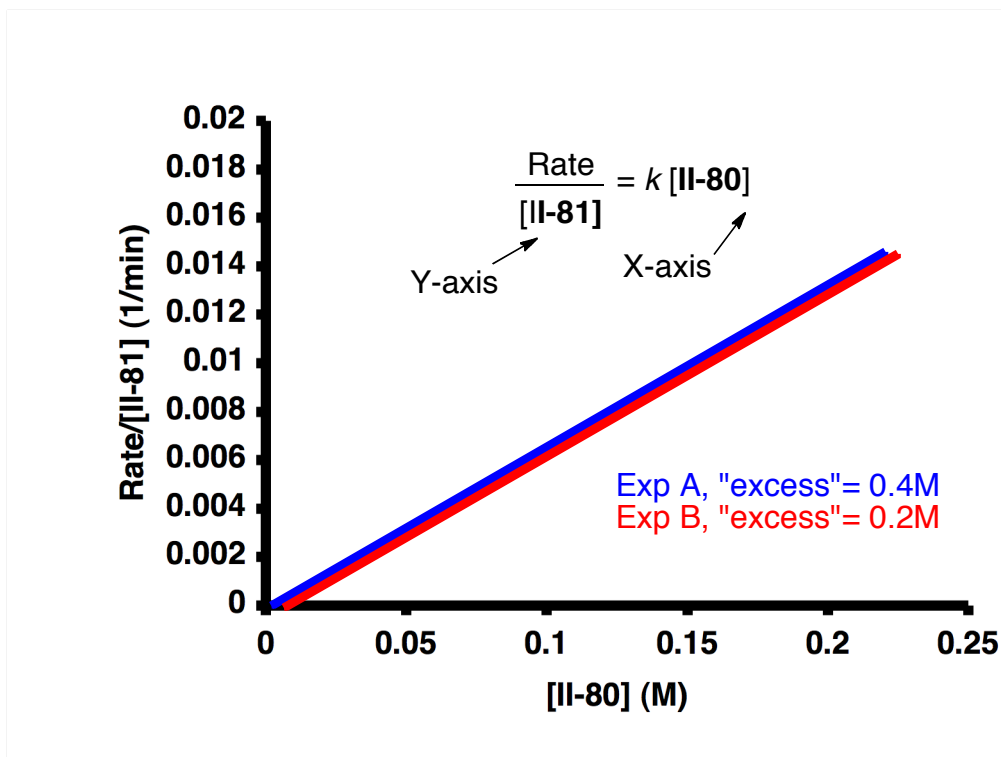
Figure II-9. Reaction rate/[**II-81**] vs [**II-80**].

example they are equal 0.2 M). The most important things here are to have different "*excess*" values for these two experiments. After collecting the data the reaction progress curves for these two experiments are derived by plotting the concentration of the dienophile vs. time (min), as depicted in Figure II-7. Looking at these two curves does not reveal the order of reaction with respect to substrates **II-80** and **II-81** but the information is there. [22,23]

The data are replotted as reaction rate vs. [**II-80**] concentration (Figure II-8). First thing to realize is that time is no longer a variable in this plot. It is important to note that *k* constant values are equal in both experiments as the reaction condition in both case are similar to actual optimized reaction conditions. In this reaction model, the plot of

both experiments results in curve that do not overlay and are also non linear (Figure II-8). This is because the concentration of both [**II-80**] and [**II-81**] change over the course of these reaction since they are both present in the rate equation, Rate = k [**II-80**] [**II-81**]. Considering any particular concentration **II-80** the concentration of **II-81** is known since the "*excess*" value for each experiment is constant at any time. Concentration for **II-81** is different at any particular concentration **II-80** as these two experiments have different *"excess"* values. These two plots do not overlay at any concentration of **II-80** (rate = k [**II-80**] [**II-81**]). Considering the rate equation explains why a curvature exists in these plots. The Y-axis is rate and the X-axis is [**II-80**], However, since the rate is dependent on the concentration of **II-81**, which is also changing, the change is not linear. Overall we have two variables change at once, which leads to the curvature in the plot. Rearranging the rate equation by dividing both sides by the concentration of **II-81** leads to a plot with one variable substrate concentration. Replotting the same data from both experiments in the rearranged form yields two straight lines that fall on each other (Figure II-9). Since the rate is normalized for the changing concentration of **II-81** the X-axis has no longer any dependence on substrate **II-81.** This rearrangement provides two things: first the straight lines suggest that the reaction is first order in [**II-80**] and the slope reveals k. Secondly, the overlay between the two curves means that the reaction is first order in substrate [**II-81**] because the normalized rate with respect to substrate **II-81** has an order of one. Two reactions with two different values of *"excess"* give reaction order of **II-80**, reaction order of **II-81** and rate constant. Basically two experiments in

110
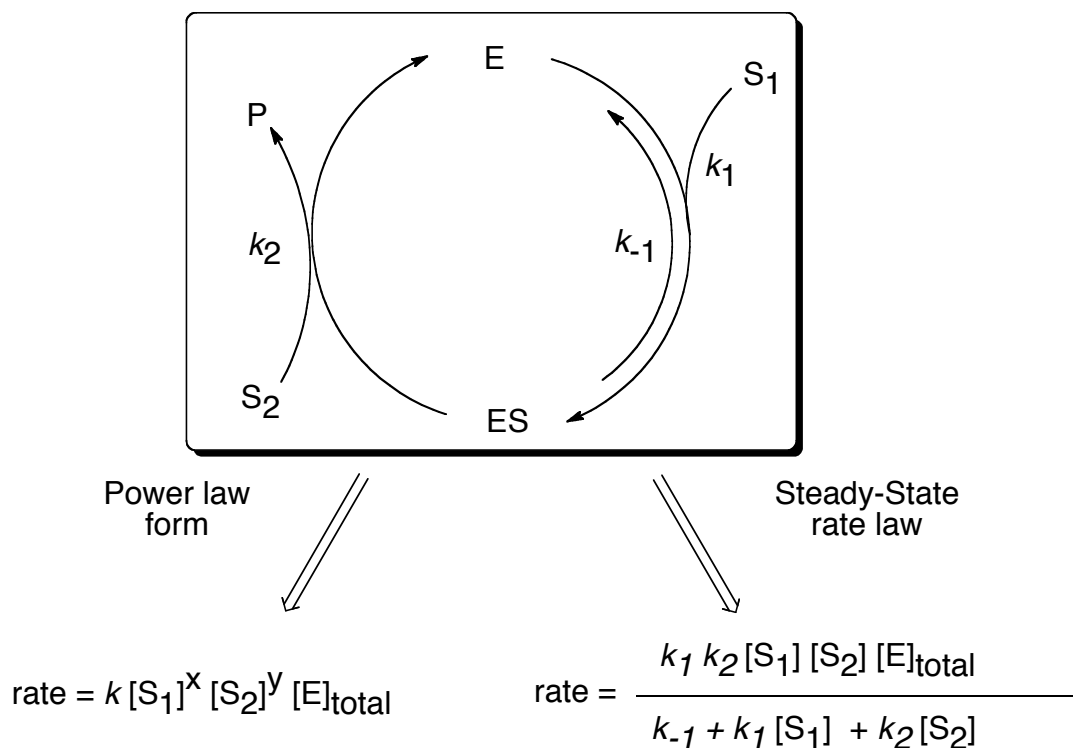
Figure II-10. Rate law for simple catalytic cycle

RPKA are equal to two sets of experiments acquired for classical kinetic methods (for this case eighteen experiments).[22,23]

In an imaginary case, a zero order reaction with respect to **II-81 (rate** = k [**II-80**]) would result in lines at different "*excess*" that would overlay perfectly on top of each other. This is because the rate of the reaction is only affected by the concentration of **II-80**. [22,23] By plotting the rate vs. **[II-80]** we would expect to have the same rate at any particular concentration of **II-80** in both experiment, which leads to the overlaying of two plots.

$$\text{rate} = k[S_1]^x[S_2]^y[E]_{total} \xrightarrow[\text{rate equation}]{\text{normalized}} \frac{\text{rate}}{[S_1]^x} = k[E]_{total}[S_2]^y$$

Y-axis   Slope   X-axis

Play around with x and y:
until we get straight line
and overlay

$\dfrac{\text{rate}}{[S_1]^x}$

$[S_2]^y$

Exp A ⎫
Exp B ⎭ Different excess experiments
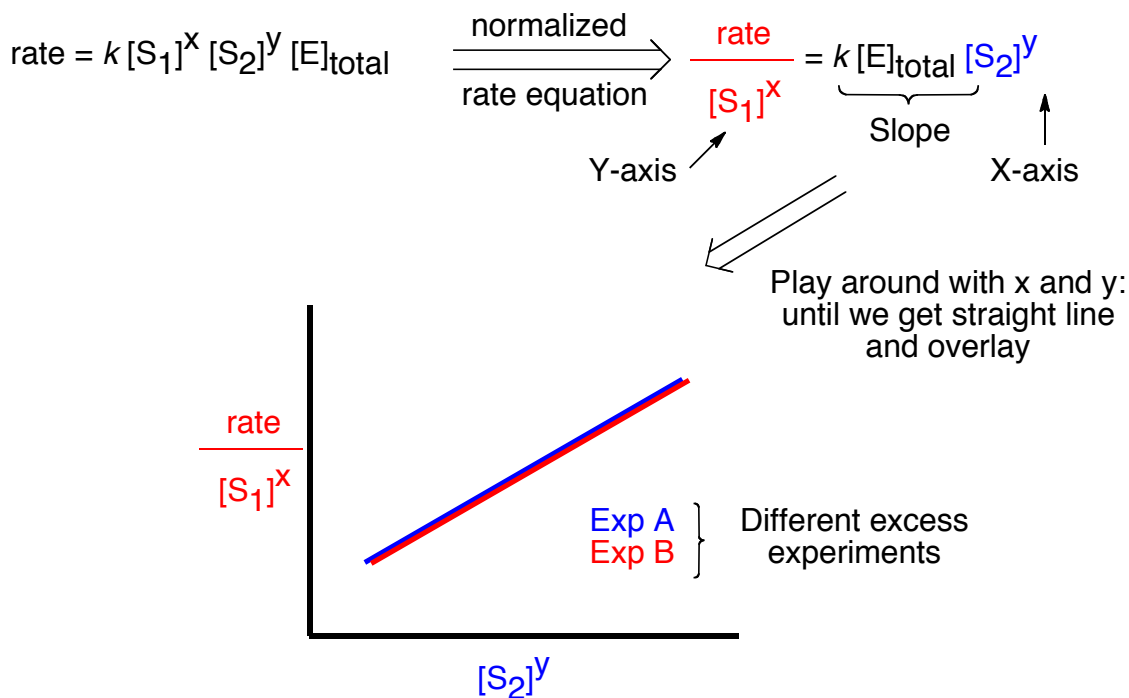
Figure II-11. Different excess protocol for a simple catalytic cycle

This simple example reveals the power of different "*excess*" protocol of RPKA for collecting valuable kinetics information from a small number of experiments. RPKA shows its power even more in analysis of complex cases such as multi-step reactions and catalytic reactions. There are a number of examples in the literature with reactants that have non-integer order in the reaction rate equation. The exact same protocol can be used to analyze the non-integer reaction orders. To better understand this, a simple catalytic cycle is shown in Figure II-10, which is the basis of the Michaelis-Menton kinetics. In this cycle, S_1 binds reversibly to catalyst E and forms the intermediate ES. S_2 then reacts irreversibly with intermediate ES to form a product and regenerate the catalyst. This catalytic system is more complex as compared to Diels – Alder reaction.

It is multi-step reaction with several rate constants and a catalyst that derives the reaction and is regenerated at the end of each cycle (constant concentration during the course of reaction). A steady state rate law for this simple catalytic cycle can be written (Figure II-10). Compared to a simple Diels – Alder reaction this rate law is more complex. The numerator of the rate law for this catalytic cycle looks very much like the rate law for the elementary reaction with three driving forces S_1, S_2, and E (all first order). But because of the complexity of the catalytic cycle S_1 and S_2 concentrations appear in the denominator (additive terms). The denominator leads to non-integer orders for S_1 and S_2 but first order for the catalyst.[22,23]

The rate law can be written in a power law form where S_1 concentration has some power of x and S_2 has some power of y but x and y can be non-integers. This is going to be a general form of the rate law. For the Diels – Alder reaction, the rate law can derived from when x and y are equal to one. The power law over some concentration range will approximate the steady state catalytic rate law.

RPKA method will use the same different "*excess*" protocol to extract non-integer values of x and y, similar to the case described for the Diels – Alder reaction. Rearrangement of power law rate equation is accomplished by dividing both sides by one of the substrate concentration to its power as shown in Figure II-11. The Y-axis is the rate/$[S_1]^x$ with *k* constant as the slope of the line. The X-axis is S_2 concentration to the y power. Iteration of x and y to achieve a straight line with the slope *k* [E] and two different "*excess*" experiment will lead to overlay two experimentally generated linear lines. For example for free copper Sonogashira coupling catalyzed by Pd, two different

113
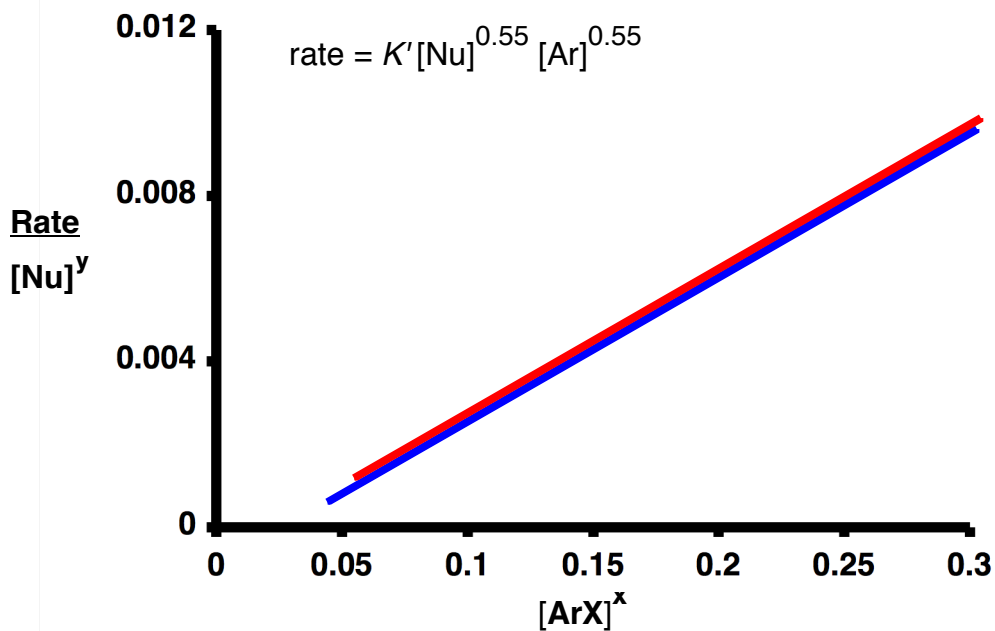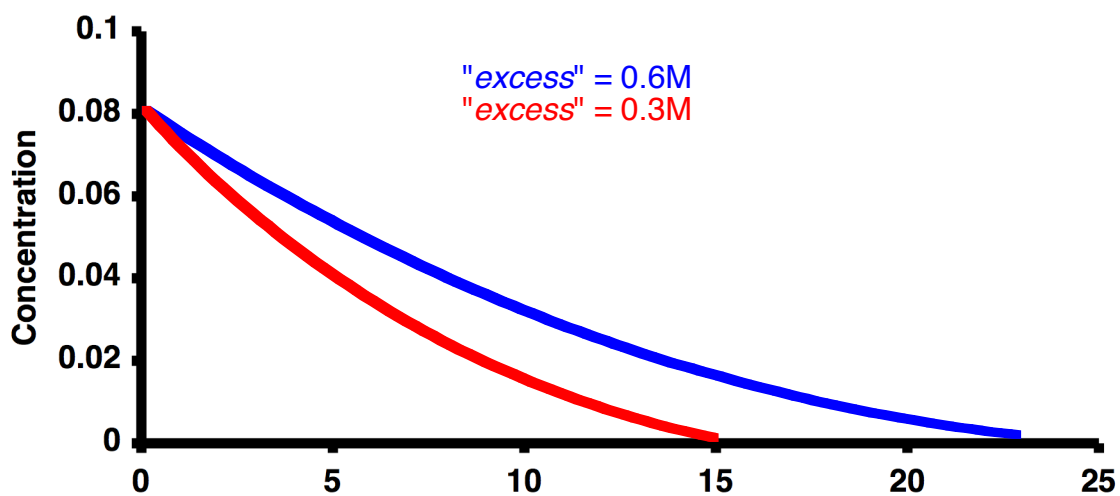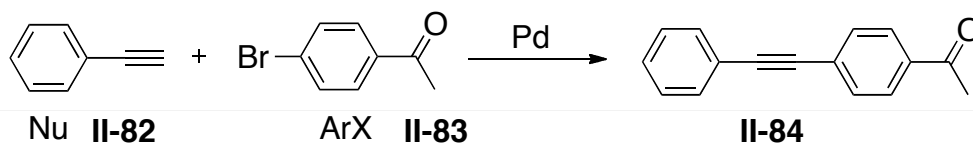
Figure II-12. Application of different "*excess*" protocol in sonogashira coupling

114

$$\text{rate} = k\,[S_1]^x\,[S_2]^y\,[E]_{total}$$

Power law
form

$$\text{rate} = \frac{k_1\,k_2\,[S_1]\,[S_2]\,[E]_{total}}{k_{-1} + k_1\,[S_1]\ +\ k_2\,[S_2]}$$

Steady-State
rate law
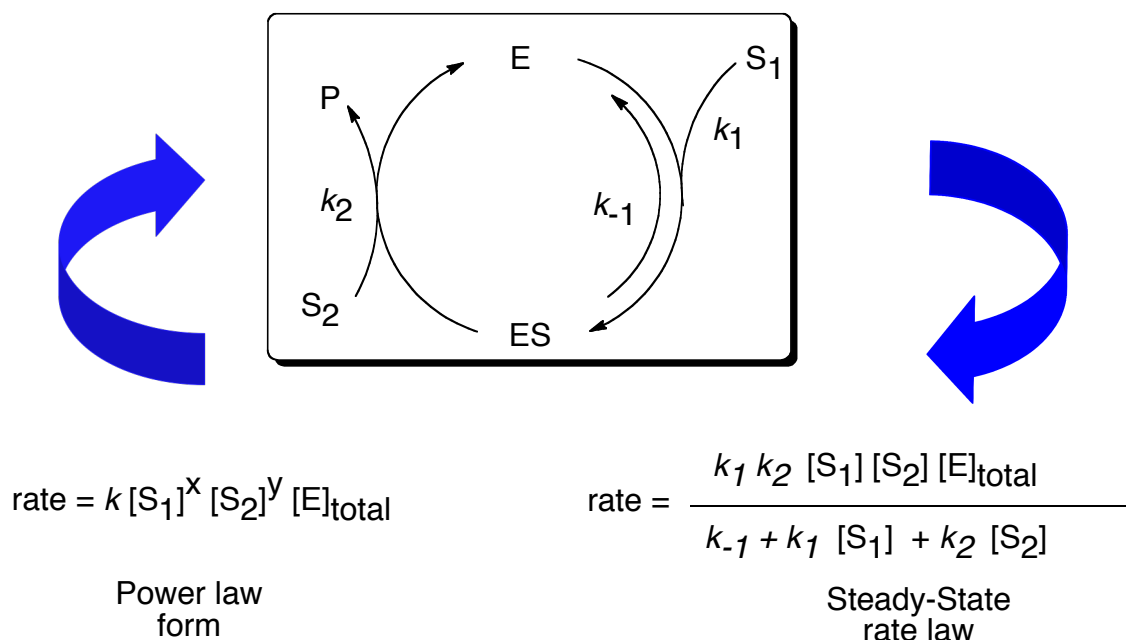
Figure II-13. What do non-integer orders mean?

experiments with "*excess*" of 0.6 and 0.3 M were carried out. As depicted in Figure II-12 the plot of the reaction progress curves cannot estimate the order of the ArX and nucleophile in this reaction. Replotting the data as rate/$[Nu]^y$ vs. $[ArX]^x$, leads to the overlaid straight lines for these two experiments at different *"excess"* values when x and y are equal to 0.55. This leads to the power law rate equation (rate = k $[ArX]^{0.55}$ $[Nu]^{0.55}$), which is the approximation of steady state rate equation. This rate equation suggests that the nucleophile and ArX are both the driving force of the reaction in almost half order.

This does not provide a mechanistic understanding, since 0.55 molecule does not react with 0.55 of another molecule. What do non-integer reaction orders mean with respect to the mechanism of a reaction? The steady state rate law is developed from

the mechanism of the reaction and reflects the proposed mechanism. The magnitude of x and y are related to how large are S_1 and S_2 in the denominator of the steady- state rate equation. If the term K_1 $[S_1]$ in denominator is large then the substrate S_1 will be close to zero order. How different x and y are from one reflects on how large the denominator terms are in the steady-state rate law. So the non-integer reaction orders do not have mechanistic meanings by themselves, however, they can provide clues to interpreting the mechanism (Figure II-13).[22,23]

A summary of different "*excess*" protocol has been illustrated in Figure II-14. Even with no proposed mechanism in mind, this chart can help reveal the order of each reactant for a particular reaction. First two experiments with different *"excess"* values

```
              Reaction at two
             different "excess"
                 values at
             standard condition
```

Plot rate vs $[S_1]$ · Plot rate/$[S_1]$ vs $[S_2]$ · Plot rate/$[S_2]$ vs $[S_1]$

Overlay — No → Overlay — No → Overlay — No → Plot rate/$[S_1]^y$ vs $[S_2]^x$

yes ↓ Zero order in S_2 · yes ↓ First order in S_1 · yes ↓ First order in S_2
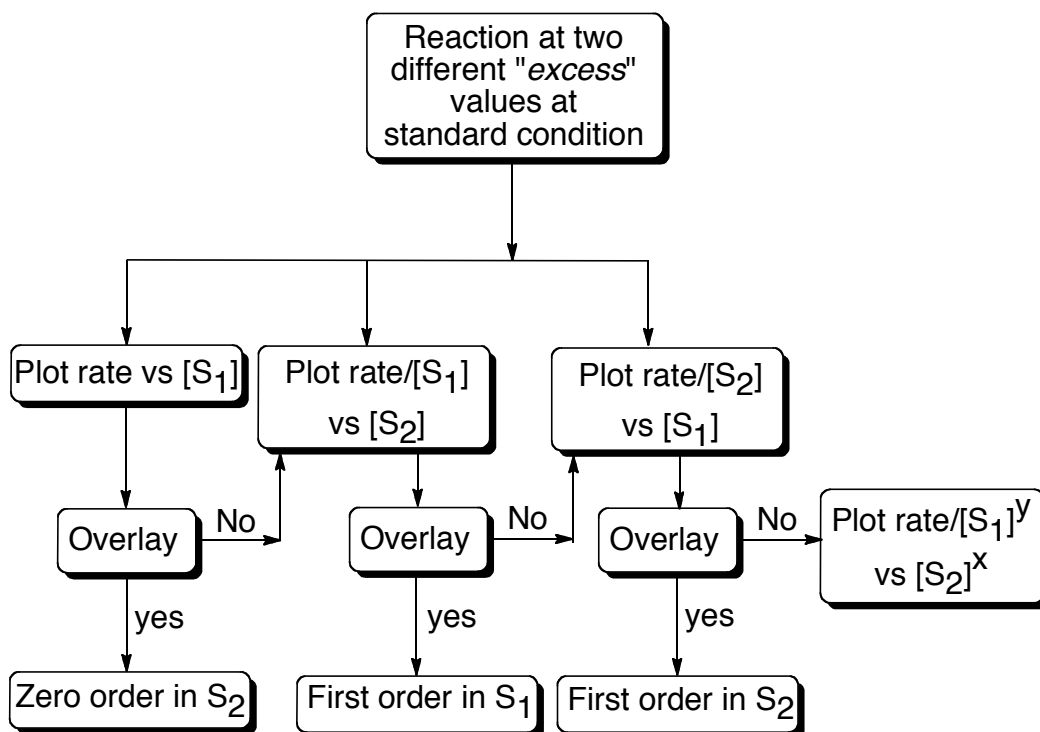
Figure II-14. A summary of different "*excess*" protocol

116

are performed and the data is collected with any spectroscopic method such as IR or NMR. Then, a plot of rate vs. any substrate (for example substrate S_1) is conducted and if there is overlay then the reaction is deemed zero order with respect to the other reactant (in this case S_2). If there is no overlay we simply need to plot rate/$[S_1]$ vs. $[S_2]$. If there is overlay of the lines, the reaction is first order with respect to S_1. If there is no overlay a plot of rate/$[S_2]$ vs. $[S_1]$ is performed. Overlay in this case suggests that the reaction is first order with respect to S_2. In case no overlay is achieved in any of mentioned cases, plot of rate/$[S_1]^x$ vs. $[S_2]^y$ and iterations of x and y to straight lines that do overlay results in approximating the non-integer order for each of the reactants.[22,23]

2.3.3: Same "*Excess*" Protocol

2.3.3.1: Catalyst Instability

Catalyst activation or deactivation can add more complexity in catalytic reactions. The rate of the reaction can be altered due to the deactivation of the catalyst over time or by inhibition of the catalyst active sites by substrate or product, the concentrations of which are changing during the course of the reaction. In classical kinetic studies these factors are not distinguishable since the focus is on the initial rate measurements only. Therefore important reaction characteristics are not observed for transformations that occur under normal concentration regimes.

RPKA is useful to uncover catalyst instabilities as a result of monitoring the reaction for a long period of time. RPKA measures the stability of the catalyst during the course of the reaction with the same "*excess*" protocol. In this protocol two separate reactions

117
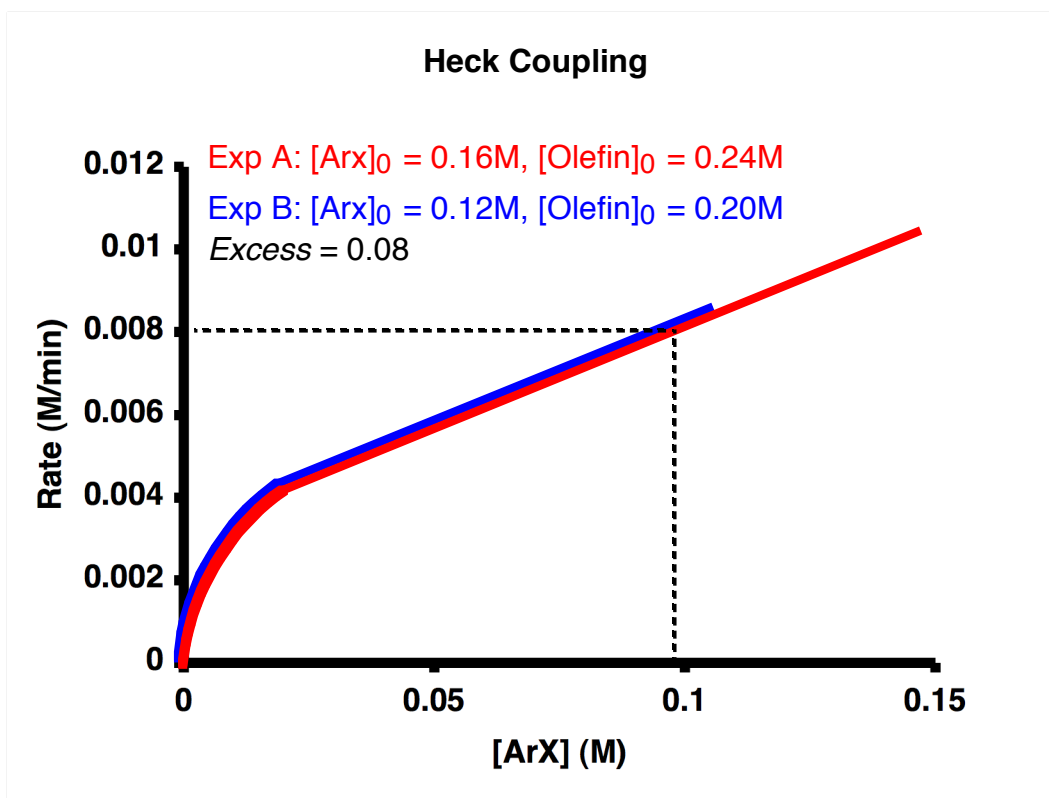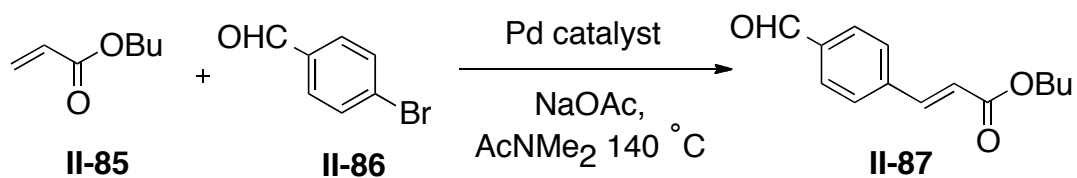
Figure II-15. Probing catalyst deactivation in Heck coupling reaction

with the same "*excess*" values but with different starting concentration are executed. These two experiments illustrate an identical reaction that start from two different starting material concentrations. Two examples below illustrate the same *"excess"* protocol.

Heck coupling of aryl halides with palladium catalyst is a commercially important carbon-carbon forming bond reaction. To understand whether this reaction is

deactivated by product or substrate, two experiments with "*excess*" value of 0.08 were carried out. In experiment A the initial concentration of the ArX and olefin are 0.16 M and 0.24 M, respectively. In the second experiment the concentrations are changed to 0.12 M and 0.20 M respectively. The two experiments with the same "*excess*" but different initial concentrations were analyzed by plotting the rate vs. olefin concentration (Figure II-15). These two experiments are identical at any ArX concentration value except for two things: 1) the reaction with higher initial concentration (Exp A) contains more product than with a lower initial concentration (Exp B). 2) Catalyst in the Exp A has completed more turnovers compare to Exp B due to having higher initial concentration. Exhibiting identical rates for both experiments in the Heck coupling reaction at any ArX concentration value means that neither product nor extra turnover catalyst in Exp A has any influence on the reaction efficiency. More specifically, the rate of the reaction A at 0.12 M ArX concentration (after 0.04 M ArX has been consumed) is equal to the rate of reaction B at 0.12 M ArX concentration (initial rate of reaction B is equal to rate of reaction A at the same ArX concentration). These two simple experiments illustrate that there is no palladium catalyst deactivation in this Heck coupling reaction.[22,23]

In the second example the cobalt-salen catalyst instability in the kinetic resolution ring opening epoxide (racemic), developed in Jacobsen's group is evaluated (Figure II-16). Two experiments with *"excess"* of 0.5 M but with different initial concentration (Exp A: $[epoxide]_0$ = 1.5 M, $[H_2O]_0$ = 2.0 M, Exp B: $[epoxide]_0$ = 1.0 M, $[H_2O]_0$ = 1.5 M) were run at room temperature. No overlay was observed after plotting the rate of each experiment against the epoxide concentration. For a given epoxide concentration, a

119
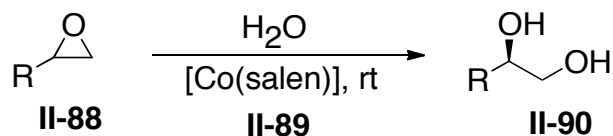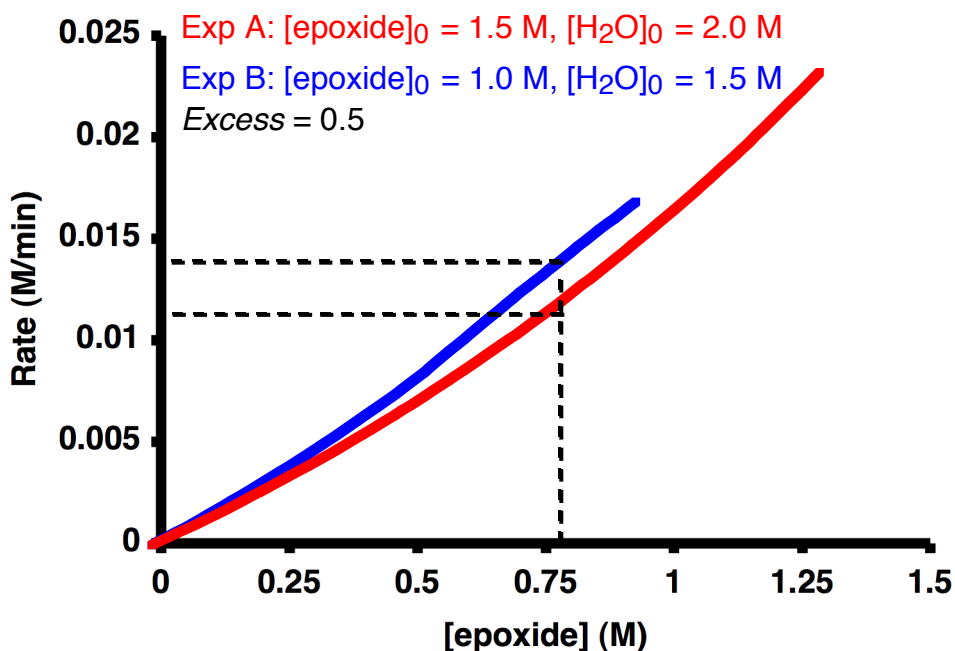
Figure II-16. Probing catalyst deactivation in epoxide ring opening reaction

higher rate was observed for experiment B with the lower initial concentration. This result suggests that either catalyst deactivation or product inhibition decreases the efficiency of the cobalt-salen catalyst. Further investigation is needed to find out which of the two scenarios is responsible for the drop in the rate of the reaction in experiment A. For instance, if addition of 0.5 M reaction product to experiment B leads to the overlay of experiment A and B, product inhibition is verified. If the later experiment does

a

$$\text{TOF} = \frac{\text{rate}}{[E]_{total}} = \frac{k_1 \, k_2 \, [S_1] \, [S_2]}{k_1 + k_1 \, [S_1] + k_2 \, [S_2]}$$

----

b

5 mol% Ni(acac)$_2$
20 mol% (-)-MIB

II-91   +   Et$_2$Zn   →   II-93

(-)-MIB =   II-92
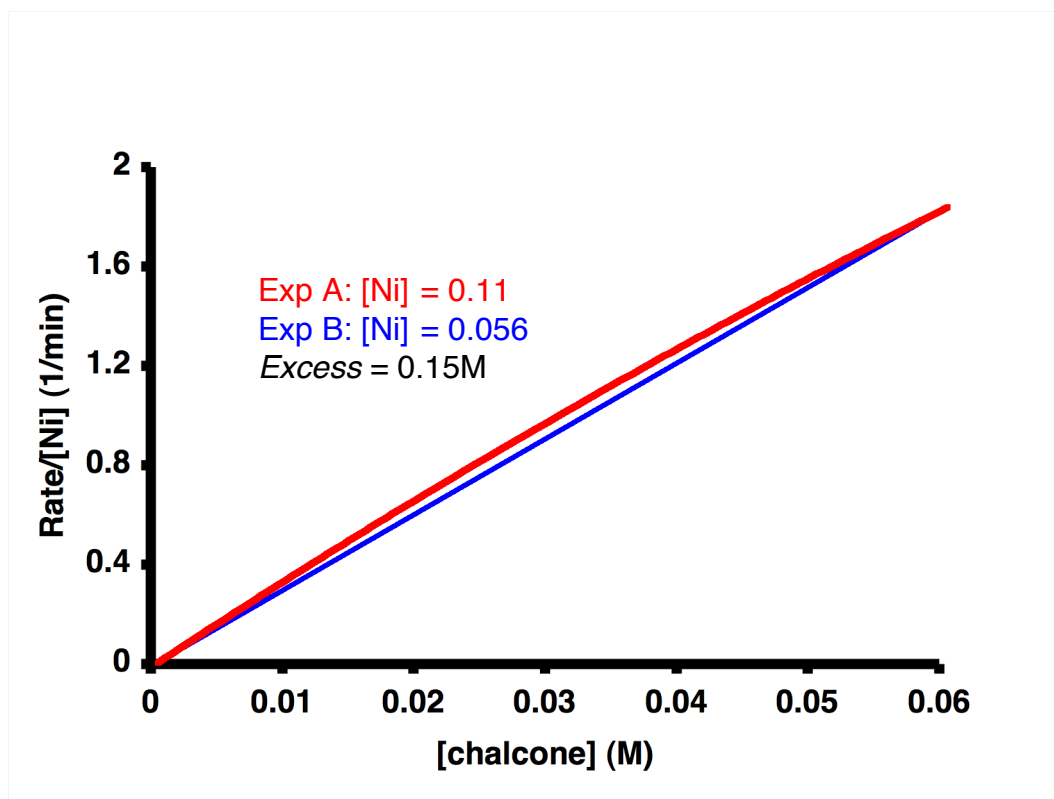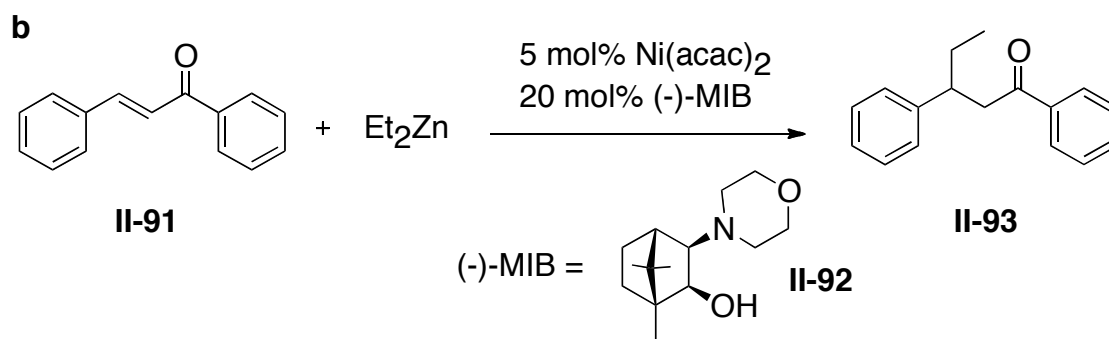
Figure II-17. Normalized rate in terms of [catalyst], b. Graphical rate equation for turnover frequency for alkylation of chalcone

not lead to overlay of experiment A on experiment B catalyst deactivation and not product inhibition is responsible for the decrease in the reaction rate of experiment A.

2.3.3.2: Turnover Frequency: Reaction Order in Catalyst

Based on the mechanism of a simple catalytic reaction (Figure II-10), One can predict that the reaction rate is proportional to the concentration of the catalyst. Most,
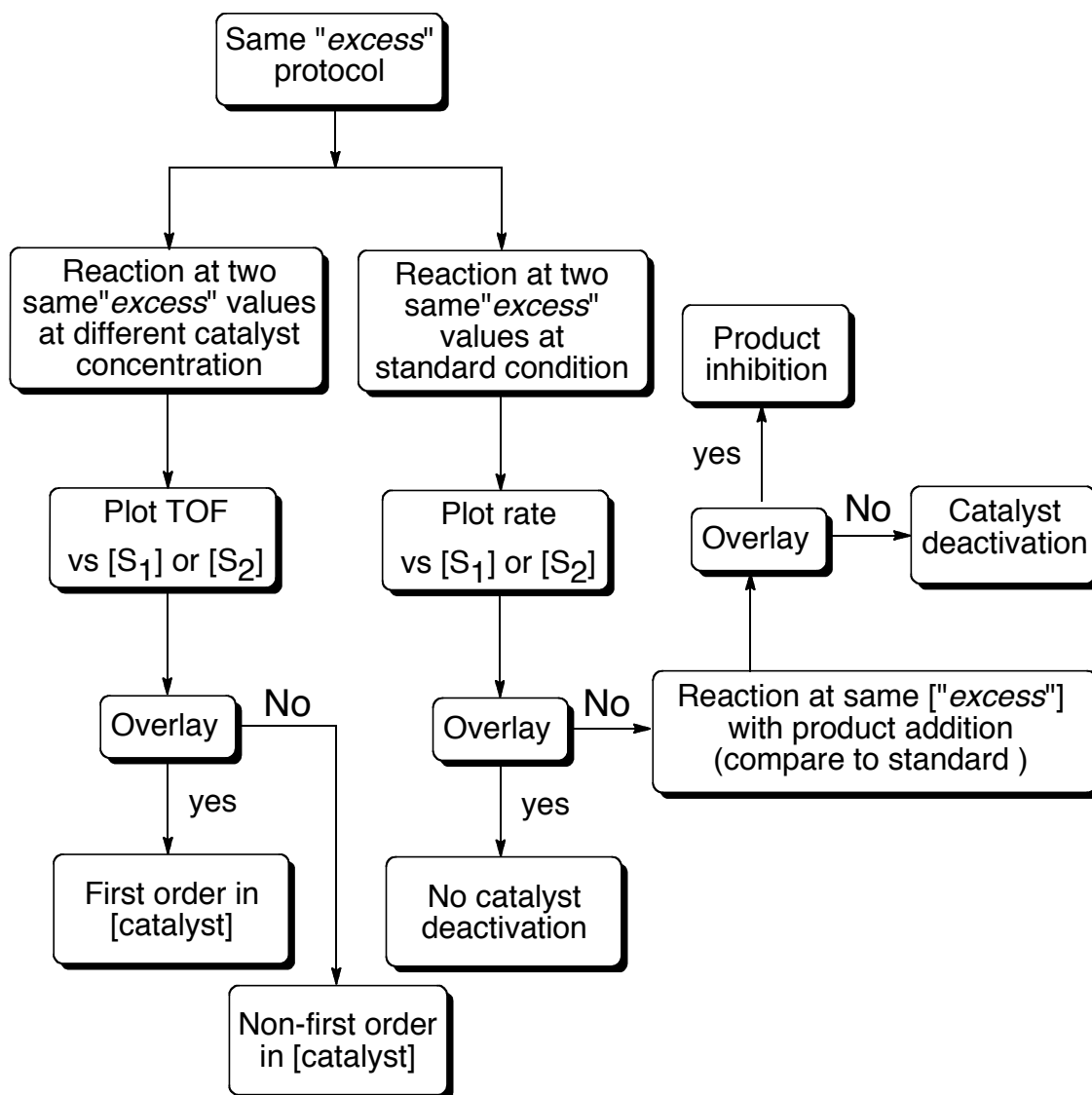
Figure II-18. Flow chart for same "*excess*" protocol

but not all, catalytic reactions do have first order behavior in catalyst concentration. The rate is normalized by dividing the steady state rate equation by catalyst concentration, which is also known as turnover frequency (TOF, Figure II-17a). To reveal the order of the catalyst in any catalytic reaction through RPKA method, two experiments with the same *"excess"* but different catalyst concentrations are performed. After plotting the TOF vs. $[S_1]$, if the two plots overlay, the reaction is first order in catalyst concentration.[22]

To show the application of the same "*excess*" protocol in revealing the catalyst order, the alkylation of chalcone with diethylzinc using Ni(acac)$_2$ and (-)-MIB ((2*S*)-(-)-3-*exo*-morpholinoisoborneol) as a chiral ligand is described. Two experiments with the *"excess"* of 0.15 M and different catalyst concentration (0.11 and 0.056 M) were carried out. After plotting the TOF vs. chalcone concentration, the curves of both experiments fall on top of each other, signifying that the catalyst is first order in the alkylation reaction. Determining the order in catalyst by this method does not require any information about the reaction order for other reagents. The same *"excess"* protocol, which was explained above, has been summarized as a flow chart in Figure II-18.[22]

2.3.4: Reaction Progress Kinetic Analysis of the Chlorolactonization Reaction:

2.3.4.1: Different *"Excess"* Protocol

As explained above different *"excess"* protocol can be applied to elucidate the order of each reagent in any catalytic or non-catalytic reaction. In the original optimized condition 0.051 M of 4-aryl-4-pentenoic acid is cyclized in the presence of 0.056 M, 1,3-
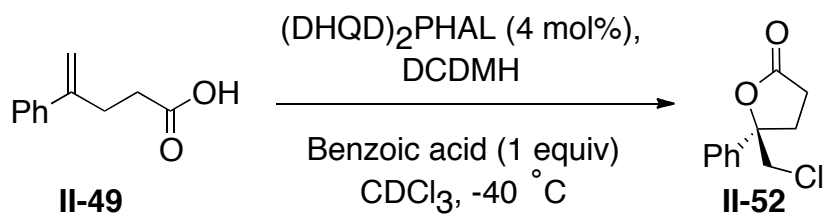
Table II-2. Different "*excess*" protocol for our asymmetric chlorolactonization

	II-49 (M)	DCDMH (M)	*excess*
Exp A	0.071	0.051	0.02
Exp B	0.091	0.051	0.04

dichloro-5,5-diphenylhydantoin, DCDMH as the chlorine source and 10 mol % (DHQD)$_2$PHAL as the chiral catalyst. The highest enantioselectivity was observed in a 1:1 mixture of chloroform and hexane and 0.051 M benzoic acid as solvent and additive, respectively. The progress of the reaction was monitored by NMR. Because 1-chloro-5,5-diphenylhydantoin, the by-product precipitates during the course of the reaction in the chosen solvent, 1,3-dichloro-5,5-dimethylhydantoin (DCDMH) was used as the chlorine source. Moreover, deuterated chloroform was used as the solvent instead of a 1:1 mixture of chloroform and hexane and only 4 mol% of the catalyst was added to slow down the reaction. These adjustments for the kinetics studies lead to only a 5% depletion of *ee* and presumably do not change the reaction mechanism.

"*Excess*" of 0.02 and 0.04 (Table II-2) were chosen for the different "*excess*" protocol with DCDMH as the limiting reagent in both experiments (Exp A: [DCDMH]$_0$ =
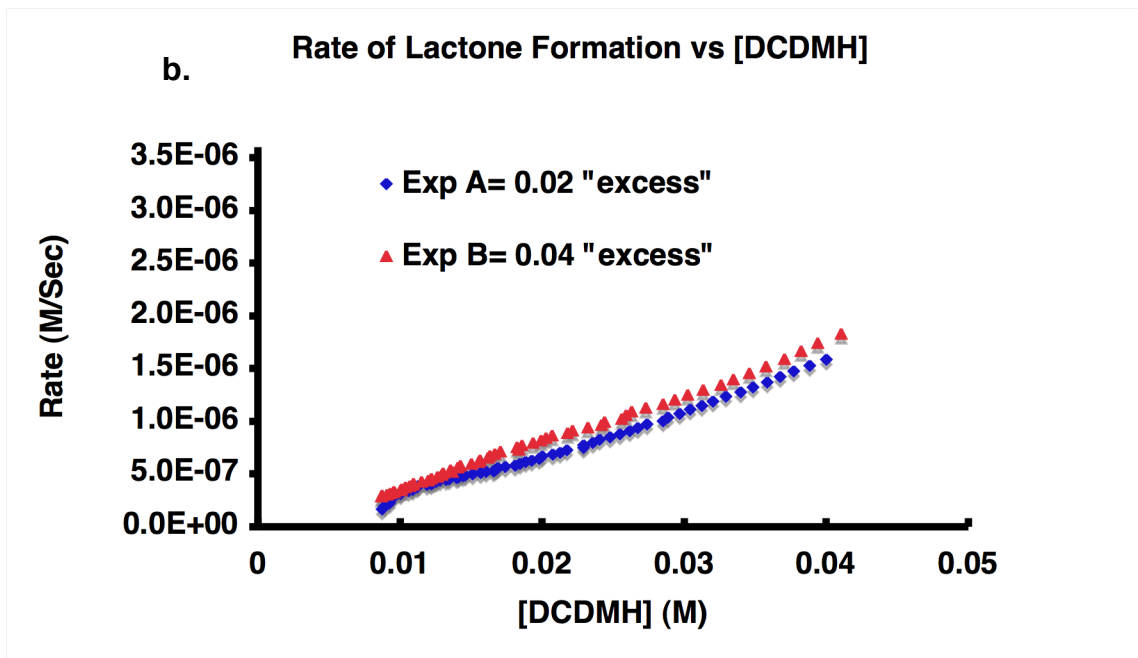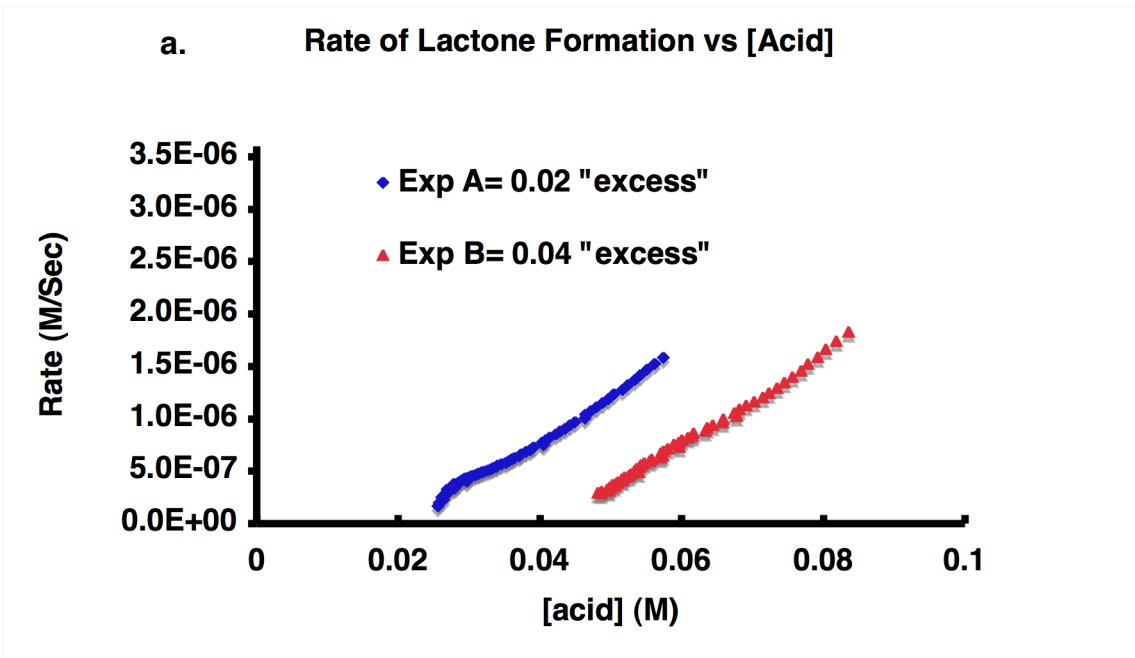
Figure II-19. a. Rate versus [Acid], b. Rate versus [DCDMH]
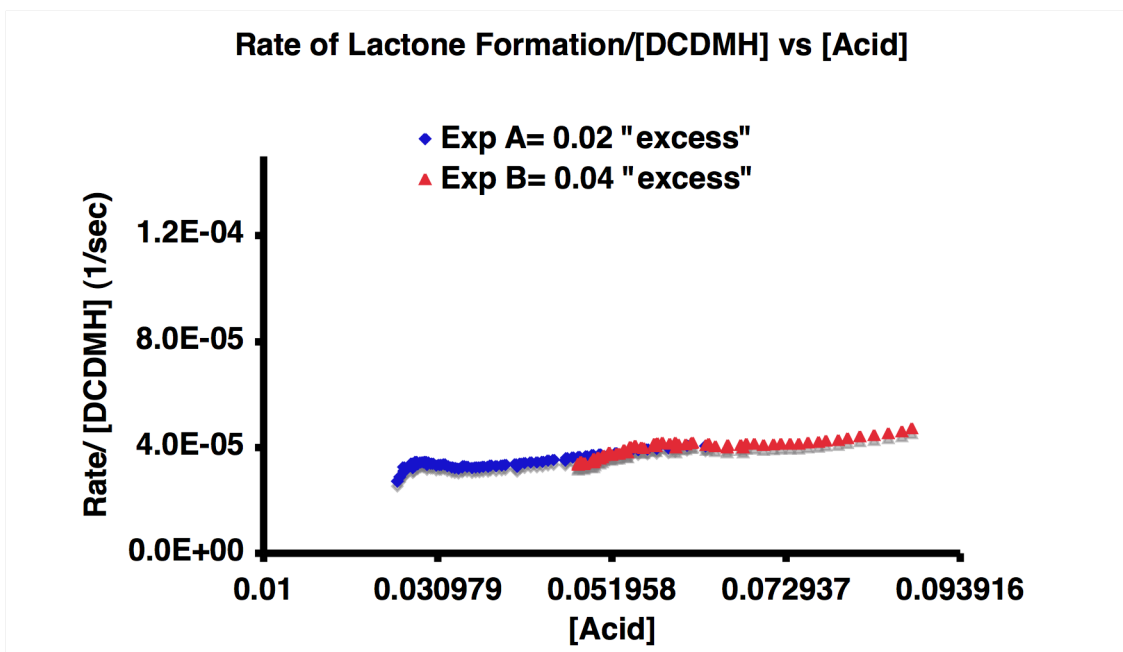
Figure II-20. Rate/[DCDMH] versus [Acid]

0.051 M and $[Acid]_0 = 0.071$ M, Exp B: $[DCDMH]_0 = 0.051$ M and $[Acid]_0 = 0.091$ M). The conditions in both experiments are close to the optimized conditions, which highlights the advantage of the RPKA method vs. classical kinetic method. In addition, in these two experiments benzoic acid not only assumes the role of the additive, it also is used as the internal standard to normalize the integral values of the product and starting materials during the course of the reaction.

After collecting the data and plotting the rate vs. 4-phenylpent-4-enoic acid **II-49** concentration, no overlay was observed (Figure II-19). Based on the different "*excess*" protocol flow chart (Figure II-14), this means that the chlorolactonization reaction is not zero order in DCDMH. On the other hand the plot of the rate vs. the concentration of

a.

Rate of Lactone Formation vs [Acid]

b.

Rate of Lactone Formation vs [DCDMH]
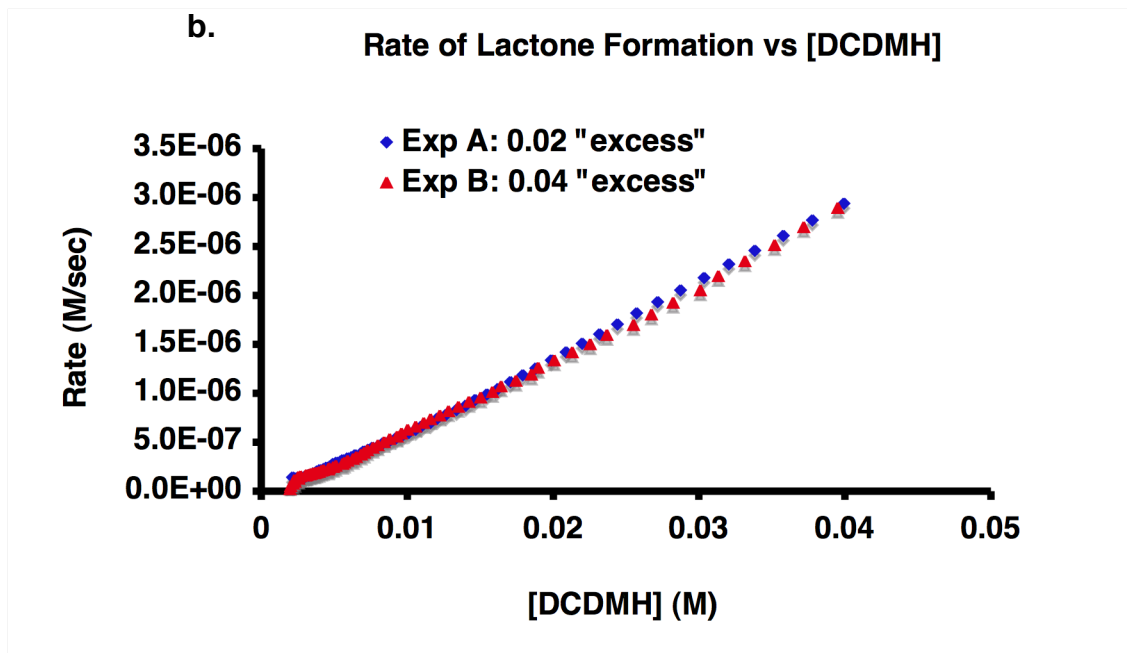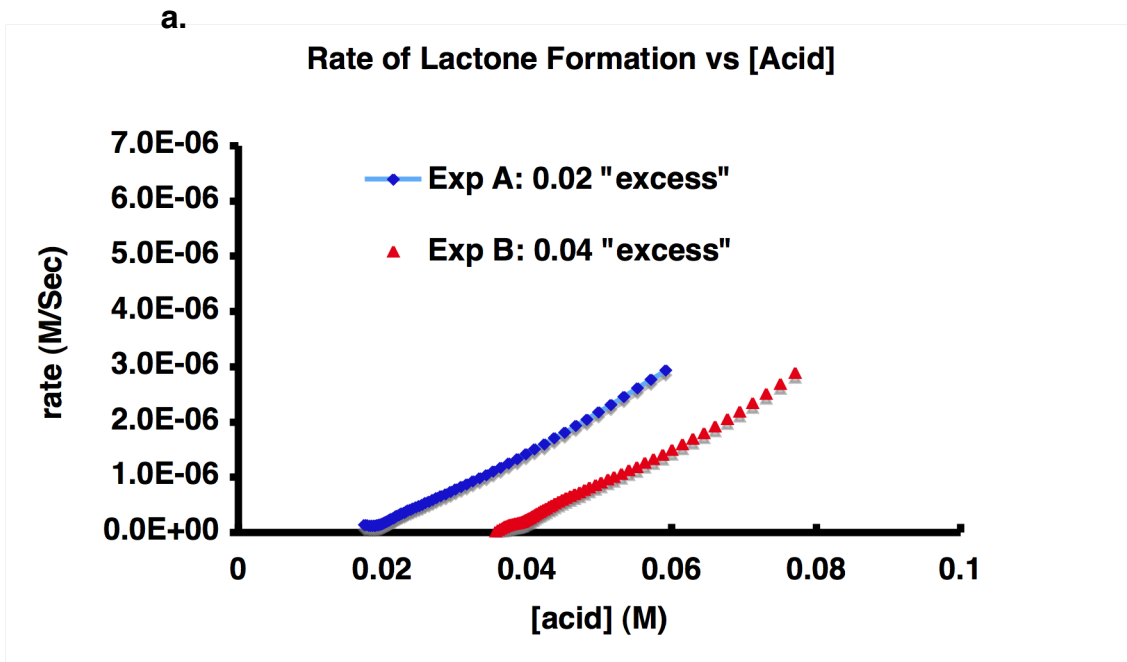
Figure II-21. a. Rate versus [Acid], b. Rate versus [DCDMH] in the absence of benzoic acid

DCDMH for both experiments A and B fall on top of each other, which suggest that 4-phenylpent-4-enoic acid **II-49** has a zero other in the rate equation of the chlorolactonization reaction. More over the straight line obtained by plotting rate vs. the concentration of DCDMH suggests that the reaction rate is first order with respect to DCDMH (Figure II-19).

At this point the rate equation for the asymmetric chlorolactonization can be expressed as rate = k [DCDMH]. Based on this equation, plotting the rate/[DCDMH] vs. [Acid] should yield overlaid horizontal straight lines for both experiments with different "*excess*" (Figure II-20).

The role of benzoic acid as an additive to increase the enantioselectivity has not been clear. To test whether or not the added benzoic acid changes the dependence of the starting material in the rate of the reaction similar kinetics studies were performed in
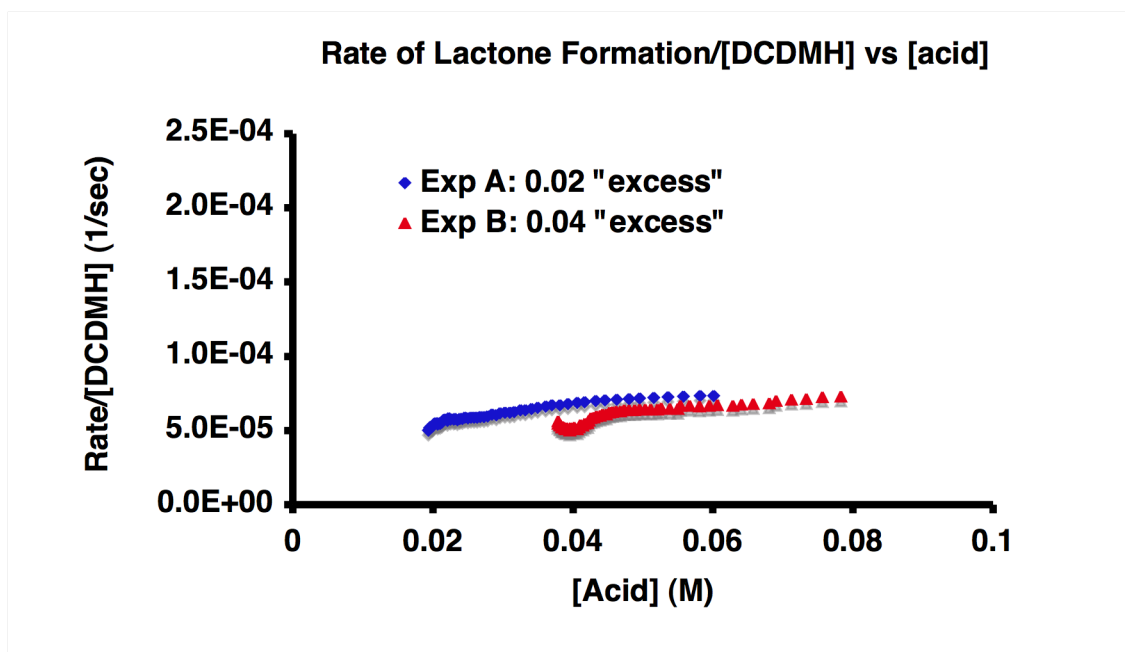
Figure II-22. Rate/[DCDMH] versus [Acid] in the absence of the benzoic acid
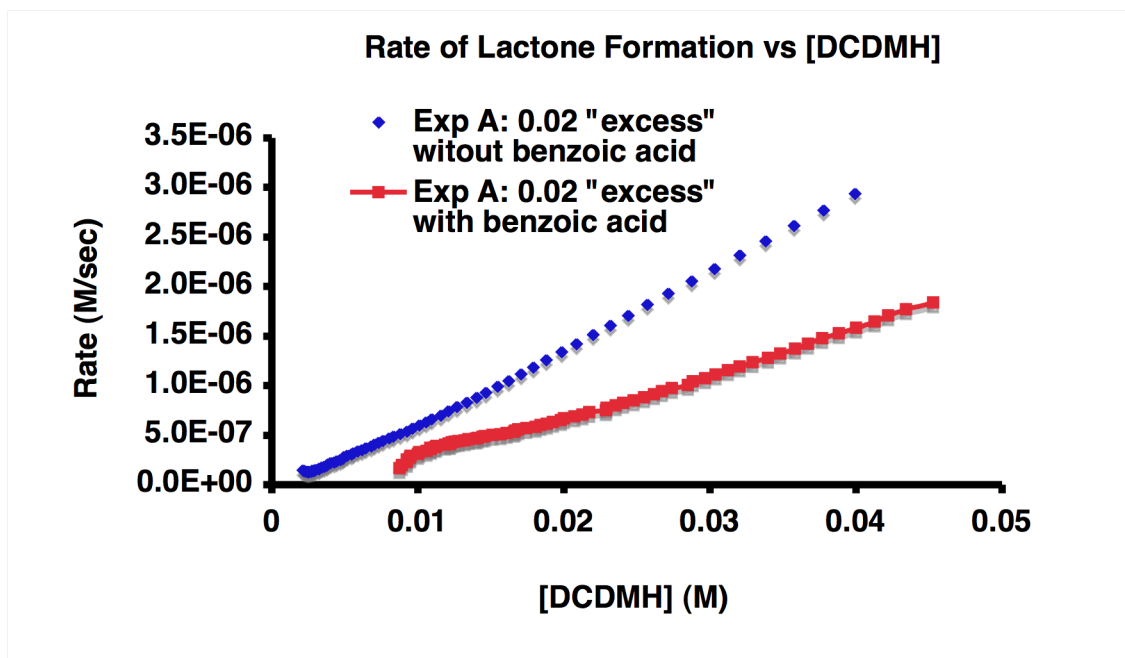
Figure II-23. Rate of the lactone formation in the absence and presence of the benzoic acid

the absence of benzoic acid. In these studies one equiv. of toluene was used as the internal standard. Plotting the rate vs. concentration of DCDMH exhibits an overlay between the two experiments with different *"excess"* (Figure II-21). As explained before this suggests that 4-phenylpent-4-enoic acid **II-49** acid is zero order with respect to the rate of equation.

Moreover, the observation of a straight line in this graphical rate suggests that DCDMH order remains the same as was observed in the presence of benzoic acid. This is confirmed again with the observation of a straight horizontal line (Figure II-22) by plotting the rate/[DCDMH] vs. [acid].

Since the addition of benzoic acid to the reaction as an additive did not change the order of DCDMH and the acid substrate, it is likely that benzoic acid does not change

129
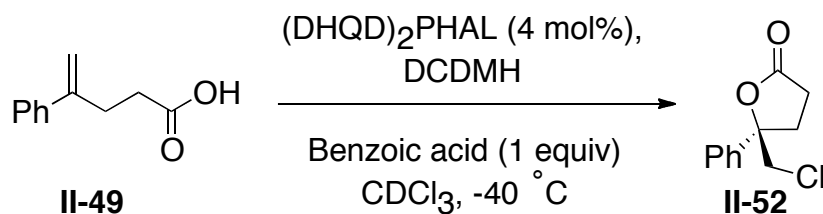
	II-49 (M)	DCDMH (M)	*excess*
Exp A	0.071	0.051	0.02
Exp B	0.091	0.071	0.02

Table II-3. Same "*excess*" protocol for our asymmetric chlorolactonization

the mechanism of the reaction. To better compare these two sets of experiments, in the absence and in the presence of the benzoic acid, Exp A rates of the both sets with the "*excess*" of 0.02 vs. the concentration of DCDMH were compared (Figure II-23). As can be seen the rate of the chlorolactonization is significantly slower in the presence of 1 equiv. of benzoic acid. This can be due to the competition between 4-phenylpent-4-enoic acid **II-49** and benzoic acid for binding with the active site of the catalyst. This behavior will be discussed in detail later on in this chapter.

2.3.4.2: Same "*Excess*" Protocol

2.3.4.2.1: Catalyst Instability

Catalyst instability could be significant for any catalytic reaction. The RPKA same "*excess*" protocol was used to understand whether the chlorolactonization system suffers from deactivation of (DHQD)$_2$PHAL during the course of the reaction or not.

130
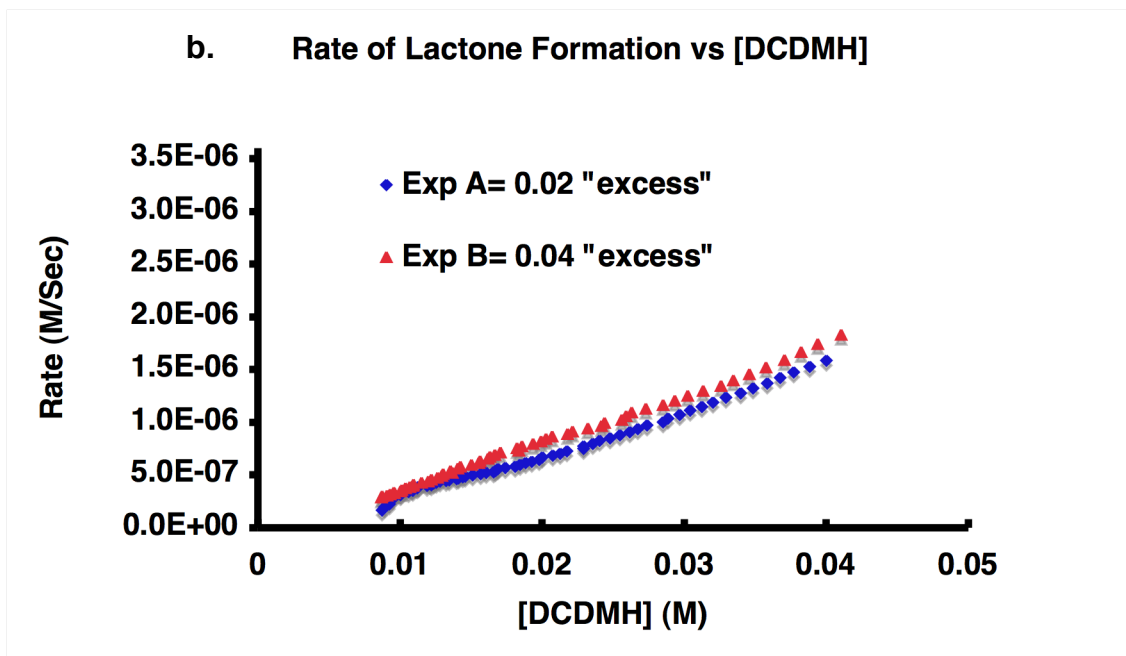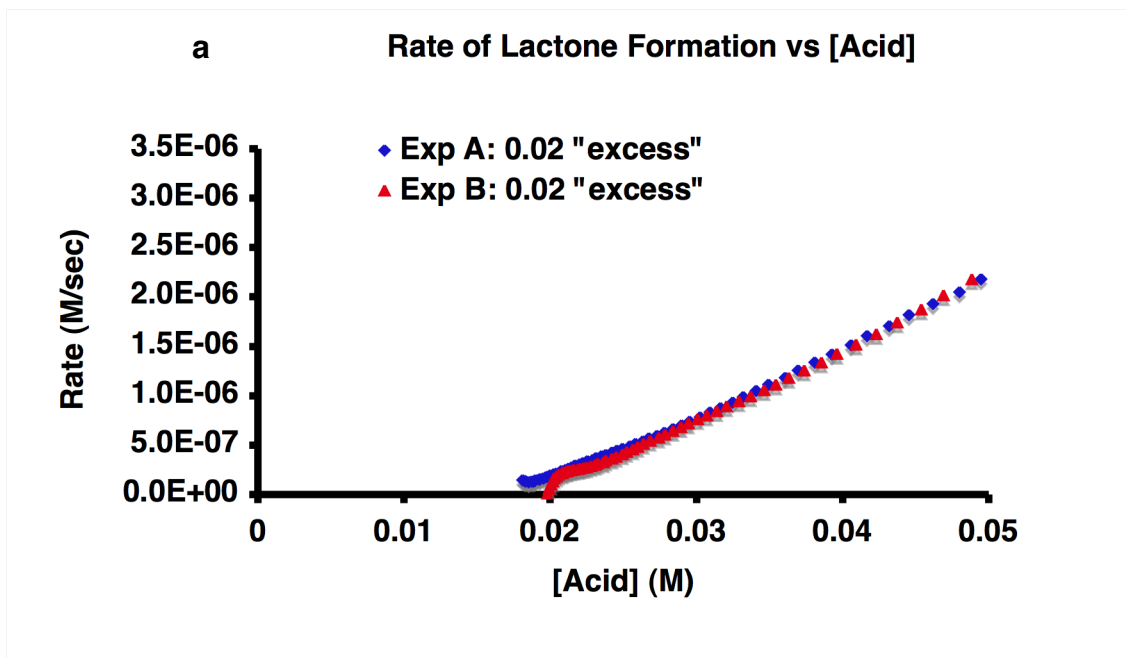
Figure II-24. Catalyst instability investigation in the presence of benzoic acid

131

a   **Rate of Lactone Formation vs [DCDMH]**

b.   **Rate of Lactone Formation vs [Acid]**
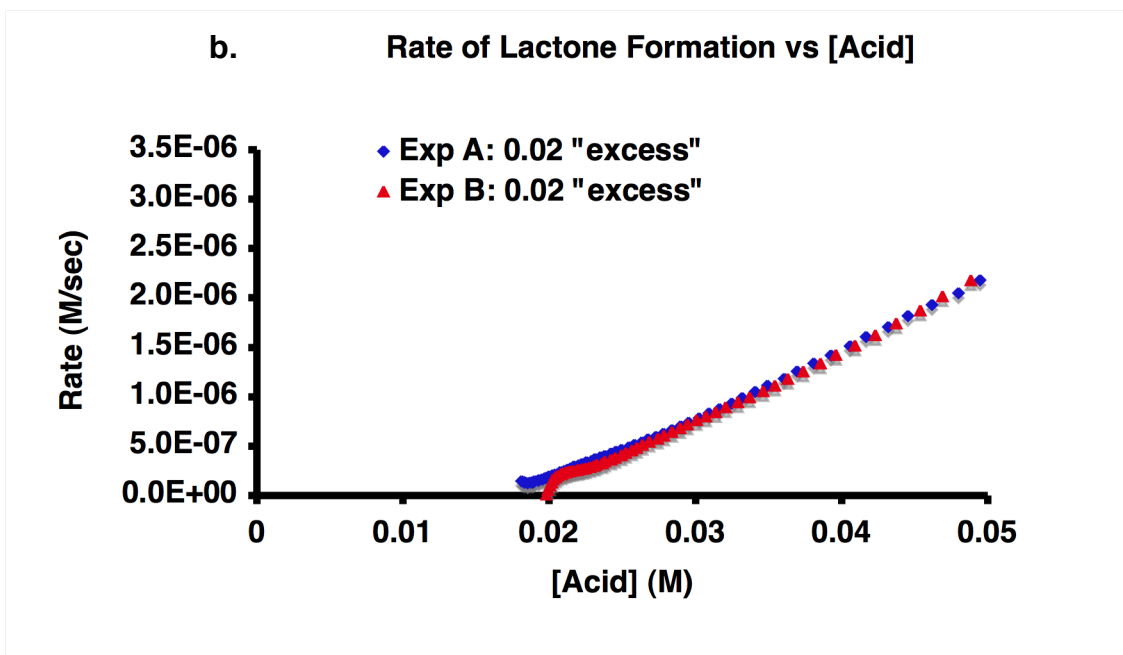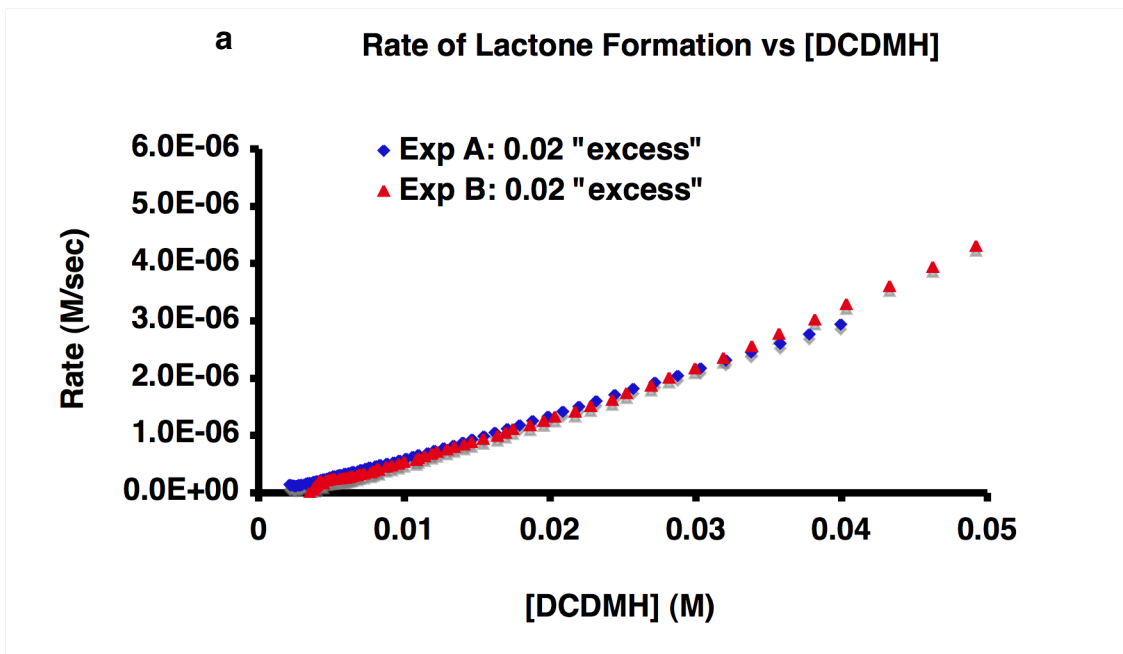
Figure II-25. Catalyst instability investigation in the absence of benzoic acid

"*Excess*" of 0.02 (Table II-3) was chosen for the same "*excess*" protocol, and DCDMH was used as the limiting reagent in both experiments (Exp A: $[DCDMH]_0 = 0.051$ M and $[Acid]_0 = 0.071$ M, Exp B: $[DCDMH]_0 = 0.071$ M and $[Acid]_0 = 0.091$ M). The plot of the rate vs. [DCDMH] or [acid], for both experiments overlay with each other completely (Figure II-24). This result indicates that Exp B at any concentration of DCDMH or acid exhibits the same rate as Exp A, although the catalyst in Exp B has completed more cycles compared to Exp A. This clearly shows that $(DHQD)_2PHAL$ does not suffer from any sort of deactivation during the course of the reaction. Similar behavior was observed by running the same experiments in the absence of the benzoic acid (Figure II-25). In this case toluene was used as the internal standard.

2.3.4.2.2: Catalyst Order

As mentioned before most, but not all, catalytic reactions are first order in catalyst concentration. To reveal the order of $(DHQD)_2PHAL$ in the asymmetric chlorolactonization reaction through RPKA method, two same "*excess*" experiments with different catalyst concentration (4 and 6 mol%) were performed. "*Excess*" of 0.02 (Table II-4) was chosen for this study and DCDMH was the limiting reagent in both experiments (Exp A: $[DCDMH]_0 = 0.051$ M and $[Acid]_0 = 0.071$ M, in the presence of the 0.00204 M $(DHQD)_2PHAL$, Exp B: $[DCDMH]_0 = 0.071$ M and $[Acid]_0 = 0.091$ M in the presence of 0.00306 M $(DHQD)_2PHAL$.). The plot of TOF vs. the concentration of DCDMH, leads to two linear lines that overlay on top of each other (Figure II-26). This suggests that like most of catalytic reactions, $(DHQD)_2PHAL$, exhibits first order rate behavior.
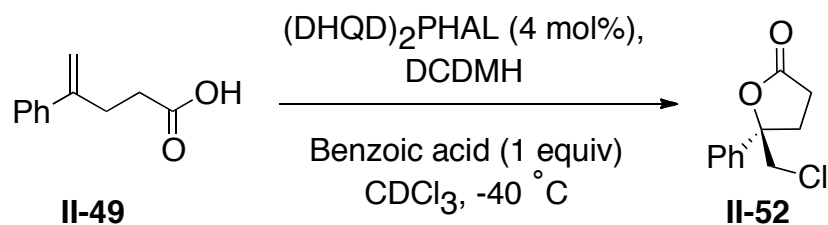
	II-49 (M)	DCDMH (M)	*excess*	Catalyst (M)
Exp A	0.071	0.051	0.02	0.002
Exp B	0.071	0.051	0.02	0.003

Table II-4. Same excess protocol in revealing the catalyst order

2.3.4.3: Rate-Determining-Step.

Based on kinetics studies discussed thus far the rate equation for the asymmetric chlorolactonization is: rate $= k$ [(DHQD)$_2$PHAL] [DCDMH]. According to the rate equation, (DHQD)$_2$PHAL and DCDMH have first order behavior and 4-phenylpent-4-enoic acid **II-49** concentration does not have any influence on the reaction rate. As a result, we can propose a catalytic cycle, depicted in Scheme II-18 that accounts for these observations. In the first step two molecules of 4-phenylpent-4-enoic acid **II-49** bind to the protonated catalyst most probably as a salt to form complex **II-95**. This equilibration cannot be the RDS, as the concentration of the acid substrate **II-49** does not appear in the rate equation. In the second step one molecule of hydantoin binds to complex **II-95** by replacing one acid substrate to form complex **II-96**. This can be the RDS as the DCDMH molecule is involved. The unreactivity of the DCDMH in the absence of the (DHQD)$_2$PHAL at -40 $^\circ$C (little to no background reaction) leads to the

134
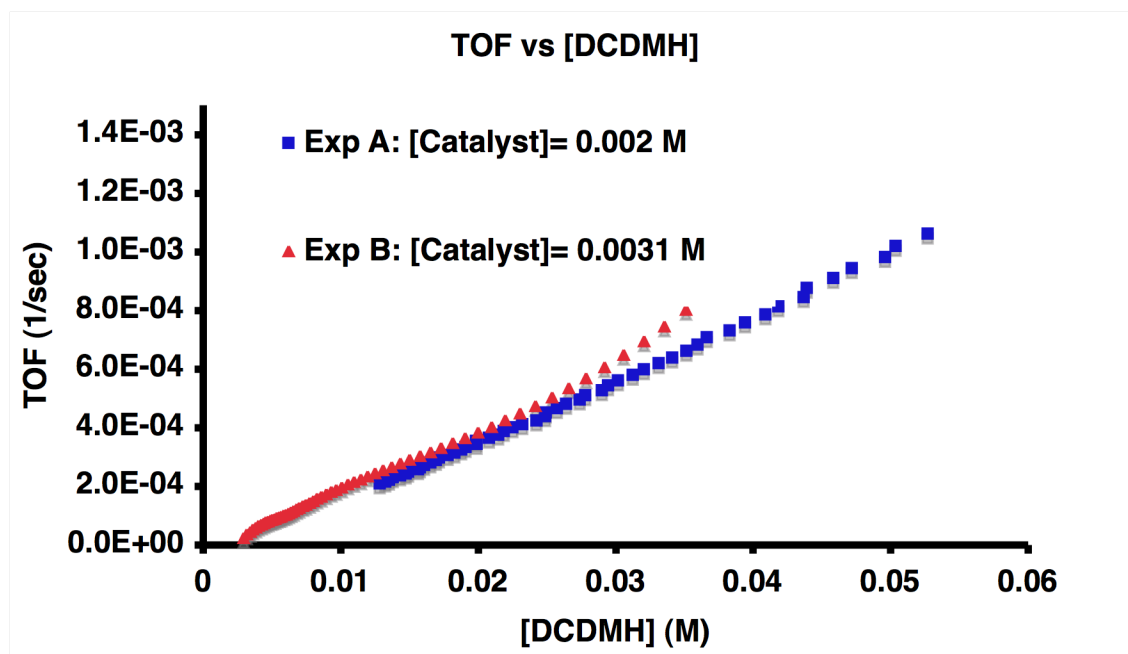
Figure II-26. TOF versus [DCDMH] graph

proposal for the second step. Hydrogen binding of DCDMH to the protonated catalyst presumably activates the DCDMH at -40 °C. NMR studies in support of this supposition are detailed in Chapter 4.

Considering the third and fourth step (chlorine delivery and cyclization) only the third step can be RDS as DCDMH is directly involved in this step. Therefore the second and third steps, DCDMH binding to the catalyst and chlorine delivery to the olefin, are considered as the rate-determining step for the chlorolactonization reaction.

During substrate scope studies it was found that 4-(3-nitrophenyl)pent-4-enoic acid substrate is unreactive under optimized conditions. This substrate provides the opportunity to kinetically segregate the second and third steps, via a competition study.
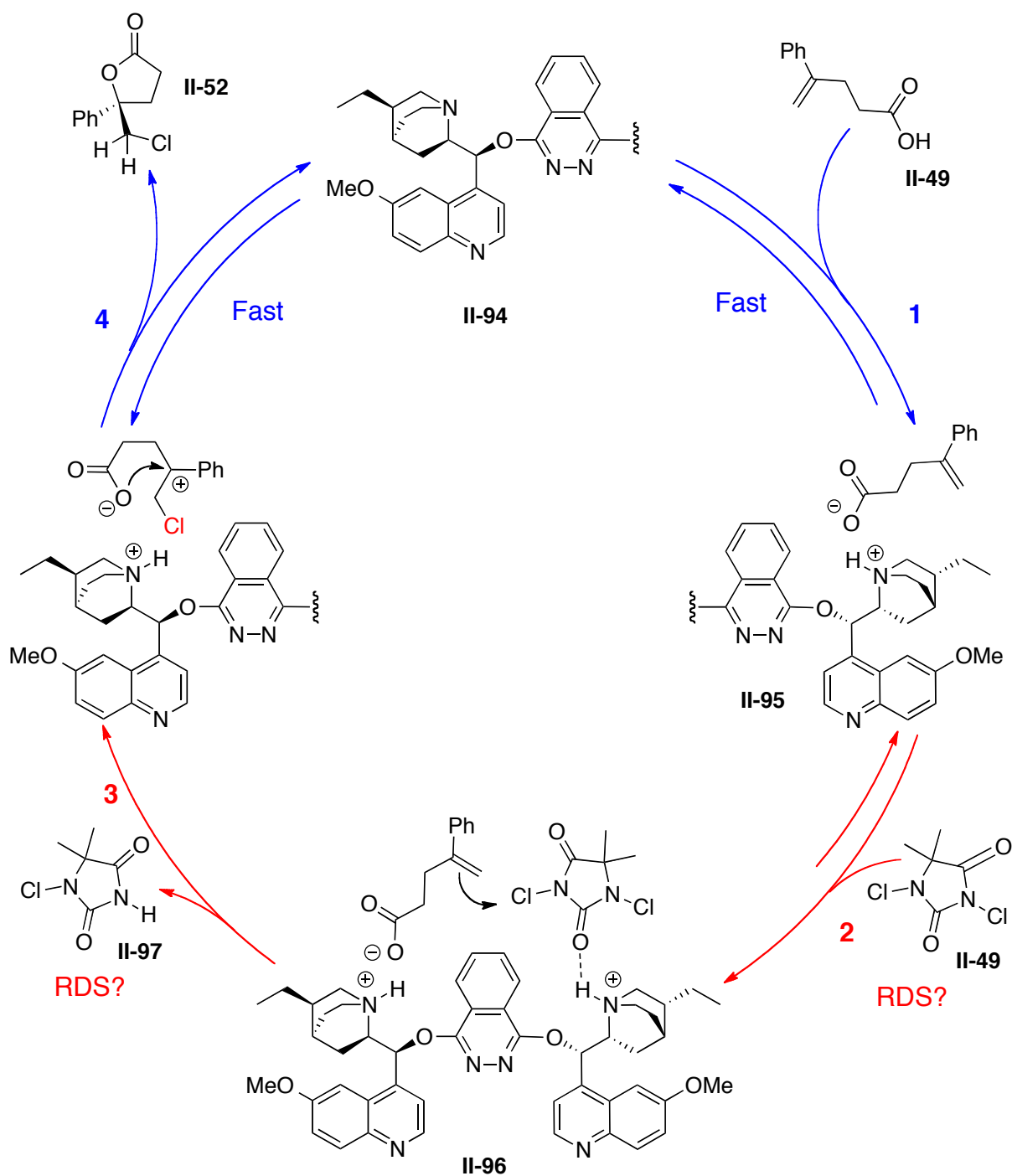
Scheme II-18. Proposed mechanism and possible RDS steps

If the second step is the RDS, addition of the 4-(3-nitrophenyl)pent-4-enoic acid substrate should not have any effect on the rate of the reaction of 4-phenylpent-4-enoic acid **II-49** substrate chlorolactonization as none of these substrates are involved in this step. If the third step, chlorine delivery, is the RDS, the presence of the non-reactive 4-(3-nitrophenyl)pent-4-enoic acid substrate should decrease the rate of the 4-phenylpent-4-enoic acid **II-49** substrate chlorolactonization. The slower rate is expected since -(3-nitrophenyl)pent-4-enoic acid substrate would compete for binding with the catalyst. Indeed, in the presence of 4-(3-nitrophenyl)pent-4-enoic acid, 4-phenylpent-4-enoic acid **II-49** and DCDMH (1:1:1) and 1.5 mol% catalyst, the rate of the chlorolactonization of 4-phenylpent-4-enoic acid **II-49** was decreased dramatically as depicted in Figure II-27 (71% slower). A 50% decrease in rate would suggest equal binding affinity of **II-98** and **II-49** with the catalyst. The larger observed inhibition indicates a greater affinity of the catalyst for **II-98**.

A similar competition study was performed between two reactive substrates, 4-phenylpent-4-enoic acid **II-49** and 4-(4-(trifluoromethyl)phenyl)pent-4-enoic acid **II-993**. Substrate **II-99** is ten times less reactive as compared to **II-49**, presumably because of having a less nucleophilic olefin moiety. In this competition study, in the presence of 4-(trifluoromethyl)phenyl)pent-4-enoic acid (as a less reactive competitor), 4-phenylpent-4-enoic acid **II-49** and DCDMH (1:1:1) and 1.5 mol% catalyst, the rate of the chlorolactonization of 4-phenylpent-4-enoic acid **II-49** was decrease 58% as depicted in Figure II-28**.**
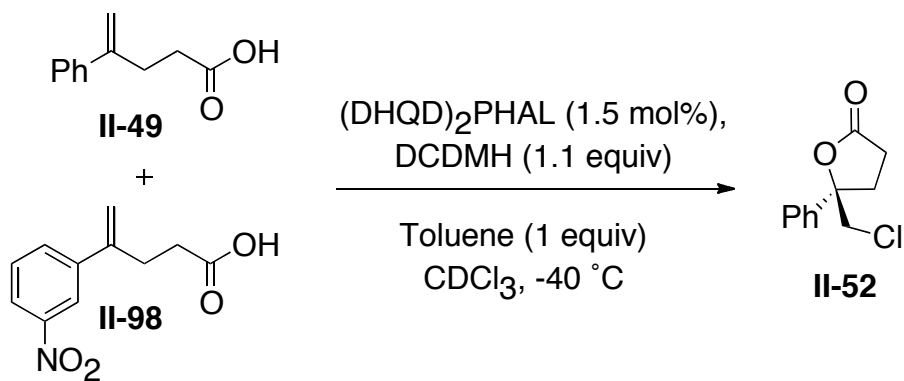
	II-49	II-98	(DHQD)$_2$PHAL	DCDMH
Exp A	0.051 (M)	0.000 (M)	0.0008 (M)	0.056 (M)
Exp B	0.051 (M)	0.051 (M)	0.0008 (M)	0.056 (M)

k' (Sec $^{-1}$) = 4.97E-5
k' (Sec $^{-1}$) = 1.46E-5
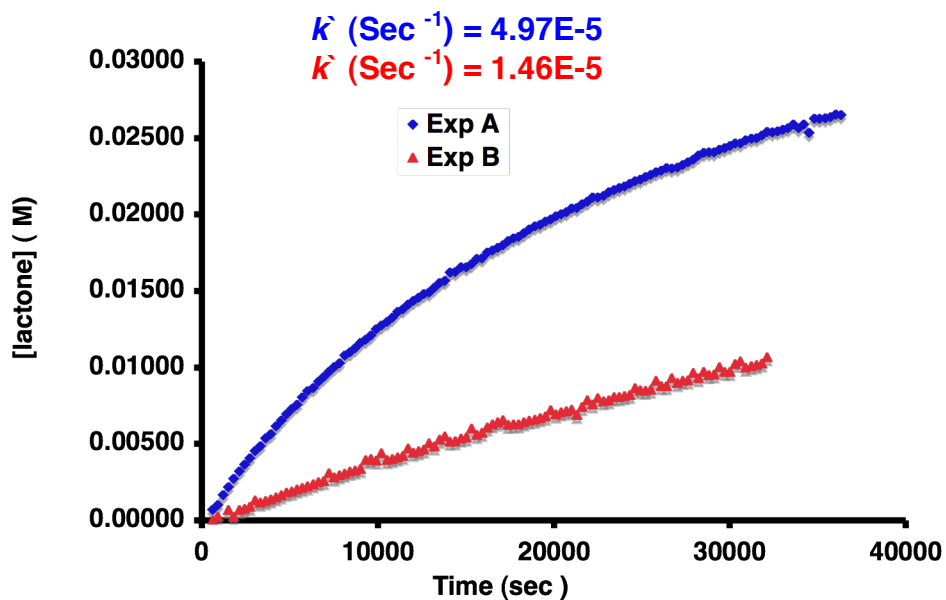
Figure II-27. Competition study between 4-(3-nitrophenyl)pent-4-enoic acid and 4-phenylpent-4-enoic acid
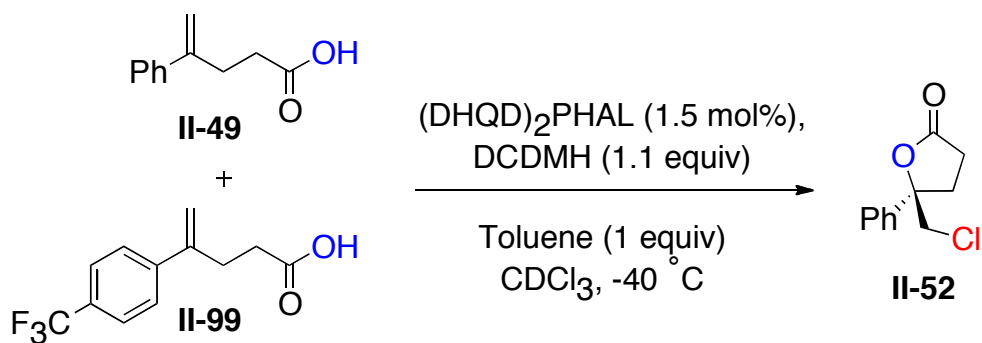
	II-49	II-99	(DHQD)₂PHAL	DCDMH
Exp A	0.051 (M)	0.000 (M)	0.0008 (M)	0.056 (M)
Exp B	0.051 (M)	0.051 (M)	0.0008 (M)	0.056 (M)
Exp C	0.000 (M)	0.051 (M)	0.0008 (M)	0.056 (M)

k (Sec^{-1}) = 4.97E-5
k (Sec^{-1}) = 2.1E-5
k (Sec^{-1}) = 5.00E-6
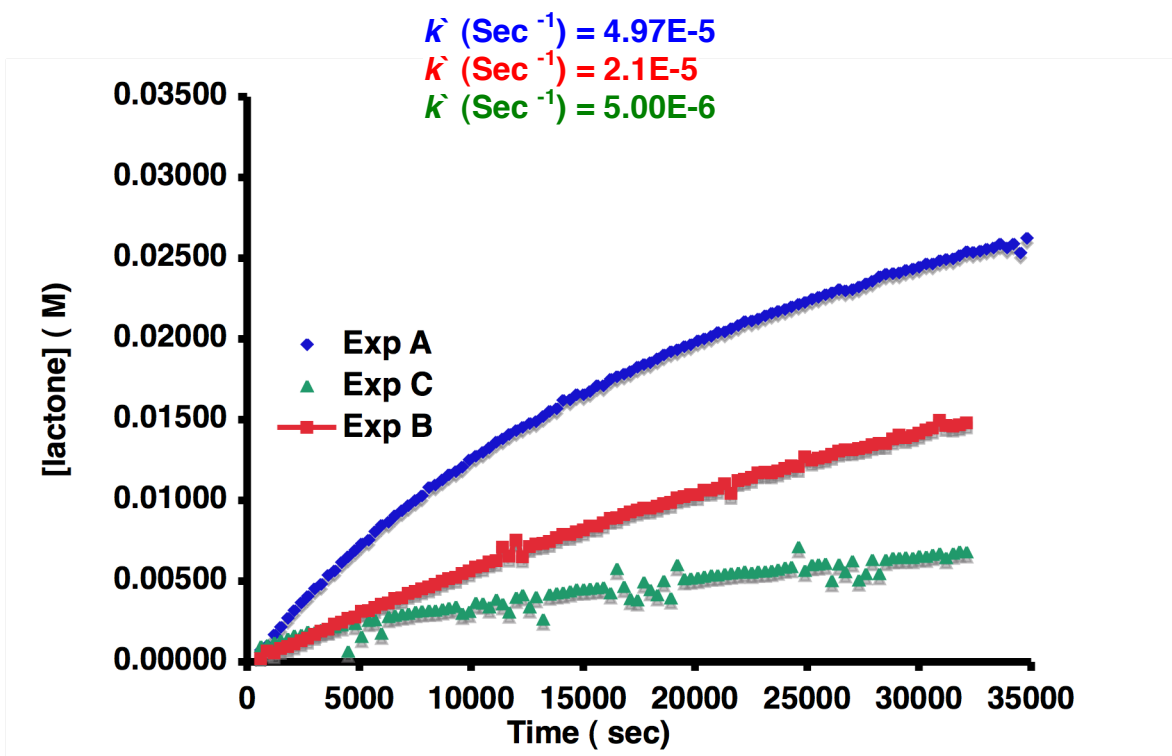
Figure II-28. Competition studiy between 4-(4-(trifluoromethyl)phenyl)pent-4-enoic acid and 4-phenylpent-4-enoic acid

Based on these two competition studies it is suggested that chlorine delivery to **II-49** in the third step is the rate-determining step in the chlorolactonization reaction (Scheme II-18 and 19).

2.3.4.4: Kinetic Isotope Effect

As described in the previous section, the chlorine delivery to the 4-phenylpent-4-enoic acid was assigned as the RDS. As depicted in Scheme II-51, in this step the nucleophilic olefin attacks the N3 chlorine on DCDMH, which is presumably activated through hydrogen binding with the protonated quinuclidine (Scheme II-51). Due to the activation of DCDMH prior to the chlorenium delivery, this process is categorized as a specific acid catalysis. It is known that the reaction will proceed faster in a specific acid catalysis by replacing the proton with the more acidic deuterium.[25-27] Based on this hypothesis, a reverse kinetic isotope effect for the catalytic asymmetric chlorolactonization is expected.

To test this hypothesis the rate of deuterated 4-phenylpent-4-enoic acid **II-49** (RCO$_2$D) was measured and compared to 4-phenylpent-4-enoic acid. This study indeed
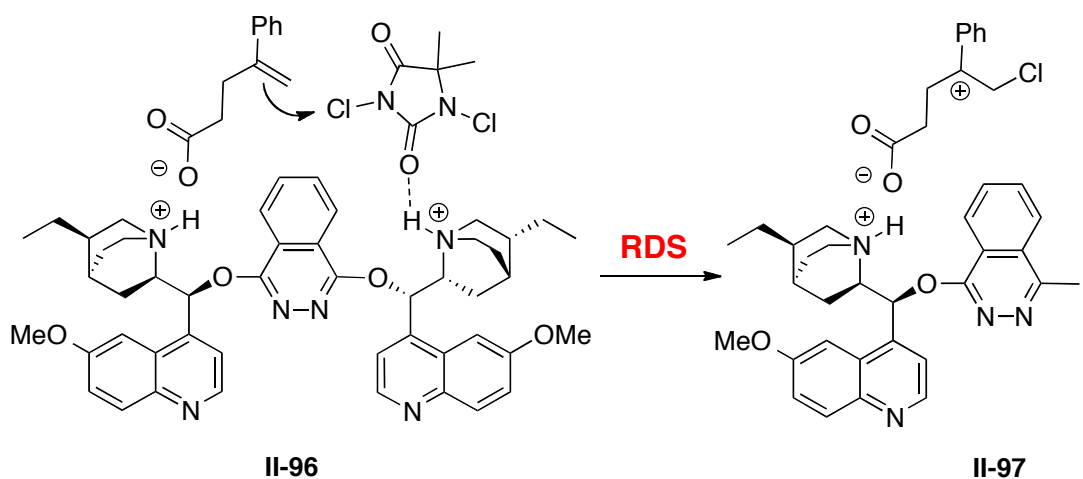
Scheme II-19. Rate determining step in asymmetric chlorolactonization

140

shows the anticipated reverse isotope effect (kH/kD = 0.81). The observed reverse isotope effect (specific acid catalysis) supports the hypothesis that DCDMH is activated presumably by hydrogen binding with the catalyst prior to the RDS.

2.4: Conclusion

Mechanistic studies of the DHQD$_2$PHAL catalyzed asymmetric chlorolactonization reaction of alkenoic acids have led to some surprising conclusions. Deuterium labeling studies of the catalyzed reaction have revealed that the high face selectivity of the delivery of the chlorenium ion to olefins is neither necessary nor a sufficient condition to deliver the product lactones with high enantioselectivities. The reaction likely proceeds via a carbocation intermediate with the enantioselectivity being imparted by the "templation" of the cyclization of the acid nucleophile by the chiral catalyst. In addition, Reaction progress kinetic analysis (RPKA) and competition studies revealed that the rate-determining step was the delivery of the chlorine ion on to the olefin. Moreover, the observed reverse isotope effect (specific acid catalysis) suggests that DCDMH is activated prior to RDS, presumably by hydrogen binding with the catalyst. Taken together, these results suggest that the rate determining step and the enantioselectivity determining step are segregated. Formation of the chloronium ion and the cyclization on to the resulting carbocation are highly stereoselective processes.

2.5: Experimental Details

2.5.1: General Information

All reagents were purchased from commercial sources and used without purification. Anhydrous chloroform stabilized with amylenes and HPLC grade 95% *n-*

hexanes were used for all asymmetric chlorolactonizations. ^{1}H and ^{13}C NMR spectra were collected on a 600, 500 or 300 MHz NMR spectrometer (VARIAN INOVA) using CDCl$_3$. Chemical shifts are reported in parts per million (ppm). Spectra are referenced to residual solvent peaks. All compounds were characterized by ^{1}H and ^{13}C NMR.

2.5.2: Procedure for Synthesis of Labeled Acid II-59 and Ester II-71

Deuterated 4-pentyne-1-ol (II-69):

4-Pentyne-1-ol (420 mg, 5 mmol, 1 equiv.) were dissolved in diethyl ether (30 mL) in 50 mL round bottom flask and cooled to 0 $^{\circ}$C. *n*BuLi, 1.6 M in hexane, (9.4 mL, 15 mmol, 3 equiv.) was added drop wise. The reaction mixture was warmed to rt and stirred for 1 h and then cooled again to 0 $^{\circ}$C and quenched with D$_2$O. The organic layer was separated and dried over anhydrous Na$_2$SO$_4$. The crude alkyne **II-69** was obtained (341 mg, 80% yield) after slow evaporation of the solvent and was used in the next reaction without purification. ^{1}H NMR (500 MHz, CDCl$_3$): δ 1.6 (1H, br), 1.75 (2H, m), 2.3 (2H, t, *J* = 7 Hz), 3.75 (2H, dt, *J* = 2.0, 6.0 Hz); ^{13}C NMR (150 MHz, CDCl$_3$): δ 14.9, 30.9, 61.30, 68.5 (t, *J* = 37.9 Hz), 83.4 (t, *J* = 7.0 Hz); IR (cm^{-1}, NaCl plate): 3335, 2588.5; HRMS (C$_4$H$_5$DO): Calc. [M]$^{+}$: 71.0481, Found [M]$^{+}$: 71.0485

Deuterated 4-phenylpent-4-en-1-ol (II-70):[20]

In a 5 mL round bottom flask alkyne **II-69** (42 mg, 0.49 mmol, 1.0 equiv.), Pd(PPh$_3$)$_4$ (17 mg, 0.015 mmol, 0.03 equiv.), phenylboronic acid (72 mg, 0.59 mmol, 1.2 equiv.), and dry 1,4-dioxane (1 mL) were added. The resulting mixture was treated with AcOH (3 μL, 0.052 mmol, 0.1 equiv.) under an argon atmosphere. The mixture was stirred for 10 min at room temperature and then for 10 h at 80 $^{\circ}$C. The reaction

mixture was concentrated and purified by column chromatography (1:4 EtOAc/hexane) to give the desired product (66 mg, 83% yield). ^{1}H NMR (600 MHz, CDCl$_3$): δ 1.22 (1H, br), 1.71 (2H, m), 2.6 (2H, t, J = 7.8 Hz), 3.65 (2H, t, J = 10.2 Hz), 5.27 (1H, s), 7.26 (1H, m), 7.32 (2H, m), 7.39 (2H, m); ^{13}C NMR (125 MHz, CDCl$_3$): δ 31.0, 31.4, 62.1, 112.3 (t, J = 20.1 Hz), 126.0, 127.3, 128.2, 140.9, 147.8; IR (cm^{-1}, NaCl plate): 3336, 2258, 1059; HRMS (C$_{11}$H$_{13}$DO): Calc. [M]$^+$: 163.1107, Found [M]$^+$: 163.1108

Deuterated 4-phenylpent-4-enoic acid (II-59):

Deuterated 4-phenylpent-4-en-1-ol (**II-70**) (65 mg, 0.4 mmol, 1.0 equiv.) was dissolved in dried DMF (2 mL) and PDC (526 mg, 1.4 mmol, 3.5 equiv.) was added. The resulting mixture was stirred at rt overnight under nitrogen gas. After completion of the reaction, monitored by TLC, the solvent was evaporated and the residue was purified by flash chromatography (1:3 EtOAc/hexane) to get desired product [71 mg, 90% yield, 83% E (5.29 ppm, integral = 0.72) 5% Z (5.08 ppm, integral = 0.05) and 12% 4-phenylpent-4-enoic acid (5.09 and 5.31 ppm, overall integral = 0.2)]. ^{1}H NMR (600 MHz, CDCl$_3$): δ 2.52 (2H, t, J = 8 Hz), 2.83 (2H, t, J = 8 Hz), 5.29 (1H, s), 7.29 (1H, m), 7.32 (2H, m), 7.39 (2H, m); ^{13}C NMR (150 MHz, CDCl$_3$): δ 30.1, 32.8, 112.7 (t, J = 23.6 Hz), 126.1, 127.7, 128.4, 140.4, 146.4, 178.6; IR (cm^{-1}, NaCl plate): 2273, 1696, 1602; HRMS (C$_{11}$H$_{11}$DO$_2$): Calc. [M-H]$^-$: 176.0822, Found [M-H]$^-$: 176.0820.

Deuterated *tert*-butyl 4-phenylpent-4-enoate (II-71):

Deuterated 4-phenylpent-4-enoic acid (50 mg, 0.282 mmol, 1.0 equiv.) and *tert*-butyl alcohol (0.042 g, 0.564 mmol, 2.0 equiv.) were dissolved in CH$_2$Cl$_2$ (1 mL), and DMAP (0.09 g, 0.0762 mmol, 0.3 equiv.) was added. Then, DCC (0.07 g, 0.34 mmol, 1.2

equiv.) was added at 0 °C. After stirring at room temperature for 24 h, the urea was filtered through the filter paper and the organic layer was concentrated in vacuum. The crude residue was purified by flash column chromatography (7% EtOAc in *n*-hexane) to give the desired deuterated *tert*-butyl 4-phenylpent-4-enoate [71 mg, 90% yield, 81% *E* (5.25 ppm, integral = 0.70) 5% *Z* (5.05 ppm, integral = 0.04) and 14% 4-phenylpent-4-enoic acid (5.07 and 5.27 ppm, overall integral = 0.24)]..^{1}H NMR (500 MHz, CDCl$_3$): δ 1.4 (9H, s), 2.37 (2H, t, *J* = 7.5 Hz), 2.77 (2H, t, *J* = 7.5 Hz), 5.25 (1H, s), 7.30 (1H, m), 7.32 (2H, m), 7.39 (2H, m); ^{13}C NMR (125 MHz, CDCl$_3$): δ 28.1, 30.6, 34.3, 80.6, 112.1 (t, *J* = 23.8 Hz), 126.1, 127.5, 128.3, 140.8, 147.0, 172.4; IR (cm^{-1}, NaCl plate): 2228, 1729, 1602; HRMS (C$_{15}$H$_{19}$DO$_2$): Calc. [M]$^+$: 233.1526, Found [M]$^+$: 233.1528

2.5.3: Procedure for Synthesis of Labeled Lactone II-62 to II-65

With DABCO to Judge the Nature of the Intermediate:

To a flame-dried screw-top vial equipped with a stir bar were added DABCO (1 mg, 0.01 mmol, 0.1 equiv), 1,3-dichloro-5,5-dimethylhydantoin (DCDMH (21 mg, 0.11 mmol, 1.1 equiv) and deuterated 4-phenylpent-4-enoic acid (18 mg, 0.1 mmol, 1 equiv, 88% deuterium labeled) These reagents were dissolved in chloroform (2 mL). The resulting mixture was stirred at rt for 12 h. The reaction mixture was poured into a 60 mL separatory funnel and diluted with chloroform (10 mL). The organics were then washed with 0.1 M aq. NaOH (10 mL). The aqueous layer was subsequently extracted with chloroform (10 mL). The combined organics were dried over anhydrous sodium sulfate and concentrated by rotary evaporation. The crude isolate was then purified by silica gel column chromatography (20% EtOAc in hexanes, KMnO$_4$ burn) to give the desired

product in 80 % yield (17 mg) as a mixture of two diastereomers (3:2). The *dr* value was measured as depicted below. For each diastereomer, a ratio was calculated by subtracting the integral of the non-labeled product from the overall integral of that diastereomer. ^{1}H NMR (500 MHz, CDCl$_3$): δ 2.5 (2H, m), 2.81 (2H, m), 3.74 (1H, s, minor diastereomer), 3.80 (1H, s, major diastereomer), 7.30-7.40 (5H, m); ^{13}C NMR (125 MHz, CDCl$_3$): δ 28.9, 31.4, 52.0 (t, *J* = 22.9 Hz), 87.0, 124.8, 128.6, 128.8, 140.7, 175.6; HRMS (C$_{11}$H$_{10}$DClO$_2$): Calc. [M]$^+$: 211.0510, Found [M]$^+$: 211.0512.

Without DABCO to Judge the Nature of the Intermediate:

To a flame-dried screw-top vial equipped with a stir bar were added 1,3-dichloro-5,5-dimethylhydantoin (DCDMH (21 mg, 0.11 mmol, 1.1 equiv.) and deuterated 4-phenylpent-4-enoic acid (18 mg, 0.1 mmol, 1 equiv. 88% deuterium labeled). These reagents were dissolved in chloroform (2 mL). The resulting mixture was stirred at rt for 48 h. The reaction mixture was poured into a 60 mL separatory funnel and diluted with chloroform (10 mL). The organics were then washed with 0.1 M aq. NaOH (10 mL). The aqueous layer was subsequently extracted with chloroform (10 mL). The combined organics were dried over anhydrous sodium sulfate and concentrated by rotary evaporation. The crude isolate was then purified by silica gel column chromatography (20% EtOAc in hexanes, KMnO$_4$ burn) to give a desired product in 60 % yield (13 mg) as a mixture of two diastereomers (1:1, dr measured as explained before for the chlorolactonization in the presence of DABCO). ^{1}H NMR (500 MHz, CDCl$_3$): δ 2.5 (2H, m), 2.81 (2H, m), 3.74 (1H, s, diastereomer one), 3.80 (1H, s, diastereomer two), 7.30-

7.40 (5H, m); ^{13}C NMR (125 MHz, CDCl$_3$): δ 28.9, 31.4, 52.0 (m), 87.0, 124.8, 128.6, 128.8, 140.7, 175.6.

With (DHQD)$_2$PHAL:[14]

To a flame-dried screw-top vial equipped with a stir bar was added (DHQD)$_2$PHAL (8 mg, 0.01 mmol, 0.1 equiv), 1,3-dichloro-5,5-diphenylhydantoin (DCDPH (32 mg, 0.11 mmol, 1.1 equiv), and benzoic acid (12 mg, 0.1 mmol, 1 equiv). These reagents were dissolved in a 1:1 mixture of chloroform and *n*-hexanes (2 mL) and cooled to -40 °C with the aid of an immersion cooler. The resulting -40 °C solution was stirred for ca. 20-30 minutes at which time the appropriate deuterated carboxylic acid **II-59** or ester **II-71** (0.1 mmol, 1 equiv) was added in one portion in solid form. The resulting mixture was stirred at -40 °C for 6 h in case of using labeled acid **II-59** and 24 h in case of using labeled ester **II-71**. The reaction mixture was poured into a 60 mL separatory funnel and diluted with chloroform (10 mL). The organics were then washed with 0.1 M aq. NaOH (10 mL). The aqueous layer was subsequently extracted with chloroform (10 mL). The combined organics were dried over anhydrous sodium sulfate and concentrated by rotary evaporation. The crude isolate was purified by silica gel column chromatography (20% EtOAc in hexanes, KMnO$_4$ burn). The resulting two enantiomers (ignoring the chiral center on the labeled carbon as it is not distinguishable by chiral HPLC) were separated using a chiralpack OJ-H column (15% IPA in hexanes; 0.8 mL/min; 254 nm; RT$_1$ = 19.6 (*R* enantiomer) and RT$_2$ = 28.6 (*S* enantiomer)) and *R* to *S ratios of* 91:9 (for cyclization of **II-59**) and 40:60 (for cyclization of **II-71**) were obtained. The *dr* for both cyclizations were measured by NMR as explained before for the chlorolactonization in

the presence of DABCO (For cyclization of **II-59:** (*R*) enantiomer was collected, dr = 95:5; For cyclization of **II-71:** (*S*) enantiomer was collected, dr = 80:20) ^{1}H NMR (500 MHz, CDCl$_3$): δ 2.5 (2H, m), 2.81 (2H, m), 3.74 (1H, s, diastereomer one), 3.80 (1H, s, diastereomer two), 7.30-7.40 (5H, m); ^{13}C NMR (125 MHz, CDCl$_3$): δ 28.9, 31.4, 52.0 (m), 87.0, 124.8, 128.6, 128.8, 140.7, 175.6.

2.5.4: Procedure for synthesis of labeled amide:

Deuterated 2-(2-phenylallyl)isoindoline-1,3-dione II-76: [28]

A mixture of *N*-propargylphthalimide **II-75** (370 mg, 2.0 mmol, 1.0 equiv.), NaBPh$_4$ (685 mg, 2 mmol, 1.0 equiv.), HOAc (114.0 *μ*L, 2.0 mmol, 1.0 equiv.), PdCl$_2$(PPh$_3$)$_2$ (42.0 mg, 0.06mmol, 0.03 equiv.), and D$_2$O (4.0 mL) was heated in a sealed tube under nitrogen at 50 °C for 12 h. The mixture was first subjected to a short silica column chromatography (ca. 5 cm of silica gel, eluted with CH$_2$Cl$_2$) to remove the water. After that, the solvents and volatiles were removed under vacuum, and the residue was then purified with column chromatography (20% EtOAc in Hex) to give the desired labeled 2-(2-phenylallyl)isoindoline-1,3-dione **II-76** as a pale yellow powder (326 mg, 62% yield). ^{1}H NMR (600 MHz, CDCl$_3$): δ 4.69 (2H, d, *J* = 1.8 Hz), 5.12 (1H, t, *J* = 1.8 Hz), 7.26 (1H, t, *J* = 7.2 Hz), 7.32 (2H, m), 7.48 (2H, dd, *J* = 7.8 Hz) 7.68 (2H, dd, *J* = 6.0, 3.0 Hz), 7.82 (2H, d, *J* = 6.0, 3.0 Hz); ^{13}C NMR (150 MHz, CDCl$_3$): δ 41.4, 113.6 (t, *J* = 23.7 Hz), 123.3, 126,4, 128.0, 128.4, 132.0, 133.9, 138.5, 142.3, 167.9. IR (cm^{-1}, NaCl plate): 2918, 2495, 1704; HRMS (C$_{17}$H$_{12}$DNO$_2$): Calc. [M+H]$^+$: 265.1088, Found [M+H]$^+$: 265.1086.

Deuterated 2-phenylprop-2-en-1-amine II-77:

The labeled 2-(2-phenylallyl)isoindoline-1,3-dione **II-76** (200 mg, 0.76 mmol, 1.0 equiv.) and hydrazine (49 mg 1.52 mmol, 2.0 equiv.) was dissolved in MeOH (2 mL) and stirred at rt for 12 h. The reaction mixture was diluted with H_2O (1 mL) and then MeOH was evaporated under reduced pressure. To the solution HCl (1 mL, 12 M) was added and the mixture was stirred for 1 h. The mixture was filtered through the filter paper; the filtrate was washed with ether (2 x 5 mL). Aqueous layer was basified with solid KOH (pH 10) and the desired product 2-phenylprop-2-en-1-amine **II-77** was extracted from aqueous layer with ether (2 x 5 mL). The organic layer was separated and dried over anhydrous Na_2SO_4. The crude 2-phenylprop-2-en-1-amine **II-77** was obtained (79 mg, 78% yield) after slow evaporation of the solvent and was used in the next reaction without purification. ^{1}H NMR (600 MHz, CDCl$_3$): δ 1.39 (2H,br s), 3.69 (2H, s), 5.19 (1H, t, J = 1.8 Hz), 7.26-7.4 (5H, m); ^{13}C NMR (150 MHz, CDCl$_3$): δ 46.1, 110.9(t, $J = 24 Hz$), 126.1, 127.6, 128.4, 139.7, 149.7;

Deuterated *N*-(2-phenylallyl)benzamide II-78:

A solution of labeled 2-phenylprop-2-en-1-amine (50 mg, 0.37 mmol, 1.0 equiv.) and pyridine (63 mg, 0.74 mmol, 2.0 equiv.) in DCM (2.5 mL) was cooled in an ice bath. To it was added benzoyl chloride (80 mg, 0.57 mmol, 1.5 equiv.) drop wise. After the addition was complete, the reaction was allowed to warm to RT. After 2 h, the reaction was diluted with an equal amount of water and extracted with DCM (3 x 5 mL). The combined organics were washed with brine (1 x 3 mL), dried over Na_2SO_4 and concentrated under reduced pressure to give the product as a yellow solid. It was recrystallized from MeOH to obtain the pure product as a colorless solid in 81% yield

[71.0 mg, 75% *E* (5.29 ppm, integral = 0.67) 7% *Z* (5.49 ppm, integral = 0.06) and 18% non-labeled *N*-(2-phenylallyl)benzamide (5.31 and 5.51 ppm, overall integral = 0.32)] after collection of two crops of crystals. ^{1}H NMR (600 MHz, CDCl$_3$): δ 4.52 (2H, d, *J* = 5.4 Hz), 5.3 (1H, t, *J* = 1.8 Hz), 6.15 (1H, br s), 7.30 (1H, t, *J* = 7.2 Hz), 7.34 (2H, t *J* = 7.2 Hz), 7.38 (2H, t, *J* = 7.8 Hz), 7.47 (3H, m), 7.69 (2H, d *J* = 8.4 Hz); ^{13}C NMR (150 MHz, CDCl$_3$): δ 43.6, 113.7 (t, *J* = 24.15 Hz), 126.0, 126.8, 128.1, 128.5, 128.6, 131.4, 134.4, 138.2, 144.1, 167.3; IR (cm^{-1}, NaCl plate): 3340, 2345, 1647. HRMS (C$_{16}$H$_{14}$DNO): Calc. [M+H]$^{+}$: 239.1294, Found [M+H]$^{+}$: 239.1297.

2.5.5: Procedure for the Catalytic Asymmetric Chlorocyclization of Labeled Unsaturated Amides II-78 [21]

DCDPH (35 mg, 0.11 mmol, 1.1 equiv) was suspended in trifluoroethanol (TFE, 2.2 mL) in a screw-capped vial equipped with a stir bar. The resulting suspension was cooled to -30 °C in an immersion cooler. (DHQD)$_2$PHAL (1.56 mg, 312 mL of a 5 mg/mL solution in TFE, 2 mol%) was then introduced. After stirring vigorously for 10 min, unsaturated amides **II-78** (24 mg, 0.10 mmol, 1.0 equiv) was added in a single portion. The vial was capped and the stirring was continued at -30 °C till the reaction was complete (TLC). The reaction was quenched by the addition of 10% aq. Na$_2$SO$_3$ (3 mL) and diluted with DCM (3 mL). The organics were separated and the aqueous layer was extracted with DCM (3 x 3 mL). The combined organics were dried over anhydrous Na$_2$SO$_4$. Pure products were isolated by column chromatography on silica gel using EtOAc-Hexanes (1:19) as the eluant in 86% yield (22 mg). The resulting two enantiomers (ignoring the chiral center on the labeled carbon as it is not distinguishable

by chiral HPLC) were separated using a chiralpack OD-H column (5% IPA in hexanes; 0.8 mL/min; 265 nm; RT_1 = 30.2 (S enantiomer) and RT_2 = 34.6 (R enantiomer)) and an R to S ratio of 95:5 was obtained. The dr (99:1, R enantiomer was collected) was measured by NMR as explained before for the chlorolactonization in the presence of DABCO. ^{1}H NMR (500 MHz, CDCl$_3$): δ 3.9 (1H, s), 4.22 (1H, d, J = 14.5 Hz), 4.49 (1H, d, J = 14.5 Hz), 7.39-7.45 (8H, m), 8.04 (2H, dd, J = 1.5, 11.5 Hz); ^{13}C NMR (125 MHz, CDCl$_3$): δ 50.8 (t, J = 23.7 Hz, 64.9, 87.5, 124.9, 127.4, 128.2, 128.3, 128.4, 128.7, 131.5, 141.5, 163.0.

2.5.6: Preparation of Alkenoic Acid Substrates for kinetic studies

Preparation of 4-phenyl-4-pentenoic acid (II-49) [14]

Methyltriphenylphosphonium bromide (1.96 g, 5.6 mmol, 1.08 equiv) was suspended in freshly distilled toluene (30 mL) and cooled to ca. 0 °C on an ice bath. Sodium bis(trimethylsilyl)amide (5.4 mL, 5.4 mmol, 1.04 equiv, 1 M solution in THF) was added drop wise by syringe and the resulting solution was stirred for 30 min. The solution was then lowered to -78 °C and methyl 3-benzoylpropionate (1.0 g, 5.2 mmol, 1 equiv) was added dropwise by syringe. The resulting solution was then stirred while warming to room temperature. The reaction mixture was then refluxed for 40 h. On cooling, the reaction was quenched by the addition of saturated ammonium chloride (40 mL) and the resulting slurry was diluted with water (50 mL) and extracted with ethyl acetate (3 X 50 mL). The combined organics were washed with brine (100 mL), dried over anhydrous Na$_2$SO$_4$, and concentrated by rotary evaporation. The residue was purified by column chromatography on silica gel (10% ethyl acetate in hexanes) to give

762 mg (77% yield) of the desired methyl 4-phenylpent-4-enoate. This substance was used immediately without characterization in the following saponification reaction. The ester (536 mg, 2.82 mmol, 1 equiv) was dissolved in THF (20 mL) and cooled to ca. 0 °C on an ice bath. A solution of lithium hydroxide monohydrate (600 mg, 14.30 mmol, 5.07 equiv.) in water (20 mL) was added dropwise over about 5 min via an addition funnel. The resulting solution was allowed to warm to room temperature while stirring for 18 h. The solution was acidified to pH <4 with 1N HCl and then extracted with diethyl ether (3 X 20 mL). The combined organics were then washed with water (60 mL) and brine (60 mL), and then dried over anhydrous Na_2SO_4. The organics were concentrated by rotary evaporation to give the desired compound **II-49** (467 mg, 94% yield). ^{1}H NMR (300 MHz, acetone-d_6): δ 2.46 (2H, m), 2.82 (2H, m), 5.12 (1H, m), 5.32 (1H, m), 7.37-7.27 (3H, m), 7.46 (2H, m); ^{13}C NMR (75 MHz, acetone-d_6): δ 30.9, 33.2, 122.7, 126.8, 128.4, 129.2, 141.5, 148.1, 171.2.

Preparation of Alkenoic acid (II-98 & II-99).[5]

These two compounds were generated by Suzuki coupling as described by Wirth and co-workers. The boronic acid (2 mmol, 1 equiv.), KF (6 mmol, 468 mg, 3 equiv.), and [$Pd_2(dba)_3$] (0.03 mmol, 28 mg, 0.015 equiv.) were dissolved in THF (1.5 mL), then 4-bromo-4-pentenoic acid tert-butyl ester (2.2 mmol, 520 mg, 1.1 equiv.), and tris-(o-tolyl)phosphine (0.08 mmol, 25 mg, 0.04 equiv.) were added. After 4–10 h, the reaction was filtered over celite. The celite pad was washed with diethyl ether (125 mL). After evaporation of the solvent, the crude product was purified by performing flash chromatography (silica gel, tert-butylmethyl ether/pentane 1:10). The purified ester (0.71

mmol, 1 equiv.) was dissolved in THF (20 mL) and cooled to ca. 0 °C on an ice bath. A solution of lithium hydroxide monohydrate (150 mg, 3.6 mmol, 5.07 equiv.) in water (5 mL) was added dropwise over about 5 min via an addition funnel. The resulting solution was allowed to warm to room temperature while stirring for 18 h. The solution was acidified to pH <4 with 1N HCl and then extracted with diethyl ether (3 X 5 mL). The combined organics were then washed with water (15 mL) and brine (15 mL), and then dried over anhydrous Na_2SO_4. The organics were concentrated by rotary evaporation to give the desired compound carboxylic acid **II-98** or **II-99**.

II-98:

^{1}H NMR (500 MHz, $CDCl_3$): δ 2.54 (2H, t, J = 7 Hz), 2.83 (2H, t, J = 7 Hz), 5.23 (1H, s), 5.46 (1H, s), 7.52 (1H, t, J = 8 Hz), 7.73 (1H, d, J = 7.5 Hz), 8.14 (1H, d, J = 8 Hz), 8.25 (1H, s); ^{13}C NMR (125 MHz, $CDCl_3$): δ 29.7, 32.5, 115.5, 121.0, 122.5, 129.4, 132.0, 142.3, 144.6, 148.5, 178.1.

II-99:

^{1}H NMR (300 MHz, $CDCl_3$): δ 2.59 (m, 2H), 2.91 (m, 2H), 5.27 (s, 1H), 5.45 (s, 1H), 7.55 (m, 2H), 7.65 (m, 2H); ^{13}C NMR (75 MHz, $CDCl_3$): δ 29.9, 32.7, 114.9, 124.1 (q, $^{1}J_{C,F}$ = 270 Hz), 125.4 (q, $^{3}J_{C,F}$ = 4 Hz), 126.4, 129.7 (q, $^{3}J_{C,F}$ = 32 Hz), 144.4, 145.4, 179.4.

2.5.7: Reaction Progress Kinetics Analysis General Procedure

Sample and NMR Instrument Preparation for RPKA Studies:

The probe of the NMR instrument was cooled to -40 °C and allowed to equilibrate for 60 minutes. A stock solution of catalyst and internal standard was prepared by

dissolving (DHQD)$_2$PHAL (16 mg, 0.0204 mmol) and benzoic acid (62 mg, 0.511 mmol) or toluene (47 mg, 0.0511 mmol) in CDCl$_3$ (2 mL). To each NMR tube 0.2 mL of this solution was added (4 mol% catalyst + 1 equiv. internal standard). Meanwhile, in two additional vials the stock solution of DCDMH (67.1 mg, 0.34 mmol) and 4-phenyl-4-pentenoic acid (60.4 mg, 0.34 mmol) were prepared by dissolving in CDCl$_3$ (1.5 mL). For each RPKA experiment the solution of the catalyst and internal standard were frozen in -78 °C and then the desired amount of the 4-phenyl-4-pentenoic acid was taken from the stock solution and added to the NMR tube. While the NMR tube was kept at -78 °C bath to freeze the sample, the desired amount of the DCDMH was taken from the DCDMH stock solution and added to the NMR tube. The solution in NMR tube was equalized to 1 mL by adding enough CDCl3 to the frozen NMR tube. This frozen sample was inserted into the NMR instrument and after 2 minutes (when the frozen sample get melted at -40 °C), the sample was ejected and shaken for a second to homogenize the solution and reinserted into the NMR instrument quickly. After locking and shimming the instrument and setting up the array experiment (six minutes after shaking the NMR tube), collection of kinetics data ensued either every five or ten minutes during 10 h. During this time the reaction, in most cases depleted in starting material to be 30%.

Data Manipulation and Analysis:

Based on the constant concentration of internal standard, concentration of the product, DCDMH and 4-phenyl-4-pentenoic acid in each data point were calculated. The AB quartet peak at 3.8 ppm (a methylene group attached to the chlorine) was used to calculate the concentration of the product at each data point. To monitor the

concentration of the carboxylic acid **II-49** and DCDMH, vinylic protons (s, 5.3 and 5.1 ppm) and methyl groups (s, 1.5 ppm) peaks were used, respectively. After fitting a six-power polynomial function to the plot of product concentration vs. time, the rate at each data point was calculated via the first derivative of the fitted polynomial function.

2.5.8: General Procedure for Competition and Kinetic Isotope Effect Studies

Sample and NMR Instrument Preparation:

Sample and NMR instrument preparation were the same as that for RPKA studies. In these experiments $[DCDMH]_o = 0.056$ M and $[Acid]_o = 0.051$ M, were used in the presence of $[Toluene]_o = 0.051$ M. Catalyst loading was decreased to 1.5 mol% to monitor the reaction slowly and collect more data points.

Data Manipulation and Analysis:

Based on the constant concentration of internal standard, concentration of the product was calculated. Product concentration was plotted against time and to an exponential grows curve by using Excel solver tool [$P_t = P_\infty (1 - Exp(-k'(t-t_0))$, was fitted to the observed data by varying t_0, k' (rate constant [catalyst]) and infinite product concentration]. The fitting proceeded to reduce the non-linear least squared regression error below 0.00002.

2.5.9: Absolute stereochemical determination of deuterated carbon

Lithium borohydride reduction of lactone **II-53** followed by sodium hydroxide mediated cyclization of the resulting chlorohydrin intermediate returned 1,1-disubstituted epoxy alcohol in good yield.[14] ROESY and NOESY studies on the corresponding
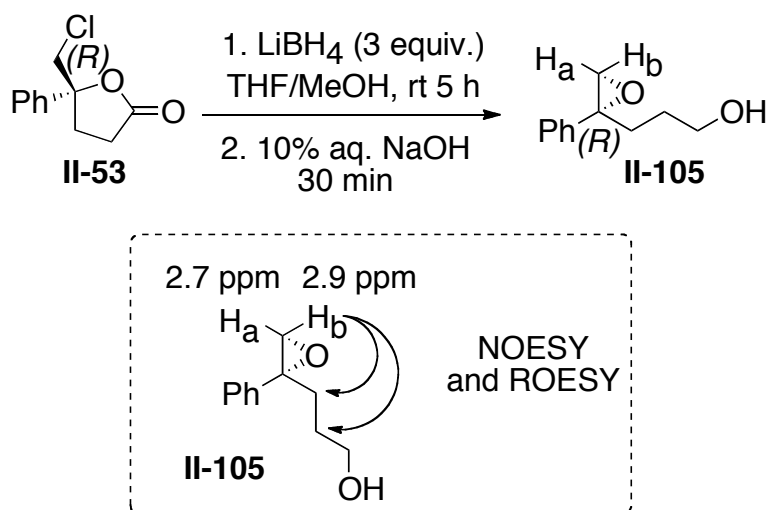
Figure II-29. Epoxy alcohol **II-105** synthesis

epoxy alcohol **II-106** show that H_a (2.73 ppm) has a *syn* orientation with the phenyl group and H_b (2.98 ppm) has a *anti* orientation with the phenyl group. After assignment of H_a and H_b, the labeled lactones **II-62** to **II-65** as a mixture (synthesized in the presence of the (DHQD)$_2$PHAL) were reduced with lithium borohydride and sodium hydroxide to yield the desired labeled epoxy alcohol **II-107**. ^{1}H NMR analysis of the epoxy alcohol **II-107** shows only a peak at 2.7 ppm, which suggests that the deuterium has an *anti* orientation with respect to the phenyl group. Based on this the deuterated carbon can be assigned as *S*-chirality carbon in the corresponding epoxy alcohol **II-107**. Since the epoxy alcohol forms through the S_N2 type cyclization of chlorohydrine intermediate **II-106**, lactone **II-62** as a major product is *R* configuration on the labeled center.

155

2.5.10: General Procedure for synthesis of labeled epoxy alcohol II-105 and II-107

Lactone **II-53** and **II-62** to **II-65** (0.17 mmol, 1.0 equiv.) was dissolved 1:1 THF-MeOH (1 mL) and cooled to 0 °C. LiBH$_4$ (11 mg, 0.5 mmol, 3.0 equiv.) was added in a single portion. The reaction was allowed to stir at ambient temperature for 5 h. The reaction was then diluted with water (1 mL) and 10% aq. NaOH solution (0.5 mL). After stirring for a further 30 min. at room temperature, the reaction was diluted with DCM (1 mL).
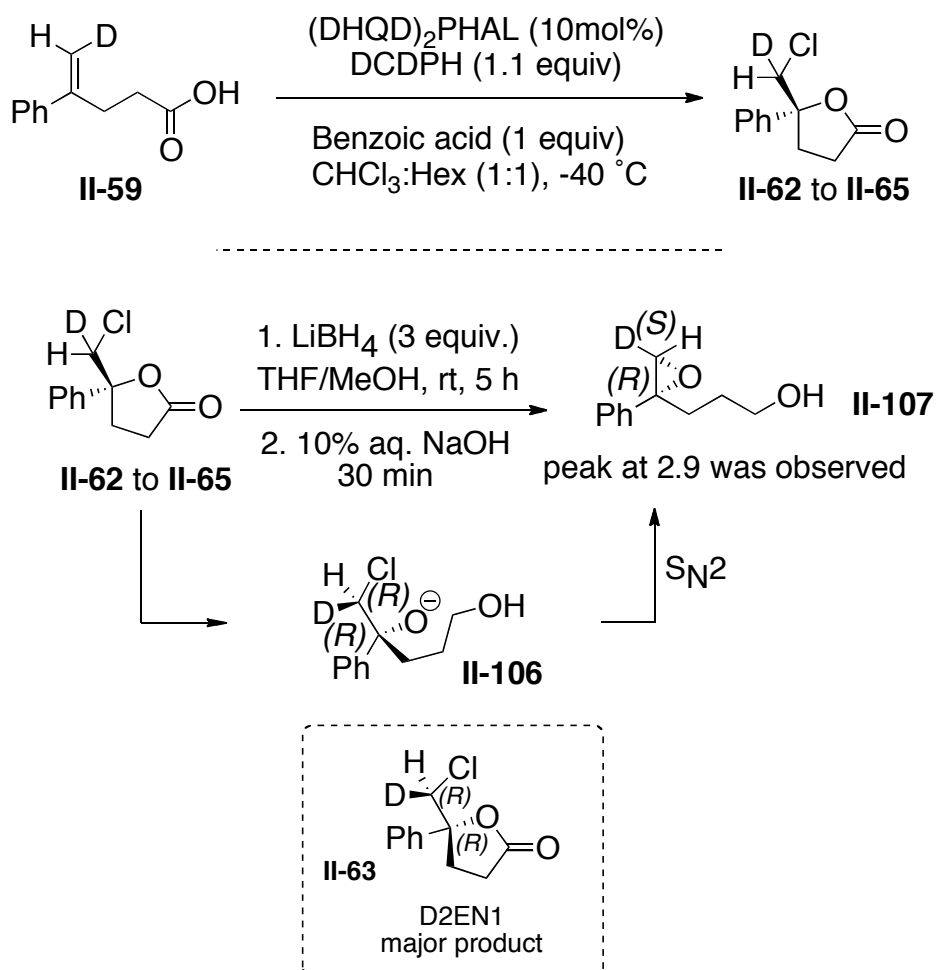
Figure II-30. Labeled carbon absolute stereochemistry determination

The aqueous and organic fractions were separated. The aqueous layer was extracted with DCM (2 X 2 mL). The combined organic fractions were dried over anhydrous Na_2SO_4 and concentrated in vacuo. The crude product was purified by silica gel column chromatography using 30% EtOAc in hexanes buffered with 1% Et_3N as eluant to give 31 mg (91%) of the desired epoxy alcohol as a colorless oil. ^{1}H NMR **II-105** (500 MHz, $CDCl_3$): δ 1.64 (3H, m), 1.76 (1H, m), 2.38 (1H, m), 2.74 (1H, d, J = 5.5 Hz), 2.97 (1H, d, J = 5.5 Hz), 3.62 (2H, br), 7.25-7.37 (5H, m); ^{13}C NMR (125 MHz, $CDCl_3$): δ 28.0, 31.8, 56.3, 60.3, 62.4, 126.0, 127.6, 128.6, 139.6. ^{1}H NMR **II-107** (500 MHz, $CDCl_3$): δ 1.64 (3H, m), 1.76 (1H, m), 2.38 (1H, m), 2.97 (1H, s), 3.62 (2H, br), 7.25-7.37 (5H, m); ^{13}C NMR (125 MHz, $CDCl_3$): δ 27.9, 31.6, 55.7(t, J = 26.9 Hz), 60.1, 62.3, 125.8, 127.5, 128.4, 139.5.

REFERENCES

REFERENCES

1. Cardillo, G.; Orena, M. *Tetrahedron* **1990**, *46*, 3321.

2. Dowle, M. D.; Davies, D. I. *Chemical Society Reviews* **1979**, *8*, 171.

3. Kitagawa, O.; Hanano, T.; Tanabe, K.; Shiro, M.; Taguchi, T. *Journal of the Chemical Society-Chemical Communications* **1992**, 1005.

4. Grossman, R. B.; Trupp, R. J. *Canadian Journal of Chemistry-Revue Canadienne De Chimie* **1998**, *76*, 1233.

5. Haas, J.; Bissmire, S.; Wirth, T. *Chemistry-a European Journal* **2005**, *11*, 5777.

6. Haas, J.; Piguel, S.; Wirth, T. *Organic Letters* **2002**, *4*, 297.

7. Garnier, J. M.; Robin, S.; Rousseau, G. *European Journal of Organic Chemistry* **2007**, 3281.

8. Cui, X. L.; Brown, R. S. *Journal of Organic Chemistry* **2000**, *65*, 5653.

9. Wang, M.; Gao, L. X.; Mai, W. P.; Xia, A. X.; Wang, F.; Zhang, S. B. *Journal of Organic Chemistry* **2004**, *69*, 2874.

10. Wang, M.; Gao, L. X.; Yue, W.; Mai, W. P. *Synthetic Communications* **2004**, *34*, 1023.

11. Ahmad, S. M.; Braddock, D. C.; Cansell, G.; Hermitage, S. A.; Redmond, J. M.; White, A. J. P. *Tetrahedron Letters* **2007**, *48*, 5948.

12. Tan, C. K.; Zhou, L.; Yeung, Y.-Y. *Synlett* **2011**, 1335.

13. Denmark, S. E.; Burk, M. T.; Hoover, A. J. *Journal of the American Chemical Society* **2010**, *132*, 1232.

14. Whitehead, D. C.; Yousefi, R.; Jaganathan, A.; Borhan, B. *Journal of the American Chemical Society* **2010**, *132*, 3298.

15. Veitch, G. E.; Jacobsen, E. N. *Angewandte Chemie-International Edition* **2010**, *49*, 7332.

16.   Murai, K.; Matsushita, T.; Nakamura, A.; Fukushima, S.; Shimura, M.; Fujioka, H. *Angewandte Chemie-International Edition* **2010**, *49*, 9174.

17.   Zhang, W.; Zheng, S.; Liu, N.; Werness, J. B.; Guzei, I. A.; Tang, W. *Journal of the American Chemical Society* **2010**, *132*, 3664.

18.   Olah, G. A.; Bollinger, J. *Journal of the American Chemical Society* **1967**, *89*, 4744.

19.   Olah, G. A.; Bollinge.Jm *Journal of the American Chemical Society* **1968**, *90*, 947.

20.   Oh, C. H.; Jung, H. H.; Kim, K. S.; Kim, N. *Angewandte Chemie-International Edition* **2003**, *42*, 805.

21.   Jaganathan, A.; Garzan, A.; Whitehead, D. C.; Staples, R. J.; Borhan, B. *Angewandte Chemie-International Edition* **2011**, *50*, 2593.

22.   Blackmond, D. G. *Angewandte Chemie-International Edition* **2005**, *44*, 4302.

23.   Mathew, J. S.; Klussmann, M.; Iwamura, H.; Valera, F.; Futran, A.; Emanuelsson, E. A. C.; Blackmond, D. G. *Journal of Organic Chemistry* **2006**, *71*, 4711.

24.   Zotova, N.; Broadbelt, L. J.; Armstrong, A.; Blackmond, D. G. *Bioorganic & Medicinal Chemistry Letters* **2009**, *19*, 3934.

25.   Mubofu, E. B.; Engberts, J. *Journal of Physical Organic Chemistry* **2004**, *17*, 180.

26.   Venkatasubban, K. S.; Schowen, R. L. *Crc Critical Reviews in Biochemistry* **1984**, *17*, 1.

27.   Schowen, K. B. J. *Solvent hydrogen isotope effects, in Transition States for Biochemical Processes*; Plenum Press: New york, 1978.

28.   Zeng, H.; Hua, R. *Journal of Organic Chemistry* **2008**, *73*, 558.

Chapter 3: On The Chloronium Source in the Asymmetric Chlorolactonization Reaction

3.1: INTRODUCTION

Several reagents have been developed as sources of chlorenium ion (Cl$^+$) in organic synthesis in lieu of using elemental chlorine. The operational benefits of these reagents are: ease of handling, reduced toxicity and tunable reactivity. Five common examples of organochlorenium sources are N-chlorosuccinimide (NCS, **III-1**), chloramine-T (**III -2**), trichloroisocyanuric acid (TCCA, **III-3**), chloro diethylsulfonium hexachloroantimonate (CDSC **III-4**) and 1,3-dichloro-5,5-dimethylhydantoin (DCDMH, **III-5**) as depicted in Scheme **III-1**.

Among these five examples, NCS has been the most common organic chlorine equivalent, which has been utilized a lot in a number chlorination and oxidation reactions.[1] Chloramine–T has been used mostly as an oxidant or nucleophilic nitrogen source, but it has been used in a few examples as a source of chlorine ion in acid.[2] The use of TCCA has been recently reviewed, but its wide-spread use as a chlorenium source is somewhat related to it's enhanced reactivity relative to NCS. For example,
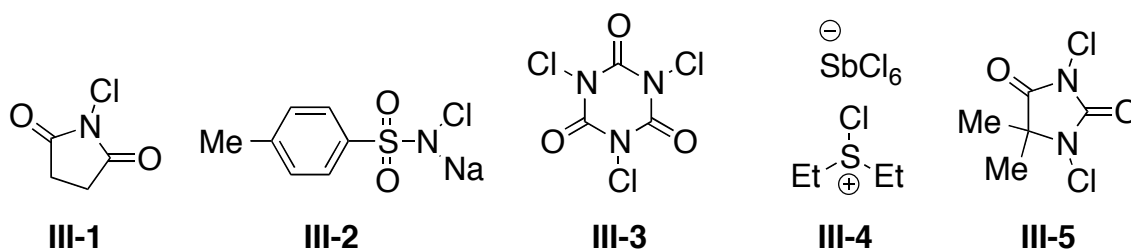
Figure III-1 Five commonly used organochlorenium sources: NCS, Chloramine-T, TCCA, CDSC and DCDMH

TCCA is known to chlorinate esters and cyclic ethers such as THF and dioxane. Moreover, TCCA is able to oxidize aliphatic ethers to their corresponding esters. This high reactivity limits the application of the TCCA in a number of solvents.[3] Very recently Snyder and coworkers introduced CDSC as a chlorine source, using it in halonium-induced polyene cyclization. CDSC is an example where a Lewis base, sulfur, activates a Lewis acid, Cl^+. Compared to NCS, DCDMH is less popular but recently it has emerged as a chlorenium ion source for different organic transformations. The use of N-chlorinated hydantoins in organic synthesis has been relatively limited as compared to the more frequently employed NCS. DCDMH is currently the only commercially available member of this reagent class, and as such has received significant attention from the synthetic community.

DCDMH has been employed as a chlorenium source for various transformations including the α-chlorination of acetophenones[4], the α-chlorination of 1-aryl-2-pyrazolin-5-ones,[5] the preparation of chlorohydrin derivatives of corticosteroids,[6] and the benzylic chlorination of 2-methylpyrazine.[7] Moreover, DCDMH was employed to trap an enolate resulting from dimethylzinc attack on an α,β-unsaturated ketone thus generating an α-chloro-β-methyl ketone functionality *en route* to a building block of Amphotericin B.[8]

Researchers at Abbott Laboratories successfully utilized DCDMH for a late stage, selective chlorination of a heavily functionalized quinolone derivative during the preparation of the antibiotic ABT-492 (Scheme IV-2, eq. 1).[9] Initially, sulfuryl chloride was employed for the transformation, but the researchers deferred to the milder

162
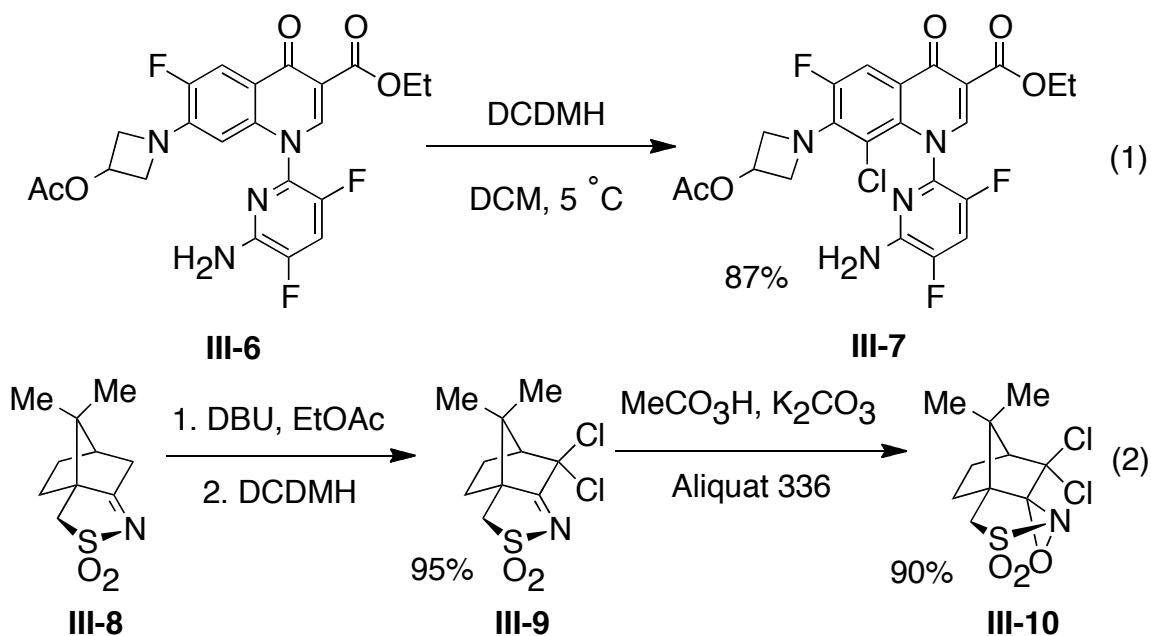
Scheme III-1. Select examples of DCDMH mediated chlorinations.

DCDMH in order to circumvent the formation of a small, albeit inseparable portion of a by-product resulting from the ring opening of the azetidine.

Researchers at Schering Plough exploited the enhanced reactivity of DCDMH relative to NCS to improve upon the large-scale preparation of Davis' oxaziridine **III-10** (Scheme III-2, eq. 2).[10,11] Employing DCDMH in lieu of NCS allowed for the reaction to be conducted at room temperature in ethyl acetate, while employing DBU as the base. This protocol represented a significant operational improvement over the established methodology, whereby **III-8** was deprotonated by NaHMDS at -78 °C in dilute anhydrous THF, and then cannulated into a -78 °C THF solution of NCS. The authors go on to note that the use of DCDMH significantly reduced the formation of

multi-chlorinated by-products, thus obviating the necessity for chromatographic purification of **IV-9**.

In addition to its use as a chlorenium equivalent, DCDMH has also been employed as an oxidant for a number of transformations including the halodeboronation of aryl boronic acids,[12] the oxidation of urazoles to provide triazolinediones,[13] the microwave-assisted cleavage of oximes,[14] and the preparation of dialkyl chlorophosphates.[15] The compound can also serve as a mild oxidant in the presence of wet silica gel in the sodium nitrite-mediated nitration of phenols[16] and in the preparation of N-nitrosoamines.[17]

If chloramine-T is replaced with DCDMH as the terminal oxidant during the course of the Sharpless asymmetric aminohydroxylation (SAA)[18-20] one can produce chiral carbamate protected amino alcohols or oxazolidinones directly (Scheme III-3). This is accomplished by utilizing DCDMH as the terminal oxidant along with the appropriate urethane nitrogen source. Historically, when carbamate based nitrogen nucleophiles were employed in the SAA reaction, *tert*-butyl hypochlorite (*t*-BuOCl) was employed as the terminal oxidant.[18-20] Barta and co-workers utilized DCDMH instead of *t*-BuOCl due to the fact that DCDMH was a commercially available solid, whereas *t*-BuOCl had to be freshly prepared each time prior to use.[21] Importantly, they noted that other more common chlorenium based co-oxidants such as NCS and TCCA were unsuccessful. After arriving at DCDMH as a suitable substitute for *t*-BuOCl, the conventional SAA reaction was extended to a one-pot preparation of chiral oxazolidinones (Scheme III-3, eq. 1). Subsequently, McLeod and co-workers used a
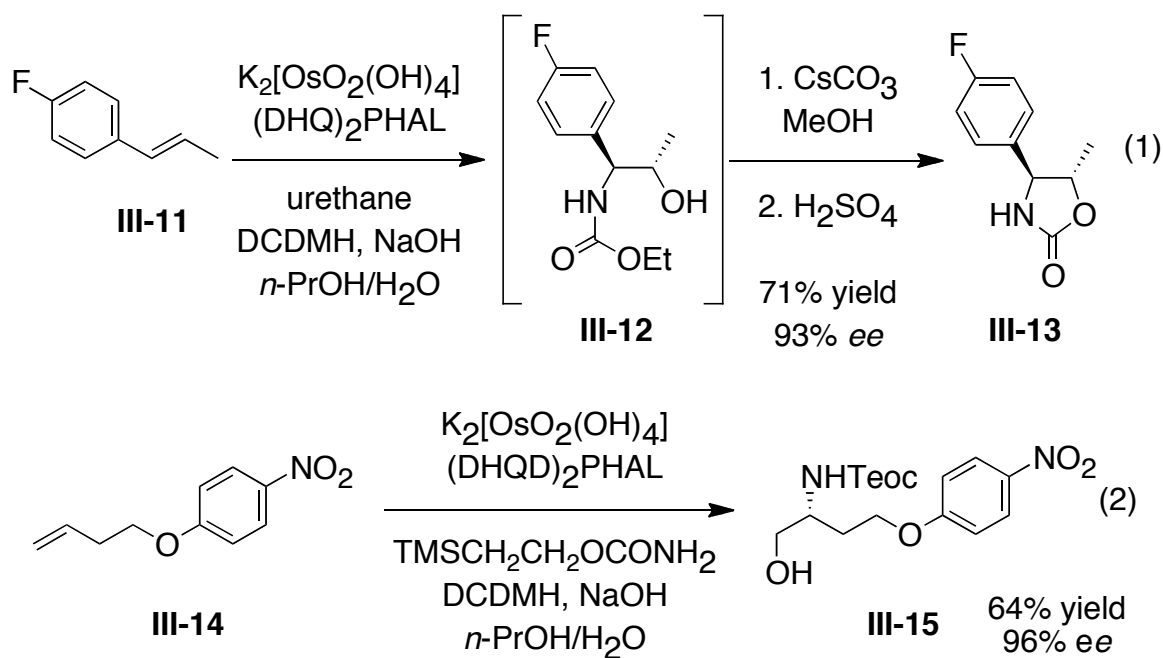
Scheme III-2. Select examples of DCDMH mediated chlorinations.

similar strategy to prepare carbamate protected 4-amino-3-hydroxybutyric acid (GABOB) precursors such as **III-15** (eq. 2).[22]

Furthermore, DCDMH has emerged as the reagent of choice for the activation, prior to loading, of silyl linkers for solid-phase organic synthesis.[23-26]   Finally, DCDMH has been used as an oxidative activator of an iridium catalyst designed for the asymmetric hydrogenation of substituted quinolines.[27] Other uses for DCDMH include employment as redox titrants in non-aqueous media,[28] and as a cheap yet safe disinfectant and bactericide for municipal water sources.[29]

Recently, as was mentioned in Chapter II, we discovered a unique catalyst system comprised of a catalytic amount of (DHQD)$_2$PHAL and chlorinated hydantoins that
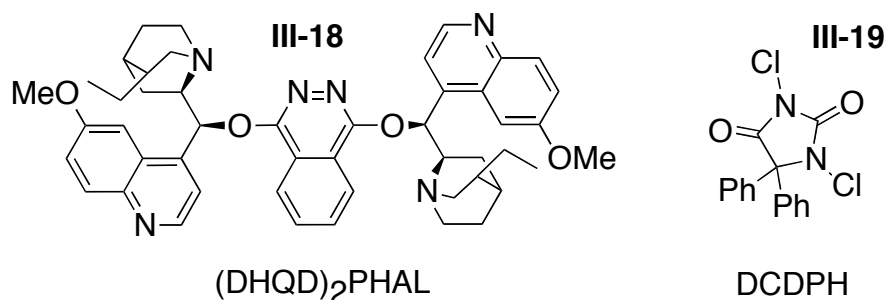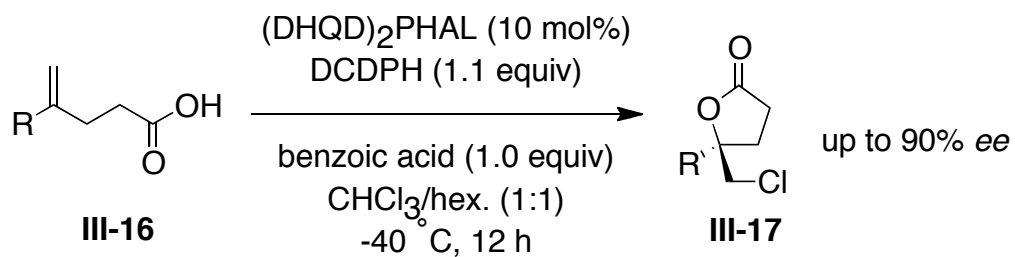
Scheme III-3. The first synthetically viable catalytic asymmetric halocyclization.

allowed for good conversions and enantioselectivities for the chlorolactonization of 4-substituted 4-pentenoic acids (**Scheme III-4**).[30]

In our original disclosure, the use of dichlorohydantoins as the chlorine source proved essential for obtaining the highest possible enantioselectivities. Here in this chapter our focus turns to understanding the mechanism of the reaction by conducting detailed studies on the role of chlorinated hydantoin, both structurally and electronically, as a chlorine source in this reaction. The results from this study can be broken down into two distinct parts.

In one part, the roles of the N1 and N3 chlorine were investigated by performing a detailed study on the influence of structurally related N1 and N3 acylated N-

chlorohydantoins on the selectivity of the chlorolactonization reaction. This study was facilitated by the development of a convenient synthetic method for the selective synthesis of N1 and N3 acylated hydantoins.[31] Additionally, in the second part of this study NMR studies were used to prove that there is an associative complex between the (DHQD)$_2$PHAL and the chlorine source that seems to be influential for the observed selectivity in the transformation.[31]

3.2. INVESTIGATHION ON THE ROLE OF THE N1 AND N3 CHLORINE ATOMS IN THE PARENT DICHLOROHYDANTOIN.

During our initial optimization studies, it became apparent that dichlorinated hydantoins (i.e. **III-19**) were suited as a perfectly tuned halenium source for our methodology. The reagent appeared uniquely wedged in reactivity between N-bromosuccinimide, which resulted in a fast but less selective bromolactonization due to the background reaction, and N-chlorosuccinimide, which was slow to react at low temperatures in the analogous chlorolactonization (Table III-1, entry one, vide infra).[30]
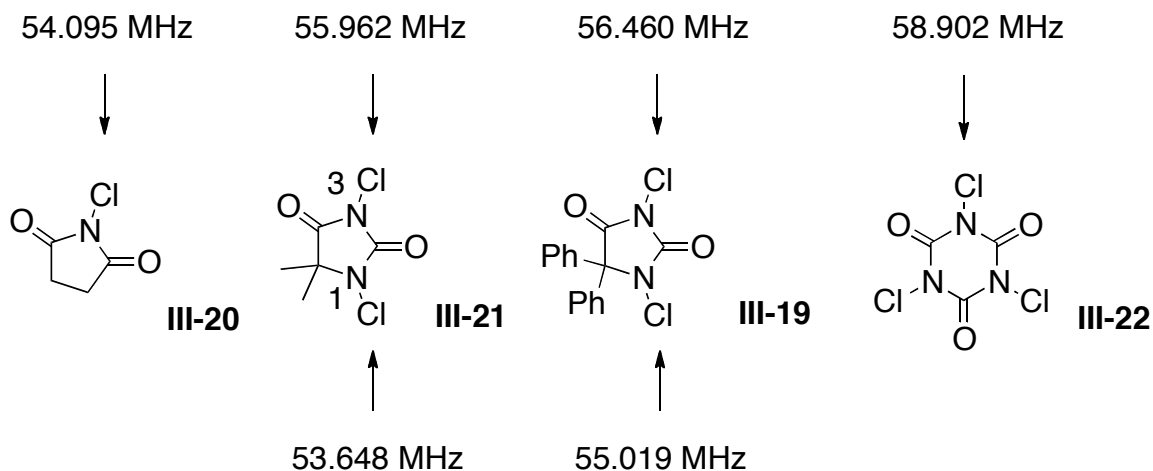
Figure III-2. ^{35}Cl NQR frequencies for various chlorenium sources.

167

The ^{35}Cl Nuclear Quadrupole Resonance (NQR) frequency has been invoked as a quantitative marker for the relative Cl$^+$ character of a given N-Cl bond. In particular, a larger Cl$^+$ character corresponds to a higher NQR resonance frequency. Several resonance frequencies are summarized in **Scheme III-5**. [32,33]

Based upon the NQR resonance frequencies collected in **Scheme III-5,** one would expect that generally the N3 chlorine (see **III-21** for numbering) of hydantoins **III-21** and **III-19** would be more electrophilic than that of NCS (**III-20**), while the N1 chlorine atom should possess roughly the same level of electrophilicity as NCS. Additionally, one would expect TCCA (**III-22**) to possess even more electrophilic Cl atoms than the N-chlorohydantoins and NCS.

This general trend, as predicted by the NQR resonance frequencies, is evident in the chlorolactonization of *p*-fluorophenyl substituted alkenoic acid **III-25** to give chlorolactone **III-26** (Table **III-1**). Under our optimized conditions, the cyclization of **III-25** governed by NCS (entry 5) proceeds in a relatively poor 15% yield with a reduced enantioselectivity of just 52% *ee*. Two dichlorinated hydantoins, DCDMH and DCDPH (**Table III-1** entry) produced the desired chlorolactone **III-26** in a much higher yield (81-87%) and markedly improved ees (84-90% *ee*) as compared to **III-20**. Chlorolactonization with the more electrophilic TCCA (**III-22**, entry 2) returned chlorolactone **III-26** in the highest yield (89%), but with a reduced 70% *ee* as compared to the N-chlorohydantoin series. The lower enantioselectivity with the more reactive TCCA is due to an inherently non-selective uncatalyzed background reaction (7.2% in

Table III-1. Investigation of terminal chlorenium sources in the cyclization of **III-25**
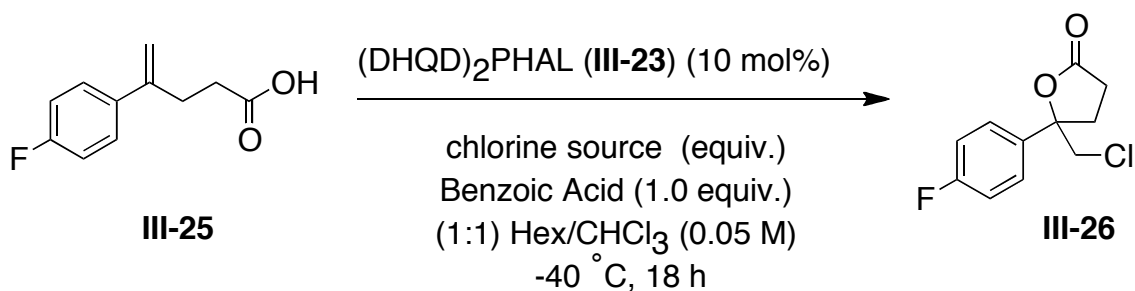
Entry	Cl+ Source	% yield (III-26)	% ee (III-26)
1	**III-20**	15	52
2	**III-22**	89	70
3	**III-21**	87	84
4	**III-19**	81	89
5	**III-23**	7	72
6	**III-24**	50	78

III-20   **III-22**   **III-21**

III-19   **III-23**   **III-24**
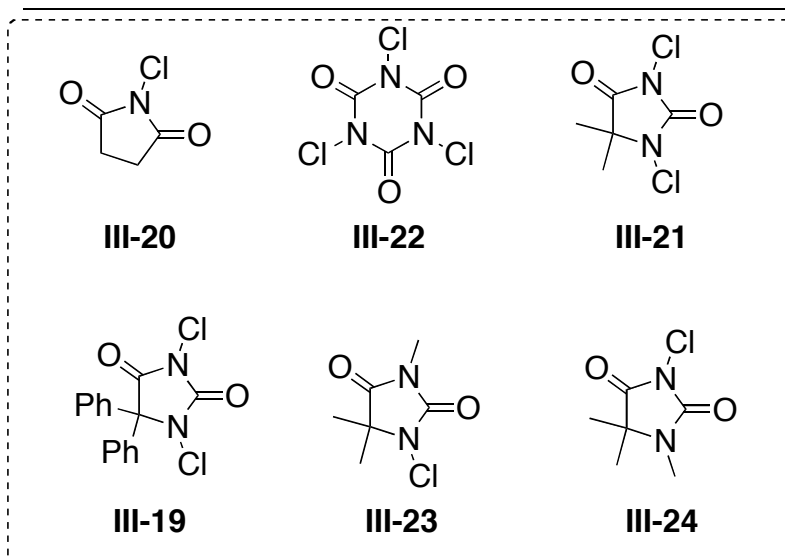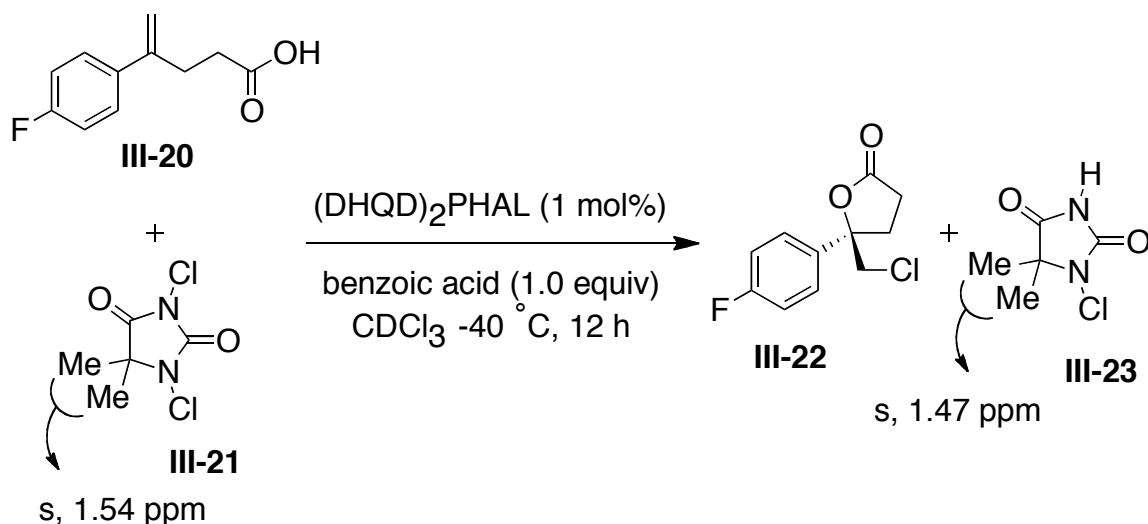
Scheme III-4. Consumption of N3-Cl of DCDMH during the course of reaction

12 h in the absence of the catalyst at -40 °C) that is avoided with the less reactive chlorohydantoins.

This trend indicates that the N3 chlorine of hydantoin **III-19** is delivered to the substrate in the chlorolactonization reaction, since the N1 chlorine atom is substantially less electrophilic. Indeed, we were able to observe the immediate formation of the 1-chloro-3-hydro hydantoin by-products by 1H-NMR during the course of the reaction by monitoring the reaction with NMR (**Scheme III-6**). From this we conclude that N1 chlorine of **III-19** must chiefly serve to inductively activate the N3 chlorine atom, most likely accounting for the molecule's enhanced N3 NQR resonance frequency as compared to NCS. A substantial amount of evidence for this supposition was collected by screening a series of N-chlorinated hydantoins.

The 1-chloro-N3-methyl-5,5-dimethylhydantoin (**III-23**, entry 5 Table III-1) was virtually inactive in the conversion of **III-25**, returning just 7% yield of **III-26** in 72% *ee*. This outcome was not unexpected, given that the remaining N1 chlorine of **III-23** is flanked by just one carbonyl and thus ought to be even less active than NCS (cf. entry 1). More interestingly, when the inductively activating N1 chlorine was replaced by a methyl (**III-24**, entry 6), the remaining N3 chlorine was substantially less activated, returning **III-26** in a reduced yield of 50% and with reduced selectivity of 78% *ee*. Clearly, some modicum of inductive activation at the N3 position via substitution at the N1 position is desirable in terms of both enhanced yield and enantioselectivity.

We posited that one might be able to rescue both yield and enantioselectivity in the transformation if the N1 chlorine of the chlorenium source were replaced by another activating group. Additionally, by incorporating a series of substitutions at the N1 site, we would be able to probe any steric demands that might arise in the associative complex between catalyst and hydantoin.

After some experimentation, we arrived at a simple method for the selective acylation of the N1 and N3 positions of 5,5-dimethylhydantoin **III-27** (Scheme III-7). The N3 position (i.e. **III-27**) could be selectively acylated under mild conditions by treating **III-27** with the appropriate acyl chloride in pyridine at room temperature. Alternatively, heating a pyridine solution of **III-27** and the acyl chloride to 170 °C gave selective access to the N1 acylated product **III-30**. Suspecting the intermediacy of **III-28** in the latter transformation, we also demonstrated its quantitative conversion to **III-30** on heating in pyridine at 170 °C. The N-acyl hydantoins were then converted to their

171
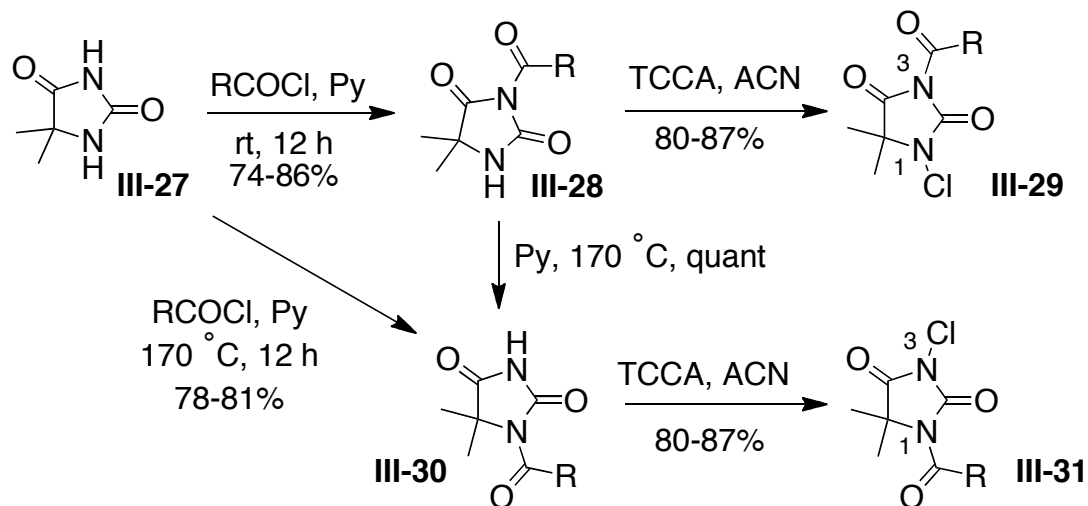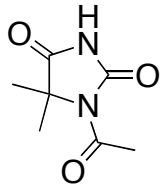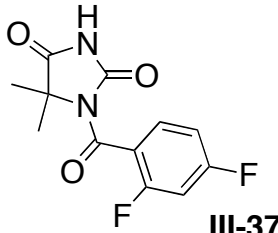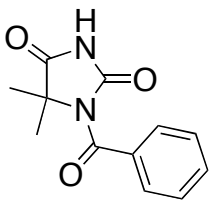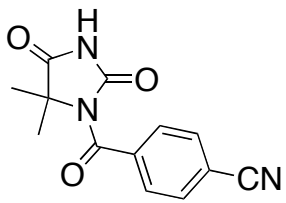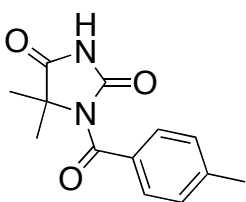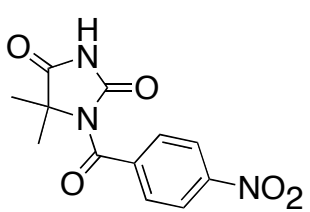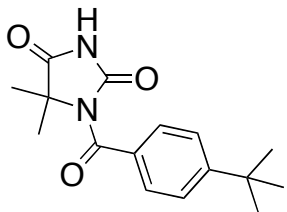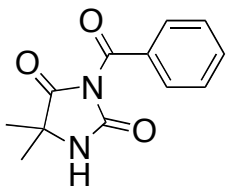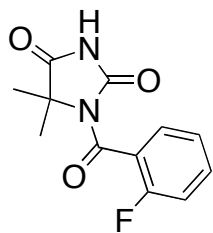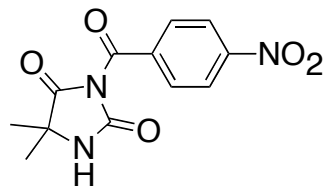
Scheme III-5. Preparation of N-acyl-N-chlorohydantions.

corresponding mono-chlorinated derivatives **III-29** and **III-31** in good yield (80-87%) by employing our TCCA mediated chlorination protocol.[34] Thus, N1 and N3 acyl and benzoyl hydantoins **III-32** - **III-41**, and corresponding chlorinated hydantoins **III-42** - **III-51** were generated, and the position of acylation and subsequent chlorination was secured unequivocally by X-ray crystallography.

With **III-42** - **III-51** in hand, they were next screened as chlorenium sources in the chlorolactonization of **III-25**, providing chlorolactone **III-26**. Confirming our prediction, all eight of the N1 acylated chlorine sources returned the desired lactone **III-26** in comparable yields and good enantioselectivities (on average 72% yield, 86% *ee*). The N1 acetylated hydantoin **III-42** gave **III-26** in 71% yield and 83% *ee* (entry 1). Interestingly, **III-42** was nearly equally selective as the parent 1,3-dichloro-5,5-dimethylhydantoin **III-21**, and markedly more active and selective than the N1 methyl

172

Table III-2. N1 or N3-Acyl hydantoins

Hydantoin	yield	Hydantoin	yield
III-32	81%	III-37	78%
III-33	80%	III-38	80%
III-34	81%	III-39	78%
III-35	79%	III-40	86%
III-36	78%	III-41	74%

Table III-3. Cyclization with modified *N*-chlorohydantoin

$$III\text{-}25 \xrightarrow[\substack{\text{benzoic acid (1.0 equiv)} \\ \text{CHCl}_3/\text{hex. (1:1)} \\ -40\,^{\circ}\text{C, 12 h}}]{\substack{\text{(DHQD)}_2\text{PHAL (10 mol\%)} \\ \text{Cl}^+ \text{ source (1.1 equiv.)}}} III\text{-}26$$
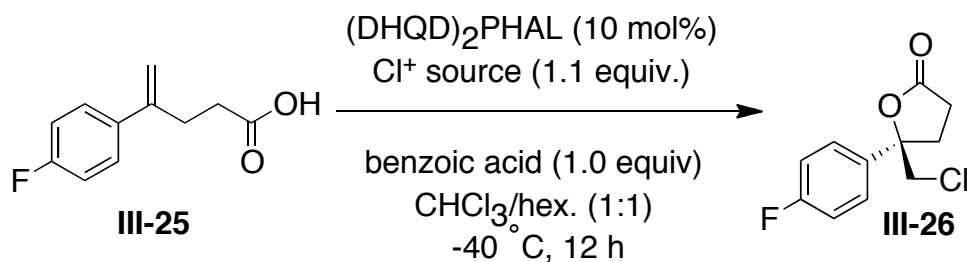
entry	Cl⁺ source	% yield[a]	% ee[b]	entry	Cl⁺ source	% yield[a]	% ee[b]
1	III-42	71	83	6	III-47 (2,6-diF-Bz)	64	87
2	III-43	78	88	7	III-48 (4-Me-Bz)	86	88
3	III-44	21	43	8	III-49 (4-*t*Bu-Bz)	64	87
4	III-45 (4-NO₂-Bz)	71	86	9	III-50 (2-F-Bz)	67	88
5	III-46 (4-NO₂-Bz)	14	46	10	III-51 (4-CN-Bz)	78	84

[a]isolated yields after column. [b]As judged by chiral GC.

174

derivative **III-24**. The N1 benzoyl derivative **III-43** surpasses the parent hydantoin **III-21** in terms of selectivity, returning **III-26** in 88% *ee* with a slightly reduced yield of 78% (entry 2). Conversely, the N3 benzoylcongener **III-44** produced **III-26** in substantially lower yield and reduced enantioselectivity (21% yield, 43% *ee*, entry 3). A second example of an N3 p-nitrobenzoyl substituted chlorohydantoin **III-46** also performed poorly in the conversion of **III-25** to **III-26** (14% yield, 46% *ee*, entry 5). The latter two examples clearly point to the need for an electron-withdrawing group on N1 for the activation and reactivity of the N3 chlorine.

Next we screened a series of N3 chlorinated hydantoins containing a variety of substituted benzoyl groups at the N1 position (**III-45**, **III-47-III-51**). Interestingly, all of the compounds returned **III-26** with good *ee*s ranging from 84 to 88% *ee* (entries 4, 6-10). To more closely probe the magnitude of the electronic effects of the N1 benzoyl substituent, we measured the rate of the formation of lactone **III-26** by NMR studies.

We employed hydantoins **III-48**, **III-43**, **III-50**, **III-47**, **III-51**, and **III-45** in order to scan a range of electron donating and withdrawing substituents. Interestingly we observed clear rate acceleration when hydantoins harboring electron withdrawing N-benzoyl substituents were employed (**Table III-4**). For example by removing the methyl group from the benzoyl group the rate constant increases from 1.6×10^{-4} to 2.1×10^{-4} (cf. **III-48** vs. **III-43**). By adding another fluoro group to the *para* postion of the hydantoin **III-50** the rate constant was almost doubled (4.2×10^{-4} vs 2.4×10^{-4}; 16 **III-50** vs. **III-47**). Moreover, the rate acceleration was even more pronounced when more strongly

Table III-4. Calculated rate constants for the formation of the lactone **III-26** by using different N1 benzoylated hydantoins (1 mol % catalyst).
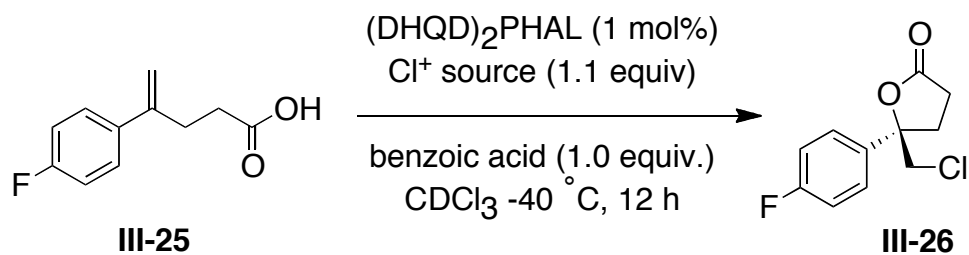
entry	Cl⁺ source	k [s⁻¹]	entry	Cl⁺ source	k [s⁻¹]
1	III-48	1.6×10^{-4}	4	III-47	4.2×10^{-4}
2	III-43	2.1×10^{-4}	5	III-51	5.6×10^{-4}
3	III-50	2.4×10^{-4}	6	III-45	7.4×10^{-4}

electron-withdrawing substituents were employed (i.e. 5.6×10^{-4} and 7.4×10^{-4} for **III-51** and **III-45**, respectively).

That the reaction maintains a comparable degree of selectivity regardless of the substitution on the N1 benzoyl substituent illustrates two interesting points. First, the overall electronics of the benzoyl substituent does not seem to influence the enantioselectivity of the transformation to any appreciable extent aside from behaving as a surrogate-activating group in place of the N1 chlorine in DCDMH **III-21** and DCDPH **III-19.** Sadly, this frustrates any strategy towards further optimization of the enantioselectivity of the transformation by means of electronic fine tuning of the N1 benzoyl substituent. Although, the electronic effects of the substituted benzoyl group do translate to the reactivity of the distal N3 chlorine to some extent as shown by the rate data in **Table III-4**.

Second, the steric demand of the substituents on the N1 benzoyl substituent seems to have a negligible effect on the selectivity of the transformation. It seems logical that since the active N3 chlorine is distal to the benzoyl group at N1, one would not expect the steric bias at the N1 position to influence the approach of the alkenoic acid to the pre-organized catalyst/chlorine source complex. More interesting is the implications of the N1 substitutent on the catalyst/hydantoin complex itself. Apparently, the N1 nitrogen and its substituent, regardless of size, must be splayed in a manner such that it does not clash with the chiral catalyst, thus allowing for high enantioselectivity. This fact, taken together with the clear dependance of *ee* on the size of the C-5 substituents (see **Table III-1** entries 3 and 4) may suggest that the complex between the catalyst and the

$(DHQD)_2PHAL$ (10 mol%)
Cl^+ source (1.1 equiv.)

benzoic acid (1.0 equiv.)
$CHCl_3$/hex. (1:1) -40 °C

III-25

III-26

III-52	**III-21**	**III-53**	**III-19**	size of the C-5 substituents
81% *ee*	84% *ee*	85% *ee*	89% *ee*	
76% yield	87% yield	82% yield	81% yield	
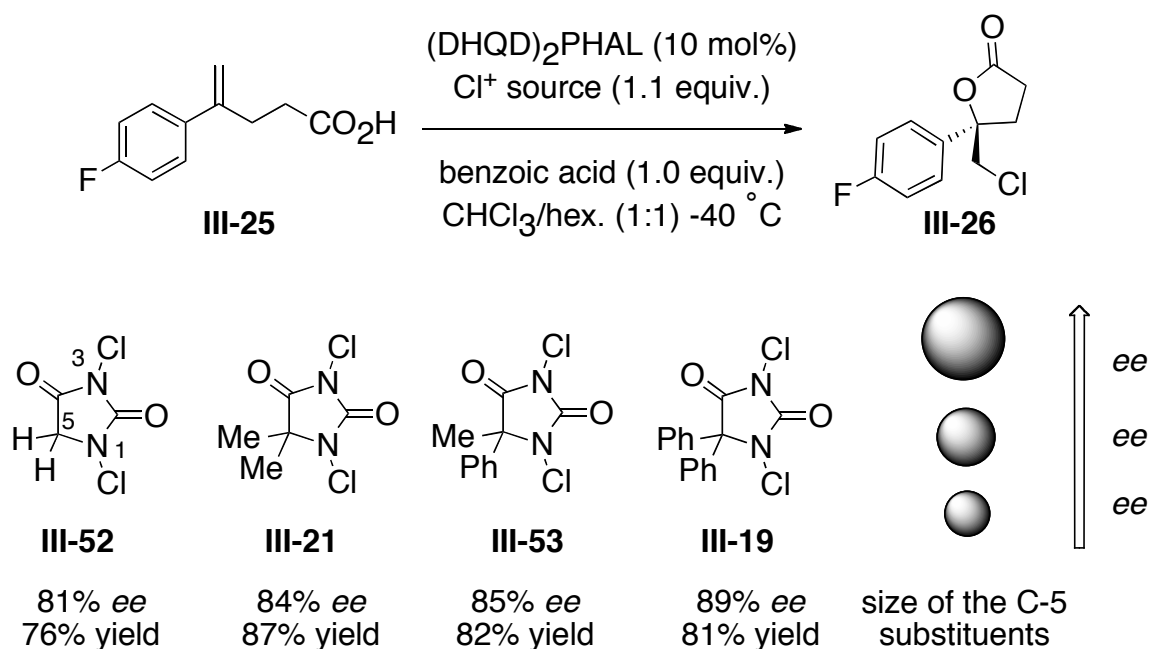
Figure III-3. Correlation between the size of the C5 substitutions and the enantioselectivity of the reaction

hydantoin is governed by a hydrogen bond to the C-4 carbonyl in lieu of that housed in the C-2 position.

3.3. POSSIBLE FORMATION OF THE ASSOCIATIVE COMPLEX BETWEEN THE $(DHQD)_2PHAL$ CATALYST AND THE CHLORINE SOURCE

During the optimization, an interesting result regarding the mechanism of the transformation came to light. In preliminary studies, an increase in selectivity was observed as the steric demand of the C-5 substituents on the terminal chlorine source increased. While lactone **III-26** was generated in 81% *ee* by action of unsubstituted **III-52**, the selectivity steadily increased on employing the dimethyl (**III-21**, 84% *ee*), methylphenyl (**III-53**, 85% *ee*), and diphenyl (**III-19**, 89% *ee*) chlorine sources (Scheme

III-8). Mechanistically these results clearly show that in this process chlorinated hydantoin is not just acting as a chlorine source to form a plausible complex **III-54** (Scheme III-9). One would expect that such a process leads to the formation of **III-26** with roughly the same degree of stereoinduction irrespective of the gross structure of the terminal chlorenium source. Conversely, the results in Scheme III-8 may indicate a more intimate relationship between the terminal halogen source and the catalyst.

Indeed, we were able to observe an associative complex between unsubstituted hydantoin **III-52** and the catalyst in a stoichiometric ^{1}H NMR experiment (Scheme III-9). In the event, the equivalent C-5 protons of dichlorohydantoin (s, 4.35 ppm) were split into a clean AB quartet (4.30 ppm, J_{AB} = 16.5 Hz) on incubation with an equivalent of (DHQD)$_2$PHAL and benzoic acid (2 equiv) in CDCl$_3$ at -40 $^\circ$C. This result clearly indicates an association between the N,N-dichlorohydantoin chlorine source and the chiral catalyst. On slowly warming the sample to RT, the association collapses and the AB quartet converges to the expected singlet at 4.35 ppm. Although premature, we are tempted to suggest complex **III-55**, invoking a hydrogen bond mediated association between the protonated catalyst and the chlorenium source. Alternatively one might imagine a tight ion pair between the chlorinated catalyst and the monochloro anion of the hydantoin chlorine source (see structure **III-56**). We believe that the associative complex between catalyst and N,N-dichlorohydantoin disclosed herein is a crucial element in the asymmetric delivery of the chlorine atom.[30]

After having these clues in hand, we decided to probe the associative hydantoin/catalyst complex observed by 1H NMR spectroscopy. We surmised that an
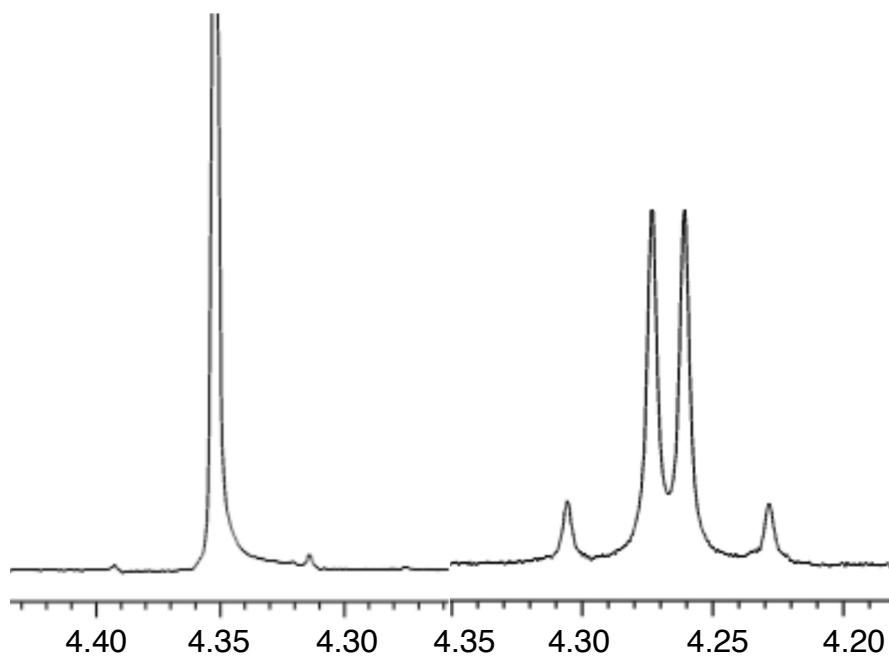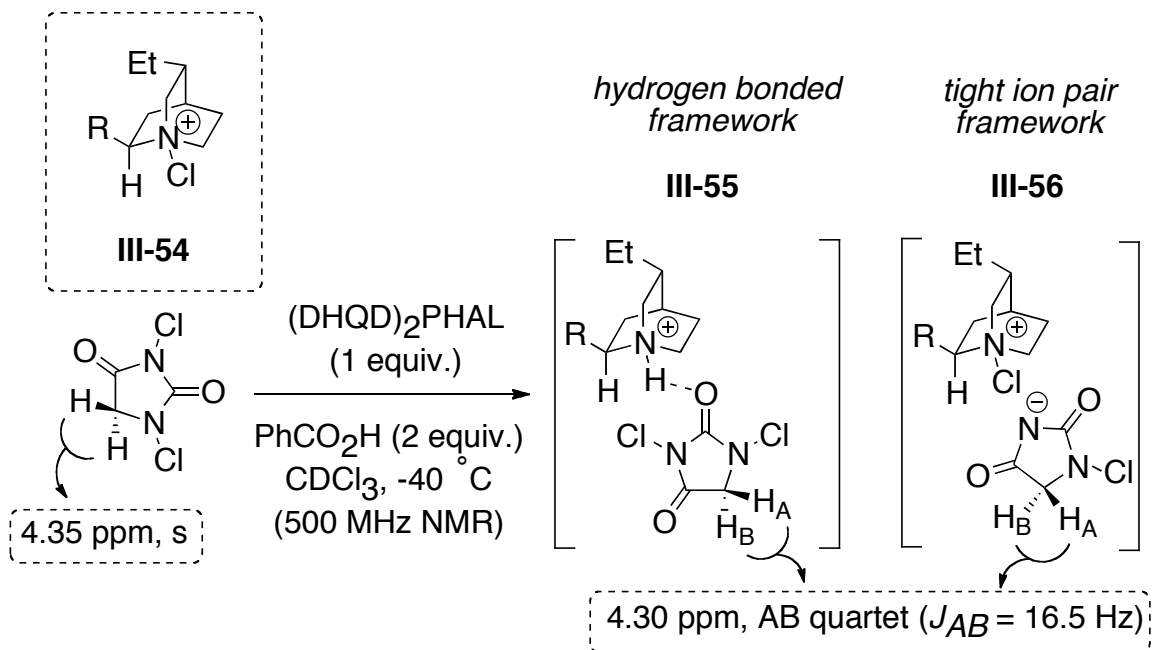
Figure III-4. The appearance of the AB quartet suggests an intimate complexation with the chiral catalyst

appropriate means of experimentally demonstrating the formation of the hydantoin/catalyst complex might be to employ a series of enantiomerically pure N-chlorinated hydantoins in the presence of the chiral catalyst in the conversion of **III-25** to **III-26**. If the enantiomerically pure hydantoins engaged in an associative interaction with the (DHQD)$_2$PHAL catalyst, then the stereochemical antipodes of the chlorine source ought to reflect matched/mismatched behavior in terms of enantioselectivity in the preparation of **III-26**. For this study, we prepared both enantiomers of 5-iso-propyl (**III-57**) and 5-benzyl-1,3-dichlorohydantoin (**III-58**). We have already demonstrated the ability to chlorinate chiral hydantoins without eroding their enantiopurity.

When the *R* and *S* enantiomers of **III-57** were employed in the cyclization of **III-25** with (DHQD)$_2$PHAL under optimized conditions, clear matched/mismatched behavior was observed (Table III-4). In the presence of (*S*)- **III-57**, lactone **III-26** was returned in 78% yield and 83% *ee*, while the *R* antipode gave **III-26** in a substantially reduced yield of 44% with an eroded enantioselectivity of 69% *ee*. This result again clearly demonstrates the formation of an associative complex between the chiral catalyst and the chlorine sources. The reduced yield for the mismatched case (i.e. with (*R*)- **III-57**) might indicate that the C-5 substituent is

displayed in the transition state in such a manner so as to prevent facile approach of the substrate to the catalyst/hydantoin complex. Importantly, the opposite effect was observed when the pseudoenantiomer (DHQ)$_2$PHAL was employed as the chiral catalyst, albeit to a lesser extent. In that case, the *R* enantiomer of **III-57** returned lactone en**III-26** in higher yield and *ee* (65% yield, 62% *ee*) as compared to the *S*

Table III-5. Matched/mismatched behavior with chiral *N*-chlorohydantoins.
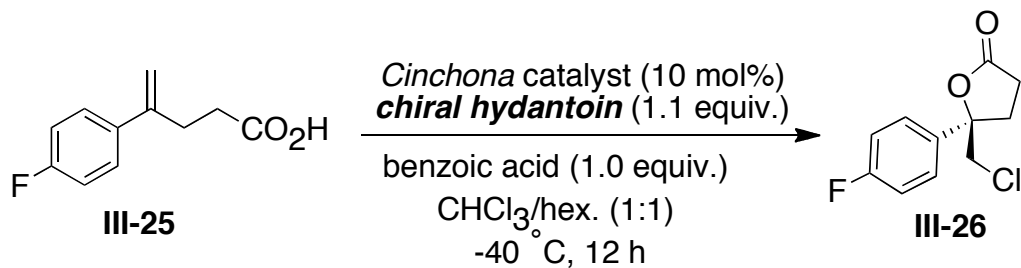
N-chlorohydantoin	(DHQD)$_2$PHAL		(DHQ)$_2$PHAL	
entry	% yield **26**	% ee **26**	% yield *ent*-**6**	% ee *ent*-**6**
1 (*S*)-**57**	78	83	30	-55
2 (*R*)-**57**	44	69	65	-62
3 (*S*)-**58**	78	79	71	-71
4 (*R*)-**58**	71	75	71	-73

antipode (30% yield, 55% *ee*). The overall lower selectivity when (DHQ)$_2$PHAL is employed is likely due to its diastereomeric relationship with its more selective pseudoenantiomer (DHQD)$_2$PHAL. A similar, but less pronounced effect was observed with (*S*) and (*R*)- **III-58** (Table III-4, entries 3 and 4), possibly as a result of benzyl's smaller steric demand as compared iso-propyl.[31]

In summary, we have probed the nature of the chlorenium source in our asymmetric chlorolactonization protocol by preparing a series of previously unknown N-acylated N-chlorohydantoins. We have conclusively secured the role of the N1 chlorine as an inductive activator of the N3 chlorine, which in turn is delivered to the substrate during the course of the chlorolactonization event. Finally, we experimentally demonstrated the formation of the associative complex between the chiral catalyst and chlorohydantoin by performing the chlorolactonization in the presence of chiral N-chlorohydantoins. In chapter four we will try to reveal the nature of this associative complex (tight ion pair or hydrogen-bonded) by series of NMR studies.

3.4: EXPERIMENTAL DETAILS

3.4.1: General Information

All reagents were purchased from commercial sources and used without purification. Anhydrous chloroform stabilized with amylenes and HPLC grade 95% *n*-hexanes was used for all asymmetric halolactonizations. ^{1}H and ^{13}C NMR spectra were collected on a 500 MHz NMR spectrometer (VARIAN INOVA) using CD$_3$Cl and CD$_3$CN. Chemical shifts are reported in parts per million (ppm). Spectra are referenced to residual solvent peaks. Samples for infrared spectroscopy were prepared as KBr pellets or KBr discs. Optical rotations were measured in chloroform and ethanol. Flash silica gel (32-63 mm) was used for column chromatography. Enantiomeric excess was judged by GC for the chlorolactone **III-26**.[1] All known compounds were characterized by ^{1}H and ^{13}C NMR and are in complete agreement with samples reported elsewhere. All new compounds were characterized by ^{1}H and ^{13}C NMR, IR, HRMS, optical rotation, melting point and in some cases by X-ray crystallography. Crystals for X-ray diffraction analyses were obtained from dichloromethane/hexane (~2:1) at -20 $^{\circ}$C. The parent chiral hydantoins of **III-57** and **III-58** were prepared in high enantiomeric purity (confirmed by optical rotation) from the corresponding chiral α-amino acids by known methodology.[2-4] All chlorinated hydantoins were prepared using our previously disclosed methodology at 2 mmol scale.[5]

3.4.2: General procedure for synthesis of hydantoins III-30

5,5-Dimethylhydantoin (7.8 mmol, 1 equiv) was suspended in pyridine (4 mL) in a sealed tube and the desired acylchloride (7.8 mmol,1 equiv) was added dropwise to the

mixture at room temperature. The sealed tube was properly sealed and the mixture was heated at 170 °C overnight. The solvent was evaporated under vacuum and the residue was dissolved in ethyl acetate and filtered with suction through a 1-cm thick pad of silica gel packed with ethyl acetate in a 50 mL fritted funnel. The silica gel pad was subsequently washed with ethyl acetate and the combined organics were concentrated by rotary evaporation to provide the crude product. The crude isolate was purified by recrystallization from ethyl acetate/hexanes. The mother liquor was then concentrated and the residue was re-subjected to recyrstallization to provide a second crop of products.

Alternatively, N3-acylated hydantoins could be converted to the corresponding N1-acylated hydantoins by heating in pyridine, overnight, in a sealed tube at 170 °C.

3.4.3: General procedure for synthesis of N3-acylated hydantoins III-28

5,5-Dimethylhydantoin (7.8 mmol, 1 equiv) was suspended in dried pyridine (4 mL) in a round bottom flask and the required acyl chloride (7.8 mmol,1 equiv) was added dropwise to the mixture and stirred at room temperature overnight. After the reaction was complete, the solvent was evaporated under vacuum without any heating or under a stream of N_2 gas. The residue was dissolved in ethyl acetate and filtered with suction through a 1-cm thick pad of silica gel packed with ethyl acetate in a 50 mL fritted funnel. The silica gel pad was subsequently washed with ethyl acetate and the combined organics were concentrated by rotary evaporation to provide the crude product. The crude isolate was purified by recrystallization from ethyl acetate/hexanes. The mother

liquor was then concentrated and the residue was re-subjected to recyrstallization to provide a second crop of products.

3.4.4: General procedure for measuring the rate of the reaction

The probe of the NMR instrument was cooled to -20 $^\circ$C and allowed to equilibrate for 60 minutes. (DHQD)$_2$PHAL (0.10 equiv, 0.0051 mmol, 4 mg) was dissolved in CDCl$_3$ (1 mL) and the catalyst solution (0.1 mL, 0.01 equiv, 0.00051 mmol, 0.4 mg) was transferred to the NMR reaction tube. Benzoic Acid (1.0 equiv, 0.051 mmol, 6.3 mg) and the appropriate hydantoin (1.1 equiv, 0.057 mmol) were dissolved in CDCl$_3$ (0.6 mL) and immediately added to the catalyst in the NMR reaction tube and cooled to -20 $^\circ$C for 10 minutes. Finally 4-(4-fluorophenyl)-4-pentenoic acid (1.0 equiv, 0.051 mmol, 10 mg) was dissolved in CDCl$_3$ (0.3 mL) and added to the NMR reaction tube and allowed to cool down to -20 $^\circ$C in the NMR probe for 5 minutes before shimming. The NMR parameters for each experiment were set so that nine acquisitions at 10-minute intervals were obtained throughout the course of the reaction. The first acquisition occurred ten minutes after the addition of the 4-(4-fluorophenyl)-4-pentenoic acid. The ortho proton resonances of benzoic acid were selected as an internal reference peak for determination of product concentration. This was done by measuring the relative integration of the benzoic acid and the chloromethylene protons (~3.75 ppm) that were unique to the product.

The plot of the product concentration vs. time (90 min) and its fit to pseudo first order kinetics, as depicted below, provided the rate constant for the formation of the lactone **III-26** by using the hydantoins **III-43**, **III-45**, **III-47**, **III-48** and **III-50**.

3.4.5: Measuring the TCCA background reaction

The probe of the NMR instrument was cooled to -40 $^{\circ}$C and allowed to equilibrate for 60 min. TCCA (1.1 equiv, 0.057 mmol, 13 mg) was dissolved in CDCl$_3$ (0.8 mL) in the NMR reaction tube and cooled to -40 $^{\circ}$C for 10 minutes.   4-(4-Fluorophenyl)-4-pentenoic acid (1.0 equiv, 0.051 mmol, 10 mg) was then dissolved in CDCl$_3$ (0.2 mL) and added slowly to the mixture. The reaction was monitored by NMR, yielding 7.2% of product after 12 h.

$$y = 0.03(1 - e^{-0.00016t}) + 0.007$$

3.4.6: Analytical data for chlorinated hydantoins and 4-nitro-*N*-chlorophthalamide:

III-42,1-Acetyl-3-chloro-5,5-dimethylhydantoin

^{1}H NMR (500 MHz, CDCl$_3$): δ 1.71 (6H, s), 2.55 (3H, s); ^{13}C NMR (125 MHz, CDCl$_3$): δ 22.74, 26.24, 65.35, 149.89, 168.87, 170.61; IR (cm^{-1}, KBr disc): 1806, 1743, 1709; HRMS (C$_7$H$_9$ClN$_2$O$_3$): Calc. [M]$^+$: 204.0302, Found [M]$^+$: 204.0295; mp = 150-151 $^{\circ}$C; 85% yield.

III-43,1-Benzoyl-3-chloro-5,5-dimethylhydantoin

^{1}H NMR (500 MHz, CDCl$_3$): δ 1.85 (6H, s), 7.42 (2H, t, *J* = 7.5 Hz), 7.52 (3H, m); ^{13}C NMR (125 MHz, CDCl$_3$): δ 23.23, 66.01, 128.10, 128.14, 132.41, 134.12, 149.23, 168.19, 170.63. IR (cm^{-1}, KBr disc): 1815, 1757, 1683; HRMS (C$_{12}$H$_{11}$ClN$_2$O$_3$): Calc. [M]$^+$: 266.0458, Found [M]$^+$: 266.0466; mp = 144-145 $^{\circ}$C; 87% yield.

III-44, 3-Benzoyl-1-chloro-5,5-dimethylhydantoin

^{1}H NMR (500 MHz, CDCl$_3$): δ 1.57 (6H, s), 7.47 (2H,), 7.64 (1H, m), 7.78 (2H, m); ^{13}C NMR (125 MHz, CDCl$_3$): δ 22.32, 66.18, 128.77, 130.36, 131.36, 134.96, 150.74,

164.94, 171.58; IR (cm^{-1}, KBr disc): 1806, 1749, 1702; HRMS (C$_{12}$H$_{11}$ClN$_2$O$_3$): Calc. [M]$^+$: 266.0458, Found [M]$^+$: 266.0457; mp = 96-97 $^\circ$C; 84% yield.

III-45, 1-(4-Nitrobenzoyl)-3-chloro-5,5-dimethylhydantoin

^{1}H NMR (500 MHz, CDCl$_3$): δ 1.87 (6H, s), 7.64 (2H, d, J = 8.5 Hz), 8.29 (2H, d, J = 8.5 Hz); ^{13}C NMR (125 MHz, CDCl$_3$): δ 23.02, 66.19, 123.44, 128.74, 139.86, 149.18, 149.57, 166.21, 170.04; IR (cm^{-1}, KBr disc): 1801, 1756, 1693; HRMS (C$_{12}$H$_{10}$ClN$_3$O$_5$): Calc. [M]$^+$: 311.0309, Found [M]$^+$: 311.0320; mp = 189-191 $^\circ$C; 85% yield.

III-46, 3-(4-Nitrobenzoyl)-1-chloro-5,5-dimethylhydantoin

^{1}H NMR (500 MHz, CDCl$_3$): δ 1.61 (6H, s), 7.92 (2H, d, J = 9.0 Hz), 8.33 (2H, d, J = 9.0 Hz); ^{13}C NMR (75 MHz, CDCl$_3$): δ 22.41, 66.25, 123.83, 131.05, 136.70, 149.98, 151.04, 163.61, 171.18; IR (cm^{-1}, KBr disc): 1808, 1752, 1713; HRMS (C$_{12}$H$_{10}$ClN$_3$O$_5$): Calc. [M]$^+$: 311.0309, Found [M]$^+$: 311.0296; mp = 160-161°C; 83% yield.

III-47,1-(2,6-Difluorobenzoyl)-3-chloro-5,5-dimethylhydantoin

^{1}H NMR (500 MHz, CDCl$_3$): δ 1.85 (6H, s), 6.96 (2H, m), 7.42 (2H, m); ^{13}C NMR (125 MHz, CDCl$_3$): δ 22.69, 65.97, 111.66 (dd, J = 4.1, 19.6 Hz), 113.68 (t, J = 20.1 Hz), 132.55 (t, J = 10 Hz), 148.61, 158.18(d, J = 6.9 Hz), 158.65, 160.18 (d , J = 6.5 Hz), 170.06; IR (cm^{-1}, KBr disc): 1812, 1759, 1697; HRMS (C$_{12}$H$_9$F$_2$ClN$_2$O$_3$): Calc. [M]$^+$: 302.0270, Found [M]$^+$: 302.0266; mp = 165-166 $^\circ$C; 80% yield.

III-48,1-(4-Methylbenzoyl)-3-chloro-5,5-dimethylhydantoin

^{1}H NMR (500 MHz, CDCl$_3$): δ 1.84 (6H, s), 2.40 (3H, s), 7.22 (2H, d, J = 8.5 Hz), 7.44 (2H, d, J = 8.5 Hz); ^{13}C NMR (125 MHz, CDCl$_3$): δ 21.66, 23.31, 66.00, 128.42, 128.82, 131.19, 143.40, 149.30, 168.14, 170.74; IR (cm^{-1}, KBr disc): 1804, 1763, 1676; HRMS (C$_{13}$H$_{13}$ClN$_2$O$_3$): Calc. [M]$^+$: 280.0615, Found [M]$^+$: 280.0618; mp = 129-130 °C; 85% yield.

III-49, 1-(4-*tert*-Butylbenzoyl)-3-chloro-5,5-dimethylhydantoin

^{1}H NMR (500 MHz, CDCl$_3$): δ 1.32 (9H, s), 1.83 (6H, s), 7.43 (2H, d, J = 8.5 Hz), 7.49 (2H, d, J = 8.5 Hz); ^{13}C NMR (125 MHz, CDCl$_3$): δ 23.31, 31.04, 35.09, 66.03, 125.11, 128.39, 131.01, 149.34, 156.39, 168.07, 170.74; IR (cm^{-1}, KBr disc): 1802, 1756, 1697; HRMS (C$_{16}$H$_{19}$ClN$_2$O$_3$): Calc. [M]$^+$: 322.1084, Found [M]$^+$: 322.1072; mp = 131-132 °C; 82% yield.

III-50,1-(2-Fluorobenzoyl)-3-chloro-5,5-dimethylhydantoin

^{1}H NMR (500 MHz, CDCl$_3$): δ 1.84 (6H, s), 7.08 (1H, t, J = 9 Hz), 7.25 (1H, t, J = 4 Hz), 7.49 (2H, m); ^{13}C NMR (125 MHz, CDCl$_3$): δ 22.94, 65.96, 115.64 (d, $^2J_{C-F}$ = 21.13 Hz), 123.51 (d, $^3J_{C-F}$ = 2.5 Hz), 124.54 (d, $^3J_{C-F}$ = 3.25 Hz), 129.37, 133.49 (d, $^3J_{C-F}$ = 8.75 Hz), 148.91, 159.32 (d, $^1J_{C-F}$ = 248.5 Hz), 163.72, 170.38; IR (cm^{-1}, KBr disc): 1813, 1755, 1688; HRMS (C$_{12}$H$_{10}$FClN$_2$O$_3$): Calc. [M]$^+$: 284.0364, Found [M]$^+$: 284.0368; mp = 146-148 °C; 80% yield.

III-51, 1-(4-Cyanobenzoyl)-3-chloro-5,5-dimethylhydantoin

^{1}H NMR (500 MHz, CDCl$_3$): δ 1.85 (6H, s), 7.58 (2H, dd, J = 6.5, 2 Hz), 7.71 (2H, dd, J = 6.5, 2 Hz); ^{13}C NMR (125 MHz, CDCl$_3$): δ 23.02, 66.15, 115.58, 117.71, 128.33, 131.94, 138.16, 149.17, 166.41, 170.09; IR (cm^{-1}, KBr disc): 1802, 1735, 1698; HRMS

($C_{13}H_{10}ClN_3O_3$): Calc. $[M]^+$: 291.0411, Found $[M]^+$: 291.0411; mp = 194-195 $^\circ$C; 83% yield.

III-57, (*R*)-1,3-Dichloro-5-(*iso*-propyl)hydantoin:

Analytical and spectroscopic data matched those reported previously.[5]

$[\alpha]_D^{20}$ = -21.8° (c = 1.00,CHCl$_3$).

III-58, (*R*)-1,3-Dichloro-5-benzylhydantoin:

Analytical and spectroscopic data matched those reported previously.[5]

$[\alpha]_D^{20}$ = -26.2° (c = 1.00, CHCl$_3$).

3.4.7: Analytical Data for parent hydantoins

III-32,1-Acetyl-5,5-dimethylhydantoin

^{1}H NMR (500 MHz, CDCl$_3$): δ 1.66 (6H, s), 2.52 (3H, s), 8.62 (1H, br); ^{13}C NMR (125 MHz, CDCl$_3$): δ 22.34, 26.30, 65.16, 152.99, 169.60, 175.63. IR (cm^{-1}, KBr disc): 1798, 1728, 1672; HRMS ($C_7H_{10}N_2O_3$): Calc. $[M]^+$: 170.0691, Found $[M]^+$: 170.0691; mp = 194-195 $^\circ$C; 81% yield.

III-33,1-Benzoyl-5,5-dimethylhydantoin

^{1}H NMR (500 MHz, CDCl$_3$): δ 1.77 (6H, s), 7.40 (2H, t, *J* = 7.5 Hz), 7.51 (3H, m), 8.59 (1H, br); ^{13}C NMR (125 MHz, CDCl$_3$): δ 22.80, 65.76, 127.99, 128.063, 132.09, 134.73, 152.29, 168.85, 175.70; IR (cm^{-1}, KBr disc): 1803, 1747, 1653; HRMS ($C_{12}H_{12}N_2O_3$): Calc. $[M]^+$: 232.0848, Found $[M]^+$: 232.0849; mp = 194-196 $^\circ$C; 80% yield.

III-40,3-Benzoyl-5,5-dimethylhydantoin

^{1}H NMR (500 MHz, CDCl$_3$): δ 1.54 (6H, s), 6.35 (1H, br), 7.47 (2H, m), 7.63 (1H, m), 7.81(2H, m); ^{13}C NMR (125 MHz, CDCl$_3$): δ 25.05, 59.19, 128.65, 130.31, 132.02, 134.61, 153.23, 166.33, 175.04; IR (cm^{-1}, KBr disc): 1806, 1753, 1702; HRMS (C$_{12}$H$_{12}$N$_2$O$_3$): Calc. [M]$^+$: 232.0848, Found [M]$^+$: 232.0853; mp = 82-84 $^\circ$C; 86% yield.

III-39.1-(4-Nitrobenzoyl)-5,5-dimethylhydantoin

^{1}H NMR (500 MHz, Acetone- d6): δ 1.78 (6H, s), 7.86 (2H, d, J = 9.0 Hz), 8.27 (2H, d, J = 9.0 Hz); ^{13}C NMR (125 MHz, Acetone- d6): δ 22.54, 65.8, 123.71, 129.69, 143.06, 149.9, 153.37, 167.86, 176.18; IR (cm^{-1}, KBr disc): 1795, 1729, 1685; HRMS (C$_{12}$H$_{11}$N$_3$O$_5$): Calc. [M]$^+$: 277.0699, Found [M]$^+$: 277.0690; mp = 257-258 $^\circ$C; 78% yield.

III-41. 3-(4-Nitrobenzoyl)-5,5-dimethylhydantoin

^{1}H NMR (500 MHz, CDCl$_3$): δ 1.54 (6H, s), 6.37 (1H, br), 7.91 (2H, dd, J = 7.0, 2 Hz), 8.30 (2H, dd, J = 7.0, 2 Hz); ^{13}C NMR (75 MHz, CDCl$_3$): δ 25.31, 59.23, 123.70, 130.97, 137.29, 150.84, 152.11, 164.77, 174.37; IR (cm^{-1}, KBr disc): 1806, 1754, 1703; HRMS (C$_{12}$H$_{11}$N$_3$O$_5$): Calc. [M]$^+$: 277.0699, Found [M]$^+$: 277.0697; mp = 151-153 $^\circ$C; 74% yield.

III-37.1-(2,6-Difluorobenzoyl)-5,5-dimethylhydantoin

^{1}H NMR (500 MHz, CDCl$_3$): δ 1.79 (6H, s), 6.92 (2H, m), 7.39 (2H, m), 8.09 (1H, br); ^{13}C NMR (125 MHz, CDCl$_3$): δ 22.26, 65.64, 111.61 (t, J = 20.12 Hz), 114.23 (t, J = 20.6 Hz), 132.14 (t, J = 10.25 Hz), 151.42, 158.16 (d, J = 7.25 Hz), 159.07 160.16 (d, J = 6.75 Hz), 174.95; IR (cm^{-1}, KBr disc): 1805, 1735, 1692; HRMS (C$_{12}$H$_{10}$F$_2$N$_2$O$_3$): Calc. [M]$^+$: 268.0649, Found [M]$^+$: 268.0659. mp = 175-176 $^\circ$C; 78% yield.

III-34.1-(4-Methylbenzoyl)-5,5-dimethylhydantoin

^{1}H NMR (500 MHz, CDCl$_3$): δ 1.78 (6H, s), 2.39 (3H, s), 7.21 (2H, d, J = 8.5 Hz), 7.44 (2H, d, J = 8.5 Hz), 8.03 (1H, br); ^{13}C NMR (125 MHz, CDCl$_3$): δ 21.63, 22.88, 65.74, 128.40, 128.68, 131.85, 142.93, 152.38, 168.82, 175.70; IR (cm^{-1}, KBr disc): 1801, 1746, 1693; HRMS (C$_{13}$H$_{14}$N$_2$O$_3$): Calc. [M]$^+$: 246.1004, Found [M]$^+$: 246.1007; mp = 157-158 $^\circ$C; 81% yield.

III-35.1-(4-*tert*-Butylbenzoyl)-5,5-dimethylhydantoin

^{1}H NMR (500 MHz, CDCl$_3$): δ 1.32 (9H, s), 1.78 (6H, s), 7.41 (2H, d, J = 8.5 Hz), 7.50 (2H, d, J = 8.5 Hz), 7.87 (1H, br); ^{13}C NMR (125 MHz, CDCl$_3$): δ 22.92, 31.07, 35.05, 65.84, 125.01, 128.36, 131.68, 152.32, 155.99, 168.75, 175.70; IR (cm^{-1}, KBr disc): 1793, 1729, 1692; HRMS (C$_{16}$H$_{20}$N$_2$O$_3$): Calc. [M]$^+$: 288.1474, Found [M]$^+$: 288.1475; mp = 209-210 $^\circ$C; 79% yield.

III-36.1-(2-Fluorobenzoyl)-5,5-dimethylhydantoin

^{1}H NMR (500 MHz, CDCl$_3$): δ 1.78 (6H, s), 7.05 (1H, t, J = 10 Hz), 7.22 (1H, t, J = 7.5 Hz), 7.46 (2H, m), 8.06 (1H, br); ^{13}C NMR (125 MHz, CDCl$_3$): δ 22.51, 65.7, 115.38 (d, $^3J_{C\text{-}F}$ = 2.6 Hz), 124.1 (d, $^2J_{C\text{-}F}$ = 15 Hz), 124.44 (d, $^3J_{C\text{-}F}$ = 3.6 Hz), 129.33 (d, $^3J_{C\text{-}F}$ = 21.12 Hz), 133.15 (d, $^3J_{C\text{-}F}$ = 8.75 Hz), 151.86, 159.28 (d, $^1J_{C\text{-}F}$ = 247.5 Hz), 164.19, 175.28; IR (cm^{-1}, KBr disc): 1806, 1758, 1660; HRMS (C$_{12}$H$_{11}$F$_1$N$_2$O$_3$): Calc. [M]$^+$: 250.0745, Found [M]$^+$: 250.0750; mp = 160-162 $^\circ$C; 78% yield.

III-38.1-(4-Cyanobenzoyl)-5,5-dimethylhydantoin

^{1}H NMR (500 MHz, CDCl$_3$): δ 1.80 (6H, s), 7.58 (2H, dd, J = 6.5, 2 Hz), 7.69 (2H, dd, J = 6.5, 2 Hz), 8.31 (1H, br); ^{13}C NMR (125 MHz, CDCl$_3$): δ 22.62, 65.90, 115.22,

117.85, 128.29, 131.86, 138.87, 151.83, 167.02, 174.82; IR (cm^{-1}, KBr disc): 1806, 1758, 1657; HRMS ($C_{13}H_{11}N_3O_3$): Calc. [M]$^+$: 257.0800, Found [M]$^+$: 257.0800, mp = 219-220 $^{\circ}$C; 80% yield.

REFERENCES

REFERENCES

1. Golebiewski, W. M.; Gucma, M. *Synthesis-Stuttgart* **2007**, 3599.

2. Agnihotri, G. *Synlett* **2005**, 2857.

3. Tilstam, U.; Weinmann, H. *Organic Process Research & Development* **2002**, *6*, 384.

4. Xu, Z. J.; Zhang, D. Y.; Zou, X. Z. *Synthetic Communications* **2006**, *36*, 255.

5. Spitulnik, M. J. *Synthesis-Stuttgart* **1985**, 299.

6. Shapiro, E. L.; Gentles, M. J.; Tiberi, R. L.; Popper, T. L.; Berkenkopf, J.; Lutsky, B.; Watnick, A. S. *Journal of Medicinal Chemistry* **1987**, *30*, 1581.

7. Karmazin, L.; Mazzanti, M.; Bezombes, J. P.; Gateau, C.; Pecaut, J. *Inorganic Chemistry* **2004**, *43*, 5147.

8. Miesch, L.; Gateau, C.; Morin, F.; Franck-Neumann, M. *Tetrahedron Letters* **2002**, *43*, 7635.

9. Barnes, D. M.; Christesen, A. C.; Engstrom, K. M.; Haight, A. R.; Hsu, M. C.; Lee, E. C.; Peterson, M. J.; Plata, D. J.; Raje, P. S.; Stoner, E. J.; Tedrow, J. S.; Wagaw, S. *Organic Process Research & Development* **2006**, *10*, 803.

10. Chen, B. C.; Murphy, C. K.; Kumar, A.; Reddy, R. T.; Clark, C.; Zhou, P.; Lewis, B. M.; Gala, D.; Mergelsberg, I.; Scherer, D.; Buckley, J.; DiBenedetto, D.; Davis, F. A. *Organic Synthesis, Vol 73* **1996**, *73*, 159.

11. Mergelsberg, I.; Gala, D.; Scherer, D.; Dibenedetto, D.; Tanner, M. *Tetrahedron Letters* **1992**, *33*, 161.

12. Szumigala, R. H.; Devine, P. N.; Gauthier, D. R.; Volante, R. P. *Journal of Organic Chemistry* **2004**, *69*, 566.

13. Zolfigol, M. A.; Nasr-Isfahani, H.; Mallakpour, S.; Safaiee, M. *Synlett* **2005**, 761.

14. Khazaei, A.; Manesh, A. A. *Synthesis-Stuttgart* **2005**, 1929.

15. Shakya, P. D.; Dubey, D. K.; Pardasani, D.; Palit, M.; Gupta, A. K. *Organic Preparations and Procedures International* **2005**, *37*, 569.

16. Zolfigol, M. A.; Ghaemi, E.; Madrakian, E.; Choghamarani, A. G. *Mendeleev Communications* **2006**, 41.

17. Niknam, K.; Zolfigol, M. A. *Journal of the Iranian Chemical Society* **2006**, *3*, 59.

18. Nilov, D.; Reiser, O. *Advanced Synthesis & Catalysis* **2002**, *344*, 1169.

19. Bodkin, J. A.; McLeod, M. D. *Journal of the Chemical Society-Perkin Transactions 1* **2002**, 2733.

20. O'Brien, P. *Angewandte Chemie-International Edition* **1999**, *38*, 326.

21. Barta, N. S.; Sidler, D. R.; Somerville, K. B.; Weissman, S. A.; Larsen, R. D.; Reider, P. J. *Organic Letters* **2000**, *2*, 2821.

22. Harding, M.; Bodkin, J. A.; Hutton, C. A.; McLeod, M. D. *Synlett* **2005**, 2829.

23. DiBlasi, C. M.; Macks, D. E.; Tan, D. S. *Organic Letters* **2005**, *7*, 1777.

24. Grela, K.; Tryznowski, M.; Bieniek, M. *Tetrahedron Letters* **2002**, *43*, 9055.

25. Kobori, A.; Miyata, K.; Ushioda, M.; Seio, K.; Sekine, M. *Chemistry Letters* **2002**, 16.

26. Komatsu, M.; Okada, H.; Akaki, T.; Oderaotoshi, Y.; Minakata, S. *Organic Letters* **2002**, *4*, 3505.

27. Zhou, Y.-G. *Accounts of Chemical Research* **2007**, *40*, 1357.

28. Radhamma, M. P.; Indrasenan, P. *Talanta* **1983**, *30*, 49.

29. Rao, Z. M.; Zhang, X. R.; Baeyens, W. R. G. *Talanta* **2002**, *57*, 993.

30. Whitehead, D. C.; Yousefi, R.; Jaganathan, A.; Borhan, B. *Journal of the American Chemical Society* **2010**, *132*, 3298.

31. Yousefi, R.; Whitehead, D. C.; Mueller, J. M.; Staples, R. J.; Borhan, B. *Organic Letters* **2011**, *13*, 608.

32. Nagao, Y.; Katagiri, S. *Chemistry Letters* **1993**, 1169.

33. Nagao, Y. K., S. *Sci. Rep. Hirosaki Univ.* **1991**, *38*, 20.

34. Whitehead, D. C.; Staples, R. J.; Borhan, B. *Tetrahedron Letters* **2009**, *50*, 656.

Chapter 4: NMR Studies on the Origin of Face Selectivity of Asymmetric Chlorolactonization

4.1: Introduction

As discussed in Chapter two, mechanistic studies of the DHQD$_2$PHAL catalyzed asymmetric chlorolactonization reaction of alkenoic acids have led to some surprising conclusions. Deuterium labeling studies of the catalyzed reaction of 4-arylpent-4-enoic acid have revealed that the high face selectivity in the delivery of the chlorenium ion to olefins is neither necessary nor a sufficient condition to deliver the product lactones with high enantioselectivities. The reaction likely proceeds via a carbocation intermediate with the enantioselectivity imparted through "templated" cyclization governed by the chiral catalyst. In addition, reaction progress kinetic analysis (RPKA) and competition studies have revealed that the rate-determining step is the delivery of the chlorenium to the olefin. Moreover, the observed reverse isotope effect (specific acid catalysis) suggests that DCDMH is activated prior to RDS, presumably by hydrogen binding with the catalyst. Taken together, these results suggest that the rate determining step and the enantioselectivity determining step are segregated. Formation of the chloronium ion and the cyclization of the resulting carbocation are highly stereoselective processes. As a result, we can propose a catalytic cycle, depicted in Scheme IV-1 that accounts for these observations. In the first step two molecules of 4-phenylpent-4-enoic acid **IV-2** bind to the protonated catalyst most probably as a salt to form complex **IV-3.** In the second step, one molecule of hydantoin binds to complex **IV-3**, presumably by replacing

one substrate. Hydrogen bonding of DCDMH to the protonated catalyst activates the

DCDMH at -40 °C. After activation of the DCDMH, the chlorenium is delivered in the

RDS to the olefin, forming the intermediate **IV-6**. The templation of the carbocation

intermediate by the catalyst will control the face selectivity in the *enantio*-determining
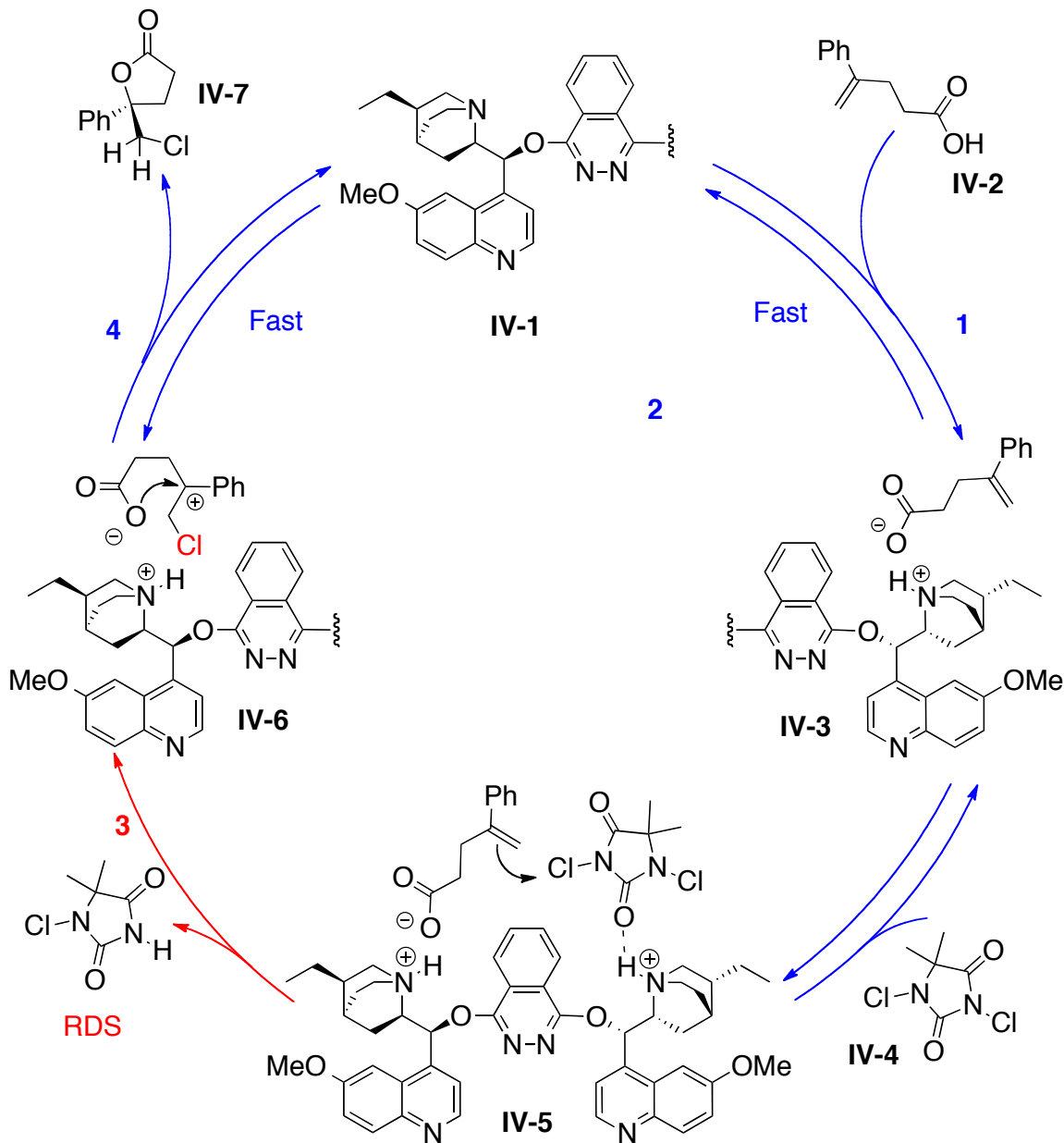
Scheme IV-1. Proposed mechanism for our asymmetric
chlorolactonization

cyclization step. In this chapter we present studies to evaluate the proposed catalytic cycle by distinguishing the origin of face selectivity in the RDS, the chlorenium delivery, and also in the *enantio*-determining cyclization step by exhaustive NMR studies.

4.2: Origin of Face Selectivity in Chlorine Delivery

As depicted in Figure IV-1 and discussed in detail in Chapter three, it is believed that there is an associative complex between the dichlorohydantoin and the catalyst, (DHQD)$_2$PHAL, based on the observed AB quartet in the ^{1}H NMR spectra.[1] The nature of this associative complex can be either a tight ion pair or a hydrogen bond as proposed before. In this section our attempts reveal the actual nature of this associative complex by a series of NMR studies.

In order for the tight ion pair complex **IV-11** to form (Scheme IV-2), first the most nucleophilic site of the (DHQD)$_2$PHAL, the nitrogen of the quinuclidine moiety, should attack the N3-chlorine, the most active chlorine,[2] of the 1,3-dichloro-5,5-dimethylhydantoin (DCDMH). Under the reaction condition, the carboxylic acid substrate and also the benzoic acid additive are present. One can imagine that the conjugated base of DCDMH, **IV-11** complex, can get protonated to form the tight ion pair complex **IV-13** (Scheme IV-2), where the benzoate acts as a counter anion to the positively charged catalyst. Tight ion pair complex **IV-13** can only form if the pK$_a$ of the substrate or benzoic acid is lower than 1-chloro-5,5-dimethylhydantoin.
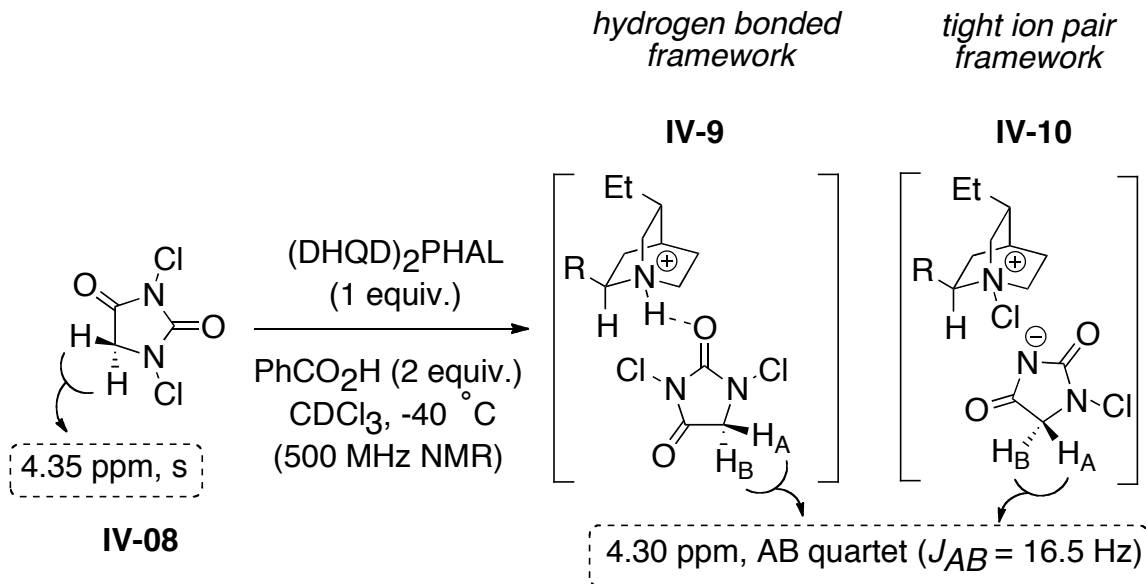
Figure IV-1. The appearance of the AB quartet suggests an intimate complexation with the chiral catalyst

The pK_a of 1-chloro-5,5-dimethylhydantoin **IV-14** (Scheme IV-3) in chloroform was estimated by titration with quinuclidine. The chemical shifts of the geminal methyl groups in 1-chloro-5,5-dimethylhydantoin and also quinuclidine methylene groups adjacent to the nitrogen were monitored by NMR (Scheme IV-3). As a result of adding one equiv. of quinuclidine to one equiv. 1-chloro-5,5-dimethylhydantoin, the chemical shift of the geminal methyl groups in 1-chloro-5,5-dimethylhydantoin, shifts from 1.48 ppm to 1.35 ppm. Moreover, the chemical shift of the quinuclidine methylenes moves from 2.83 ppm to 3.01 ppm. These changes in chemical shifts are the consequences of deprotonation of the 1-chloro-5,5-dimethylhydantoin by quinuclidine. This suggests that the pK_a of 1-chloro-5,5-dimethylhydantoin is lower than the protonated quinuclidine in chloroform (pK_a in H_2O = 11). One equiv. of benzoic acid (pK_a in H_2O = 4.2) was added

to this mixture. Protonation of the conjugated base of 1-chloro-5,5-dimethylhydantoin results in the down field shift of the methyl groups to 1.43 ppm. These changes in the chemical shift of the methyl groups suggests that the pK_a of 1-chloro-5,5-dimethylhydantoin is between that of benzoic acid (or carboxylic acid substrate) and the
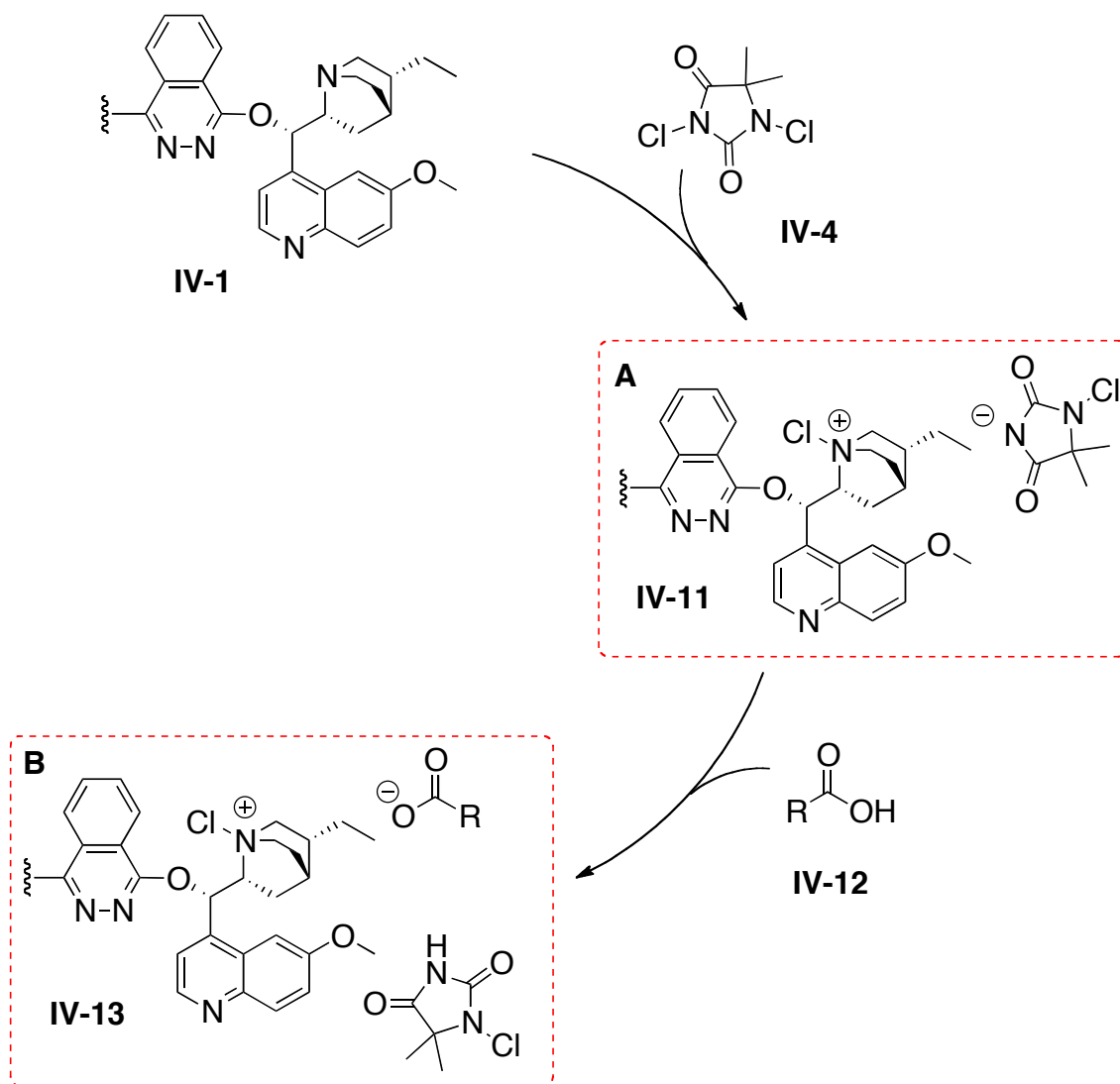
Scheme IV-2. Two possible tight ion pair complexes: complex A and B

protonated quinuclidine. If tight ion pair is a plausible complex, we should look for evidence of the formation of complex **IV-13,** not **IV-11** (Scheme IV-2)**,** as the pK_a of 1-chloro-5,5-dimethylhydantoin (pK_a in H_2O = 7.17)[3,4] is higher than benzoic acid (or the carboxylic acid substrate).

On the other hand, if the hydrogen-bonded complex forms **IV-9**, the quinuclidine moieties of the (DHQD)$_2$PHAL will deprotonate the substrate or benzoic acid and thus the DCDMH will bind to the catalyst through hydrogen bonding. In this case, the benzoate or the deprotonated substrate will be the counter anion for the protonated catalyst **IV-21** (Scheme IV-4)
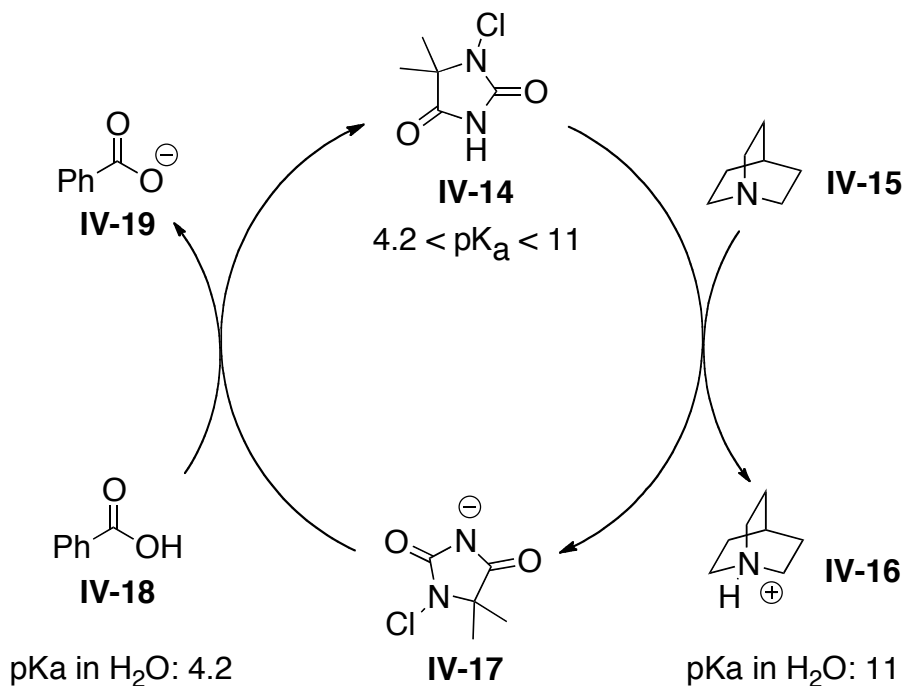
Scheme IV-3. Estimating the MCDMH pKa

The two possible complexes are **IV-13** and **IV-21** (Schemes II-2 and II-4), 1-chloro-5,5-dimethylhydantoin is produced in complex **IV-13**, which is identifiable by NMR spectroscopy. In the other plausible complex, **IV-21**, DCDMH stays intact, forming an associative complex with catalyst through hydrogen bond.

In order to find which associative complex (tight ion pair **IV-13** or hydrogen-bonded complex **IV-21**) forms under the reaction conditions, it is necessary to know the
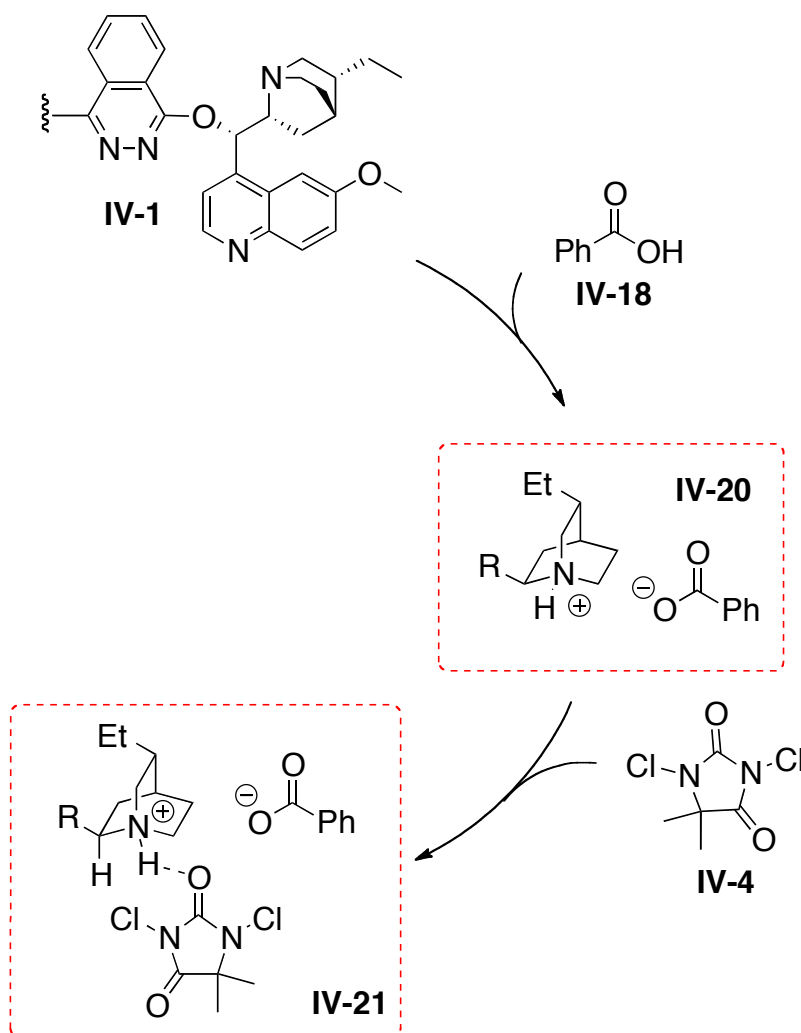
Scheme IV-4. Hydrogen-bonded complex

chemical shift of the geminal methyl groups for 1-chloro-5,5-dimethylhydantoin and DCDMH under the reaction conditions. When 1-chloro-5,5-dimethylhydantoin was mixed with (DHQD)$_2$PHAL (1 equiv.) and benzoic acid (2 equiv.) at -40 $^\circ$C, two methyl resonances at 1.34 and 1.39 ppm were observed for the geminal methyl groups in the ^{1}HNMR, presumably due to tight binding to the (DHQD)$_2$PHAL (methyl groups are not in the same environment). In another experiment, DCDMH (1 equiv.) was added to the mixture of benzoic acid (2 equiv.) and (DHQD)$_2$PHAL (1 equiv.) at -40 $^\circ$C . If the associative complex **IV-13** forms, two resonances corresponding to the 1-chloro-5,5-dimethylhydantoin (1.34 and 1.39 ppm) should be observed. However, under these condition a single peak at 1.54 ppm was observed (Figure IV-2), which closely
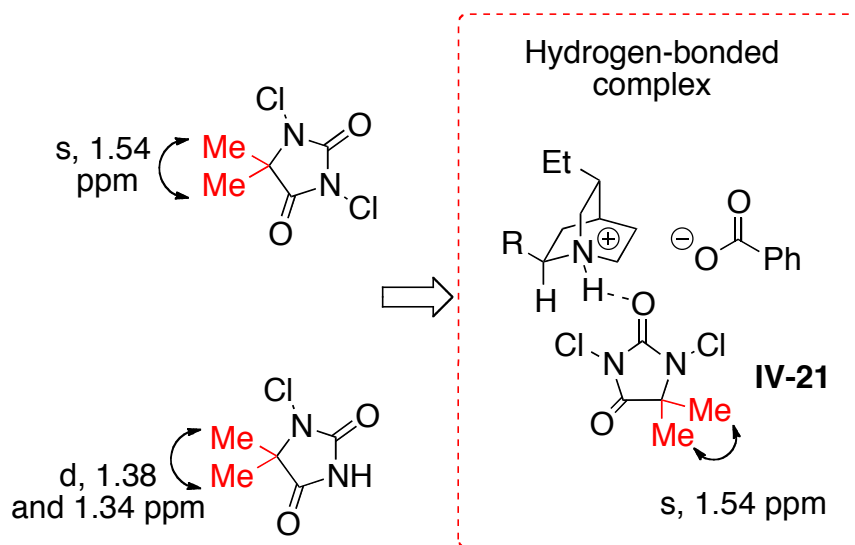
Figure IV-2. Hydrogen-bonded associative complex

204

resembles the chemical shift of free DCDMH (1.53 ppm) in CDCl$_3$ at − 40 $^{\circ}$C. In addition, deshielding of the methylene groups adjacent to the nitrogen of quinuclidine suggests that the quinuclidine moiety of the (DHQD)$_2$PHAL is protonated. The latter series of NMR experiments suggests that hydrogen bond plays an important role in the formation of the proposed associative complex between DCDMH and protonated catalyst. It is believed that the intermolecular hydrogen bond activates DCDMH and presumably controls the face selectivity in chlorenium delivery to the olefin.

4.3: Origin of Face Selectivity in the Ring-Closing Step

As explained in Chapter two, high face selectivity in chlorine delivery to the *tert*-butyl ester substrate, a substrate that cannot bind to (DHQD)$_2$PHAL as a counter anion, suggests that the origin of face selectivity in chlorine delivery to the olefin is different than that of the ring closing step (Figure II-3). NMR studies in the previous section suggests that face selectivity in chlorine delivery is a consequence of the hydrogen bond between the DCDMH and (DHQD)$_2$PHAL. As the reaction proceeds through the carbocation intermediate, the associative complex between the hydantoin and the catalyst cannot be responsible for the high enantioselectivity in the second step. The presence of the catalyst as a counteranion for the carbocation intermediate leads to the facial discrimination of the sp^2 hybridized carbon. In this section, the possible binding elements, which control the face selectivity of the *enantio*-determining step will be investigated.

To elucidate these binding elements, it is necessary to know the conformation of the (DHQD)₂PHAL under the reaction conditions. It has been shown that quinidine (the unsaturated monomer of (DHQD)₂PHAL) has four different conformations, *anti*-closed, *syn*-closed, *anti*-open and *syn*-open, as depicted in Scheme IV-5. These four conformations interconvert by rotation around the C8-C9 and C9-C4´.[5-7] It is known that quinidine prefers to have the *anti*-open conformation when the quinuclidine nitrogen is protonated.[8] As discussed in the previous section deshielding of the methylene groups adjacent to the quinuclidine nitrogen in the presence of DCDMH, benzoic acid and (DHQD)₂PHAL suggests that the quinuclidine moiety is protonated. One would
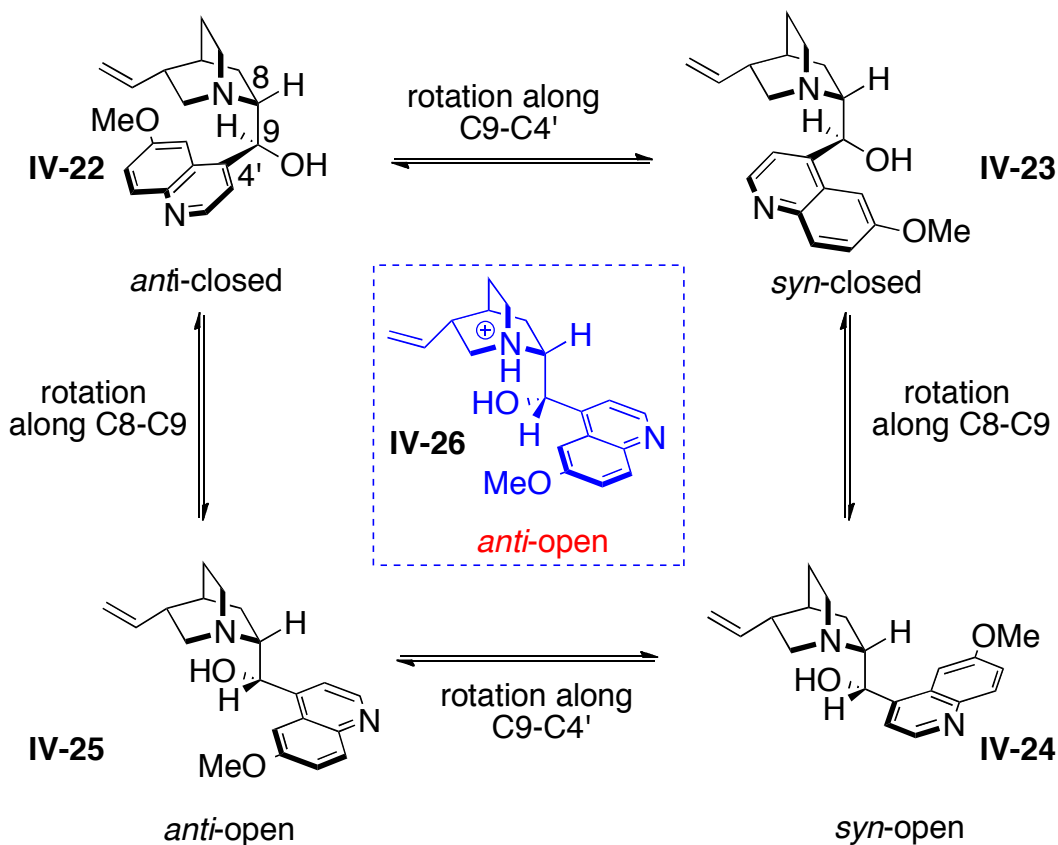
Scheme IV-5. Four conformers of quinidine

206

assume that, (DHQD)$_2$PHAL under the real reaction conditions (where only 10 mol% catalyst is present along with 200 mol% carboxylic acid) adopts the *anti*-open conformation.

To confirm this hypothesis and elucidate the conformation of (DHQD)$_2$PHAL, exhaustive ROESY analysis was performed on a 2:1 mixture of 4-(4-fluorophenyl)pent-4-enoic acid substrate **II-29** and (DHQD)$_2$PHAL in CDCl$_3$ at -40 °C. 4-(4-Fluorophenyl)pent-4-enoic acid **II-29** was used as the substrate since its aromatic protons (ortho to fluoro) do not overlap with the aromatic protons of the catalyst. The ^{1}HNMR spectrum of the (DHQD)$_2$PHAL and substrate at -40 °C shows only one set of peaks for the alkaloid, which suggests that the catalyst has on average a C2 symmetric conformation in the presence of the carboxylic acid substrate. Moreover, ROESY experiments show a series of intermolecular correlation, depicted in Figure IV-3, that highlight close proximity of the ethyl group and the back ring of the phthalazine, and also the phthalazine and the quinoline. In 1998 Ammalahti and co-workers proposed a method to estimate the distances between protons that show ROESY correlations.[9,10] By taking advantage of this method, we were able to measure the distance between the linker and ethyl groups of the quinuclidine moiety, and also the quinoline ring as shown in Figure IV-3. These ROESY correlations, with their corresponding distances, and also the small coupling constant between H$_a$ and H$_b$ (a broad singlet peak was observed for H$_b$) suggest that (DHQD)$_2$PHAL rests in a C2 symmetric *anti* open conformation (**IV-27**), with respect to an axis through the plane of the phthalazine linker and therefore a preferred *anti*–arrangements of the two DHQD units. This proposed conformation for
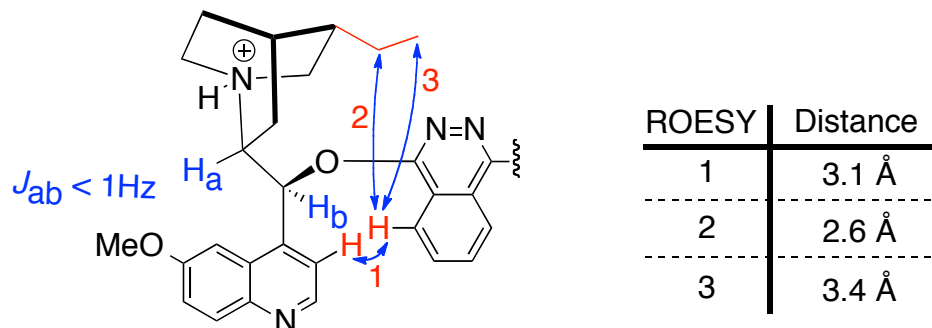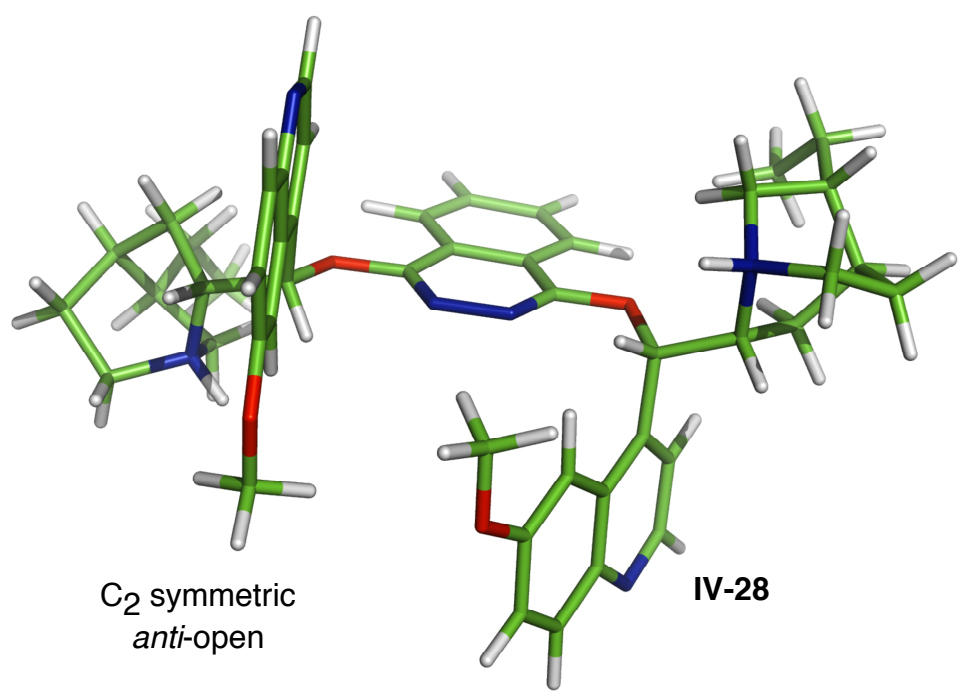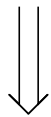
Figure IV-3. *Anti*-open with C$_2$ symmetric conformation

protonated $(DHQD)_2PHAL$ is similar to the crystal structure of the $(DHQD)_2PHAL.$[11] The protonated $(DHQD)_2PHAL$, having a C2 symmetric *anti* open conformation, provides a proper binding pocket for the substrate in its resting state and possibly in the ring closing transition state.

Moreover, during the ROESY NMR study, it was observed that the vinylic protons and also two methylene groups of 4-(4-fluorophenyl)pent-4-enoic acid **II-29** are highly shielded (by ~0.5 ppm) as shown in Figure IV-4c. This shielding can be the result of the deprotonation of the substrate by the catalyst and also the binding of the corresponding carboxylate to the catalyst. In a control experiment, quinuclidine was used as a base to measure the magnitude of shielding for the deprotonated carboxylic acid **II-30**. In this experiment the highest shielding (0.19 ppm) was observed for the methylene group adjacent to the carboxylate moiety. Chemical shifts of the rest of the protons showed a slight change (~0.04 ppm) due to deprotonation (Figure IV-4b). As expected, deprotonation does not account fully for the large shielding, observed with the catalyst–bound substrate. In the proposed complex, **IV-31**, 4-(4-fluorophenyl)pent-4-enoic acid **II-29** presumably rests in the shielding cone of the phthalazine and/or quinoline moieties.

This hypothesis is also supported by the observed intermolecular ROESY between 4-(4-fluorophenyl)pent-4-enoic acid **II-29** and $(DHQD)_2PHAL$ (Figure IV-5). The OMe groups of the quinoline group show ROESY interactions to the methylene groups of the substrate and also to the phenyl group (ortho protons to fluorine). Based on the observed ROESY correlations and the experimentally calculated distances, a resting

a IV-29

	ppm
1	2.52
2	2.80
3	5.06
4	5.25
5	7.36
6	7.01

CDCl$_3$, -40 °C

b IV-30

	ppm	Δ ppm
1	2.33	-0.19
2	2.74	-0.06
3	5.02	-0.04
4	5.21	-0.04
5	7.39	+0.04
6	6.95	-0.06

c

	ppm	Δ ppm
1	2.00	-0.52
2	2.37	-0.43
3	4.62	-0.46
4	4.71	-0.54
5	7.13	-0.23
6	6.82	-0.29

IV-31
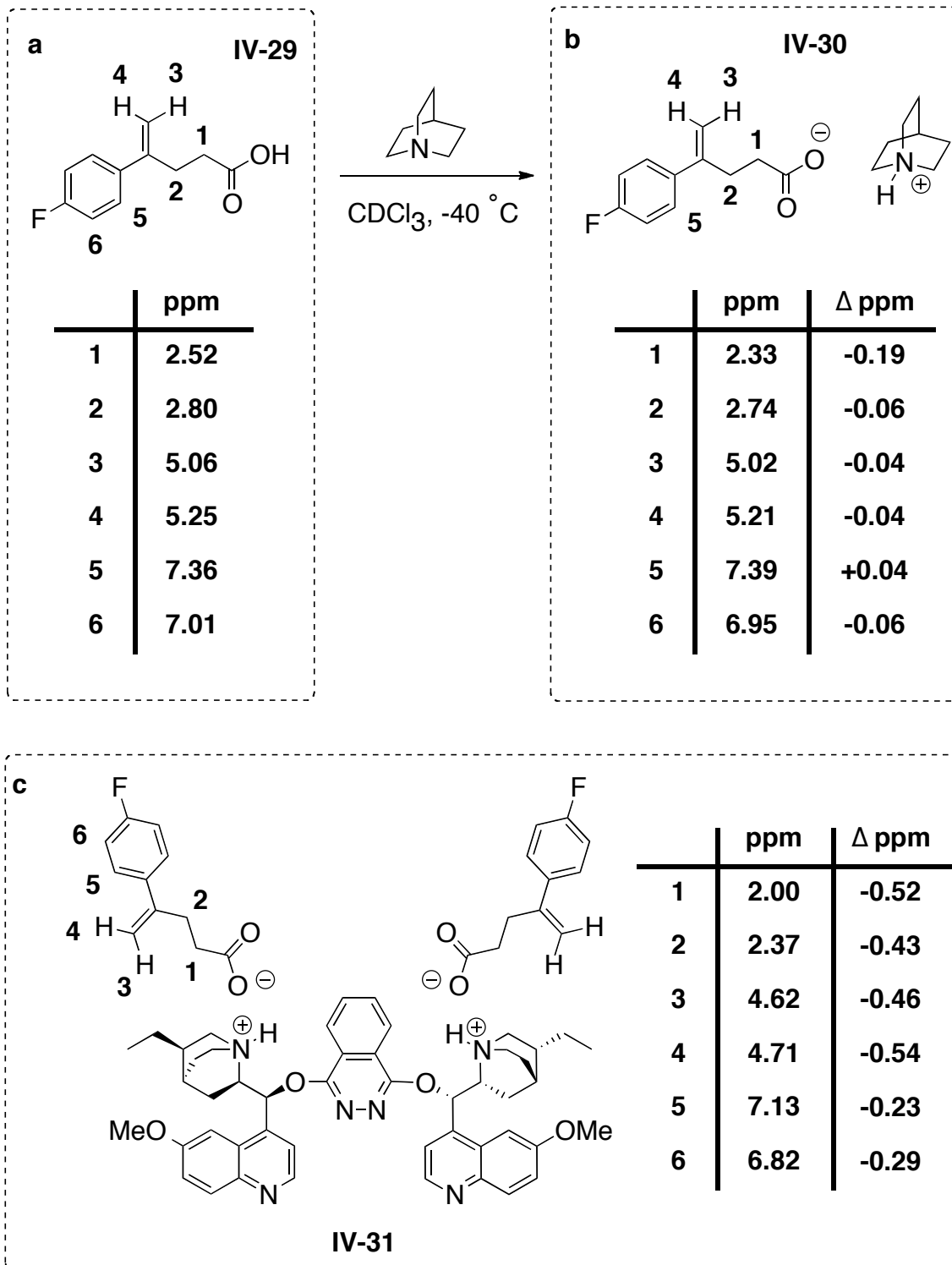
Figure IV-4. 4-(4-Fluorophenyl)pent-4-enoic acid substrate chemical shift change in the presence of quinuclidine or (DHQD)$_2$PHAL

model for the binding of the substrate with (DHQD)$_2$PHAL is proposed as depicted in Figure IV-5. In this proposed model the carboxylate substrate binds to the protonated (DHQD)$_2$PHAL as a counter anion in a manner that positions the phenyl group out of the binding pocket of (DHQD)$_2$PHAL. In this proposed model the vinylic protons and also the two methylene groups of the carboxylate substrate reside in the shielding cone of the quinoline moieties, which explains the observed upfield shield of their resonances. In addition, OMe groups of the quinoline in this proposed resting model are approximately 3 Å away from the methylene groups of the substrate in agreement with observed ROESY correlations. Further computational studies are needed to evaluate and minimize this proposed resting model.

As mentioned in Chapter 2, 4-(3-nitrophenyl)pent-4-enoic acid **II-33** is unreactive under the chlorolactonization reaction conditions. This unreactive substrate provides the opportunity to further investigate the proposed resting model in the presence of 1,3-dichlorohydantoin as a surrogate substrate.

Similar shielding behavior was also observed with a 2:1 mixture of 4-(3-nitrophenyl)pent-4-enoic acid substrate and (DHQD)$_2$PHAL, which suggest that this unreactive substrate binds in a similar orientation to the catalyst (Figure IV-6). Addition of four equivalent of 4-(3-nitrophenyl)pent-4-enoic acid **IV-33** to (DHQD)$_2$PHAL resulted in an average spectra, indicating a fast equilibrium (based on the NMR time scale) between bonded and non-bonded forms. Due to this fast equilibration, one does not

211

ROESY	Distance
1	3.1 Å
2	3.0 Å
3	3.8 Å
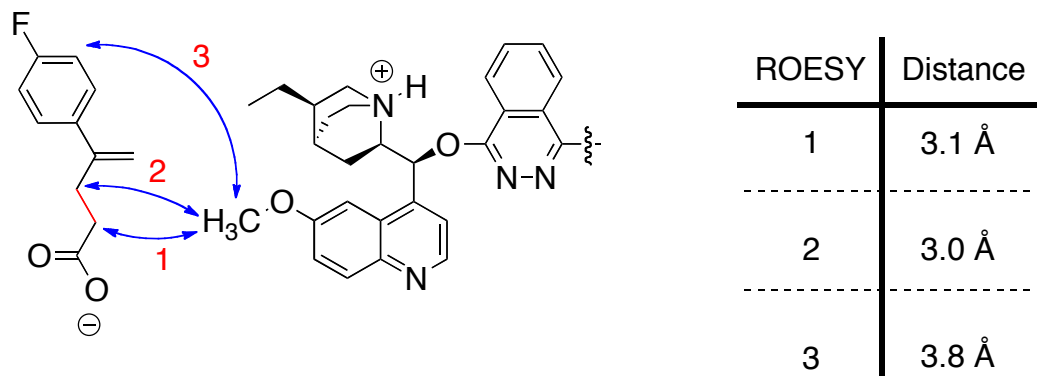
front view:
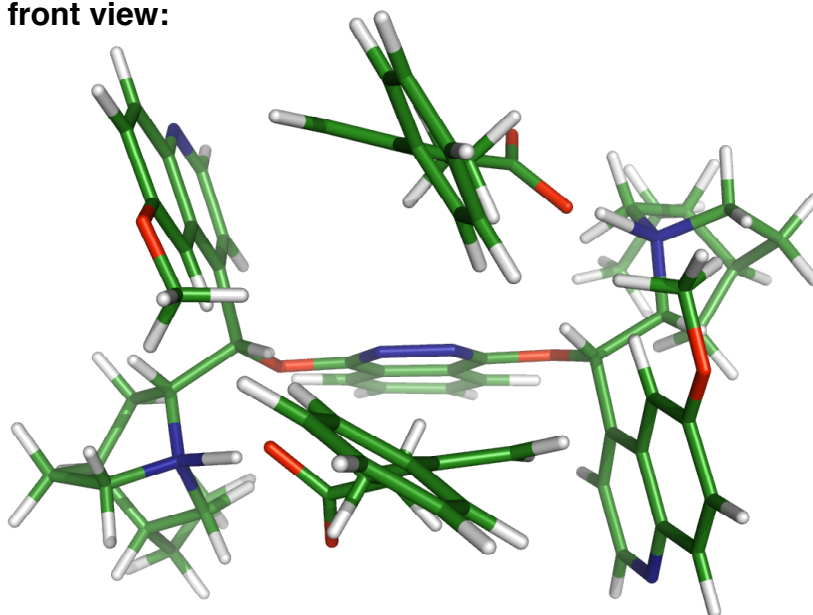
side view:
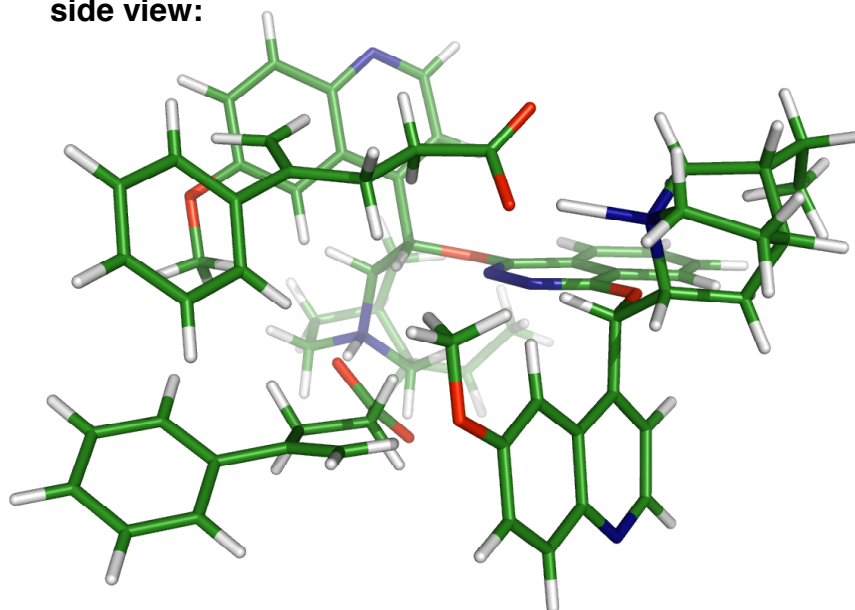
Figure IV-5. Intramolecular ROESY between 4-(4-fluorophenyl)pent-4-enoic acid substrate and $(DHQD)_2PHAL$ and the proposed resting state

observe two sets of peaks for non-bonded and bonded forms but an average chemical shift, which is equal to the average of the **IV-32** and **IV-33** species (Figure IV-7).

(DHQD)$_2$PHAL, a dimeric cinchona alkaloid, has the potential to bind to two substrates at the same time, as speculated in the proposed resting model. As mentioned in chapter two in the presence of 4-(3-nitrophenyl)pent-4-enoic acid, 4-phenylpent-4-enoic acid and DCDMH (1:1:1) and 1.5 mol% catalyst, the rate of the chlorolactonization of 4-phenylpent-4-enoic acid was decreased by 71%, which can suggest a greater affinity of the catalyst for 4-(3-nitrophenyl)pent-4-enoic acid. Simply stated the nitrophenyl substrate acts as a competitive inhibitor of the cinchona alkaloid-binding pocket. In an another experiment, a 1:1 mixture of 4-(3-nitrophenyl)pent-4-enoic acid **IV-32** and 4-phenylpent-4-enoic acid **IV-2** (1:1) was mixed with one equiv.

	IV-32	IV-33	Δ ppm
1	2.56	2.07	-0.49
2	2.84	2.4	-0.44
3	5.23	4.74	-0.49
4	5.46	4.79	-0.67
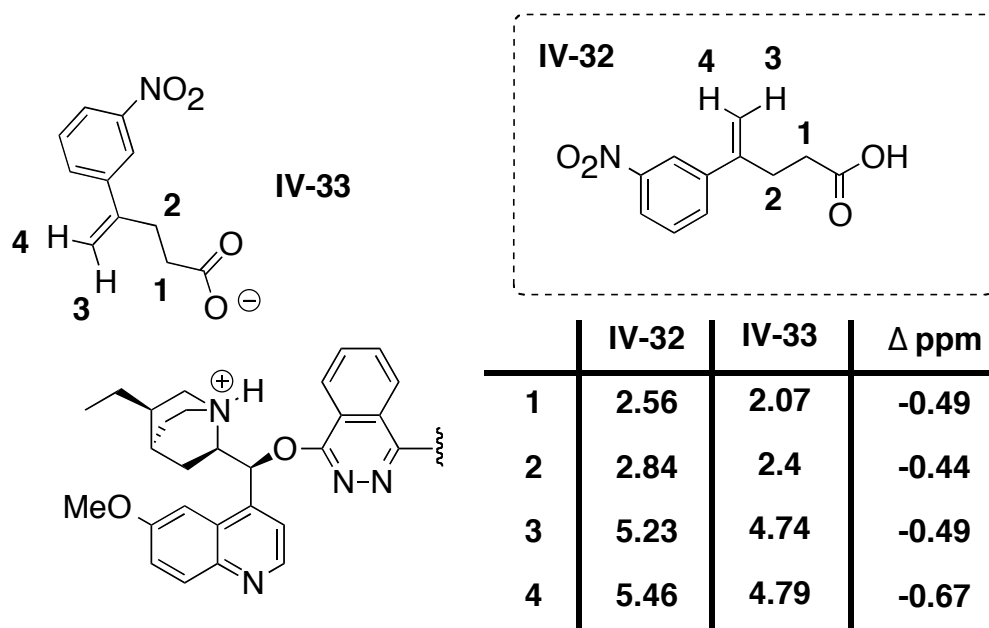
Figure IV-6. 4-(3-nitrophenyl)pent-4-enoic acid substrate chemical shift change in the presence of (DHQD)$_2$PHAL (2:1).

213

(DHQD)$_2$PHAL. Surprisingly in this NMR experiment, a similar shielding behavior were observed for 4-(3-nitrophenyl)pent-4-enoic acid **IV-32** and 4-phenylpent-4-enoic acid **IV-2** as compared to when a 2:1 mixture of the 4-(3-nitrophenyl)pent-4-enoic acid and (DHQD)$_2$PHAL (or 2:1 mixture of the 4-phenylpent-4-enoic acid and (DHQD)$_2$PHAL) was used (Figure IV-8). The catalyst with a single binding site should have resulted in more shielding of 4-(3-nitrophenyl)pent-4-enoic acid resonances in the latter experiment, as the catalyst has greater affinity for it. Since the same degree of chemical shift is observed, it suggests that there is no competition for both substrates to bind to the catalyst in a 1:1:1 complex. These results let us to propose that (DHQD)$_2$PHAL can bind two substrates at the same time. In addition, observation of broad peaks, when

	IV-32	IV-33 (2 equiv.)	IV-33 (4 equiv.)
1	2.56	2.07	2.22
2	2.84	2.4	2.58
3	5.23	4.74	4.94
4	5.46	4.79	5.07
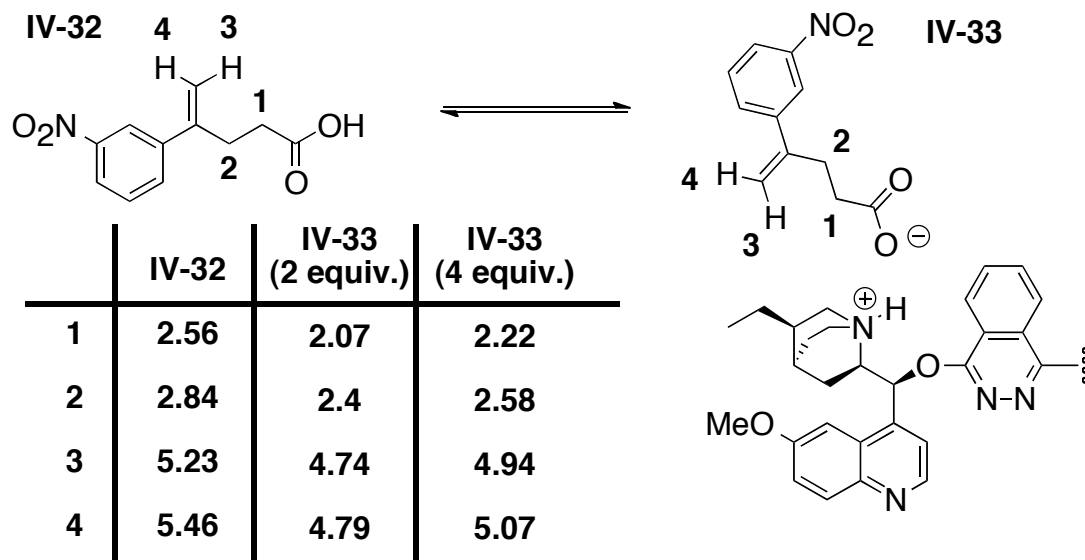
Figure IV-7. Fast equilibration in NMR time scale between non-bonded and bonded 4-(3-nitrophenyl)pent-4-enoic acid substrate.

catalyst and substrate were mixed in a 1:1 ratio also supported this hypothesis. These sets of experiments suggest that in the optimized conditions two molecules of substrate can bind to catalyst at the same time.

The higher affinity of the catalyst to 4-(3-nitrophenyl)pent-4-enoic acid were also evaluated again in a control experiment. In this experiment 4-(3-nitrophenyl)pent-4-enoic acid **IV-32**, 4-phenylpent-4-enoic acid **IV-2** and (DHQD)$_2$PHAL were mixed togther in a 2:2:1 ratio, respectively. As the catalyst has two presumed binding sites, we expect to observe more shielding of 4-(3-nitrophenyl)pent-4-enoic acid **IV-32** substrate. This expectation comes from the fact that the catalyst can accommodate half of the substrates presents in the solution and the nitro phenyl substrate has higher binding affinity. Indeed as depicted in Figure IV-8d, vinylic protons of the 4-(3-nitrophenyl)pent-4-enoic acid are shielded more than 0.4 ppm by the catalyst in comparison to the same protons of 4-phenylpent-4-enoic acid that are shielded by (~0.1ppm).

In another experiment, to the 2:1 mixture of 4-(3-nitrophenyl)pent-4-enoic acid substrate and (DHQD)$_2$PHAL, 1 equiv. 1,3-dichlorohydantoin was added. Surprisingly, no AB quartet pattern was observed for the methylene group of the 1,3-dichlorohydantoin. At this stage, we cannot conclude that in the presence of the acid substrate hydantoin cannot bind to the catalyst. The disappearance of the AB quartet can be due to having the bigger counter anion (deprotonated substrate), in the binding pocket instead of benzoate, with which we were able to observe the AB quartet. By replacing one of the substrate molecules with benzoic acid in this experiment, a small

IV-32

or/and

IV-2

(DHQD)₂PHAL
1 equiv.

a
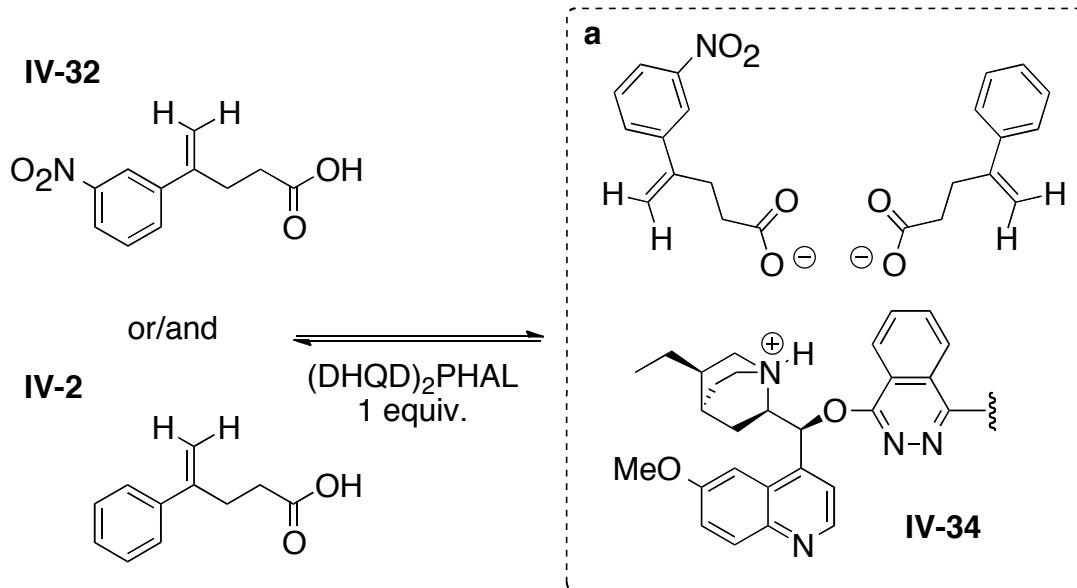
IV-34

b

	IV-34 (2 equiv.)	IV-34 (4 equiv.)
1	4.74	4.94
2	4.79	5.07

c

	IV-34 (2 equiv.)	IV-34 (4 equiv.)
3	4.69	4.81
4	4.89	5.02

d

	IV-34 (1:1)	IV-34 (2:2)
1	4.65	4.83
2	4.65	4.93
3	4.73	4.90
4	4.94	5.12

Figure IV-8. NMR studies to evaluate the number of binding sites on (DHQD)₂PHAL

splitting of the methylene protons was observed, which can be an indication for the possible hydrogen bond even in the presence of the deprotonated substrate.

By considering the disappearance of the AB quartet and the fact that hydrogen bonds are weaker than ionic bonds, the proposed catalytic cycle (Scheme IV-1) is revised. In the second step of the proposed catalytic cycle a molecule of DCDMH replaces one carboxylate substrate, which is an energetically uphill process. On the other hand, as mentioned before the lack of reactivity of the DCDMH in the absence of the catalyst, the match-mismatch behavior and also the inverse isotope effect are the clues for the possible binding and activation of the DCDMH by protonated $(DHQD)_2PHAL$. Based on these facts, one can imagine that DCDMH can bind to the protonated $(DHQD)_2PHAL$ through hydrogen binding without replacing a carboxylate substrate. Indeed, in this new proposed catalytic cycle (Scheme IV-6), $(DHQD)_2PHAL$, a dimeric C_2 symmetric catalyst, is able to catalyze two chlorolactonization reactions at the same time.

4.4: Summary

In summary, NMR studies in this chapter show that in the asymmetric chlorolactonization reaction, DCDMH or DCDPH is activated through hydrogen bonding with protonated $(DHQD)_2PHAL$. This result is in agreement with the observed inverse isotope effect as discussed in Chapter two. Moreover, ROESY NMR studies and corresponding distances leads to the proposed resting state for the substrate in the binding pocket of $(DHQD)_2PHAL$. In this proposed model substrate binds to the catalyst

217
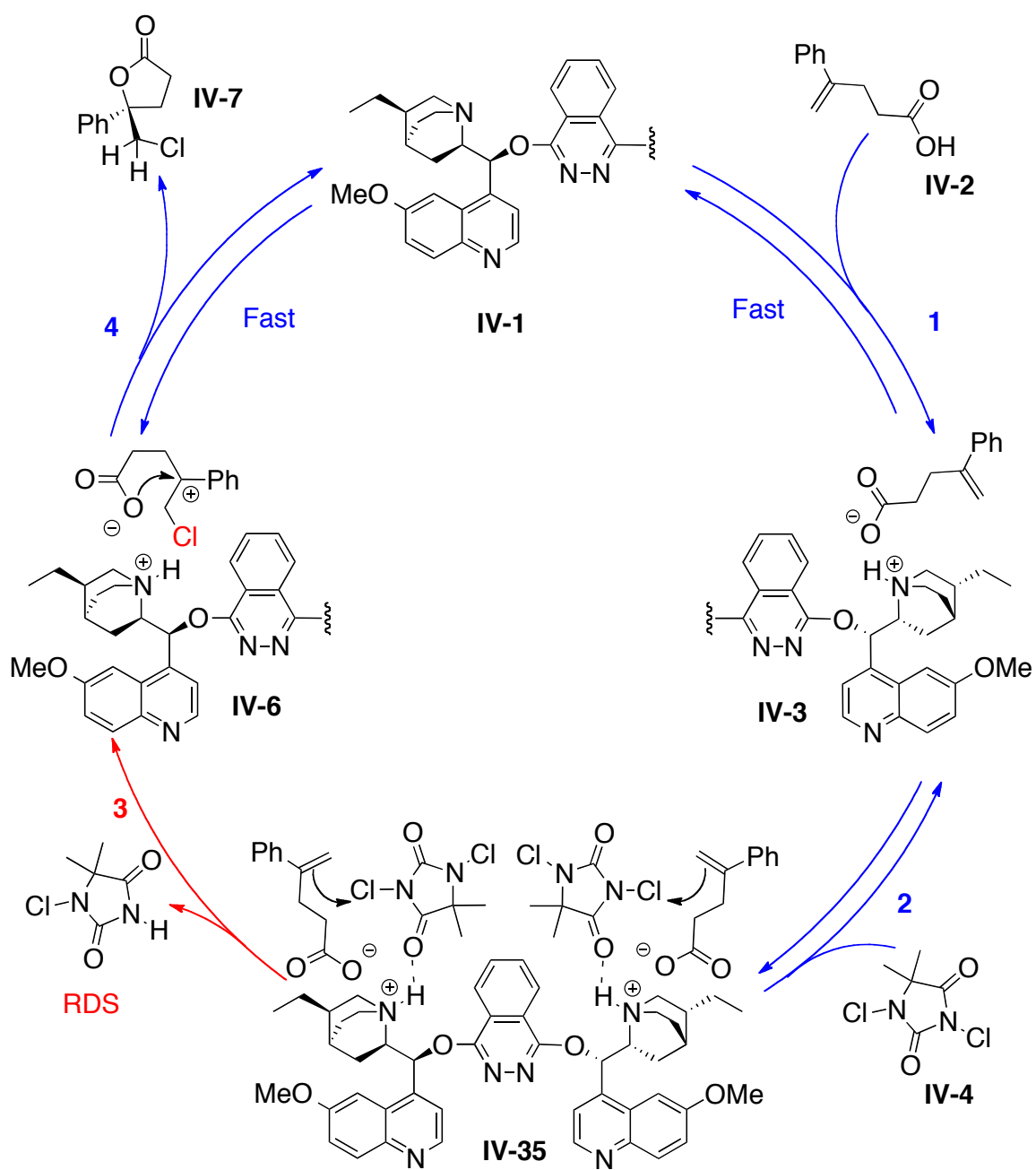
Scheme IV-6. A revised mechanism for the asymmetric chlorolactonization reaction

as a counter ion in a way that vinylic protons stay in the shielding cone of the quinoline moieties. Taken together, we believe that face selectivity in the first step is controlled by the hydrogen bond formation between DCDMH and protonated $(DHQD)_2PHAL$. In addition, NMR studies suggest that face selectivity in the ring closing step is controlled by templation of the cyclization event in the $(DHQD)_2PHAL$ chiral binding pocket.

4.5: Experimental Details

4.5.1: General Information

All reagents were purchased from commercial sources and used without purification. All 1D and 2D NMR spectra were collected on a 600 or 500 MHz NMR spectrometer (VARIAN INOVA) using $CDCl_3$. Chemical shifts are reported in parts per million (ppm).

4.5.2: Sample and NMR Instrument Preparation for ^{1}HNMR Studies

The probe of the NMR instrument was cooled to -40°C and allowed to equilibrate for 60 minutes. A stock solution of catalyst and different substrates were prepared and desired volume were calculated and added to the NMR tube. In all ^{1}HNMR studies, the solution in NMR tube was equalized to 1 mL by adding enough $CDCl_3$.

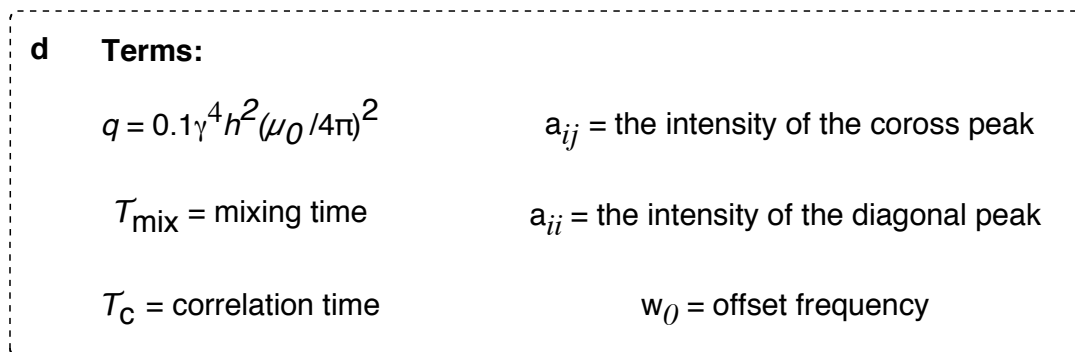## 4.5.2: Sample and NMR Instrument Preparation for ROESY Studies

600 MHz NMR instrument was used for all ROESY studies due to higher stability of the NMR instrument at lower temperature, which helped to minimize artifacts, especially

in the aromatic region. Prior to any ROESY study, the probe of the NMR instrument was cooled to -20 $^\circ$C (-20 $^\circ$C was chosen because of 600 MHz NMR instrument limitation) and allowed to equilibrate for two hours. A stock solution of catalyst and substrate were prepared and the desired volume of catalyst and substrate were calculated and added to the NMR tube. In all ROESY studies, the solution in NMR tube was equalized to 1 mL by adding enough $CDCl_3$. After preparing the sample, Freeze-Pump-Thaw degassing method was used to remove dissolved oxygen from the sample. The NMR tube was sealed properly with Teflon tape and then inserted to the NMR instrument. The sample was equilibrated in the NMR instrument for 10 minutes. After tuning the carbon and proton, and locking and shimming the sample, PW 90° was measured and set for the ROESY study.

4.5.2: Measuring the Distances in ROESY Studies

The intensity-ratio method (developed by Ammalahti)[9,10] was used to measure the distances in our ROESY experiments. Several effects such as HOHAHA type magnetization and also an offset dependence of the spin-locked conditions influence ROESY cross peaks intensities. Ammalahti and coworkers has shown that ROESY cross peaks can be used to estimate the distances between desired protons by carefully adjusting the measuring condition. To minimize these undesired effects on the ROESY peaks, the spin lock pulse was positioned at the far low side of the spectrum (3599 Hz) and also moderate spin-lock field (5758 Hz) was used.

To measure the distance based on this method, equation 1 (Figure IV-9a) was

a

$$r_{ij} = \left\{ \frac{-2qT_{mix}}{\ln\left[\dfrac{a_{ii}c_{ii} + a_{ij}c_{ij}}{a_{ii}c_{ii} - a_{ij}c_{ij}}\right]} \left(\frac{6T_c}{1 + 4\omega^2 T^2_c} - T_c\right) \right\}^{1/6}$$

$$\Downarrow$$

$$\text{Constant} = -2qT_{mix}\left(\frac{6T_c}{1 + 4\omega^2 T^2_c} - T_c\right)$$

$$\Downarrow$$

$$\mathbf{1:}\quad r_{ij} = \left(\frac{\text{Constant}}{\ln\left[\dfrac{a_{ii}c_{ii} + a_{ij}c_{ij}}{a_{ii}c_{ii} - a_{ij}c_{ij}}\right]}\right)^{1/6}$$

b

c

$$c_{ij} = \frac{1}{(\sin^2\theta_i \sin^2\theta_j)}$$

$$c_{ii} = \frac{1}{(\sin^2\theta_i \sin^2\theta_i)}$$

$$\tan\theta_i = \frac{\gamma B_1}{(\omega_i - \omega_0)}$$

d **Terms:**

$$q = 0.1\gamma^4 h^2 (\mu_0/4\pi)^2 \qquad a_{ij} = \text{the intensity of the coross peak}$$

$$T_{mix} = \text{mixing time} \qquad a_{ii} = \text{the intensity of the diagonal peak}$$

$$T_c = \text{correlation time} \qquad w_0 = \text{offset frequency}$$
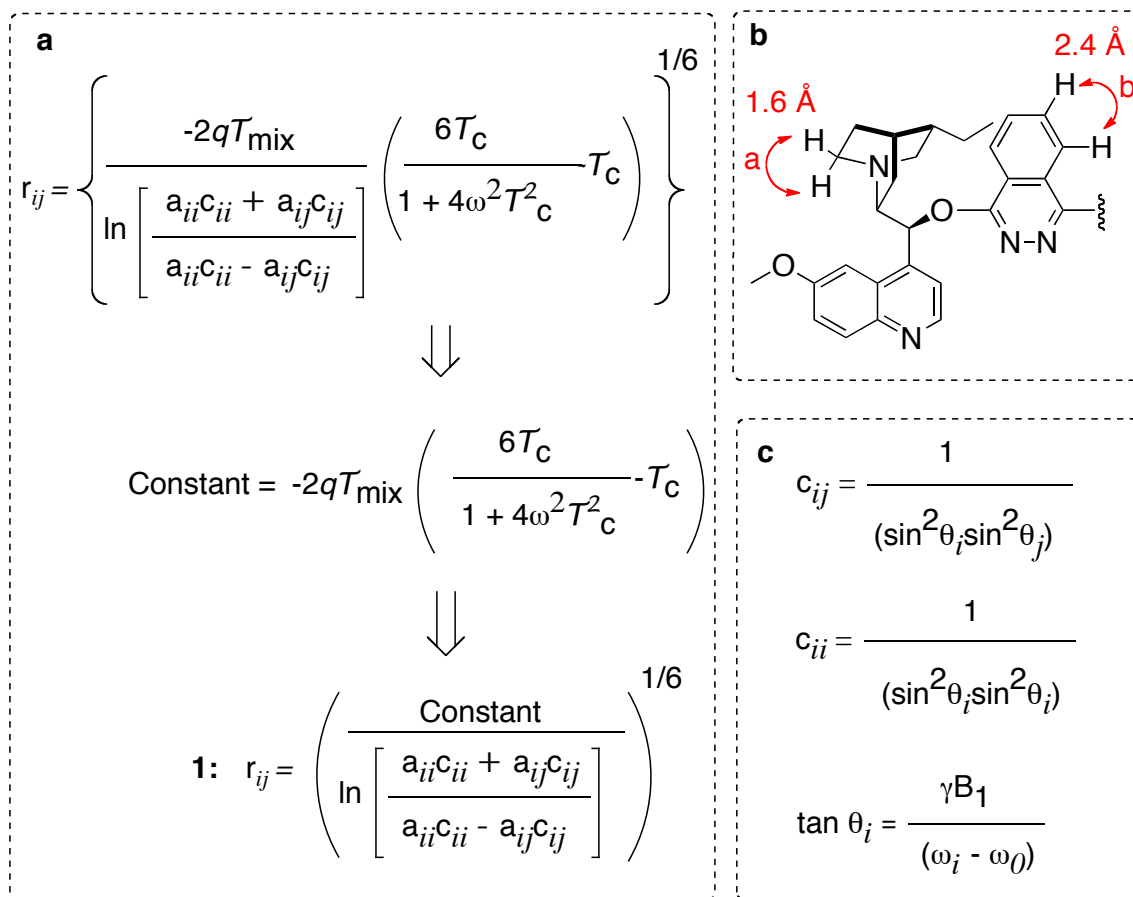
Figure IV-9. a) Modified intensity-ratio method's equation to measure ROESY distances. b) Two chosen-fixed distances. c) Correction factor's equations. d) Terms.

221

Table IV-1. Interproton intensities, correction factors and distances.

ROESY Correlations	Cross Peak Intensity	Diagonal Peak Intensity	C_{ij}	C_{ii}	Distance Å
2.8 ppm to 3.11 ppm	8.64	36.4	1.208	1.109	1.6
7.3 ppm to 8.5 ppm	3.56	135.5	1.086	1.017	2.3
2.4 ppm to 3.67 ppm	0.62	152.6	1.207	1.140	3.2
2.0 ppm to 3.67 ppm	0.77	133.7	1.238	1.169	3.0
3.67 ppm to 6.85 ppm	0.29	191.4	1.067	1.059	3.8
8 ppm to 8.3 ppm	3.24	100	1.106	1.044	2.2
1.69 ppm to 8.3 ppm	1.78	125	1.273	1.202	2.6
7.25 ppm to 8.3 ppm	0.65	135	1.078	1.017	3.1
8.35 ppm to 0.94 ppm	0.46	165	1.354	1.278	3.4
3.66 ppm to 7.15 ppm	0.97	191.4	1.0746	1.059	3.1

used. To apply this equation, correction factors based on the equations in Figure IV-9c were calculated. The constant value was calculated as well by having a reference ROESY with a fixed distance. Two references, Figure IV-9b, with the fixed distance were chosen to calculate the constant number. Reference "a" was chosen with 1.6 Å fixed distance to calculate the "constant number". To evaluate whether this method is accurate in for this purpose or not, reference "b" distance was measured (2.25 Å) by using the equation 1 (Figure IV-9a) and the calculated constant, and then the result was compared with its actual distance from $(DHQD)_2PHAL$ crystal structure (2.4 Å). This control experiment shows that Ammalahati method is a reliable method with a marginal

error. These calculations are summarized in Table IV-1, which were used to predict the

catalyst conformation proposed for the resting state of substrate in catalyst binding

pocket.

REFERENCES

REFERENCES

1. Whitehead, D. C.; Yousefi, R.; Jaganathan, A.; Borhan, B. *Journal of the American Chemical Society* **2010**, *132*, 3298.

2. Yousefi, R.; Whitehead, D. C.; Mueller, J. M.; Staples, R. J.; Borhan, B. *Organic Letters* **2011**, *13*, 608.

3. Akdag, A.; Worley, S. D.; Acevedo, O.; McKee, M. L. *Journal of Chemical Theory and Computation* **2007**, *3*, 2282.

4. Corral, R. A.; Orazi, O. O. *Journal of Organic Chemistry* **1963**, *28*, 1100.

5. Burgi, T.; Baiker, A. *Journal of the American Chemical Society* **1998**, *120*, 12920.

6. Dijkstra, G. D. H.; Kellogg, R. M.; Wynberg, H. *Journal of Organic Chemistry* **1990**, *55*, 6121.

7. Dijkstra, G. D. H.; Kellogg, R. M.; Wynberg, H.; Svendsen, J. S.; Marko, I.; Sharpless, K. B. *Journal of the American Chemical Society* **1989**, *111*, 8069.

8. Olsen, R. A.; Borchardt, D.; Mink, L.; Agarwal, A.; Mueller, L. J.; Zaera, F. *Journal of the American Chemical Society* **2006**, *128*, 15594.

9. Ammalahti, E.; Bardet, M.; Cadet, J.; Molko, D. *Magnetic Resonance in Chemistry* **1998**, *36*, 363.

10. Ammalahti, E.; Bardet, M.; Molko, D.; Cadet, J. *Journal of Magnetic Resonance Series A* **1996**, *122*, 230.

11. Kolb, H. C.; Andersson, P. G.; Sharpless, K. B. *Journal of the American Chemical Society* **1994**, *116*, 1278.